

TRANSACTINIUM ISOTOPE NUCLEAR DATA (TND)

VOL.III

**PROCEEDINGS OF AN ADVISORY GROUP MEETING
ON TRANSACTINIUM ISOTOPE NUCLEAR DATA
ORGANIZED BY THE
IAEA NUCLEAR DATA SECTION
IN CO-OPERATION WITH THE
OECD NUCLEAR ENERGY AGENCY
HELD AT THE KERNFORSCHUNGSZENTRUM
KARLSRUHE, 3-7 NOVEMBER 1975**



**A TECHNICAL DOCUMENT ISSUED BY THE
INTERNATIONAL ATOMIC ENERGY AGENCY, VIENNA, 1976**

**PLEASE BE AWARE THAT
ALL OF THE MISSING PAGES IN THIS DOCUMENT
WERE ORIGINALLY BLANK**

The IAEA does not maintain stocks of reports in this series. However, microfiche copies of these reports can be obtained from

INIS Microfiche Clearinghouse
International Atomic Energy Agency
Kämtner Ring 11
P.O. Box 590
A - 1011 Vienna, Austria

on prepayment of US \$0.65 or against one IAEA microfiche service coupon.

FOREWORD

The IAEA Nuclear Data Section, in cooperation with the OECD Nuclear Energy Agency, convened an Advisory Group Meeting on Transactinium Isotope Nuclear Data at Karlsruhe, FRG, from 3-7 November 1975. The meeting was attended by 45 representatives from 13 countries and 3 international organizations. It was the first international meeting on this topic.

The general conclusion of the meeting participants was that transactinium isotopes are becoming more and more important in nuclear technology, and that the present knowledge of nuclear data required to evaluate the effects of actinides in nuclear technology is not satisfactory. One of the basic recommendations, which resulted from the meeting was to initiate an internationally coordinated programme to measure, calculate, and evaluate needed transactinium isotope nuclear data which would span the next ten years. The principal aim of this effort would be to improve the status of actinide nuclear data required for nuclear technology.

Table of Contents

VOLUME I

Summary Report

Introduction	1
General Recommendations	3
Conclusions and Recommendations of the Working Group on Thermal Reactors	7
Conclusions and Recommendations of the Working Group on Fast Reactors	17
Conclusions and Recommendations of the Working Group on Waste Management and Isotope Application	25
List of Review Papers	29
Meeting Programme	31
List of Participants	33

Session A, Survey of TND Applications

Review Paper No. A1: General Survey of Applications which require Actinide Nuclear Data	39
Review Paper No. A2: Importance of Transactinide Nuclear Data for the Physics of Fast and Thermal Reactor Cores	113
Review Paper No. A3: Transactinium Isotope Build-up and Decay in Reactor Fuel and Related Sensitivities to Cross Section Changes	139
Review Paper No. A4: The Requirements for Trans- actinium Nuclear Data for the Design and Operation of Nuclear Power Plants	167
Review Paper No. A5: Importance of Transactinium Nuclear Data for Fuel Handling	175
Review Paper No. A6: European Programmes in Waste Management (Incineration) of Actinides	191
Review Paper No. A7: Some Activities in the United States Concerning the Physics Aspects of Actinide Waste Recycling	201
Review Paper No. A8: Importance of Transactinium Nuclear Data (TND) for Fuel Analysis	215
Review Paper No. A9: Radiation and Energy Sources, Tracer Techniques, Applications in Life Sciences, Agriculture and Industry	227

Table of Contents

VOLUME II

Review Paper No. B1: Status of Measured Neutron Cross Sections of Transactinium Isotopes for Thermal Reactors. . .	1
Review Paper No. B2: Status of Neutron Cross Sections of Transactinium Isotopes in the Resonance Region - Linear Accelerator Measurements	71
Contributed Papers to Topic B2:	
Neutron Capture Cross Sections of the Actinides	115
Total Neutron Cross-Section Measurements on the Trans- actinium Isotopes ^{241}Am , ^{243}Am , ^{244}Am , ^{245}Am , ^{246}Am , ^{248}Cm . . .	121
Measurement of the Fission Cross-Section of ^{237}Np between 100 keV and 2 MeV	135
High Resolution Measurements of Fission Cross Sections of ^{238}U and ^{239}Pu as compared with ^{235}U	141
Fission Cross-Section and Resonance Parameters of ^{241}Am . .	149
Measurement of σ_f for ^{243}Am	159
Review Paper No. B3: Status of Neutron Cross Sections of Transactinium Isotopes in the Resonance and fast Energy Regions - Underground Nuclear Explosion Measurements	161

VOLUME III

Review Paper No. B4: Status of Measured Neutron Cross Sections of Transactinium Isotopes in the Fast Region . . .	1
Review Paper No. B5a: Status of Transactinium Isotope Evaluated Neutron Data in the Energy Range 10^{-3} eV to 15 MeV	165
Contributed Paper to Topic B5a: The Transactinides in the Main Evaluated Neutron Data Files	195
Review Paper No. B5b: Theoretical Calculation of Trans- actinium Isotope Nuclear Data for Evaluation Purposes . . .	201
Contributed Paper to Topic B5b: A Survey of Cross Section Evaluation Methods for Heavy Isotopes	237
Review Paper No. B6: The Experimental Investigation of the Alpha Decay of Transactinium Isotopes	249
Review Paper No. B7: Status of Beta- and Gamma-Decay and Spontaneous Fission Data from Transactinium Isotopes	265

Status of Measured Neutron Cross Sections of
Transactinium Isotopes in the Fast Region

S. Igarasi

Japan Atomic Energy Research Institute,
Tokai-mura, Naka-gun,
Ibaraki, Japan

This paper reviews present status of measured neutron cross sections of transactinium isotopes from a viewpoint of requested data in application field of the nuclear data. The measured cross sections from 1 keV to 15 MeV are examined. The status of the data is illustrated with many graphs and short notes, instead of detailed explanation on each data set. Except for the fission cross section, the measured data are very scarce. Therefore, comparison between different data sets is mainly performed on the fission cross sections.

This work has been done with the following collaborators;

Y. Kanda,	Kyushyu University
H. Matsunobu,	Sumitomo Atomic Energy Industries, Ltd.
T. Murata,	Nippon Atomic Industry Group Co., Ltd.
T. Ohsawa,	Kyushyu University
Y. Kikuchi,	Japan Atomic Energy Research Institute

1. Introduction

An aim of this review is to examine the status of the experimental data for which requested data are entered in WRENDA 74¹⁾. CINDA 74²⁾ is used as an information source of literatures concerned. Energy range is limited from 1 keV to 15 MeV. The literatures examined are mainly those issued after 1960, but some old literatures are often adopted. Though an effort is made to examine every appropriate literature, some

may be missed. However, present status of the experimental data must be described in substance.

There are many contributions to this review. Britt presented his works³⁻⁵⁾ with his colleague concerning indirect estimates of the fission cross sections using fission probabilities measured with ($^3\text{He},\text{df}$), ($^3\text{He},\text{tf}$) and (t,pf) reactions. In addition to these, he informed his future plan of measurements using Cm, Bk, Cf and Es targets. He plans further to develop techniques using other direct reactions in order to get excitation energies corresponding to equivalent neutron energies of 14 MeV or greater.

Boldeman contributed his works^{6,7)} with his colleague dealing with $\bar{\nu}$ studies. He informed that his measurements of $\bar{\nu}$ on ^{230}Th , ^{231}Pa and ^{232}Th were in progress, and that he was also doing measurements of fission cross section for ^{233}U and ^{235}U with absolute neutron flux facility on VdG. He calculated the energy dependence of $\bar{\nu}$, and found consistent structure in $\bar{\nu}$ and \bar{E}_k (average total kinetic energy of fragments) for ^{233}U . This dependence could be explained in terms of the hypothesis of Blyumkina et al.⁸⁾ However, the calculation applied to ^{235}U showed that the energy dependence of $\bar{\nu}$ was linear. This agrees with his experimental data.⁹⁾ Concerning the status of $\bar{\nu}$ for ^{235}U and ^{239}Pu , Tsukada¹⁰⁾ presented his review privately.

Browne presented his informal report¹¹⁾ on transactinium nuclear cross section measurements at Lawrence Livermore Laboratory 100 MeV linac. Measurements of $^{234}\text{U}(\text{n},\text{f})$ and $^{236}\text{U}(\text{n},\text{f})$ cross sections relative to $^{235}\text{U}(\text{n},\text{f})$ cross section had been performed by Behrens et al. in the neutron energy 0.1 to 30 MeV. The data were presented at the Conference on Nuclear Cross Sections and Technology held at Washington D.C., March, 1975. Future plans of this ratio measurement are for the fission cross sections of ^{238}Pu , ^{240}Pu , ^{241}Pu , ^{242}Pu and ^{244}Pu . This technique is supposedly dependent only on an atomic ratio between the isotope of interest and ^{235}U . At LLL, they have future plans for measurements of the fission cross

section of ^{242}Am , ^{243}Cm , ^{245}Cm , ^{247}Cm and ^{249}Cf , in the energy range from 0.01 eV to 14 MeV. They have a plan for measurement of $\bar{\nu}$ as a function of incident neutron energy from 0.01 eV to 14 MeV.

Nishi et al.¹²⁾ contributed their recent measurement of (n,2n) cross section for ^{237}Np at 9.6 and 14.2 MeV. They obtained the cross section for a residual state with $T_{1/2} = 22.5$ h. The data are 0.34 ± 0.05 barns at 9.6 MeV and 0.36 ± 0.05 barns at 14.2 MeV.

Glover and Patrick notified integral experiments^{13,14)} for the production of ^{242}Cm from ^{241}Am in ZEBRA Reactor. The production cross section of ^{244}Cm from ^{243}Am is also measured with the similar technique. These measurements must be valuable in the application field of the nuclear data.

Weston also presented his recent works¹⁵⁻¹⁷⁾ with his colleague concerning measurements¹⁵⁾ of capture cross section for ^{240}Pu , ^{241}Pu and ^{241}Am , measurements¹⁶⁾ of capture and fission cross sections of ^{239}Pu , and measurements¹⁷⁾ of fission and absorption cross sections of ^{239}Pu and ^{241}Pu . They have planned the measurements of capture cross sections for ^{242}Pu , ^{237}Np and ^{243}Am .

In the following sections, these contributions will serve as the valuable information of the present status for the experimental data. In the next section, an outline of the requested and experimental data is presented in order to see their rough correlation. In section 3, the status of the experimental data is shown with many graphs. Comparisons between the requested accuracies and the experimental errors are discussed, as well as the comparison between the different experimental data sets. In graphs showing the requested accuracies (dashed line) and the experimental errors (solid line), vertical bars or widths of bands stand for the assigned accuracies or errors in the literature. The length or width of 1 cm corresponds with 10%. Summary and conclusion of this review are given in section 4. Some problems concerning measurements and data utilization are discussed.

In this work, many data are illustrated in the graphs. Majority of these data are taken from CCDN. Some of these are probably preliminary data which should not be quoted without permission. In this review, however, we should exhibit as many data as possible. In this sense, it would be permitted to quote the preliminary data.

2. Outline of Requested and Experimental Data

In order to see the status of data requirement, contents of WRENDA 74¹⁾ were surveyed at the first stage of this review work. Schematic representation of the data requests is shown in Figs. 1 (a) through 1 (e). Circles in upper part of each block mean the strength of the requests. It is seen in these figures that the cross sections of fission and capture are required eagerly. Number of neutrons per fission and the total cross section for heavier isotopes are also requested.

According to a correspondence from Dierckx, reviewer of A8, the following quantities are needed for destructive fuel analysis and for dosimetry work (neutron spectra measurements). They are (1) capture cross section of ^{242m}Am , absorption cross section of ^{236}Pu , ^{238}Pu , ^{244}Cm , and (n,2n) reaction cross section of ^{238}U , (2) absorption cross section of ^{241}Am , ^{242}Am , capture or absorption cross sections of ^{234}U , ^{236}U , ^{237}Np , ^{240}Pu , ^{241}Pu , ^{242}Pu , ^{243}Am , cross sections of ^{241}Am (n, γ) ^{242m}Am , and ^{241m}Am (n, γ) ^{242}Am reactions. Required accuracy is 10% for the quantities in (1) and 20% for the quantities in (2). Most quantities in (1) and (2) are already entered in the request lists of WRENDA 74¹⁾, except for the absorption cross section of ^{236}Pu .







In the lower part of each block in Fig. 1, triangles show degrees of the experimental performance for nuclear data measurements. Hence, from these figures, a rough correlation between the needed data and the experimental ones can be found. It seems apparent that the data for ^{236}U , ^{237}Np and ^{240}Pu are so accumulated that the requests may be satisfied. However, there is a variety of contents for accuracies and reasons behind

the requests. Hence, in general, it is difficult or impossible to determine whether the experimental data satisfy the requests or not. In this work, any serious comparison between the experimental and requested data will not be performed. For comparison of their accuracies, some figures will be shown in section 3.

Some data for the other nuclides are available. For example, some data of Th isotopes have been measured. However, these data have not been requested in WRENDA 74, except for ^{232}Th . This is the reason why no isotopes of Th are shown in Fig. 1. These data will be also reviewed in the next section.

There are some requests for the data of Es and Fm in WRENDA 74, but no experimental data have been found in this survey. Hence, it may be considered that the available experiments in the fast region are limited for the nuclides from Th to Cf, at this moment.

Captions on Figures 1(a) through 1(e).

Comparison between requests listed in WRENDA 74 and status of the experimental data. Symbols ,  and  mean the number of requests, 1 or 2, 3 or 4, and more than 4, respectively. Symbols ,  and  mean the number of experiments, 1 or 2, 3 or 4, and more than 4, respectively. Left-half of each block shows the energy region from 1 keV to 1 MeV, and right-half shows above 1 MeV.

Nuclides shown here are required their data in WRENDA 74, but the nuclides whose data are obtained experimentally but not requested are excluded from these figures.

	σ_{tot}	$\sigma_{n,r}$	$\sigma_{n,n'}$	$\sigma_{n,f}$	$\sigma_{n,2n}$	$\sigma_{n,3n}$	$\bar{\nu}$ or ν_p	$\sigma_{n,p}$	$\sigma_{\text{el.}}$	Miscell
^{231}Pa		○ ○		△ △						△
^{232}U	△	○ ○		○ ○ △ △					△	△
^{234}U	△	⊙ ⊙		○ △ △	○	○	○ ○	△		
^{236}U	△	⊙ ⊙ △ △	○	○ ⊙ △ △			○ ⊙ △ △		△	△
^{237}U		○ ○		○ ○ △ △						
^{239}U	△	○ ○		○ ○						
^{237}Np	△	○ ○ △ △		⊙ ⊙ △ △	⊙ △			△		

Fig. 1 (a)

	$\bar{\sigma}_{\text{tot}}$	$\bar{\sigma}_{n,r}$	$\bar{\sigma}_{n,n'}$	$\bar{\sigma}_{n,f}$	$\bar{\sigma}_{n,2n}$	$\bar{\sigma}_{n,3n}$	$\bar{\nu}$ or ν_p	$\bar{\sigma}_{n,p}$	$\bar{\sigma}_{\text{el.}}$	Miscell
^{239}Np		○ ○								
^{236}Pu				○ ○						
^{237}Pu		○ ○		○ ○						
^{238}Pu		⊙ ⊙		○ ⊙	○		○ ○			
^{240}Pu	○ ○ △ △	⊙ ○ △	○ ⊙ △ △	⊙ ⊙ △ △			○ ⊙ △ △		△ △	○ △
^{241}Pu	○ ○ △	⊙ ○		⊙ ⊙ △ △			○ ○ △ △			⊙ ○ △
^{242}Pu		⊙ ⊙ △		○ ○ △ △			⊙ ⊙	○		△ △ △

Fig. 1 (b)

	$\bar{\sigma}_{\text{tot}}$	$\bar{\sigma}_{n,\gamma}$	$\bar{\sigma}_{n,n'}$	$\bar{\sigma}_{n,f}$	$\bar{\sigma}_{n,2n}$	$\bar{\sigma}_{n,3n}$	$\bar{\nu}$ or ν_p	$\bar{\sigma}_{n,p}$	$\bar{\sigma}_{\text{el.}}$	Miscell.
^{241}Am		⊙ ⊙ △		⊙ ⊙ △ △			⊙ ○			
^{242}Am	○	⊙ ○		○ ○ △ △			○ ○			
^{243}Am	○	○ ○		○ ○ △ △			○ ○			
^{242}Cm		⊙ ○		⊙ ○ △			⊙ ○			
^{243}Cm	○	○		○ △ △						
^{244}Cm		○ ○		○ ○ △ △			○ ○			△
^{245}Cm	○	○		○ △ △						

Fig.1 (c)

	$\bar{\sigma}_{\text{tot}}$	$\bar{\sigma}_{n,r}$	$\bar{\sigma}_{n,r'}$	$\bar{\sigma}_{n,f}$	$\bar{\sigma}_{n,2n}$	$\bar{\sigma}_{n,3n}$	$\bar{\nu}$ or ν_p	$\bar{\sigma}_{n,p}$	$\bar{\sigma}_{\text{el.}}$	Miscell.
^{246}Cm	○	○		○ △ △						
^{247}Cm	○	○		○ △ △						
^{248}Cm	○	○		○ △ △						
^{249}Bk	○	○		△ △						
^{249}Cf				○ △ △						
^{250}Cf	○	○		○						
^{251}Cf		○								

Fig.1 (d)

	σ_{tot}	$\sigma_{n,r}$	$\sigma_{n,n'}$	$\sigma_{n,f}$	$\sigma_{n,2n}$	$\sigma_{n,3n}$	$\bar{\nu}$ or ν_p	$\sigma_{n,p}$	$\sigma_{\text{el.}}$	Miscell.
^{252}Cf		○		○ △ △						
^{253}Cf		○								
^{253}Es				○						
^{254}Es		○		○						
^{255}Fm				○						
^{257}Fm				○						

Fig. 1 (e)

3. Survey of Experimental Data

In this section, status of the experimental data are surveyed on the basis of some selected literature . The selected literature are mainly those issued after 1960. Short notes are presented for the literature concerning the data and experiments. In the note, form of the compiled data is shown in three letters E, T, and G which stand for EXFOR, Table and Graph, respectively. The note is not necessarily unified on the contents.

3.1 Thorium

There are no requests in WRENDATA 74 for the data of this element, except for ^{232}Th . However, the fission cross sections of ^{228}Th , ^{229}Th and ^{230}Th have been measured, in order to investigate a structure near the threshold of the fission. This structure of the cross section was observed by 59 Gokhberg, 67 Vorotnikov, 71 Yuen and 72 James, in particular, for ^{230}Th with the energy resolutions of about 20 keV, 30 keV, 5 keV and 2-5 keV, respectively. The data obtained by these measurements are shown in Fig. 3.1 (a), in which the data are mainly transcribed from the graphs.

There is a large systematic difference between the former two measurements and the latter two. This may be due to the different data sets used for the normalization. A measurement with the nuclear explosion (71 Muir) obtained the data which support the latter two measurements (Fig. 3.1 (b)). The data by 71 Muir were obtained by using Davey's evaluated $^{239}\text{Pu}(n,f)$ cross section¹⁹⁾.

The measurements of the fission cross section have been carried out up to 3 MeV, at most, except for an experiment at 14.6 MeV by 60 Kazarinova.

$^{228}\text{Th}(n,f)$

Ref.	Energy Range	Data
72 Vorotnikov	160 keV - 5 MeV	E. G. T.
	Electrostatic accelerator. $^7\text{Li}(p,n)$, $^3\text{H}(p,n)$, $^2\text{H}(d,n)$ sources. Fission fragment glass detectors. Energy resolution about 50 keV.	

 $^{229}\text{Th}(n,f)$

59 Gokhberg	6 keV - 1.2 MeV	E. G.
	$^3\text{H}(p,n)$ source. VdG. Plane-parallel ionization chamber. Neutron monitored by long counters.	

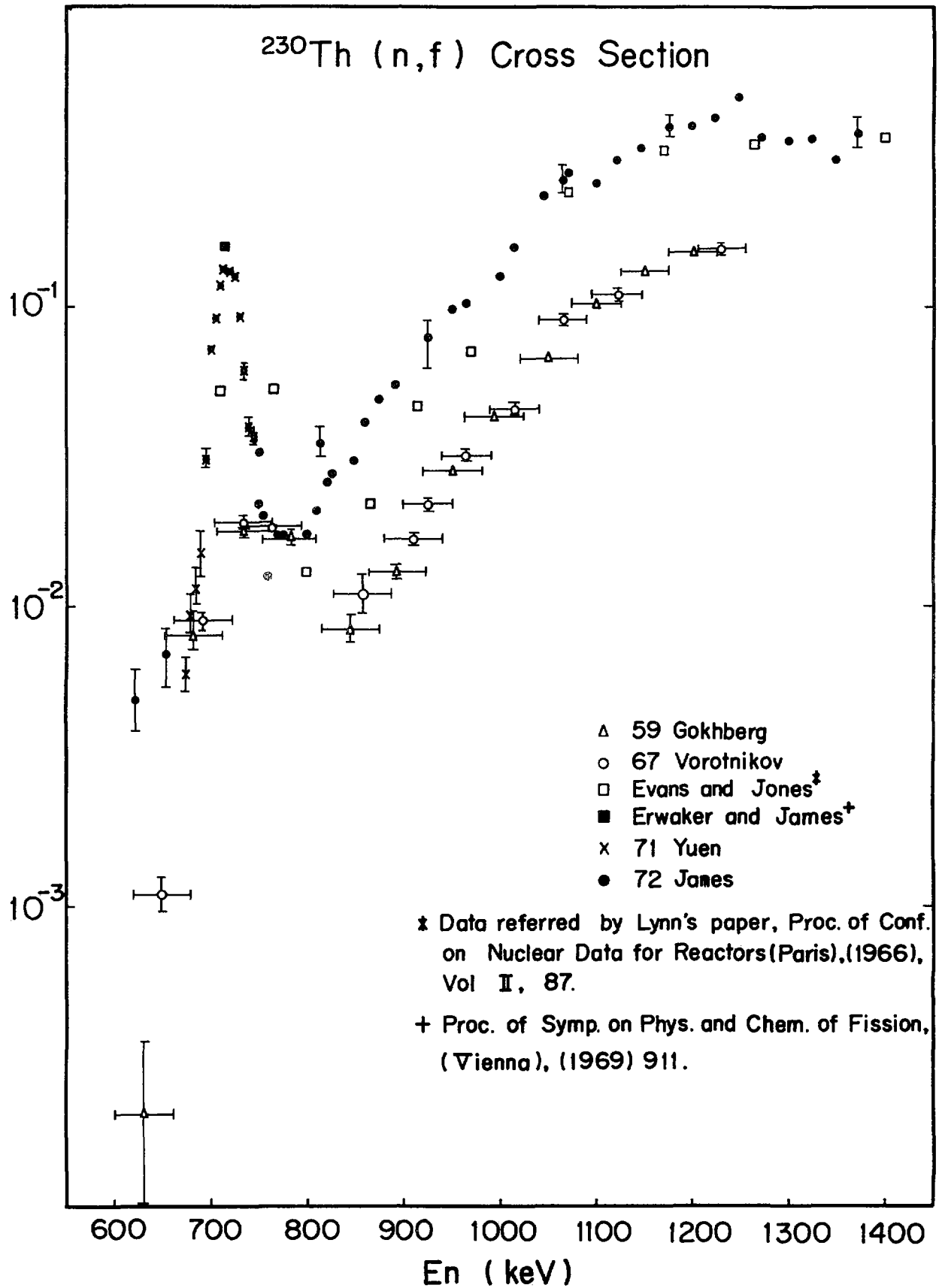
 $^{230}\text{Th}(n,f)$

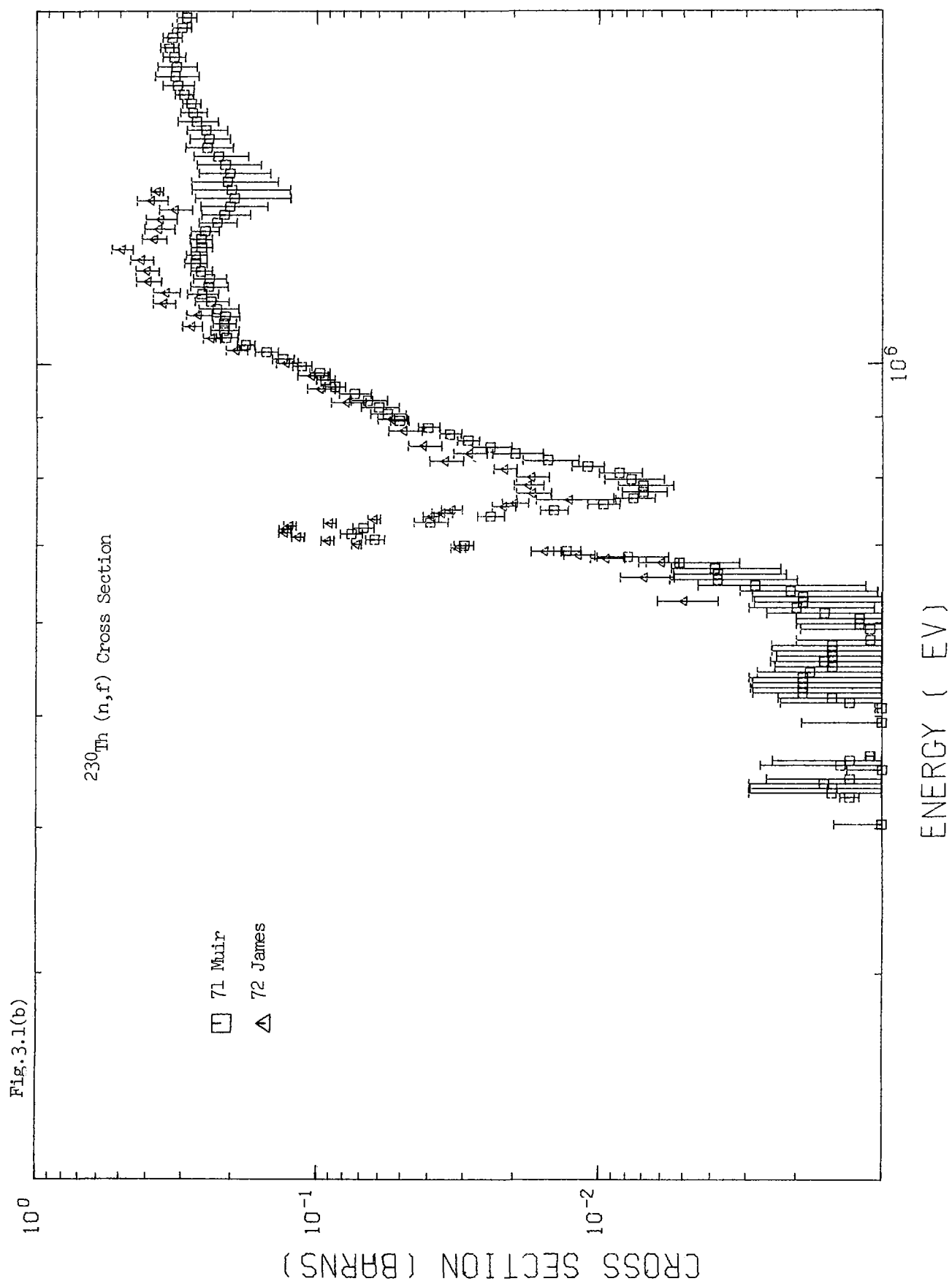
59 Gokhberg	670 keV - 1.2 MeV	E. G.
	$^3\text{H}(p,n)$ source. VdG. Plane-parallel ionization chamber. Neutron monitored with long counters. Energy resolution about 20 keV. Angular anisotropic fission cross sections also measured.	
60 Kazarinova	2.5 MeV and 14.6 MeV	E.
	Double fission chamber. Neutron monitored with long counters. Absolute measurement at 14.6 MeV.	
64 Lamphere	620 keV - 3 MeV	G.
	$^7\text{Li}(p,n)$, $^3\text{H}(p,n)$ sources. Back-to-back fission counters. Relative to $^{235}\text{U}(n,f)$ data of BNL-325. Angular anisotropy also measured.	

$^{230}\text{Th}(\text{n},\text{f})$

Ref.	Energy Range	Data
67 Vorotnikov	690 keV - 1.2 MeV	G.
	Electrostatic accelerator. $^3\text{H}(\text{p},\text{n})$ source. Glass detectors. Neutron monitored with long counters. Energy resolution about 30 keV. Fragment angular distributions also measured.	
70 James	675 keV - 850 keV	G.
	IBIS VdG. $^7\text{Li}(\text{p},\text{n})$ source. Fragment angular distribution determined by polycarbonate foil technique.	
71 Muir	100 keV - 3 MeV	E. G.
	Measurements with neutron beam of 0.6 ns/m resolution from nuclear explosion. Relative to Davey's $^{239}\text{Pu}(\text{n},\text{f})$ evaluated data. Fission fragment detectors at 100° and 165° .	
71 Yuen	682 keV - 1 MeV	T. G.
	$^7\text{Li}(\text{n},\text{p})$ ^7Be neutron source. ANL Dynamitron used. Polycarbonate resin detector for detection of fission fragments.	
72 James	625 keV - 1.4 MeV	E. G. T.
	$^7\text{Li}(\text{p},\text{n})$ source. IBIS VdG. Fission fragments detected by Si-Au surface-barrier detector. BF_3 counters for neutron monitoring. Fragment angular distribution determined by polycarbonate foil technique.	

Fig.3.1(a)





References for Review on Th Data

59 Gokhberg

Gokhberg, B.M., Otroshchenko, G.A., Shigin, V.A.,
AEC-tr-6398 (1959) 59,
Proc. of Conf. on Peaceful Uses of Atomic Energy (Tashkent),
(1959)

60 Kazarinova

Kazarinova, M.I., Zamyatnin, Yu.S., Gorbachev, V.M.,
Sov. Atom. Energy 8 (1960) 125
Atom. Energ. 8 (1960) 139

64 Lamphere

Lamphere, R.W.,
ORNL-3582 (1964)
ORNL-P-1082 (1964)

67 Vorotnikov

Vorotnikov, P.E., Dubrovina, S.M., Otroshchenko, G.A.,
Shigin, V.A.,
Sov. J. Nucl. Phys. 5 (1967) 207
Yad. Fiz. 5 (1967) 295

70 James

James, G.D.,
Proc. of Conf. on Nuclear Data for Reactors (Helsinki) I
(1970) 267

71 Muir

Muir, D.W., Veaser, L.R.,
Proc. of 3rd Conf. on Neutron Cross Sections and Technology
(Knoxville) (1971) 292

71 Yuen

Yuen, G., Rizzo, G.T., Behkami, A.N., Huizenga, J.R.,
Nucl. Phys. A171 (1971) 614

72 James

James, G.D., Lynn, J.E., Earwaker, L.G.,
Nucl. Phys. A189 (1972) 225
AERE-R 6901 (1971)

72 Vorotnikov

Vorotnikov, P.E., Gladkikh, Z.S., Davydov, A.V., Dubrovina, S.M., Otroshchenko, G.A., Pal'sin, E.S., Shigin, V.A., Shubko, V.M.,

Sov. J. Nucl. Phys. 16 (1973) 505

Yad. Fiz. 16 (1972) 916

Yad. Fiz. Letters 14 (1972) 6

3.2 Protactinium

The neutron capture cross section of ^{231}Pa from thermal to 10 MeV is requested with 10% accuracy. This is only one request above 1 keV in WRENDA 74. However, no data can be found in this survey.

There are some experiments dealing with the fission cross section of ^{231}Pa , delayed neutron yield of ^{231}Pa and fission cross section of ^{233}Pa . The last one obtained an averaged value with the fission neutron spectrum (67 von Gunter). The average value of 775 ± 190 mb was obtained based on a fission cross section of 142 mb for ^{232}Th .

The fission cross section of ^{231}Pa is reported by 71 Muir and 70 Vorotnikov which may be the same experiment as 64 Dubrovina. The data of 64 Dubrovina are entered in the data library of the four centers. The cross section curve shown in Fig. 3.2 reveals a nonmonotonic dependence on energy near the threshold. Three peaks were observed at the energies 320, 550 and 870 keV. These peaks were reobserved by 71 Muir which used a nuclear explosion technique. In this experiment, a new subthreshold fission resonance was detected at 158 ± 3 keV, of which maximum value is 100 ± 25 mb and the width is 4 ± 1 keV. This resonance coincides almost with a dip at 0° in the fragment angular distribution observed by 70 Vorotnikov. This fact confirms the assumption of a small number of channels in the fission reaction in this energy region, as discussed by 70 Vorotnikov.

The fission cross section of ^{231}Pa at 14 MeV was obtained by 72 Iyer. The value was estimated as 1.33 b. There are a few experiments for total cross section measurements below a few keV. These were performed for obtaining the resonance parameters.

$^{231}\text{Pa}(\text{n},\text{f})$

Ref.	Energy Range	Data
44 Williams	0.43 MeV - 3 MeV	E. G.
	Normalized to $^{235}\text{U}(\text{n},\text{f})$ data. Graph in BNL-325, 2nd ed. Suppl. No. 2.	
64 Dubrovina	0.15 MeV - 1.7 MeV	E.
	Peaks near 330, 550 and 880 keV.	
70 Vorotnikov	0.14 MeV - 1.3 MeV	G.
	Measurements for fragment angular distributions. Glass plate detector. Favourable results for the assumption of a small number of channels.	
71 Muir	0.1 MeV - 3.0 MeV	E. G.
	Measurements with neutron beam of 0.6 ns/m resolution from nuclear detonation. Relative to Davey's $^{239}\text{Pu}(\text{n},\text{f})$ evaluated data. Structure of the cross section near threshold is studied.	
72 Iyer	14 MeV	
	Fission track technique. Relative to $^{235}\text{U}(\text{n},\text{f})$ data.	

$^{231}\text{Pa}(\text{delayed neutrons})$

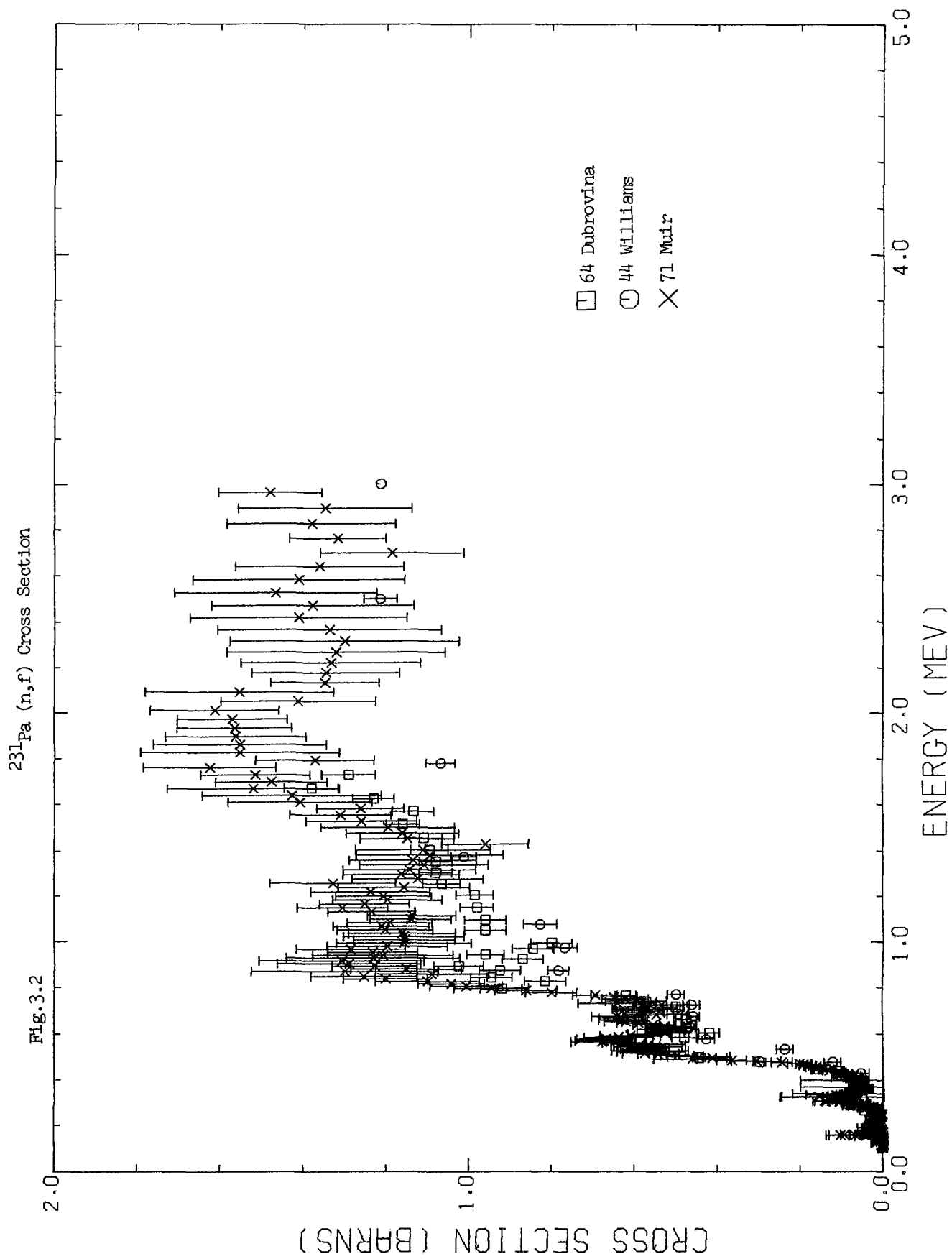
70 Chrysochoides	fission neutrons	T.
	Measurements are performed for the first three groups. Four BF_3 counters are used. Average values for yields are shown in table.	

$^{231}\text{Pa}(\text{delayed neutrons})$

Ref.	Energy Range	Data
71 Brown	14.8 MeV	T.
Effect of incident neutron energy on group delayed neutron yields. BF_3 counters used for delayed neutron counting. Yields per 100 fissions are presented in tables. Errors estimated to be about 25%.		

$^{233}\text{Pa}(\text{n,f})$

67 von Gunter	fission neutrons	E. T.
Back-to-back fission counter with ^{232}Th . Heavy-water reactor DIORIT spectrum used. Average cross section is given, relative to $^{232}\text{Th}(\text{n,f})$.		



References for Review on Pa Data

44 Williams

Williams, J.H.,
LA-150 (1944)

64 Dubrovina

Dubrovina, S.M., Shigin, V.A.,
INDSWG-64E (1964) 23
Sov. Phys. - Doklady 9 (1964) 579

67 von Gunter

von Gunter H.R., Buchana, R.F., Wyttenbach, A., Behringer, K.,
Nucl. Sci. Eng. 27 (1967) 85

70 Chrysochoides

Chrysochoides, N.G., Perricos, D.C., Zikides, C.C.,
J. Nucl. Energy 24 (1970) 157

70 Vorotnikov

Vorotnikov, P.E., Dubrovina, S.M., Otroshchenko, G.A., Shigin,
V.A.,
Sov. J. Nucl. Phys. 10 (1970) 280

71 Brown

Brown, M.G., Lyle, S.J., Martin, E.B.M.,
Rad. Chi. Acta 15 (1971) 109

71 Muir

Muir, D.W., Veaser, L.R.,
3rd Conf. on Neutron Cross Sections and Technology, Univ.
of Tennessee, Knoxville, (1971) 292

72 Iyer

Iyer, R.H., Sagu, M.L., Sampathkumer, R.,
BARC 628 (1972) 94

3.3 Uranium

There are many requests for the quantities of U-isotopes, even if the three big nuclides, ^{233}U , ^{235}U and ^{238}U were deleted. As Fig. 1 shows, the requested data for U-isotopes are the capture and fission cross sections of ^{232}U , ^{234}U , ^{236}U , ^{237}U and ^{239}U , inelastic scattering cross section of ^{236}U , (n,2n) and (n,3n) cross sections of ^{234}U , $\bar{\nu}_p$ and $\bar{\nu}$ of ^{234}U and ^{236}U . Measurements have been performed on these isotopes. Hence, these five nuclides are examined here.

3.3.1 Uranium-232

The fission cross sections were measured by 70 Farrell and 71 Vorotnikov. These data are shown in Fig. 3.3.1 (a). The former reported mainly the resonance cross sections measured with the nuclear explosion. Estimated errors seem rather large in this experiment.

The measurements of the fission cross section and fragment angular distributions were reported by 71 Vorotnikov. The absolute values of the fission cross section at 1 MeV were obtained by determination of the number of ^{232}U atoms, (1) with counting α -particles from the decay of ^{232}U and (2) with comparison between the number of fissions in ^{232}U layer and in a layer of natural uranium. Obtained cross section was 2.2 ± 0.3 b. This process may decrease the systematic error.

The requested accuracy and the experimental errors estimated from the above mentioned measurements are shown in Fig. 3.3.1 (b), in which the energy range and accuracy of the requested data are shown in dashed line, and those of the experimental data are in solid line. The vertical line shows the error of per cent, 1 mm stands for 1%.

For the capture cross section, 58 Miskel is only the experiment. The information about the data is not published yet.

3.3.2 Uranium-234

Precise measurement of the fission cross section was performed by 62 Lamphere with $^{235}\text{U}(n,f)$ cross section as a standard. The data of this measurement were examined by Davey^{18,19)} in his evaluation, as well

as the data of 62 Babcock, 65 Perkin, 65 White and 67 White. These data are shown in Fig. 3.3.2 (a), except for the data by 65 Perkin.

After this evaluation, a few experiments were found in the literatures. Though 72 James is a progress report, the measured cross section relative to ^{235}U (n,f) seems to show a different feature from Davey's evaluation above 1.5 MeV. This may be a problem below 4 MeV.

The requested accuracies are rather large, 15-20%, but no data exist in 6-14 MeV region. Hence, the present status of the experimental data is not necessarily satisfy the requests (see Fig. 3.3.2 (b)). As mentioned in Introduction of this report, Browne¹¹⁾ reported that the cross section of ^{234}U (n,f) had been obtained with about 5% from 0.1 to 30 MeV by Behrens et al. at LLL. This experiment may be expected to fill the requests.

A measurement of $\bar{\nu}_p$ was performed by 65 Mather, relative to $\bar{\nu}$ of ^{252}Cf . This is only one experiment (see Fig. 3.3.2 (c)) and was adopted by Davey²⁰⁾ in his evaluation. However, more experiments are wanted in order to fulfill the request. Concerning the capture cross section, no data could be found.

3.3.3 Uranium-236

Davey^{18,19)} examined the fission cross sections by 50 Nyer, 56 Lamphere, 57 Henkel, 65 Perkin, 65 White and 67 White. Most data of these experiments were measured relative to the data of ^{235}U (n,f) cross section. After the Davey's evaluation, the measurements were performed by 68 Stein, 70 Cramer-1 and 72 Rösler.

68 Stein measured the fission cross section ratio, relative to ^{235}U (n,f) cross section, with pulsed monoenergetic neutrons. TOF background discrimination technique was used in order to subtract precisely the background pulses. The errors of the ratio are estimated about 2.2%. The ratio of the cross sections is 5% lower than that by 56 Lamphere.

The nuclear explosion technique was used by 70 Cramer-1. Correction of errors seems to be poor (see Figs. 3.3.3 (a) and (b)). High resolution cross section measurement was performed by 72 Rösler, with 7 keV resolution,

in the energy range 0.5 to 2.6 MeV. Two sets of the cross sections were given by using two kinds of neutron flux monitors. Peaks in the cross section curves at 0.75, 0.95, 1.15 and 1.4 MeV may correspond to the members of collective vibrational levels.

The data by 68 Stein and 72 Rösler were obtained by the precision experiment, but the data are requested from very low energy to 15 MeV (see Figs. 3.3.3 (c) and (d)). Moreover, the values of the cross section ratio adopted by Davey¹⁹⁾ seem to be about 6% higher than those by 68 Stein. Hence, more works on experiments and evaluations must be needed.

The measurements of the capture cross section were carried out by 61 Barry and 70 Carlson. In the former experiment, the cross section was obtained by the activation method. The neutron flux was determined by using the $^{235}\text{U}(n,f)$ cross section.

Main purpose of 70 Carlson was the measurement of the resonance cross sections. The averaged cross section was presented above 1 keV. The assigned errors were dependent on the energy intervals.

There are no data in the region from 20 keV to 360 keV (see Fig. 3.3.3 (e)). Hence, more experiments must be needed.

The measurement of $\bar{\nu}_p$ was made by 71 Condé. They used a value of $\bar{\nu} = 3.756$ for spontaneous fission of ^{252}Cf as a standard value. Accuracy may be 2% (see Fig. 3.3.3 (f)).

3.3.4 Uranium-237 and 239

For these nuclides with very short lives, indirect measurements proposed by 70 Cramer-2 may be efficient. For estimation of ^{237}U fission cross section, they used $^{236}\text{U}(t,pf)$ reaction in which compound nucleus was assumed to be ^{238}U . Though this method is interesting, preciseness of the data is not expected, at least for the present.

Fission cross section of ^{237}U was measured by 74 McNally with the underground nuclear explosion technique. The neutron flux was determined by $^6\text{Li}(n,\alpha)$ and $^{235}\text{U}(n,f)$ cross sections. Comparison between the data by 74 McNally and by 70 Cramer-2 showed large difference above 500 keV.

$^{232}\text{U}(\text{total})$

Ref.	Energy Range	Data
67 Simpson	0.01 eV - 10 keV	E. G.
	Material testing reactor - fast chopper. TOF. Multilevel parameters.	

 $^{232}\text{U}(\text{n},\text{f})$

70 Farrell	10 eV - 21 keV	E. T. G.
	75 eV resonance peak is normalized to 1000 b. Corrections for resolution and target impurities are not done.	

71 Vorotnikov	100 keV - 1.5 MeV	E. G.
	Glass detectors. Absolute and relative cross sections to natural U at 1 MeV. Also anisotropy of fragments are measured.	

 $^{232}\text{U}(\text{n},\gamma)$

58 Miskel	240 eV - 65 MeV	E.
	Private Communication.	

 $^{234}\text{U}(\text{total})$

69 James	1 eV - 32 keV	G.
	Linac. Li Glass Scintillator. Resonance parameters are deduced.	

$^{234}\text{U}(\text{n},\text{f})$

Ref.	Energy Range	Data
62 Babcock	13 MeV - 18 MeV	E.
	Cited in Davey's evaluation. (1962)	
62 Lamphere	50 keV - 4.054 MeV	E. T. G.
	(p,n) neutron sources. Fission chamber. Relative to $^{235}\text{U}(\text{n},\text{f})$. Numerical data in ORNL-3306. Fragment angular distribution is also measured.	
65 Perkin	24 keV	T.
	Absolute neutron flux by three methods. Ionization chamber.	
65 White	40 keV - 500 keV	T. G.
	$^7\text{Li}(\text{p},\text{n})$. Back-to-back ionization chamber. Relative to $^{235}\text{U}(\text{n},\text{f})$.	
67 White	1 MeV - 14 MeV	E. T. G.
	(p,n) and (d,n) reactions are used as neutron sources. Back-to-back ionization chamber. Relative to $^{235}\text{U}(\text{n},\text{f})$.	
68 Behkami	200 keV - 1.184 MeV	
	No measured cross sections are given. Anisotropy of fragments is measured.	
72 James	180 keV - 6 MeV	G.
	TOF. Si - Au Surface barrier detector. Cross sections are normalized to Lamphere's values near 1 MeV.	

$^{234}\text{U}(\bar{\nu}_p)$

Ref.	Energy Range	Data
65 Mather	0.99 MeV - 4.02 MeV	E. T. G.
	Pulsed neutron source. Large liquid scintillator. Relative to $\bar{\nu}$ (^{252}Cf).	

$^{234}\text{U}(n,\gamma)$

70 Elwyn	550 keV, 2.2 MeV	
	No measured cross sections are given. A half-life of short-lived fission isomer is assigned.	

$^{236}\text{U}(\text{total})$

73 Bockhobb	10 eV - 800 eV, 0.4 keV - 2.4 keV	
	Linac. Resonances. Evaluation of the data in progress.	

73 Mewissen	30 eV - 1800 eV	
	Linac.	

$^{236}\text{U}(\text{scat.})$

72 Poortmans	20 eV - 2 keV	
	Linac. ^3He -high pressure gaseous scintillator. Analysis in progress.	

$^{236}\text{U}(\text{n},\text{f})$

Ref.	Energy Range	Data
50 Nyer	14 MeV Relative to $^{238}\text{U}(\text{n},\text{f})$	
56 Lamphere	0.688 MeV - 4.00 MeV $^3\text{H}(\text{p},\text{n})$. Fission chamber. Relative to $^{235}\text{U}(\text{n},\text{f})$.	E. T. G.
57 Henkel		
65 Perkin	24 keV Absolute neutron flux by three methods. Ionization chamber.	T.
65 White	40 keV - 500 keV $^7\text{Li}(\text{p},\text{n})$. Back-to-back ionization chamber. Relative to $^{235}\text{U}(\text{n},\text{f})$.	T. G.
67 White	1 MeV - 14 MeV (p,n) and (d,n) reactions are used as neutron sources. Back-to-back ionization chamber. Relative to $^{235}\text{U}(\text{n},\text{f})$.	E. T. G.
68 Stein	1 MeV - 5 MeV One nsec pulsed neutron source. TOF background discrimination. Relative cross section to $^{235}\text{U}(\text{n},\text{f})$.	T. G.
70 Cramer-1	35 eV - 2.9 MeV Underground nuclear explosion Pommard. Mean cross sections of 55° and 90° data are given.	E. T. G.

$^{236}\text{U}(n,f)$

Ref.	Energy Range	Data
72 Rösler	500 keV - 2.6 MeV	G. ORELA, Fission chamber. Neutron flux is measured by both ^{235}U fission chamber and plastic scintillator. Cross section curves are given for the both neutron flux measurements.

 $^{236}\text{U}(\bar{\nu})$

71 Condé	770 keV - 6.7 MeV	T. G. Large liquid scintillator. Relative to 3.756 for ^{252}Cf spontaneous fission. Values of $\bar{\nu}$ for the spontaneous fission of ^{236}U and ^{238}U are also measured.
----------	-------------------	--

 $^{236}\text{U}(n,\gamma)$

61 Barry	360 keV - 3.97 MeV	E. T. G. Activation method. Neutron flux is determined by U-235 fission chamber.
70 Carlson	0.01 eV - 20 keV	G. Linac. Large liquid scintillator. Averaged cross sections at high energy and resonance parameters at low energy are given.

$^{237}\text{U}(n,f)$

Ref.	Energy Range	Data
70 Cramer-2	500 keV - 2.25 MeV	T. G. Cross sections are deduced from (t,pf) with the aid of an optical model calculation.
70 McNally	43 eV - 2 MeV	E. T. G. Preliminary report of 74 McNally.
74 McNally	43 eV - 2 MeV	G. Underground nuclear explosion, Pommard. Two solid state detectors at 55° and 90°. Numerical data are given in 70 McNally.

 ^{239}U

70 Cramer-2	500 keV - 2.25 MeV	T. G. Cross sections are deduced from (t,pf) with the aid of an optical model calculation.
-------------	--------------------	---

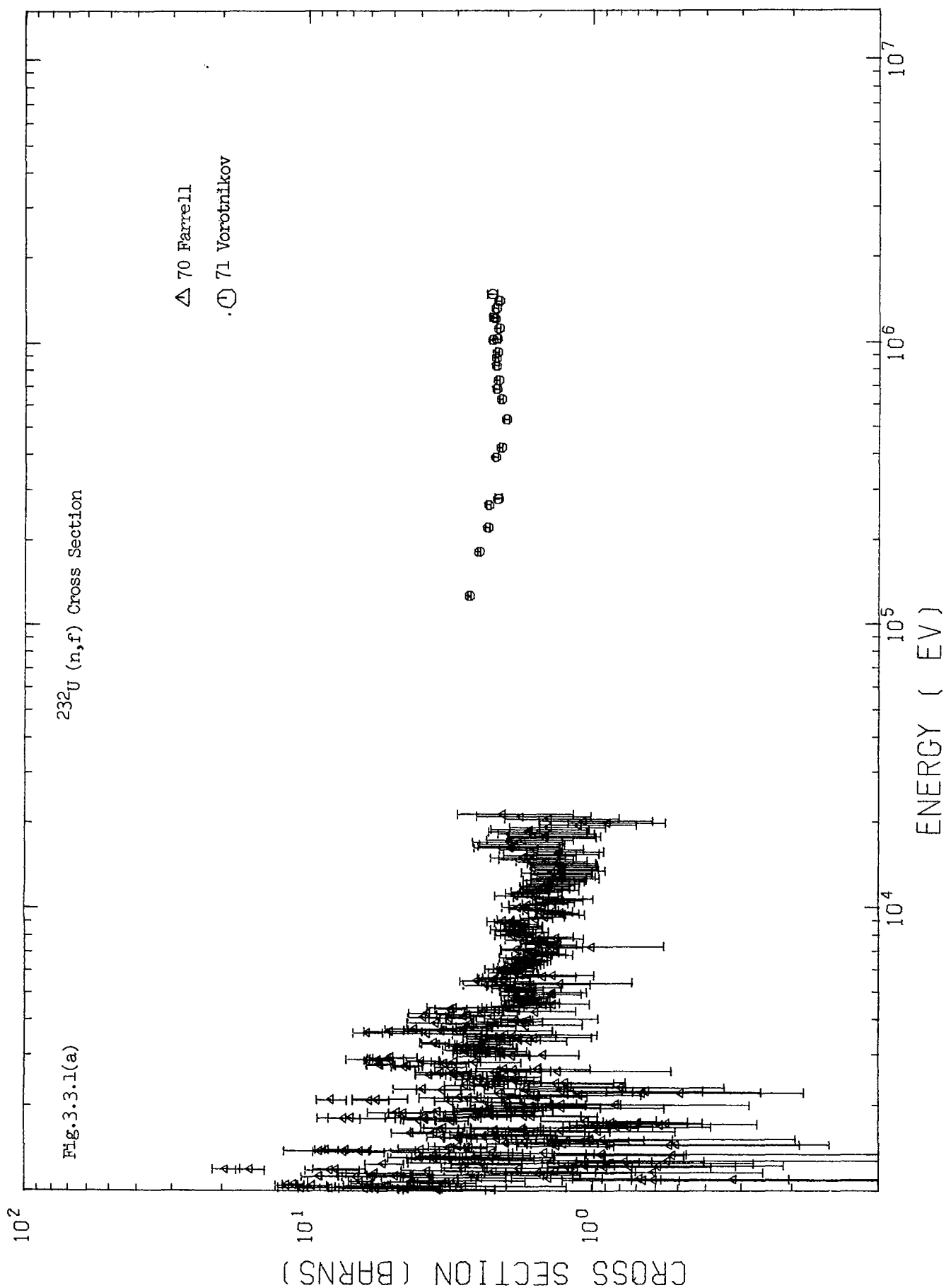
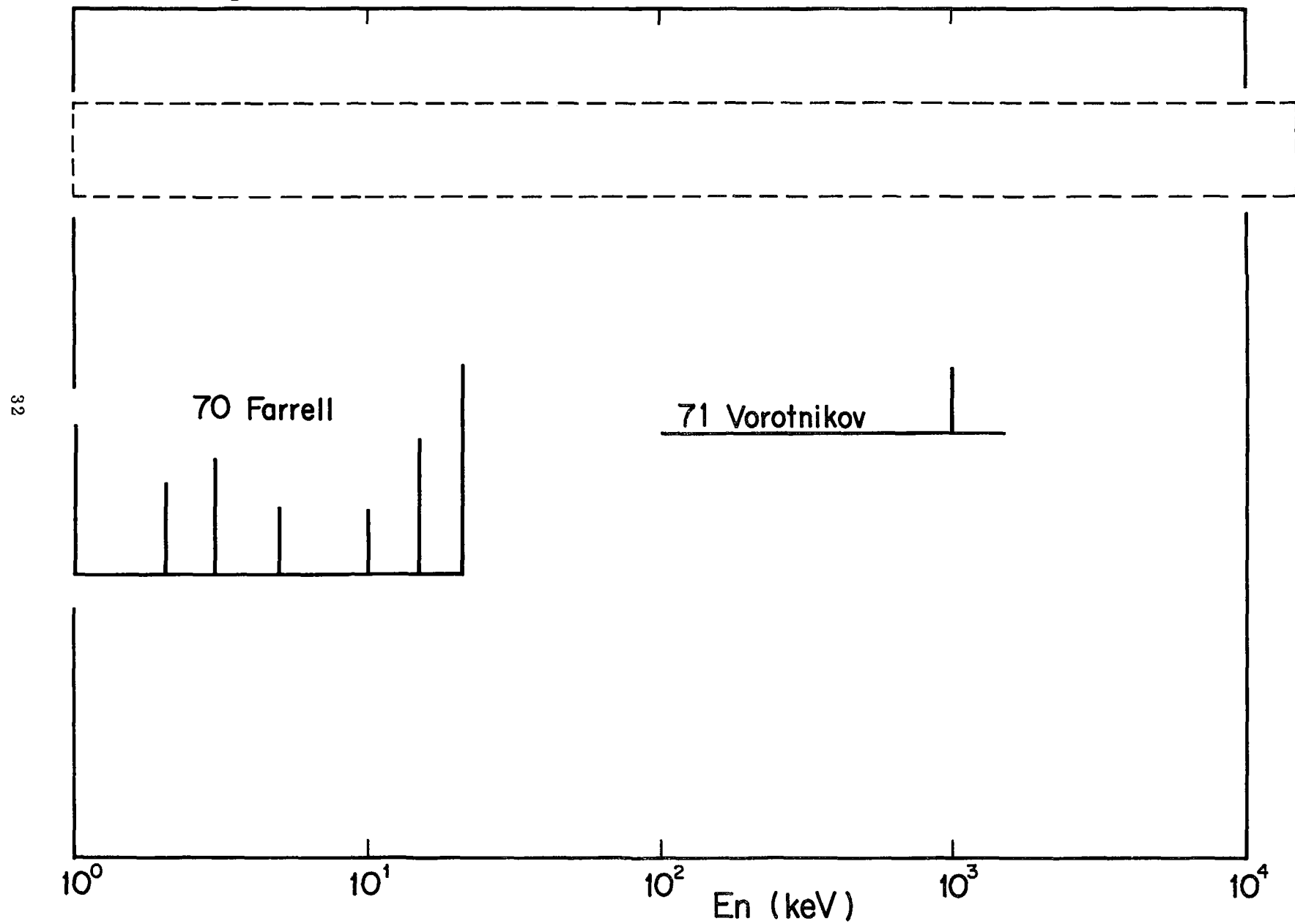


Fig.3.3.1(b)

$^{232}\text{U}(n,f)$



$^{232}\text{U}(n,\sigma)$

Fig.3.3.1(c)

58 Miskel

10^0 10^1 10^2 10^3 10^4
En (keV)

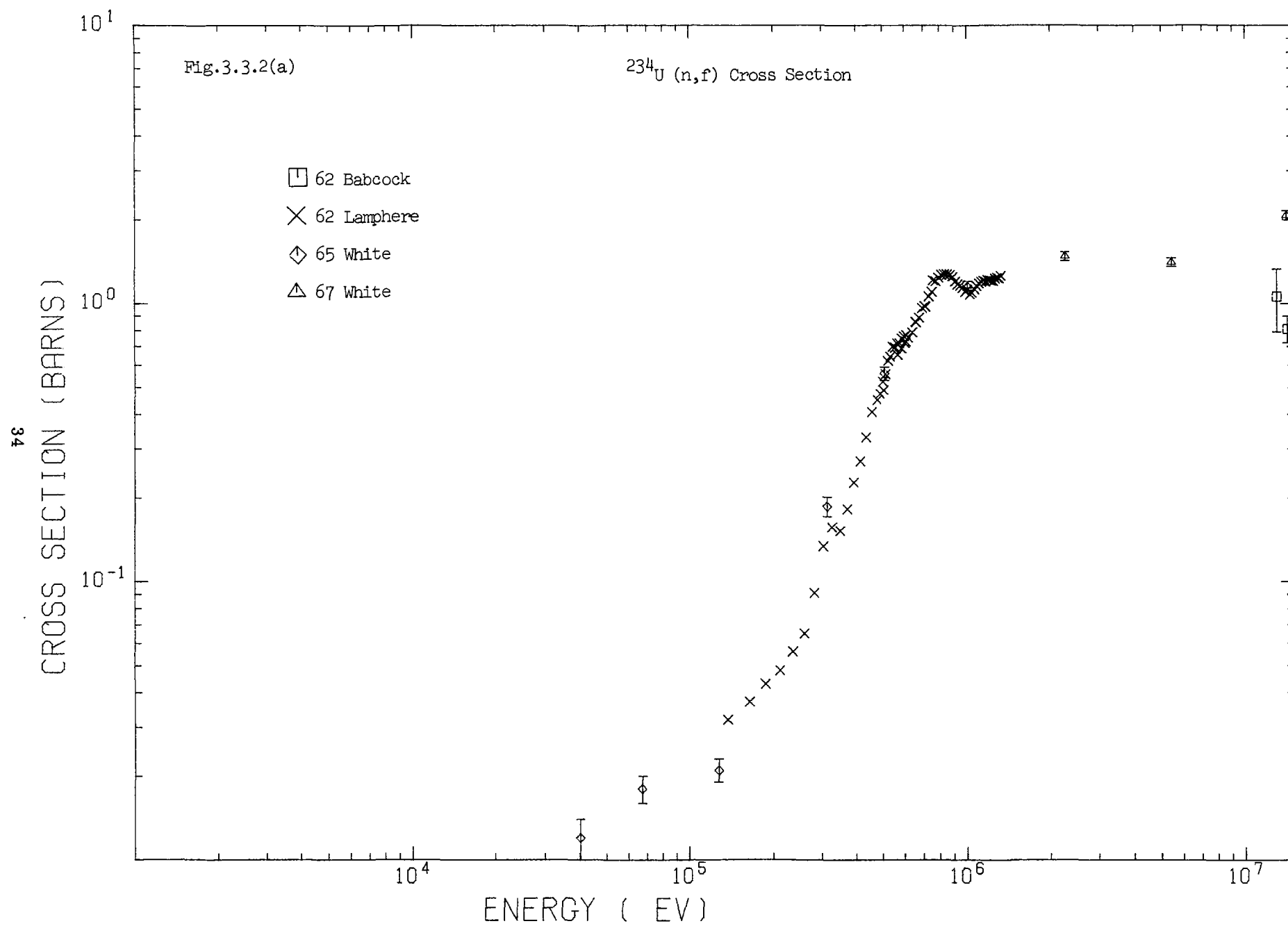


Fig.3.3.2(b)

$^{234}\text{U}(\text{n},\text{f})$

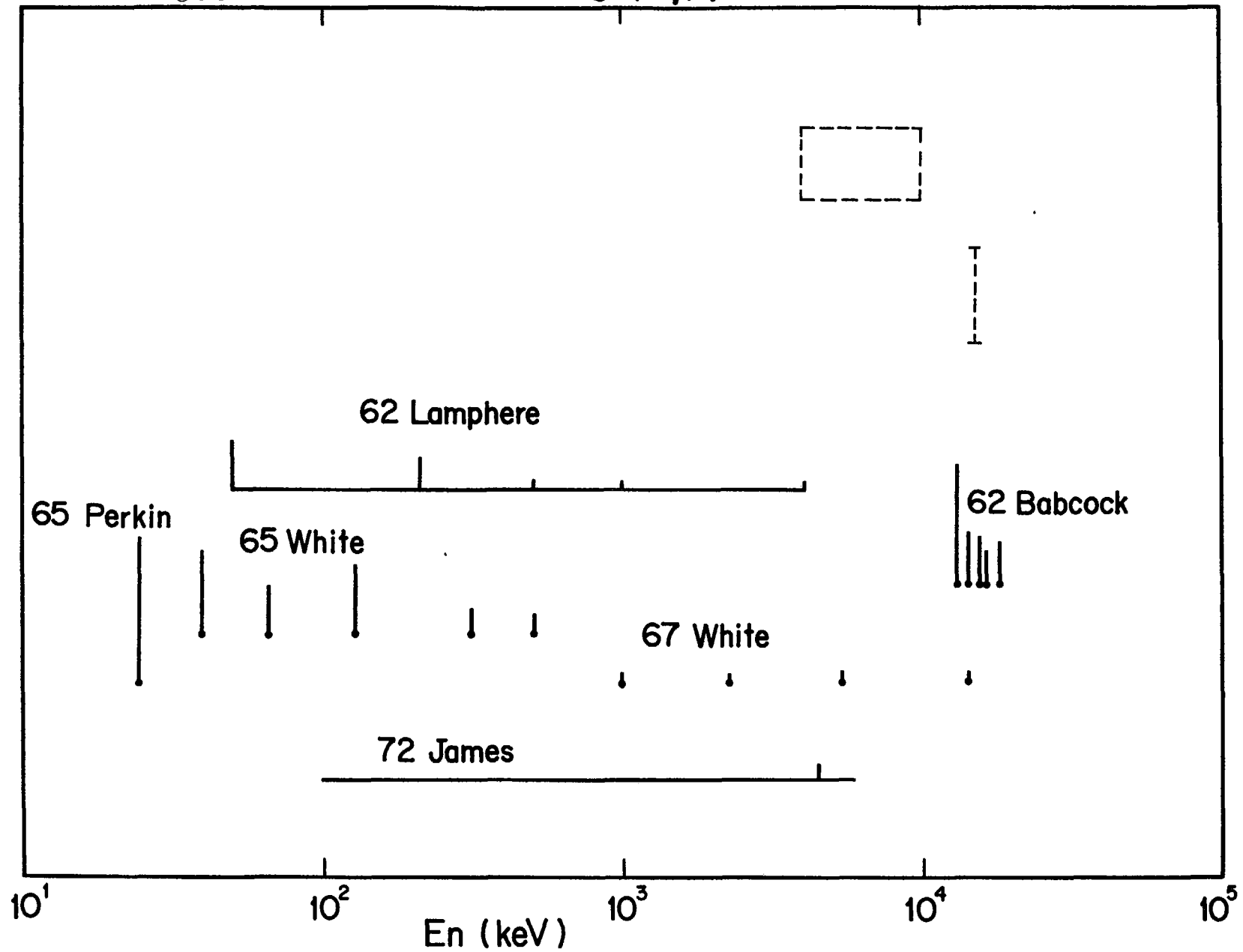
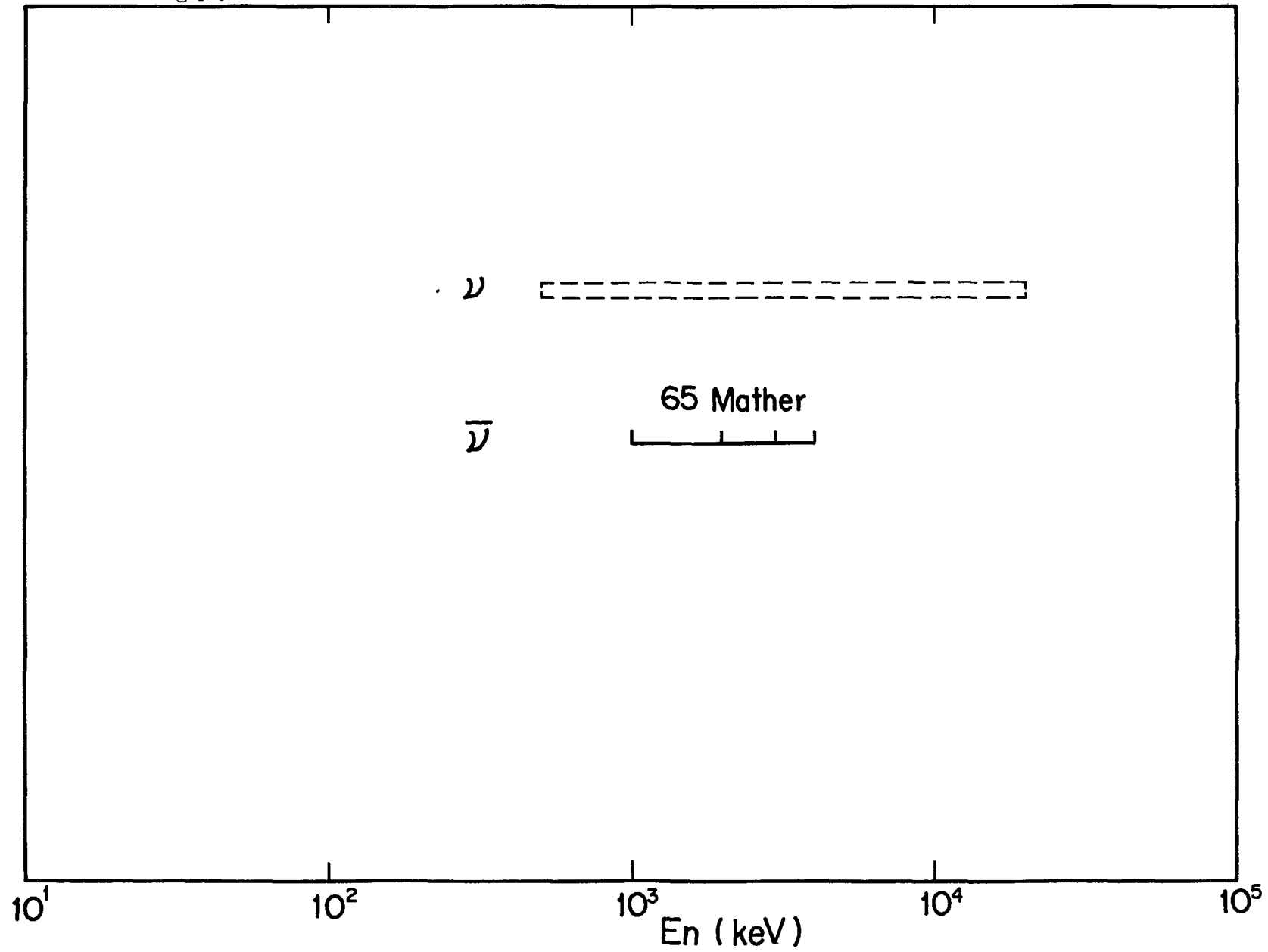
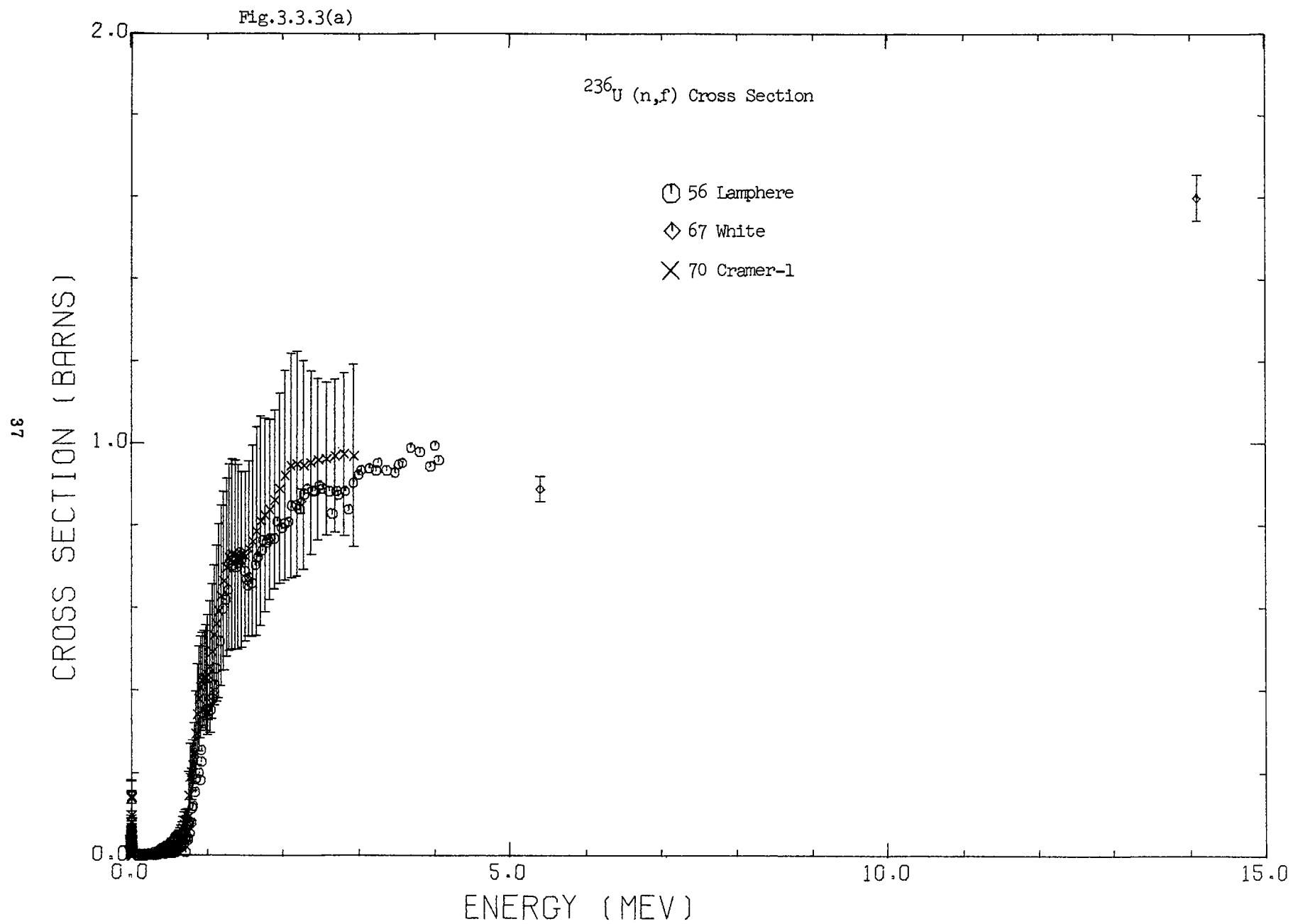


Fig.3.3.2(c)

$^{234}\text{U}(\nu)$





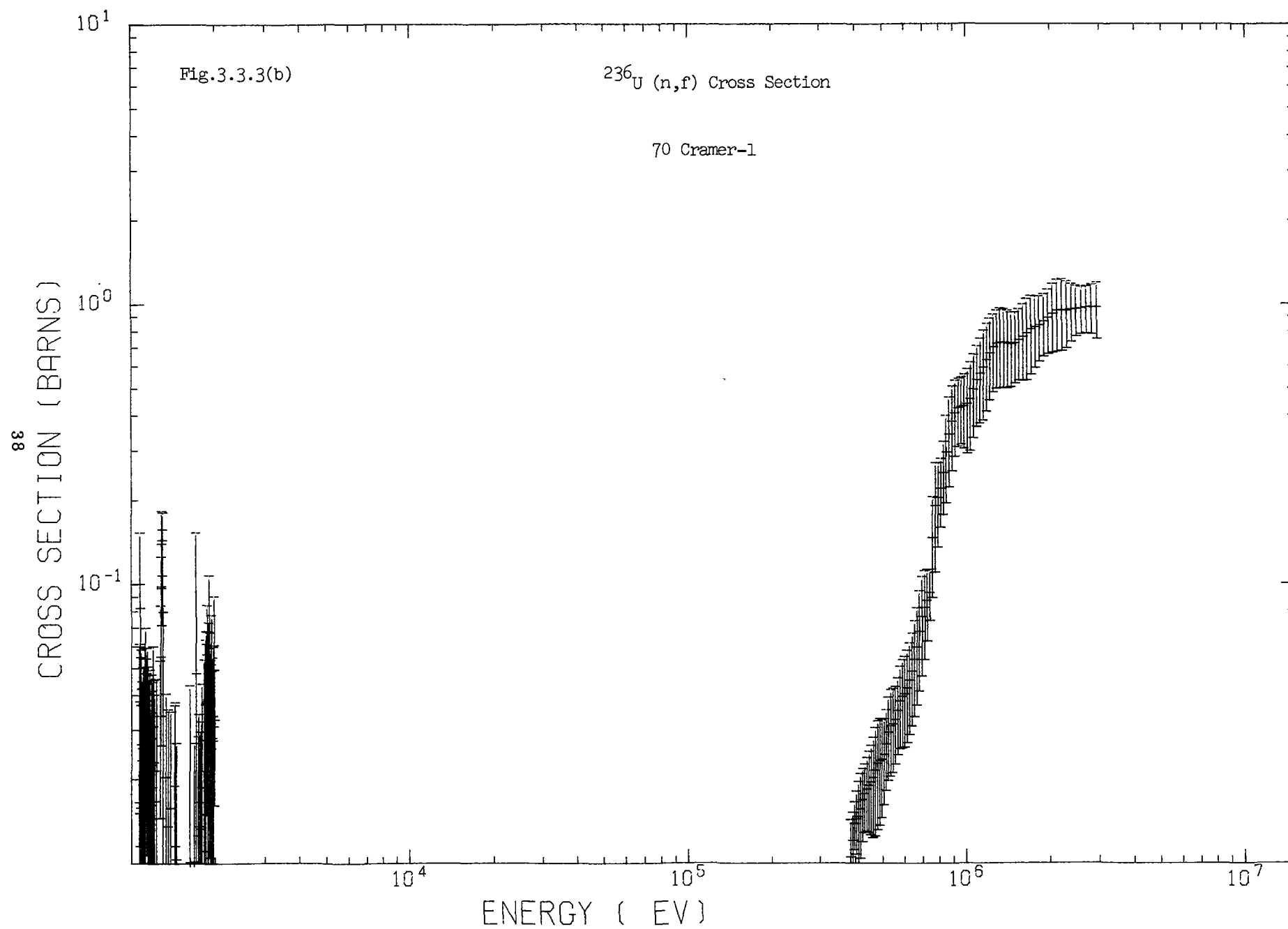


Fig.3.3.3(c)

$^{236}\text{U} (n,f)$

68

Ratio to ^{235}U fission cross section

56 Lamphere

50 Nyer

63

65 Perkin

50

65 White

39

67 White

68 Stein

10^0

10^1

10^2

10^3

10^4

En (keV)

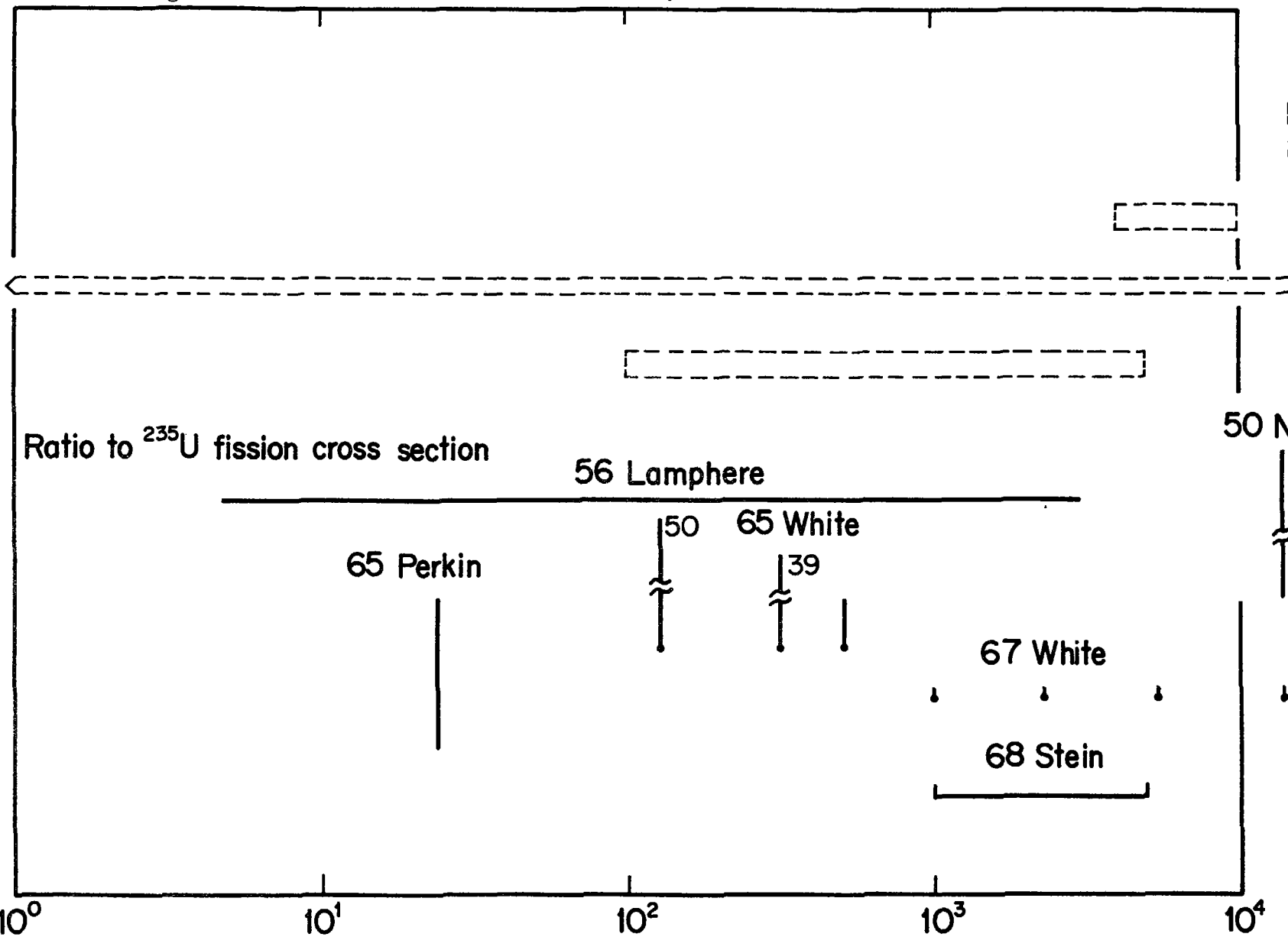
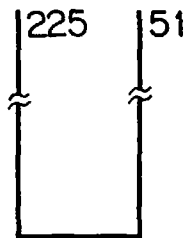


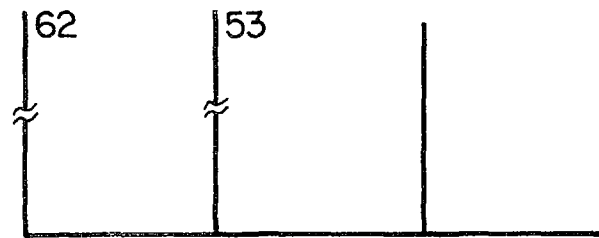
Fig.3.3.3(d)

$^{236}\text{U}(n,f)$

Absolute cross section



70 Cramer-1



72 Rösler



40

10^0

10^1

10^2

10^3

10^4

En (keV)

Fig.3.3.3(e)

$^{236}\text{U}(n,\bar{\nu})$

41

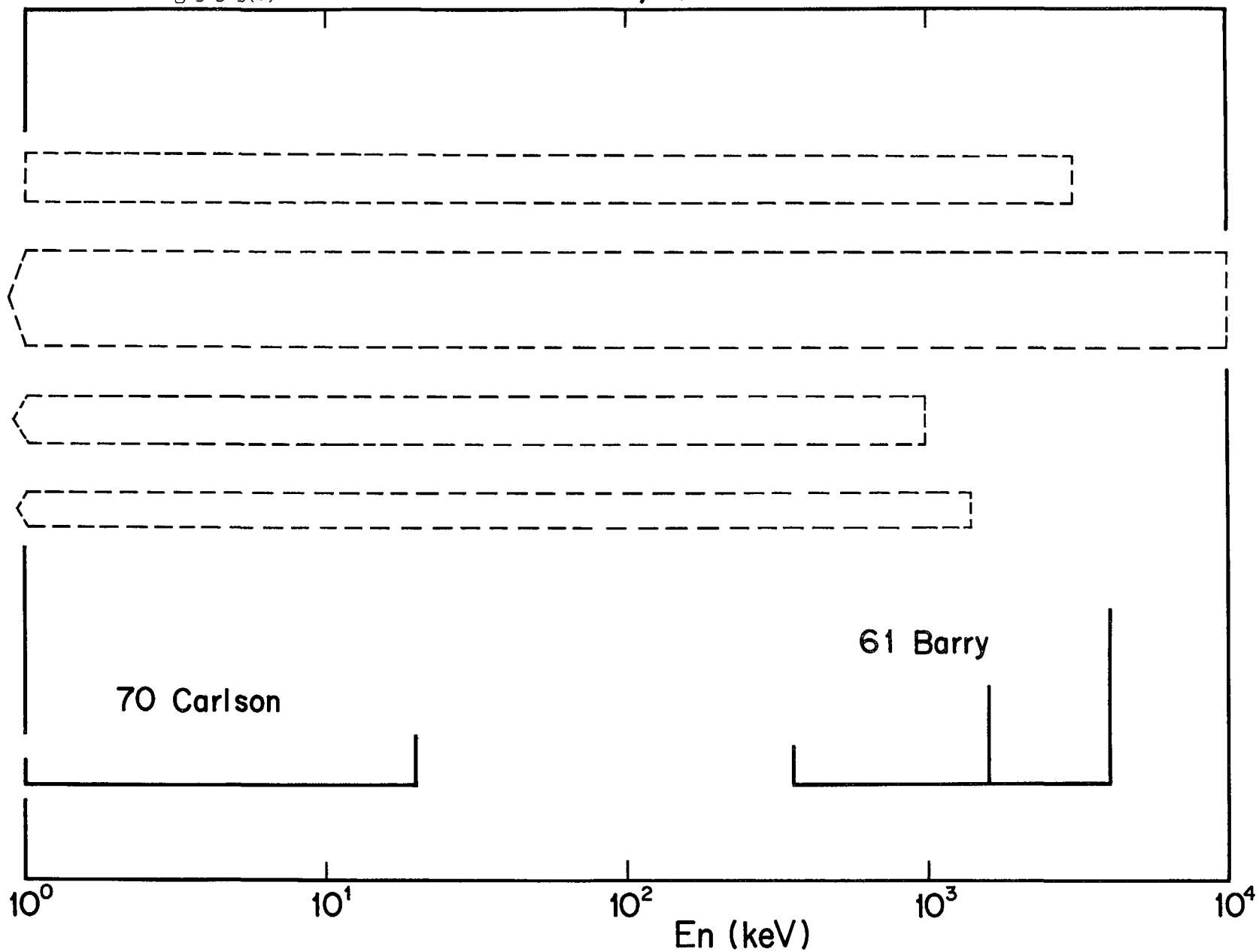


Fig.3.3.3(f)

$^{236}\text{U}(\nu)$

42

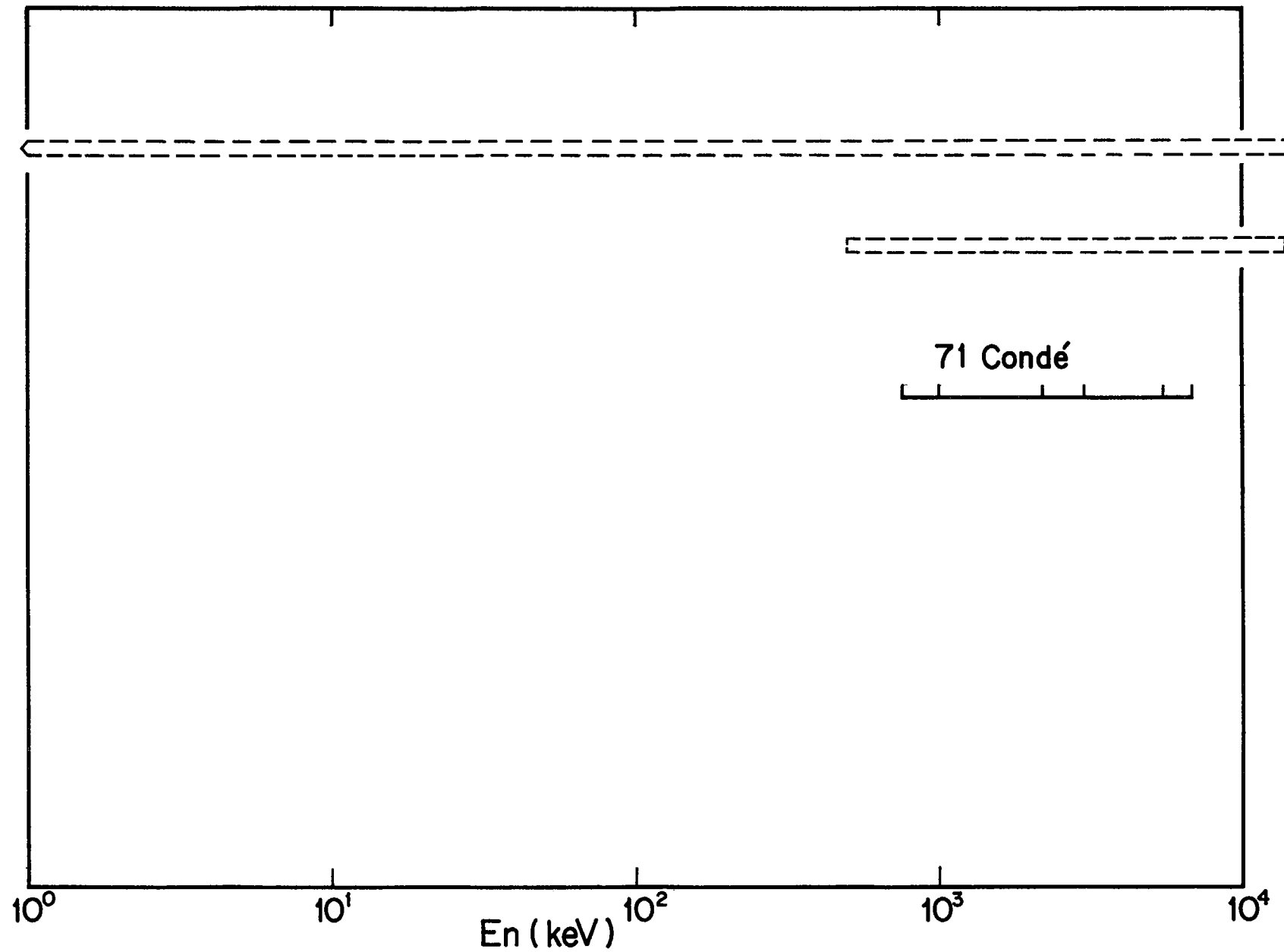


Fig.3.3.4(a)

$^{237}\text{U} (n,f)$

43

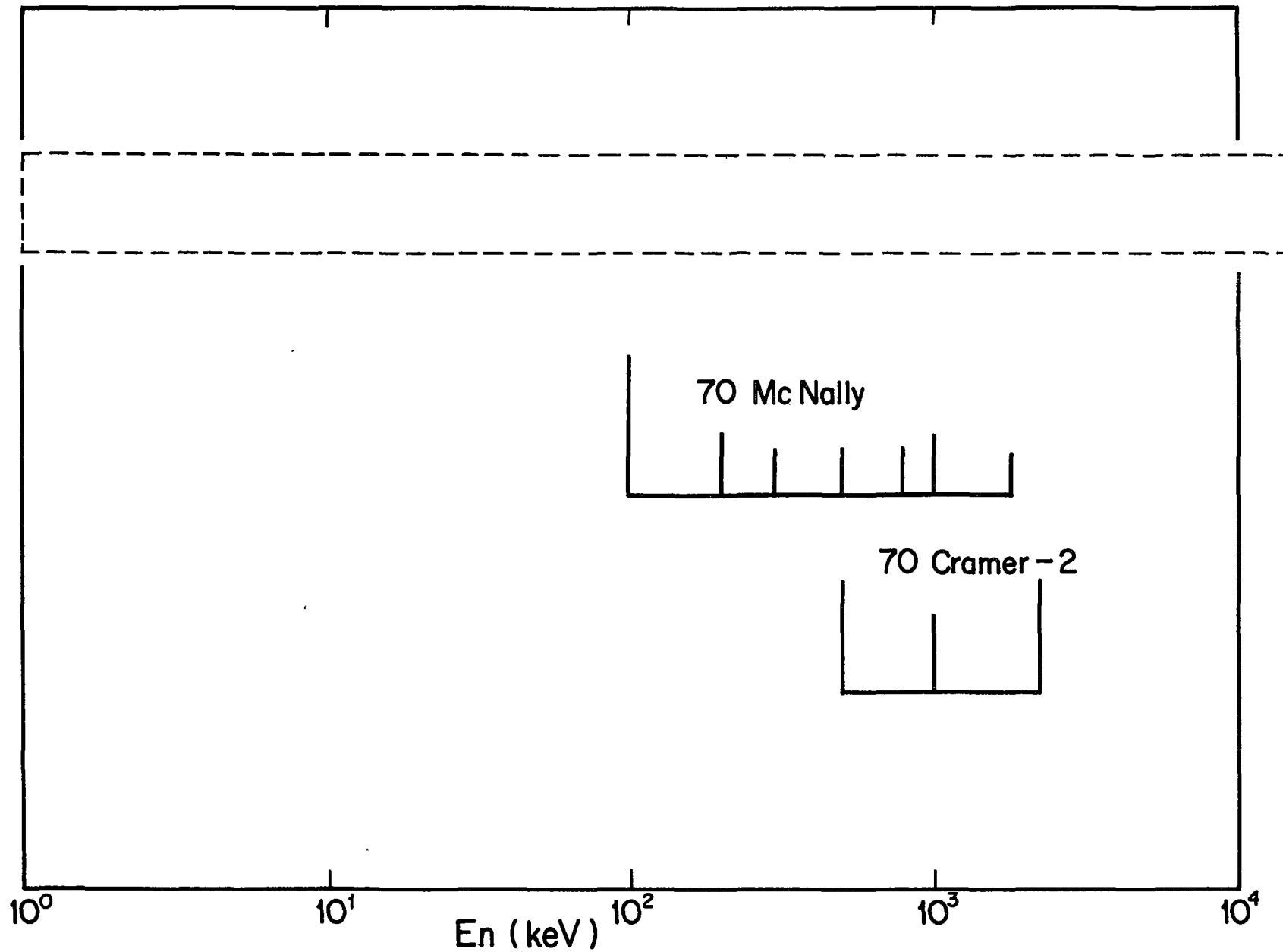


Fig.3.3.4(b)

$^{239}\text{U}(n,f)$

70Cramer-2

44

10^0

10^1

10^2
En (keV)

10^3

10^4

References for Review on U Data

50 Nyer

Nyer, W.,
LAMS-938,
Los Alamos Scientific Laboratory (1950); Cited by Davey

56 Lamphere

Lamphere, R.W.,
Phys. Rev., 104 (1956) 1654

57 Henkel

Henkel, R.L.,
LA-2122,
Los Alamos Scientific Laboratory (1957); Cited by Davey

58 Miskel

Miskel,
Private communication in CINDA

61 Barry

Barry, J.F., Bunce, J.L., Perkin, J.L.,
Pros. Phys. Soc., 78 (1961) 801

62 Babcock

Babcock, R.V.,
BNL-732
Brookhaven National Laboratory (1962); Cited by Davey

62 Lamphere

Lamphere, R.W.,
Nucl. Phys. 38 (1962) 561

65 Mather

Matner, D.S., Fieldhous, P., Moat, A.,
Nucl. Phys. 66 (1965) 149

65 Perkin

Perkin, J.L., White, P.H., Fieldhous, P., Axton, E.J.,
Cross, P., Robertson, J.C.,
J. Nucl. Energy A/B 19 (1965) 423

65 White

White, P.H., Hodgkinson, J.G., Wall, G.J.,
Proc. Salzburg Conf. on Phys. and Chem. of Fission, 1
(1965) 219

67 Simpson

Simpson, O.D., Moore, M.S., Berreth, J.R.,
Nucl. Sci. Eng. 29 (1967) 415

67 White

White, P.H., Warner, G.P.,
J. Nucl. Eng. 21 (1967) 671

68 Behkami

Behkami, A.N., Roberts, J.H., Loveland, W., Huijenga, H.G.
Phys. Rev. 171 (1968) 1267

68 Stein

Stein, W.E., Smith, R.K., Smith, H.L.,
Proc. 2nd Conf. on Neutron Cross Section and Tech. Washington
1 (1968) 627

69 James

James, G.D., Slaughter, G.G.,
Nucl. Phys. A139 (1969) 471

70 Carlson

Carlson, A.D., Friesenhahn, S.J., Lopez, W.M., Fricke, M.P.,
Nucl. Phys. A141 (1970) 577

70 Cramer-1

Cramer, J.D., Bergen, D.W.,
LA-4420 (1970)

70 Cramer-2

Cramer, J.D., Britt, H.C.,
Nucl. Sci. Eng. 41 (1970) 177

70 Elwyn

Elwyn, A.J., Ferguson, A.T.G.,
Nucl. Phys. A148 (1970) 337

70 Farrell

Farrell, J.A.,
LA-4420 (1970)

70 McNally

McNally, J.H., Barnes, J.W., Dropesky, B.J., Seeger, P.A.,
Wolfsberg, K.,
LA-4420 (1970)

71 Condé

Condé, H., Holmberg, M.,
J. Nucl. Eng. 25 (1971) 331

71 Vorotnikov

Vorotnikov, P.E., Dubrovina, S.M., Otroshchenko, G.A.,
Shigin, V.A., Davydov, A.V., Pal'skin, E.S.,
Sov. J. Nucl. Phys. 12 (1971) 259

72 James

James, G.D., Langsbord, A., Miss Khatonn, A.,
AERE-PR/NP-19, (1972) 16

72 Poortmans

Poortmans, F., Theobaldx, J., Wartena, J., Weigannx, H.,
EANDC (E) 150 "U" (1972) 171

72 Rösler

Rösler, H., Plasil, F., Schmitt, H.W.,
Phys. Letters 38B (1970) 501

73 Bockhobb

Bockhobb, K.H., Carrora, G., Brusegan, A., Dufrasne, A.,
Rohr, G., Weigmann, H.,
EANDC(E) 150 "U" (1972) P.115

73 Mewissen

Mewissen,
EANDC(E)-163U (1973)

74 McNally

McNally, J.H., Barnes, J.W., Dropesby, B.J., Seeger, P.A.,
Wolfsberg, K.,
Phys. Rev. C9 (1974) 717

3.4 Neptunium

Data are required for the cross sections of $^{237}\text{Np}(n,\gamma)$, $^{237}\text{Np}(n,f)$, $^{237}\text{Np}(n,2n)$ and $^{239}\text{Np}(n,\gamma)$ reactions. Experimental data have been obtained only for those of ^{237}Np , in the region above 1 keV.

Two measurements by 67 Stupugia and 71 Nagel were performed for the cross section of $^{237}\text{Np}(n,\gamma)$ reaction. The cross sections were obtained by the activation method. Both data are shown in Fig. 3.4 (a). Large difference between the two data sets may be due to the difference of the used γ -ray detectors (NaI in 67 Stupugia and Ge(Li) in 71 Nagel). Though the statistical errors shown in Fig. 3.4 (b) are rather small, this large systematic deviation must be reduced.

For $^{237}\text{Np}(n,2n)$ cross section, Nishi et al.¹²⁾ contributed their recent measurement to this meeting. They obtained the data with activation method. Their data are 0.34 ± 0.05 b at 9.6 MeV and 0.36 ± 0.05 b at 14.2 MeV. These are comparable to the data by 61 Perkin and 73 Landrum. These may satisfy the requests (Fig. 3.4 (c)).

Recent data of the $^{237}\text{Np}(n,f)$ cross section are shown in Fig. 3.4 (d). Though many experiments had been carried out, the data obtained after 1965 are plotted here. Davey¹⁸⁾ adopted 65 White as well as Otroshenko and Shigin, and Henkel²¹⁾ in his first evaluation. With the precise ratio measurements of fission cross section ($^{237}\text{Np} / ^{235}\text{U}$) by 66 Stein and 67 White, he revised¹⁹⁾ his evaluated fission cross section of ^{237}Np . The latter evaluation gave a little bit higher values of the first plateau than the former. Two measurements with underground nuclear explosion technique by 70 Brown and 72 Jiacoletti showed slightly higher values than the Davey's evaluation.

Comparisons between the requested accuracies and the assigned errors of the experimental data are shown in Figs. 3.4 (e) and 3.4 (f). As far as the quoted errors are concerned, the requested accuracies seem to be satisfied. However, there are systematic deviations of about 10% or so in the energy region above 1.0 MeV.

$^{237}\text{Np}(n,\gamma)$

Ref.	Energy Range	Data
67 Stupigia	0.15 MeV - 1.5 MeV	E. T.
VdG. Activation method. NaI crystal used for gamma-ray detection.		
71 Nagle	0.1 MeV - 3.0 MeV	G.
VdG. Activation method. Ge (Li) detectors used for gamma-ray detection.		

 $^{237}\text{Np}(n,2n)$

61 Perkin	14.5 MeV	T.
$^3\text{H}(d,n)$ source. Neutron monitored by $^{27}\text{Al}(n,\alpha)$ reaction. Gridded ionization chamber to count the α -particles.		
73 Landrum	13.7 MeV - 14.9 MeV	T. G.
ICT neutron generator. Activation method.		

 $^{237}\text{Np}(n,f)$

65 Perkin	24 keV	T.
Sb-Be source. Neutron flux determined by absolute flat response detectors. Ionization chamber.		
65 White	40 keV - 500 keV	T. G.
VdG. Back-to-back ionization chamber. Relative values to $^{235}\text{U}(n,f)$ data.		

$^{237}\text{Np}(n,f)$

Ref.	Energy Range	Data
66 Stein	1.0 MeV - 4.5 MeV	E. T. G. Electrostatic accelerator. Relative values to $^{235}\text{U}(n,f)$ data.
67 White	1.0 MeV - 14.1 MeV	E. T. G. Back-to-back fission chamber. Relative values to $^{235}\text{U}(n,f)$ data.
67 Grundl	1.07 MeV - 8.07 MeV	E. T. VdG. Foil-activation measurement via gross beta-gamma counting.
68 Stein	1.0 MeV - 4.5 MeV	E. T. G. VdG. Back-to-back solid state detectors. Relative values to $^{235}\text{U}(n,f)$ data.
68 Rago	12.5 MeV - 17.5 MeV	E. T. G. VdG. Fission track detector. Relative values to $^{238}\text{U}(n,f)$ data.
69 Iyer	14.0 MeV	E. T. Relative values to $^{238}\text{U}(n,f)$ data.
70 Brown	32 eV - 2.8 MeV	E. G. Nuclear explosion (Pommard). Neutron flux measured by using $^{235}\text{U}(n,f)$ and $^6\text{Li}(n,\alpha)$ reactions. SSD
72 Jiacoletti	40 keV - 6.2 MeV	T. Nuclear explosion (Physics-8). Relative to $^{235}\text{U}(n,f)$ data. Neutron flux determined by $^{235}\text{U}(n,f)$ and $^6\text{Li}(n,\alpha)$ reactions. SSD.

$^{237}\text{Np}(n, f)$

Ref.	Energy Range	Data
73 Kobayashi	3.5 MeV - 4.9 MeV	E. T. G.
	VdG. SSD. Fission spectrum averaged cross section also measured.	

Fig.3.4(a)

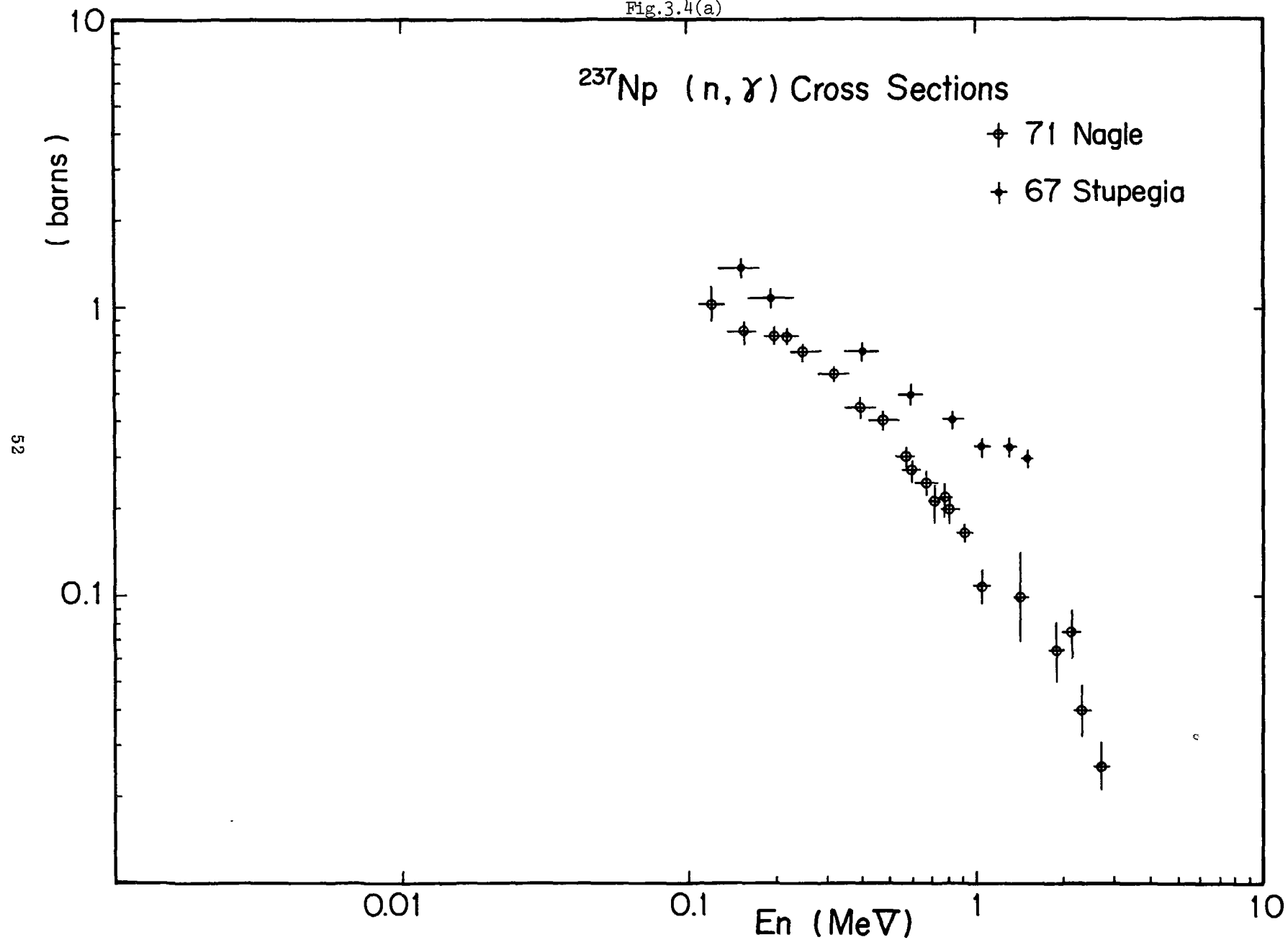


Fig.3.4(b)

$^{237}\text{Np} (n, \gamma)$

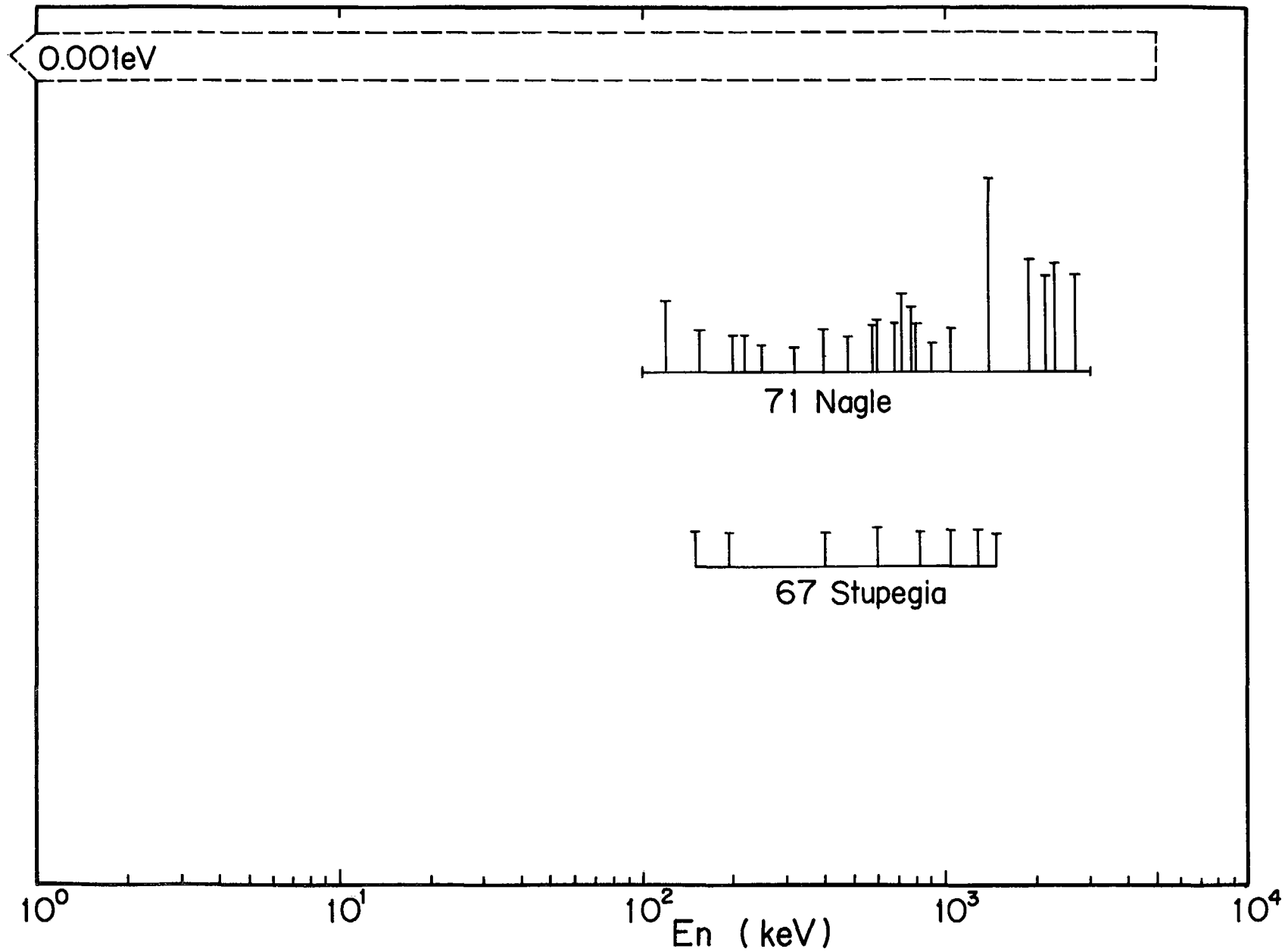


Fig.3.4(c)

^{237}Np (n, 2n)

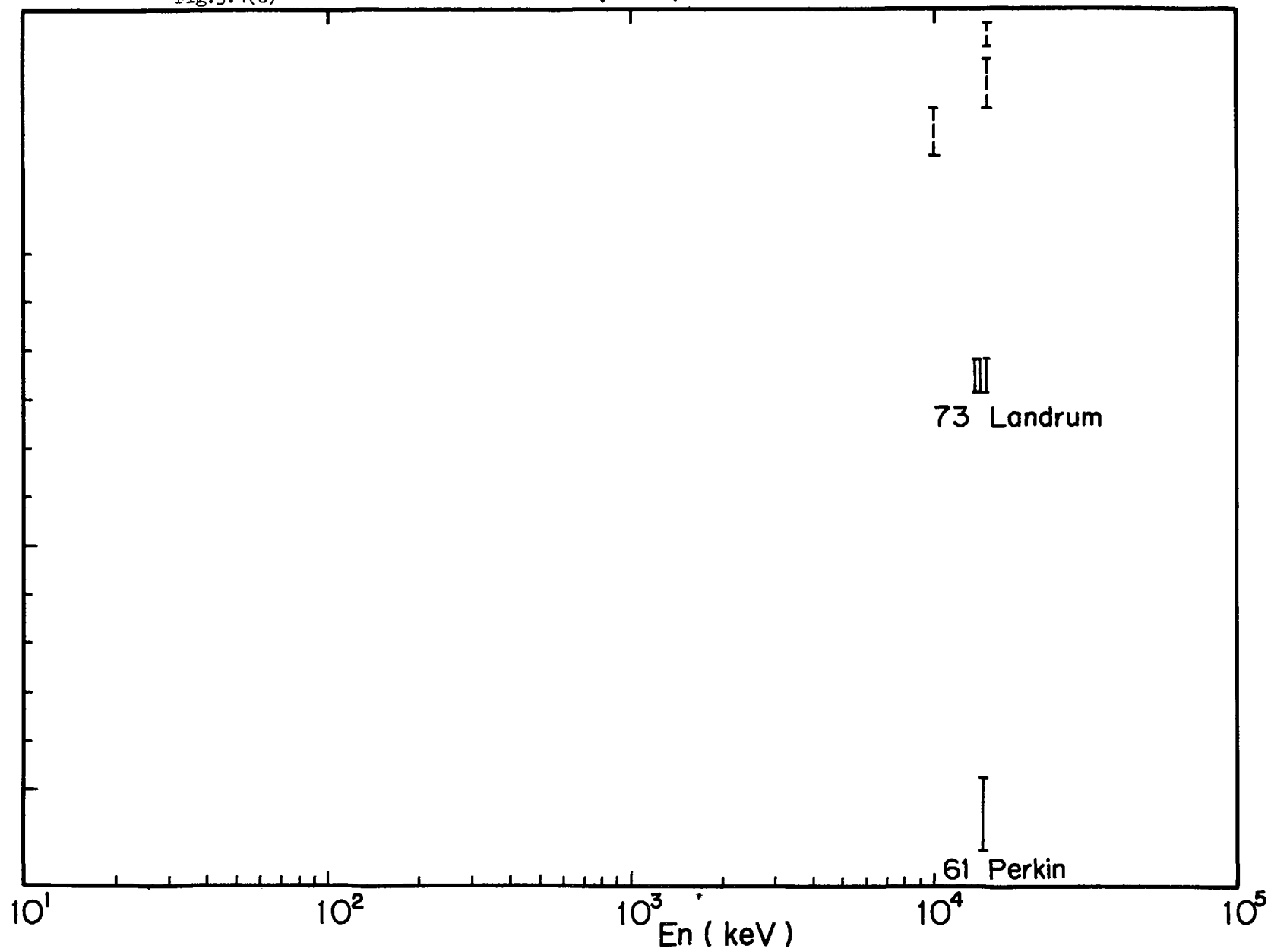
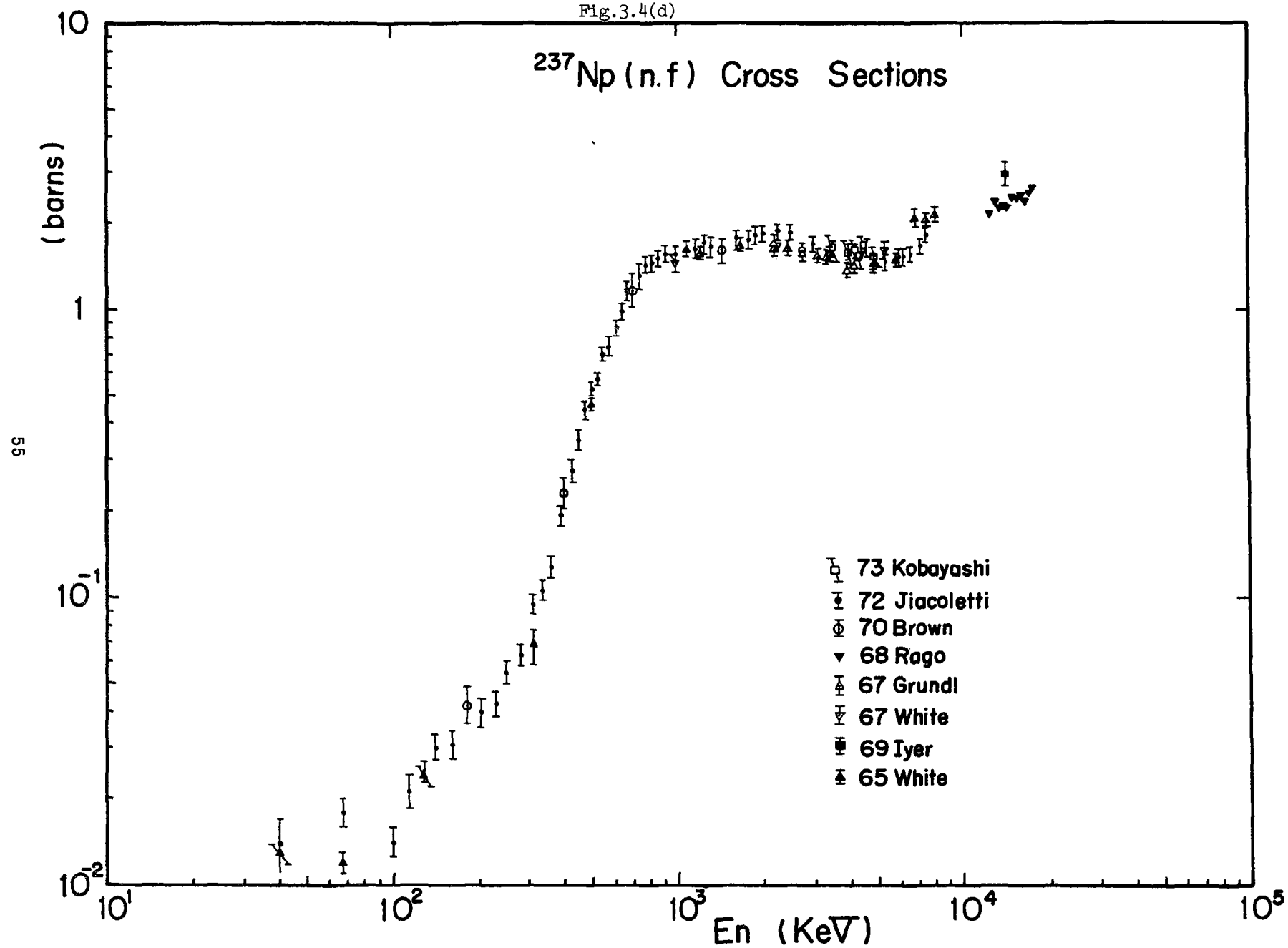


Fig.3.4(d)



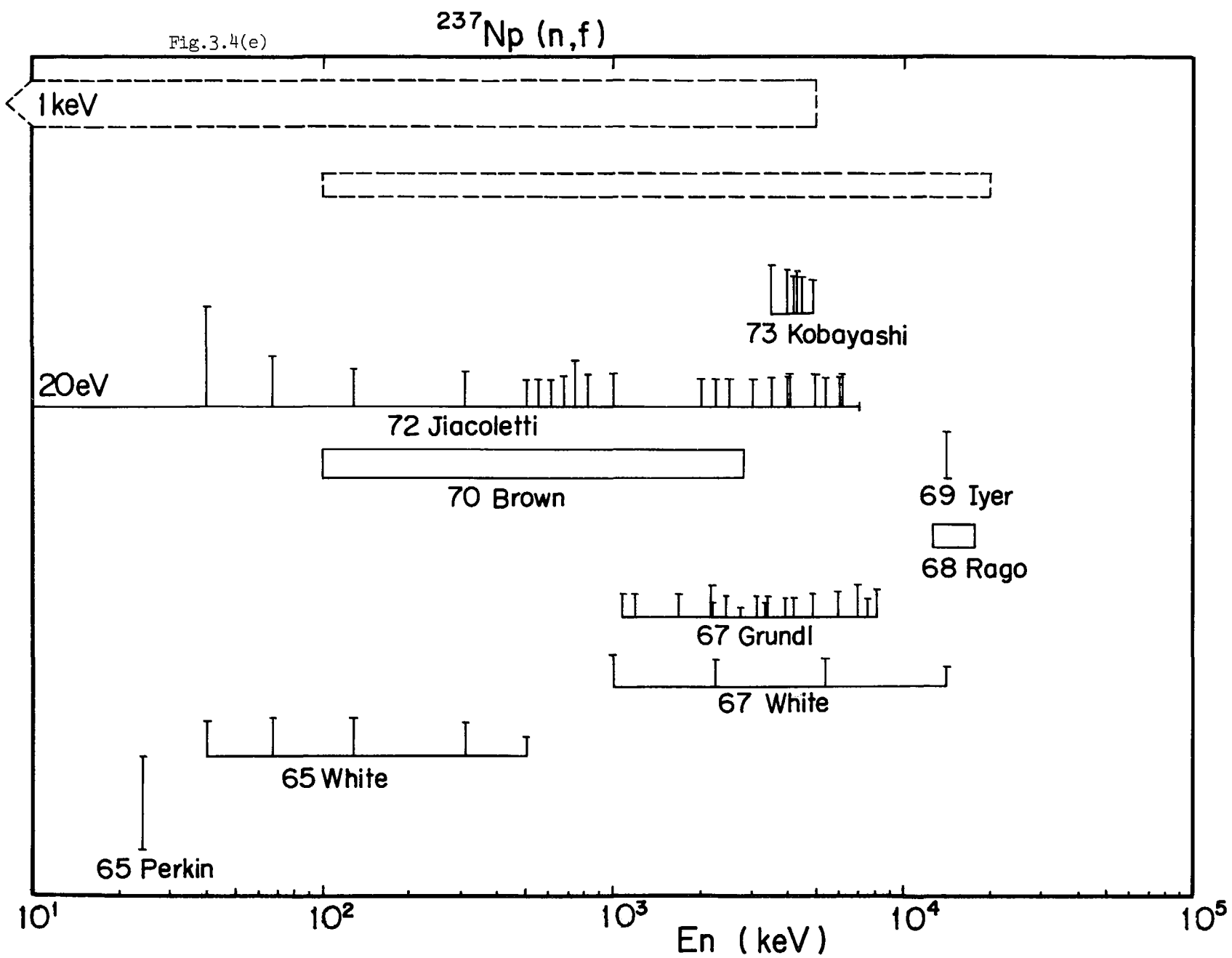
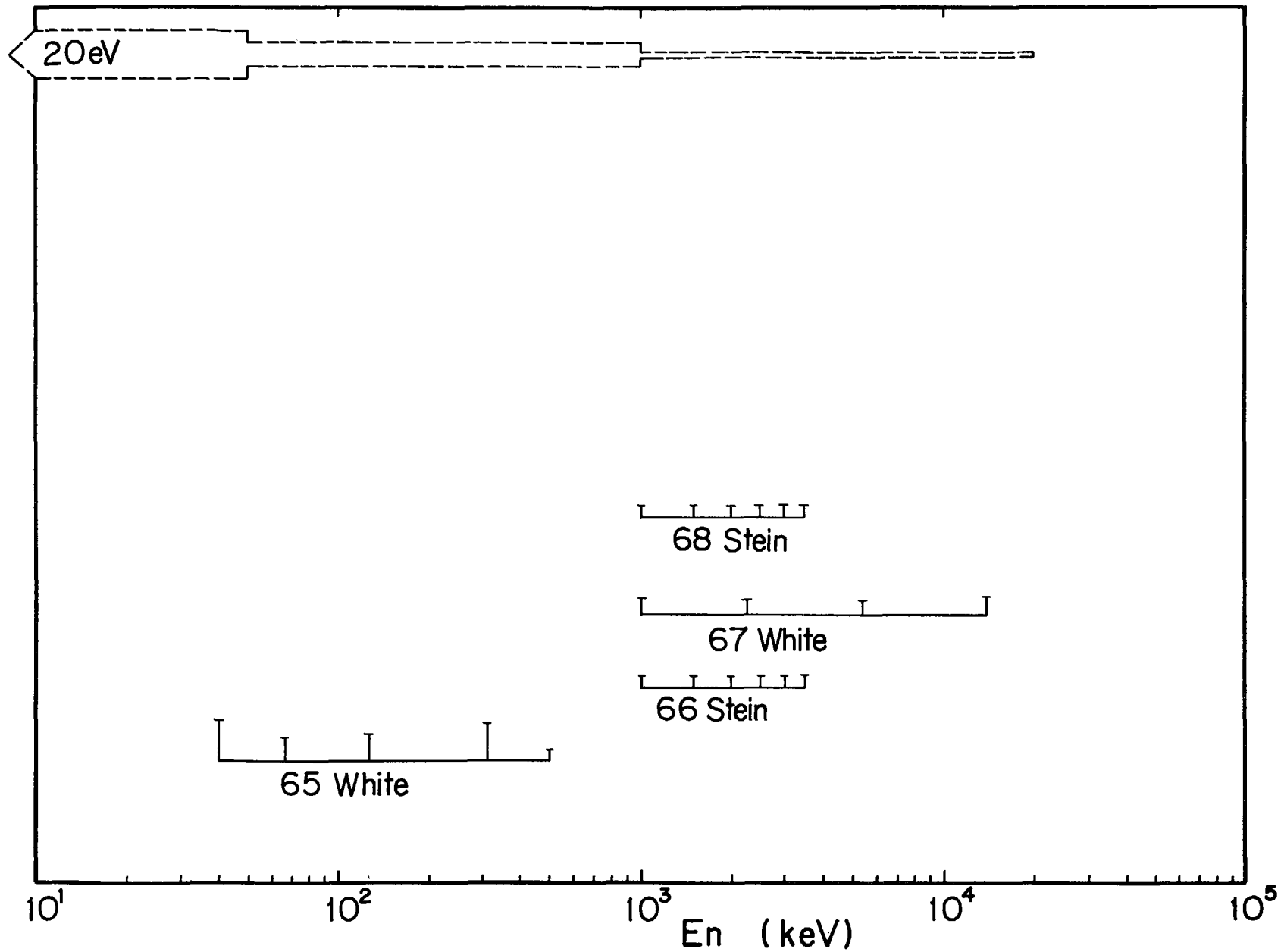


Fig.3.4(f)

Np(n,f) – Ratio relative to $\sigma_f(^{235}\text{U})$



References for Review on Np Data

61 Perkin

Perkin, J.L., Coleman, R.F.,
J. Nucl. Energy 14 (1961) 69

65 Perkin

Perkin, J.L., White, P.H., Fieldhouse, P., Axton, E.J.,
Cross, P., Robertson, J.C.,
J. Nucl. Energy A/B 19 (1965) 423

65 White

White, P.H., Hodgkinson, J.G., Wall, G.J.,
Proc. of Symp. on Phys. and Chem. of Fission (Saltzburg) I
(1965) 219

66 Stein

Stein, W.E., Smith, R.K., Grundl, J.A.,
Proc. of 1st Conf. on Neutron Cross Section and Technology
(Washington) (1966) 623

67 Grundl

Grundl, J.A.,
Nucl. Sci. Eng. 30 (1967) 39

67 Stupiega

Stupiega, D.C., Schmidt, M., Keedy, C.R.,
Nucl. Sci. Eng. 29 (1967) 218

67 White

White, P.H., Warner, G.P.,
J. Nucl. Energy 21 (1967) 671

68 Rago

Rago, P.E., Goldstein, N.,
Health Phys. 14 (1968) 595

68 Stein

Stein, W.E., Smith, R.K., Smith, H.L.,
Proc. of 2nd Conf. on Neutron Cross Sections and Technology
(Washington) (1968) 627

69 Iyer

Iyer, R.H., Sampathkumar, R.,
Proc. of Nucl. Phys. and Solid State Phys. Symp.
(Roorkee) Vol. II (1969) 287

70 Brown

Brown, W.K., Dixon, D.R., Drake, D.M.,
Nucl. Phys. A156 (1970) 609
LA-4372 (1970)

71 Nagle

Nagle, R.J., Landrum, J.H., Lindner, M.,
Proc. of 3rd Conf. on Neutron Cross Section and Technology
(Knoxville), (1971) 259

72 Jiacoletti

Jiacoletti, R.J., Brown, W.K., Olson, H.G.,
Nucl. Sci. Eng. 48 (1972) 412

73 Kobayashi

Kobayashi, K., Kimura, I., Gotoh, H., Yagi, H.,
Ann. Report of the Research Reactor Institute, Kyoto
University, 6 (1973) 1,
EANDC (J) 26L (1972) 39

73 Landrum

Landrum, J.H., Nagle, R.J., Lindner, M.,
Phys. Rev. C8 (1973) 1938

3.5 Plutonium

Various kinds of data for the Pu-isotopes have been requested. In particular, the capture cross section of ^{240}Pu and ^{242}Pu , the fission cross section of ^{240}Pu and ^{241}Pu , and neutrons per fission of ^{240}Pu are required eagerly. For the fission cross section, many experiments have been performed by many researchers with various techniques. Therefore, the data are so accumulated that the data seem to satisfy the requests. Further measurements¹¹⁾ are designed for the fission cross section ratios

of ^{238}Pu , ^{240}Pu , ^{241}Pu , ^{242}Pu and ^{244}Pu relative to ^{235}U over the energy range 0.1 to 30 MeV.

On the other hand, measurements for the other quantities shown in Fig. 1 (b) are not necessarily made enough to satisfy the requests. A plan is proposed by a Harwell group¹⁴⁾ to measure the capture cross section of ^{241}Pu and ^{242}Pu with the integral measurements.

3.5.1 Plutonium-238

According to the WRENDA 74, there are three requests for the fission cross section with 10 to 20%. Roughly speaking, these requests seem to be satisfied (see Fig. 3.5.1 (d)). In fact, the data of the recent experiments shown in Fig. 3.5.1 (b) agree well with each other. In Fig. 3.5.1 (a), the data obtained by the accelerators are shown. Comparing between these, the old data by 63 Butler and by 66 Vorotnikov are systematically 20 to 30% larger than the data by the other experiments.

The data by 70 Drake and by 73 Silbert-2 shown in Fig. 3.5.1 (c) were measured with underground nuclear explosion technique. These data show a strong intermediate structure in the fission sub-threshold energy region. The averaged cross section in this energy region does not show a characteristic of even-even nuclei but of odd-A nuclei with large s-wave component. Near 1 MeV, these two data sets show some difference with each other.

Angular anisotropy of the fission fragment distributions (70 Fomushkin) may be smaller than that of ^{240}Pu and of ^{242}Pu .

3.5.2 Plutonium-240

There are many requested quantities in WRENDA 74. For these requests, there are one or two experiments for the total, capture, inelastic scattering cross sections and delayed neutrons emitted per fission. Comparisons between the requested accuracies and the experimental errors are shown in Figs. 3.5.2 (d) through 3.5.2 (j).

Some experimental data of fission cross section are shown in Fig. 3.5.2 (a). The data obtained by the ratio measurements such as 64 Ruddick,

66 Gilboy and 57 Henkel are reduced the cross sections by using Matsunobu's evaluated fission cross section²²⁾ of ^{235}U . The data obtained by 66 Byers with underground nuclear explosion technique and by 68 Mingeco with linac are averaged within some proper energy intervals. The former data by 66 Byers are larger than the other data (see also Figs. 3.5.2 (b) and (c)). Their errors are also large, including 8.7% correlated errors.

After Davey's evaluation, the data were obtained by 70 Sabin-1, 71 Androsenko, 72 Hockenbury and 74 Frehaut. The data by 70 Sabin-1 seem to show some structures near 1 MeV. But their deviation is rather large. The data by 74 Frehaut cover the energy region from 8 to 14 MeV, where the other data have not been observed. In this sense, they are very valuable data. Including them, the fission cross section of this isotope reveal the saw-tooth structure in MeV region.

Angular anisotropy of the fission fragment distributions was measured by 71 Androsenko, and the number of neutrons per fission was observed by 60 Kuzminov, 66 DeVroey, 70 Sabin-2 and 74 Frehaut. Though the quantities concerning fission reaction were obtained rather abundantly, the total cross section, inelastic scattering and capture cross sections have been measured only slightly (see short notes). In order to satisfy the requests, more data must be needed for these quantities.

3.5.3 Plutonium-241

The requests are made in WRENDA 74 for the total cross section, fission cross section, capture cross section and number of neutrons per fission. For these requests, the experimental data are not necessarily satisfactory, except for the fission cross section. Figs. 3.5.3 (c) through 3.5.3 (e) show the comparison between the requested accuracies and the experimental errors.

There have been many experiments for the fission cross section measurements. Generally speaking, the assigned errors of the measured fission cross sections are within 10%. However, some systematic deviations appear between 61 Butler, 66 Simpson and 70 Szabo (Figs. 3.5.3 (a) and (b)). These may be due to the different standardization of the cross sections.

The number of neutrons per fission have been measured by 68 Condé, 74 Frehaut and 74 D'yachenko. The data of the former two experiments were obtained by relative measurements to the data of ^{252}Cf , and the latter by observing the fission yields and the kinetic energy of the fission fragments. Agreements among them seem to be good.

The measurements of the total and capture cross sections are very poor. Concerning the capture cross section, in particular, there is only one experiment by 72 Weston whose aim was a measurement of α -value.

3.5.4 Plutonium-242,-243 and -244

There are five experiments for the fission cross section of ^{242}Pu . Recent measurements are by 70 Bergen, 70 Fomushkin and 71 Auchampaugh. These data are shown in Figs. 3.5.4 (a) and (b). The data by 70 Fomushkin were obtained by integrating the angular distributions of the fission fragments. These are 10 to 20% smaller than those obtained by 70 Bergen and 71 Auchampaugh with the underground nuclear explosion technique. The data by 70 Bergen and by 71 Auchampaugh agree well with those by 60 Butler, below 1 MeV.

Above 1 MeV, the two data sets reveal the angular anisotropy of the fission. The data by 71 Auchampaugh obtained with a detector at 55° direction from the incident neutrons are about 15 to 20% larger than those obtained at 90° direction (Fig. 3.5.4 (b)). However, the difference between the data by 70 Fomushkin and the data by underground nuclear explosion measurements seems to be larger than that estimated with the angular anisotropy.

The errors in the sub-threshold energy region are very large. These data were measured with the underground nuclear explosion technique. In Figs. 3.5.4 (b) and (c), the data for ^{242}Pu and ^{244}Pu are shown. The status of the data are not enough to satisfy the requests (Figs. 3.5.4 (d) and (e)).

$^{238}\text{Pu}(\text{total})$

Ref.	Energy Range	Data
67 Young	0.008 eV - 6.5 keV	E. G.
	MTR fast chopper. Transmission. Also, resonance and average resonance parameters.	

$^{238}\text{Pu}(\text{n}, \gamma)$

73 Silbert-1	18 eV - 200 keV	T. G.
	Underground nuclear explosion "Persimmon". TOF. Modified Moxon-Rae. Flux monitored by $^3\text{He}(\text{n}, \text{p})$, $^6\text{Li}(\text{n}, \alpha)$ and $^{235}\text{U}(\text{n}, \text{f})$. Also, resonance and average resonance parameters.	

$^{238}\text{Pu}(\text{n}, \text{f})$

63 Butler	0.4 MeV - 1.4 MeV	E.
	VdG; $^7\text{Li}(\text{p}, \text{n})$. Back-to-back gas scintillation counter.	
66 Vorontnikov	50 keV - 1.4 MeV	E. G.
	VdG; $^7\text{Li}(\text{p}, \text{n})$, $\text{T}(\text{p}, \text{n})$. Four angle measurement with grided ion chamber. Flux measured by calibrated long counters.	
67 Barton	1 MeV - 3 MeV, 14.9 MeV	E. T. G.
	VdG; $\text{T}(\text{p}, \text{n})$, C&W; $\text{D}(\text{d}, \text{n})$, $\text{T}(\text{d}, \text{n})$. Three angle measurement. Relative to $^{235}\text{U}(\text{n}, \text{f})$. (C&W = Cockcroft - Walton accelerator)	
67 Fomushkin	14.5 MeV	E. T.
	$\text{T}(\text{d}, \text{n})$. Glass detector. Relative measurement to ^{238}U and ^{237}Np fission. Also, fragment angular distribution.	

$^{238}\text{Pu}(n,f)$

Ref.	Energy Range	Data
67 Stubbins	2 eV - 300 eV, 0.12 MeV - 5 MeV	E. G.
	Linac. TOF. Fission spark chamber. Relative measurement to $^{239}\text{Pu}(n,f)$. High energy measurement to normalize the low energy data. Also, resonance parameters.	
68 Ermagambetov	0.5 MeV - 16.9 MeV	E. T. G.
	VdG; T(p,n), D(d,n), T(d,n). Cylindrical glass detector. Relative measurement to $^{235}\text{U}(E_n \leq 1.5 \text{ MeV})$ and $^{238}\text{U}(E_n \geq 1.5 \text{ MeV})$ fissions.	
69 Ermagambetov	2.7 keV - 1 MeV	G.
	VdG. ^{235}U reference. Relation between resonance fission width and sub-barrier average fission width is discussed.	
70 Drake	32 eV - 2.6 MeV	E. T. G.
	Underground nuclear explosion "Pommard". TOF. Measurement at 55° and 90°. No correction for target impurities and source resolution.	
70 Ermagambetov	2.4 keV - 2.4 MeV	T. G.
	VdG; T(p,n). Glass detectors (0° - 150°). Relative to $^{235}\text{U}(n,f)$.	
70 Fomushkin	0.45 MeV - 3.6 MeV	T. G.
	VdG; T(p,n). Dielectric detectors (5 angles). Relative to $^{235}\text{U}(n,f)$. Also, fragment angular distributions: Legendre expansion coefficients.	

$^{238}\text{Pu}(\text{n},\text{f})$

Ref.	Energy Range	Data
72 Shpak	13.4 MeV - 14.8 MeV	G. T(d,n). Multiangle glass detector. Fragment angular anisotropy. Fission cross section ratio to ^{232}Th .
73 Silbert-2	18 eV - 3 MeV	(E). T. G. Underground nuclear explosion "Persimmon". TOF. Measurement at 55°, 80° and 90°. Flux monitor $^{235}\text{U}(\text{n},\text{f})$, $^3\text{He}(\text{n},\text{p})$ and $^6\text{Li}(\text{n},\alpha)$.

$^{240}\text{Pu}(\text{n},\text{f})$

57 Dorofeev	0.03 MeV - 5 MeV	E. T. Radio isotope neutron sources. Absolute measurement for Sb-Be source, relative for other sources. Spherical ion chamber.
57 Henkel	0.27 MeV - 8.12 MeV	E. T. G. Back-to-back ion chamber. Relative measurement to $^{235}\text{U}(\text{n},\text{f})$.
60 Kazarinova	2.5 MeV, 14.6 MeV	E. T. D(d,n), T(d,n) reaction. Fission chamber. Relative measurement to $^{238}\text{U}(\text{n},\text{f})$.

$^{240}\text{Pu}(n,f)$

Ref.	Energy Range	Data
62 Nesterov	0.04 MeV - 4 MeV, (15 MeV)	E. T. G.
	VdG; T(p,n), C&W; T(d,n). Double fission chamber. Relative measurement to $^{239}\text{Pu}(n,f)$.	
64 DeVroey	0.03 MeV - 2.0 MeV	G.
	Relative measurement to $^{235}\text{U}(n,f)$.	
64 Ruddick	60 keV - 500 keV	E. T. G.
	VdG; Li(p,n). Gas scintillation double fission counter. Relative measurement to $^{235}\text{U}(n,f)$.	
65 Perkin	24 keV	T.
	Sb-Be neutron source. Fission chamber. Absolute measurement.	
66 Byers	20 eV - 1 MeV	E. T. G.
	Underground nuclear explosion "Petrel". TOF. Flux monitor $^{235}\text{U}(n,f)$.	
66 Gilboy	14 keV - 173 keV	E. G.
	VdG Li(p,n). TOF. Xe gas scintillation fission counter. Relative measurement to $^{235}\text{U}(n,f)$.	
67 White	1.0 MeV - 5.4 MeV, 14.1 MeV	E. T. G.
	T(p,n), D(d,n) and T(d,n) reaction. Back-to-back fission counter. Relative measurement to $^{235}\text{U}(n,f)$.	

$^{240}\text{Pu}(\text{n},\text{f})$

Ref.	Energy Range	Data
68 Migneco	200 eV - 8 keV	E. G. Linac. TOF. Fission neutron liquid scintillation counter. Normalized to the integrated resonances of ^{239}Pu impurity. Also, resonance parameters.
70 Sabin-1	0.52 MeV - 3.73 MeV	E. G. Linac. TOF. Prompt fission γ liquid scintillation detector. Relative measurement to $^{235}\text{U}(\text{n},\text{f})$.
71 Androsenko	0.1 MeV - 1.5 MeV	T. G. VdG T(p,n). Glass detectors. Fragment angular anisotropy data only.
72 Hockenbury	20 eV - 30 keV	G. See $^{240}\text{Pu}(\text{n},\gamma)$
74 Frehaut	1.8 MeV - 14.8 MeV	T. G. Tandem T(p,n), D(d,n). Double fission chamber. Relative measurement to $^{235}\text{U}(\text{n},\text{f})$. Also, $\bar{\nu}_p$ ratio to that of ^{235}U .

$^{240}\text{Pu}(\text{total})$

72 Smith	0.1 MeV - 1.5 MeV	T. G. VdG $^7\text{Li}(\text{p},\text{n})$. Transmission. BF_3 ; proton recoil counter.
----------	-------------------	--

$^{240}\text{Pu}(n,n)$

Ref.	Energy Range	Data
72 Smith	0.3 MeV - 1.5 MeV	T. G. VdG $^7\text{Li}(p,n)$. TOF. Measurement at 8 angles. Relative to $C(n,n)$. Angular distributions; Legendre expansion coefficients.

 $^{240}\text{Pu}(n,n')$

72 Smith	0.35 MeV - 1.5 MeV	T. G. Excitation cross sections for $E_x = 42 \pm 5, 140 \pm 10, 300 \pm 20, 600 \pm 20, 900 \pm 50$ keV levels. See $^{240}\text{Pu}(n,n)$.
----------	--------------------	--

 $^{240}\text{Pu}(n,\gamma)$

72 Hockenbury	20 eV - 30 keV	T. G. Linac. TOF. Large liquid scintillation detector for capture γ and prompt fission γ rays. Absolute detection efficiency and flux obtained by resonance area analysis.
75 Weston	thermal - 350 keV	G. Linac. TOF. Liquid scintillation counter. Cross section normalized to that of ENDF/B-IV at 0.025 eV. Energy dependence of neutron flux measured with a $^{10}\text{BF}_3$ chamber and a ^6Li glass detector.

 $^{240}\text{Pu}(\bar{\nu}_p)$

60 Kuzminov	3.6 MeV, 15 MeV	E. T. $D(d,n), T(d,n)$. Gas counter. Relative to $\bar{\nu}_p$ of ^{239}Pu thermal neutron fission.
-------------	-----------------	--

$^{240}\text{Pu}(\bar{\nu}_p)$

Ref.	Energy Range	Data
66 DeVroey	0.1 MeV, 1.0 MeV, 1.6 MeV	E. T.
	VdG $^7\text{Li}(p,n)$, $T(p,n)$. TOF associated with fission. Relative to $\bar{\nu}_p$ of ^{235}U .	
70 Sabin-2	1.0 MeV - 4.0 MeV	T. G.
	Linac. TOF. Liquid scintillation detector. Relative to ^{252}Cf spontaneous fission $\bar{\nu}_p = 3.772$	
74 Frehaut	1.8 MeV - 15 MeV	T. G.
	Tandem. Fission chamber and Gd loaded liquid scintillation counter. ^{252}Cf spontaneous fission $\bar{\nu}_p$ standard (3.782).	

$^{240}\text{Pu}(\text{delayed neutron})$

57 Keepin	near fission neutron spectrum	T.
	Bare critical assembly (GODIVA). Absolute total yields, as well as six group half-lives and yields for each group.	
69 East	14.9 MeV	T.
	C&W $T(d,n)$. Fission counter, Slab detector. absolute yield = 0.057 ± 0.0007	

$^{242}\text{Pu}(\text{total})$

70 Young	0.0015 eV - 8 keV	E. G.
	MTR fast chopper. Transmission. Also, resonance and average resonance parameters.	

$^{242}\text{Pu}(n,\gamma)$

Ref.	Energy Range	Data
67 Bell	10 keV	T. Estimation of capture cross sections and capture to fission ratios of Pu isotopes ($A = 242 - 254$) to explain the abundance data of neutron exposed ^{242}Pu target with nuclear explosion "Tweed".
73 Poortmans	20 eV - 1.3 keV	G. Linac. TOF. Moxon-Rae detector. Also, measured scattering and total cross section. Resonance and overage resonance parameters.

 $^{242}\text{Pu}(n,f)$

60 Butler *		
67 Fomushkin	14.5 MeV	E. T. G. See $^{238}\text{Pu}(n,f)$.
70 Bergen	50 eV - 5 keV, 0.1 MeV - 3 MeV	E. T. G. Underground nuclear explosion "Pommard". TOF. Measurement at 55° and 90° . Relative to $^{235}\text{U}(n,f)$. Missed data in the energy range 5 keV - 0.1 MeV.
70 Fomushkin	0.45 MeV - 3.6 MeV	E. T. G. See $^{238}\text{Pu}(n,f)$
71 Auchampaugh	20 eV - 10 MeV	E. G. Underground nuclear explosion. TOF. Measurement at 55° and 90° . Relative to $^6\text{Li}(n,\alpha)$ and $^{235}\text{U}(n,f)$. Also, resonance parameters including class I and class II fission data.

$^{242}\text{Pu}(\text{delayed neutron})$

Ref.	Energy Range	Data
70 East	14.7 MeV	T. Six components group half-lives and relative yields.
72 Krick	0.7 MeV - 1.3 MeV	T. Averaged yield data in 0.7 MeV - 1.3 MeV. Revised values given in Nucl. Sci. Eng. <u>50</u> (1973) 80

$^{243}\text{Pu}(\text{n},\gamma)$

67 Bell	10 keV	T.
See $^{242}\text{Pu}(\text{n},\gamma)$.		

$^{243}\text{Pu}(\text{n},\text{f})$

67 Bell	10 keV	T. Estimated capture to fission ratio. See $^{242}\text{Pu}(\text{n},\gamma)$.
70 Cramer	0.5 MeV - 2 MeV	T. G. Estimated fission cross section using measured (t,pf) probability and calculated compound nucleus formation cross section.

$^{244}\text{Pu}(\text{n},\gamma)$

67 Bell	10 keV	T.
See $^{242}\text{Pu}(\text{n},\gamma)$		

$^{244}\text{Pu}(\text{n},\text{f})$

Ref.	Energy Range	Data
71 Auchampaugh See $^{242}\text{Pu}(\text{n},\text{f})$.	20 eV - 10 MeV	E. G.

*

60 Butler	0.1 MeV - 1.7 MeV	E. G.
$^7\text{Li}(\text{p},\text{n})$ source. VdG. Double gas scintillator. Relative measurement to $^{235}\text{U}(\text{n},\text{f})$. Quoted error is 6 to 12%.		

$^{241}\text{Pu}(\text{total})$

Ref.	Energy Range	Data
61 Simpson	0.02 eV - 2 keV	E. G.
MTR fast chopper, TOF, transmission. BF_3 proportional counters.		
63 Pattenden	3 eV - 5 keV	E. G.
Linac, TOF, transmission Li glas scintillator		

$^{241}\text{Pu}(\text{n},\text{f})$

60 Kazarinova	2.5 MeV and 14.6 MeV	E. T.
61 Butler	20 keV - 1.8 MeV	E. T. G.
Ratio to $^{235}\text{U}(\text{n},\text{f})$. VdG. Back-to-back gas scintillation counter.		

62 Smith	120 keV - 21 MeV	E. T. G.
	Ratio to $^{235}\text{U}(\text{n},\text{f})$. VdG. Back-to-back fission chamber.	
65 James	0.01 eV - 3 keV	E. G.
	Linac, TOF, SSD.	
65 Perkin	24 keV	T. G.
	Sb-Be photoneutron source. Fission chamber.	
65 White	40 keV - 505 keV	T. G.
	Ratio to $^{235}\text{U}(\text{n},\text{f})$. Back-to-back fission chamber.	
66 James	1 keV - 25 keV	T.
	TOF. Gas scintillation	
	Relative measurment, normalized to $^{241}\text{Pu}(\text{n},\text{f})$ by 65 James.	
$^{241}\text{Pu}(\text{n},\text{f})$		
Ref.	Energy Range	Data
66 Simpson	20 eV - 100 keV	E. T. G.
	Underground detonation. SSD.	
67 White	1 MeV - 14 MeV	E. T. G.
	Ratio to $^{235}\text{U}(\text{n},\text{f})$. Back-to-back fission chamber.	
70 James	10 eV - 2 keV	T.
	TOF	
70 Migneco	10 eV - 2 keV	E. T. G.
	Normalized as RI (4.65 - 10 eV) = 193.6b	
70 Szabo	17 keV - 1 MeV	E. T. G.
	VdG, Fission chamber	

70 Szabo 1 MeV - 2.6 MeV E. T. G.
VdG, Fission chamber

73 K  ppler 5 keV - 1.2 MeV E. T. G.
Ratio to $^{235}\text{U}(\text{n},\text{f})$. VdG. Gas scintillation.

73 Blons 0 - 30 keV E. T. G.
Linac, TOF, Gas scintillation. Normalized as
 $\int_{20}^{70} \sigma_f \, dE = 2367.5 \text{ b.eV}$

$^{241}\text{Pu}(\nu_p)$

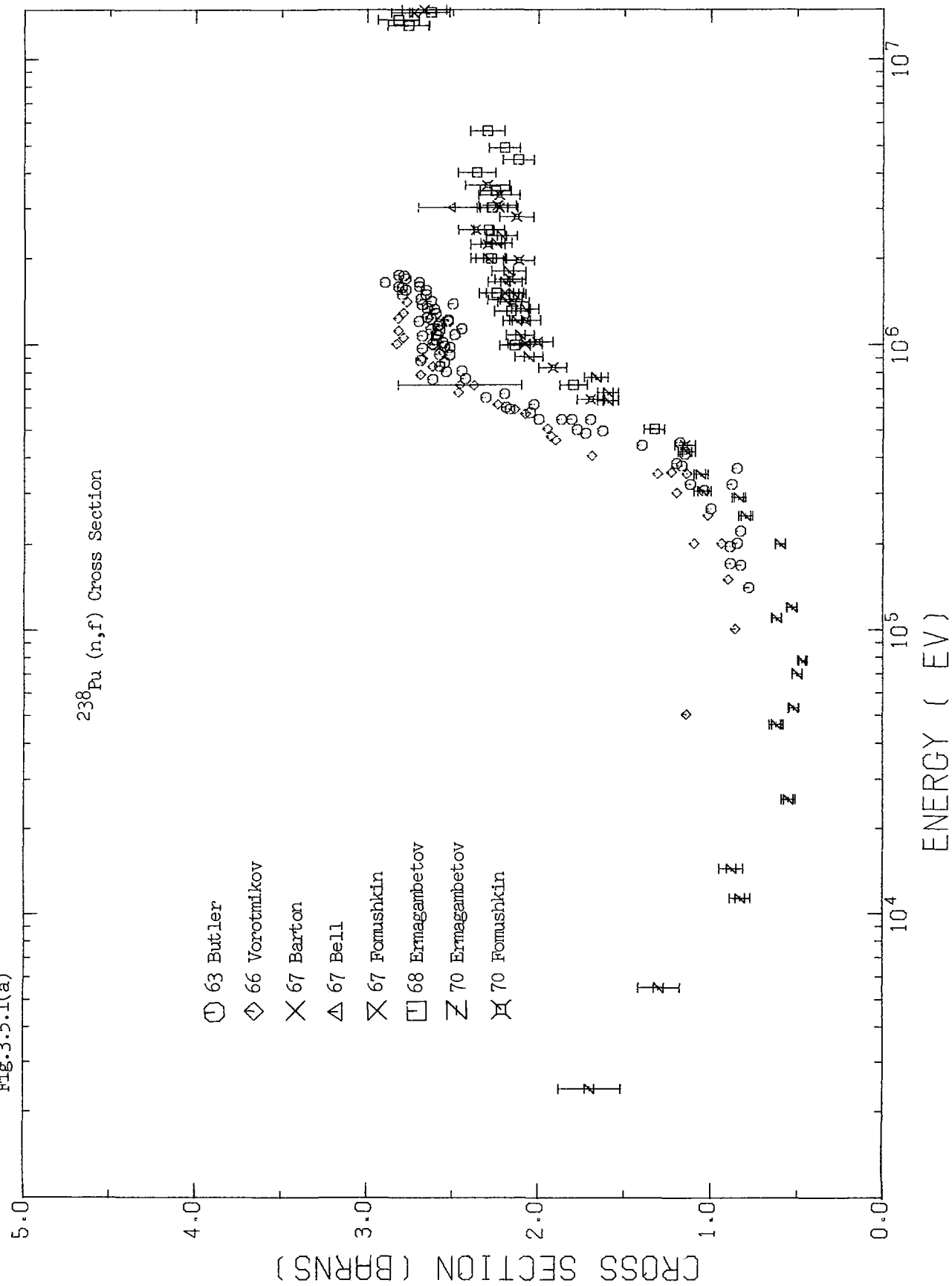
Ref.	Energy Range	Data
------	--------------	------

68 Conde	0.52 MeV - 14.8 MeV VdG. Large liquid scintillator Normalization : $\nu_p (^{252}\text{Cf}) = 3.764$	E. T.
----------	--	-------

74 Frehaut	1.5 MeV - 15 MeV VdG. Large liquid scintillator Normalization : $\nu_p (^{252}\text{Cf}) = 3.732$	T.
------------	---	----

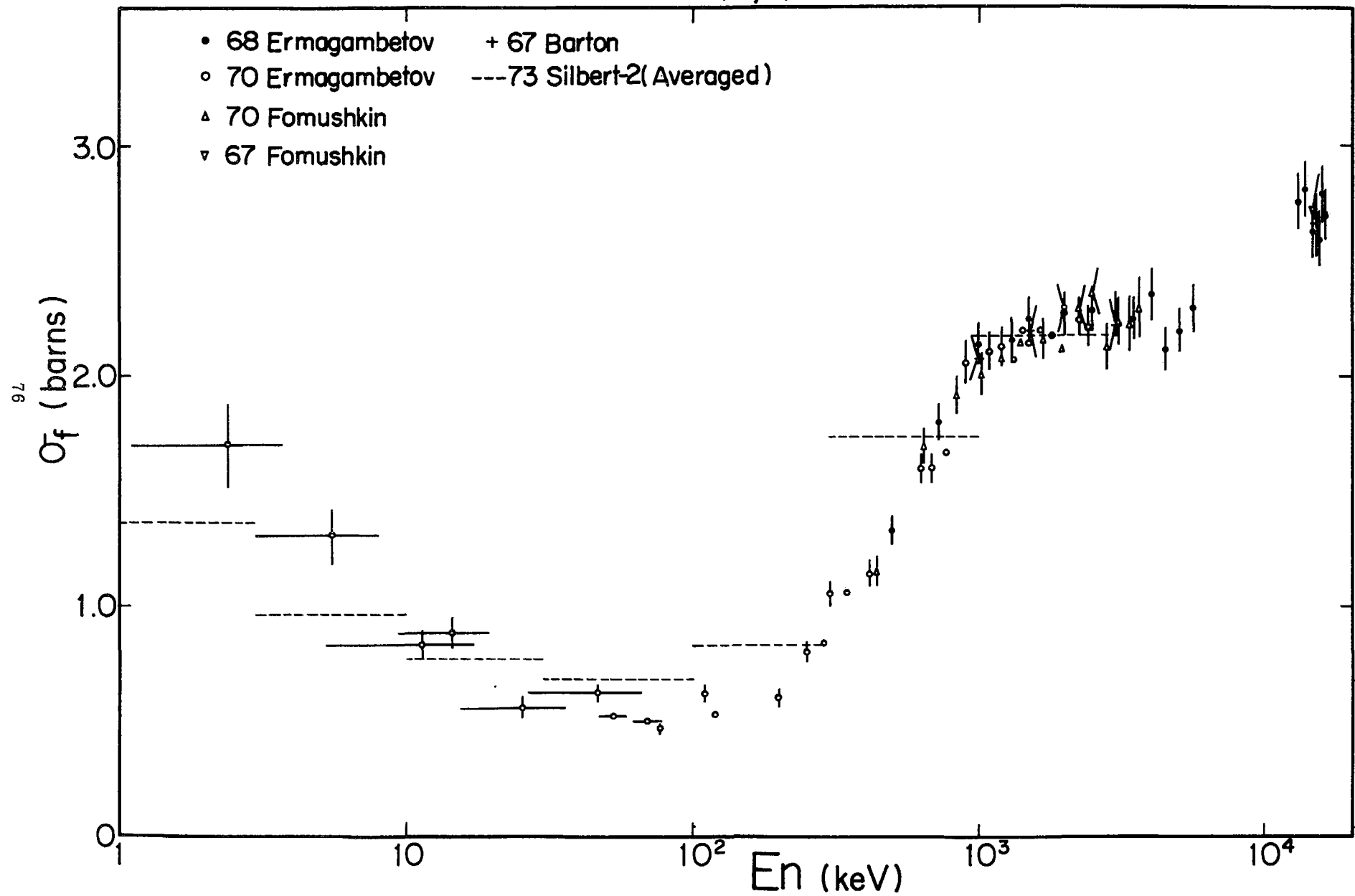
74 D'yachenko	0.28 MeV - 5 MeV Calculated from energy dependence of fission yield and of fission fragment K.E.	T. G.
---------------	--	-------

Fig.3.5.1(a)



$^{238}\text{Pu} (n, f)$

Fig.3.5.1(b)



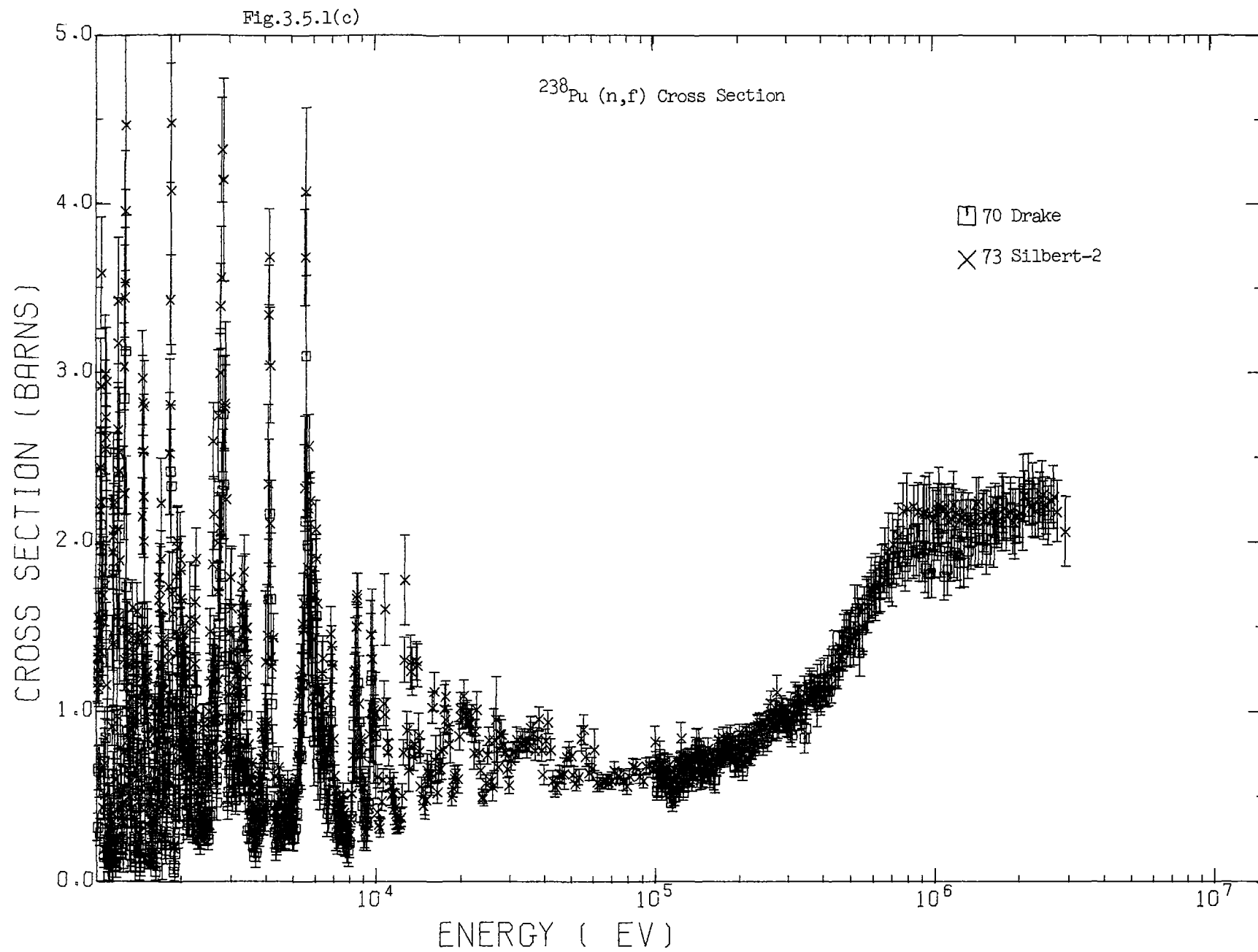


Fig.3.5.1(d)

^{238}Pu (n,f)

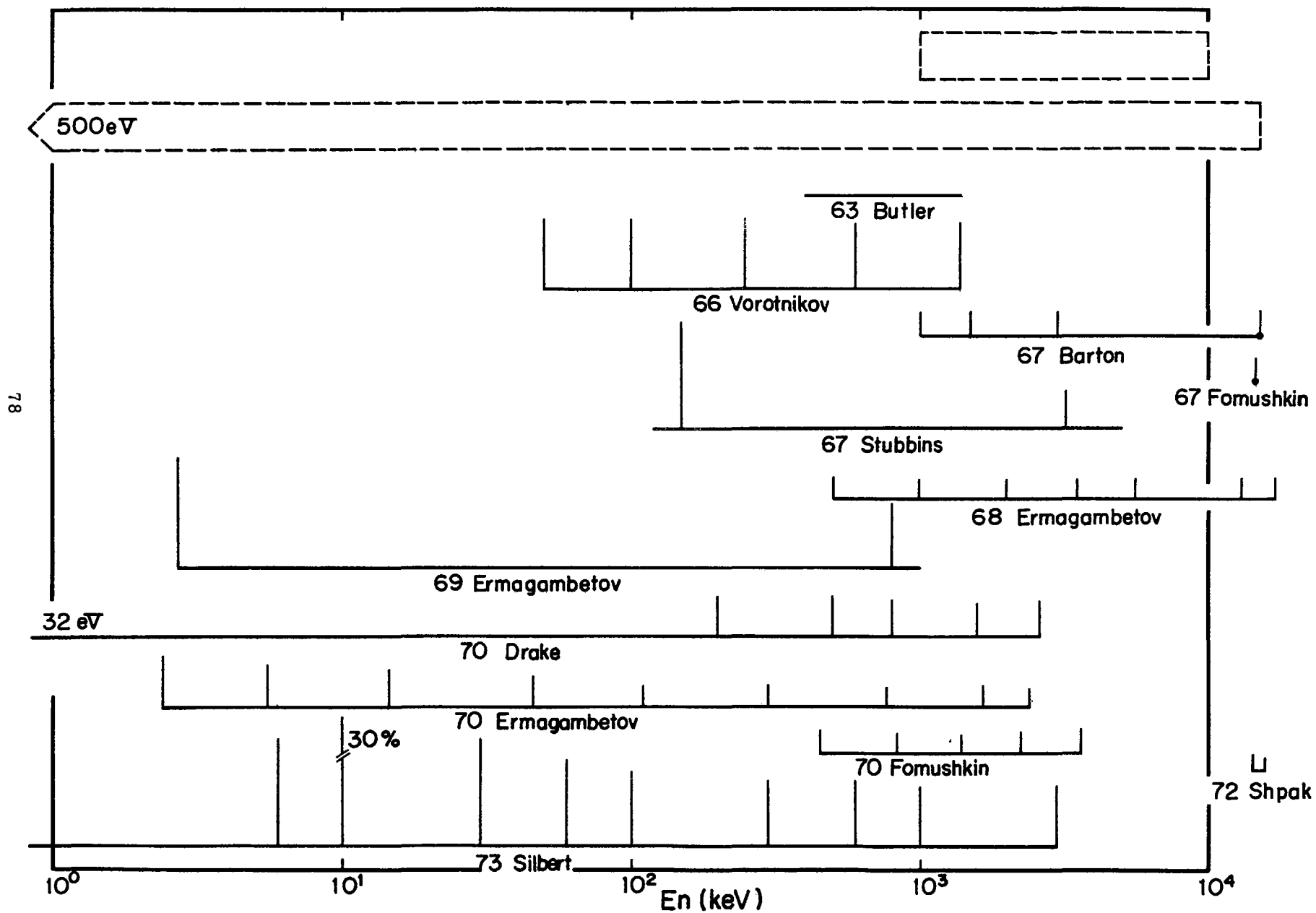


Fig.3.5.1(e)

^{238}Pu (n, γ)

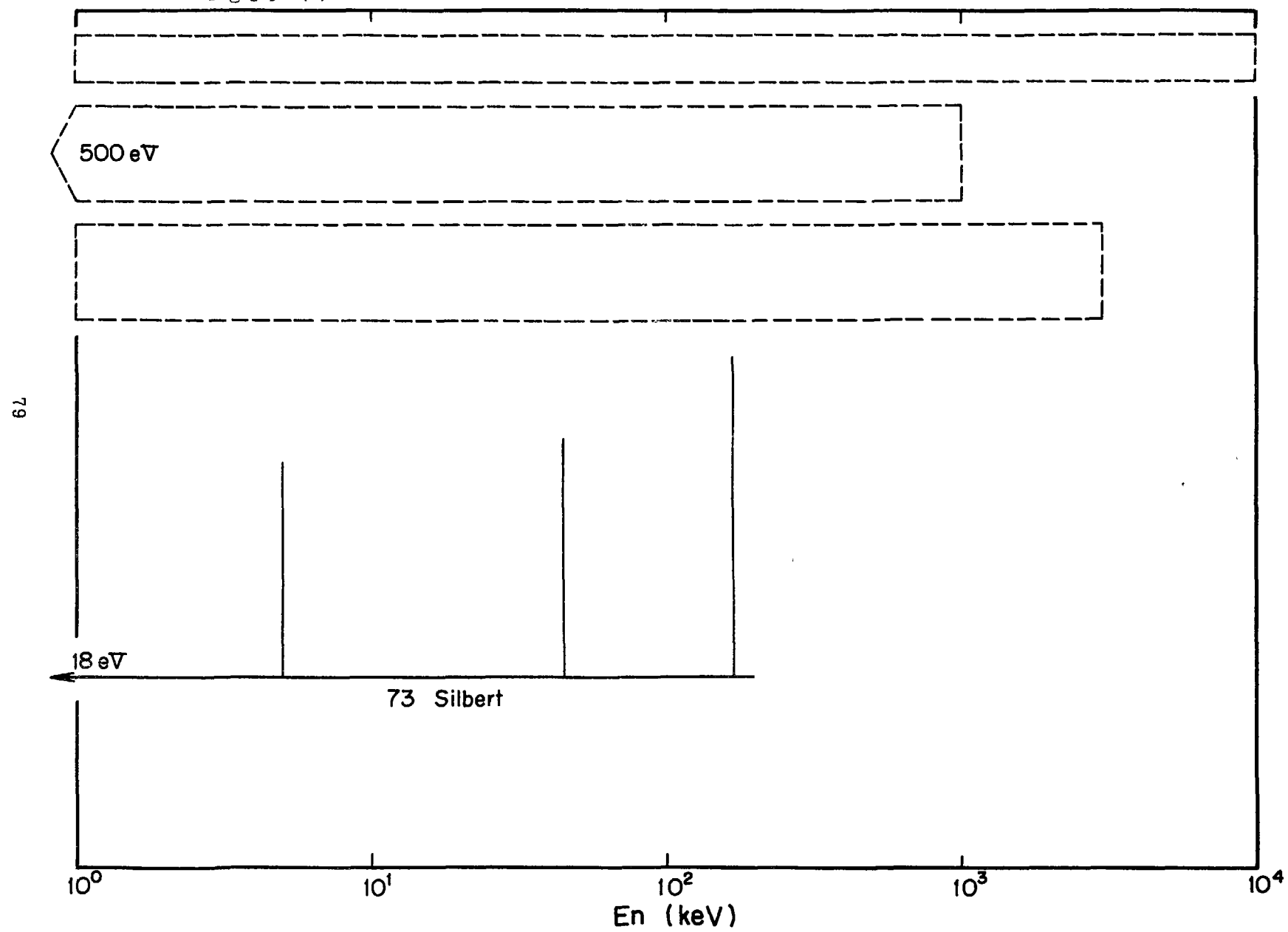
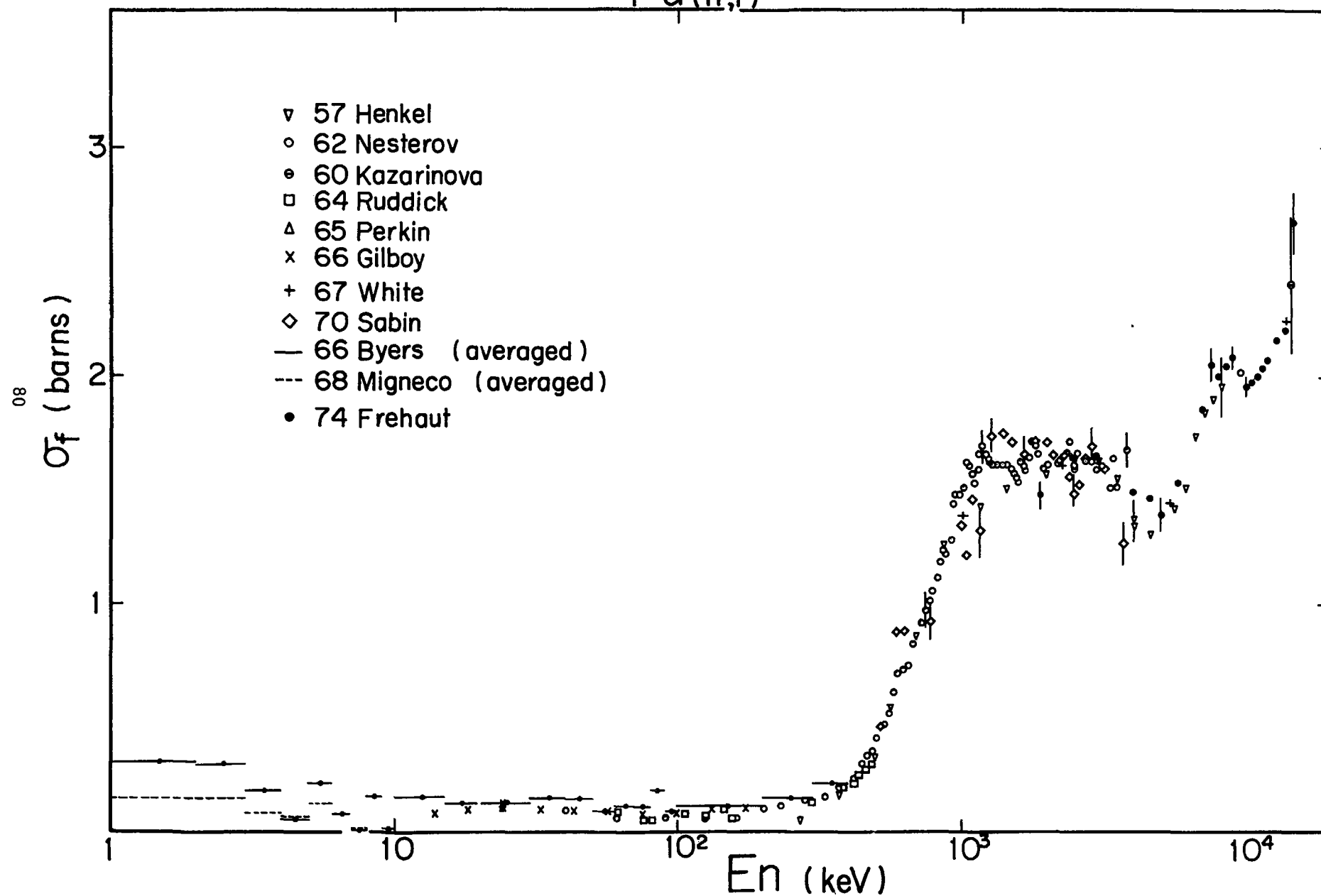
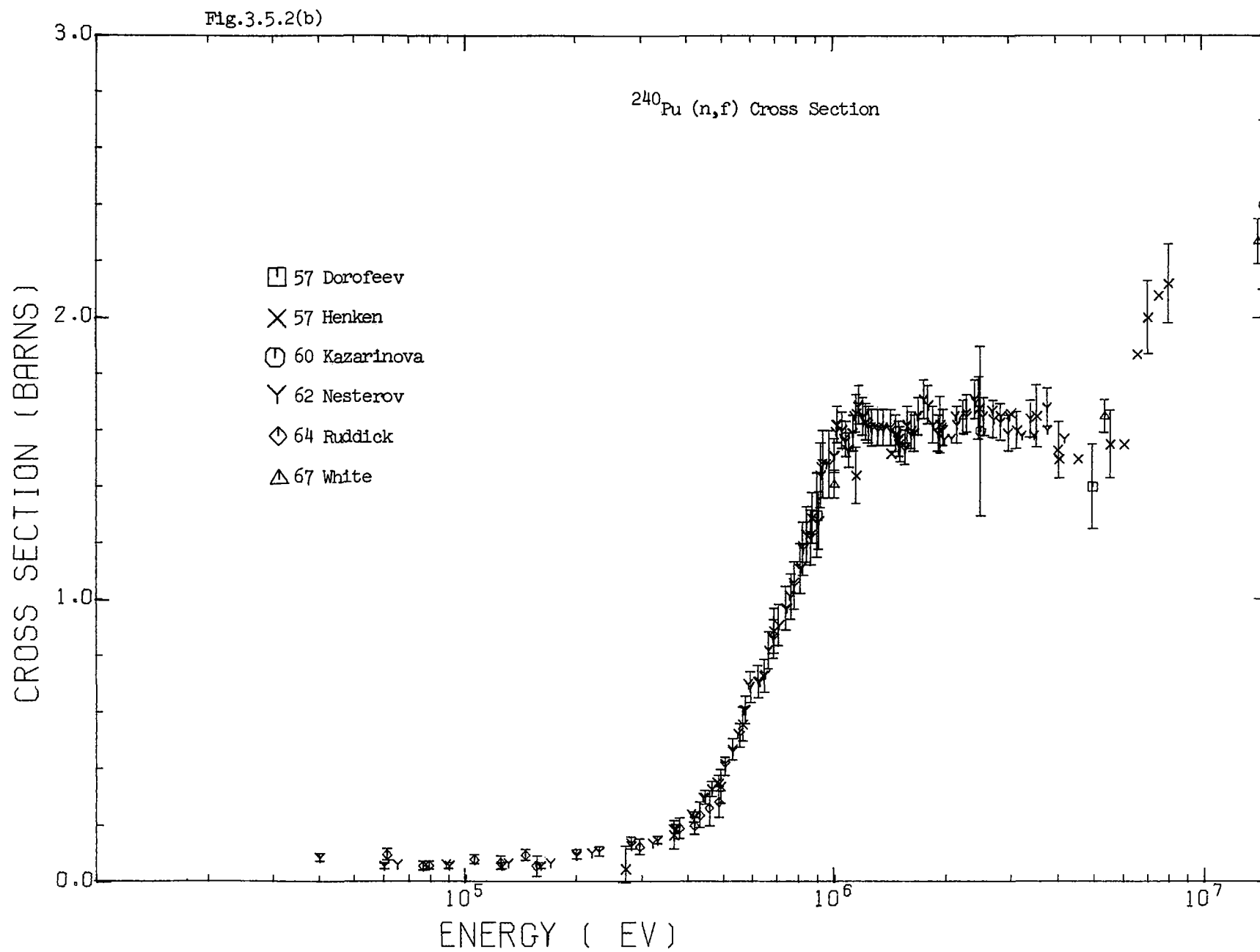


Fig.3.5.2(a)

 $^{240}\text{Pu}(n,f)$ 



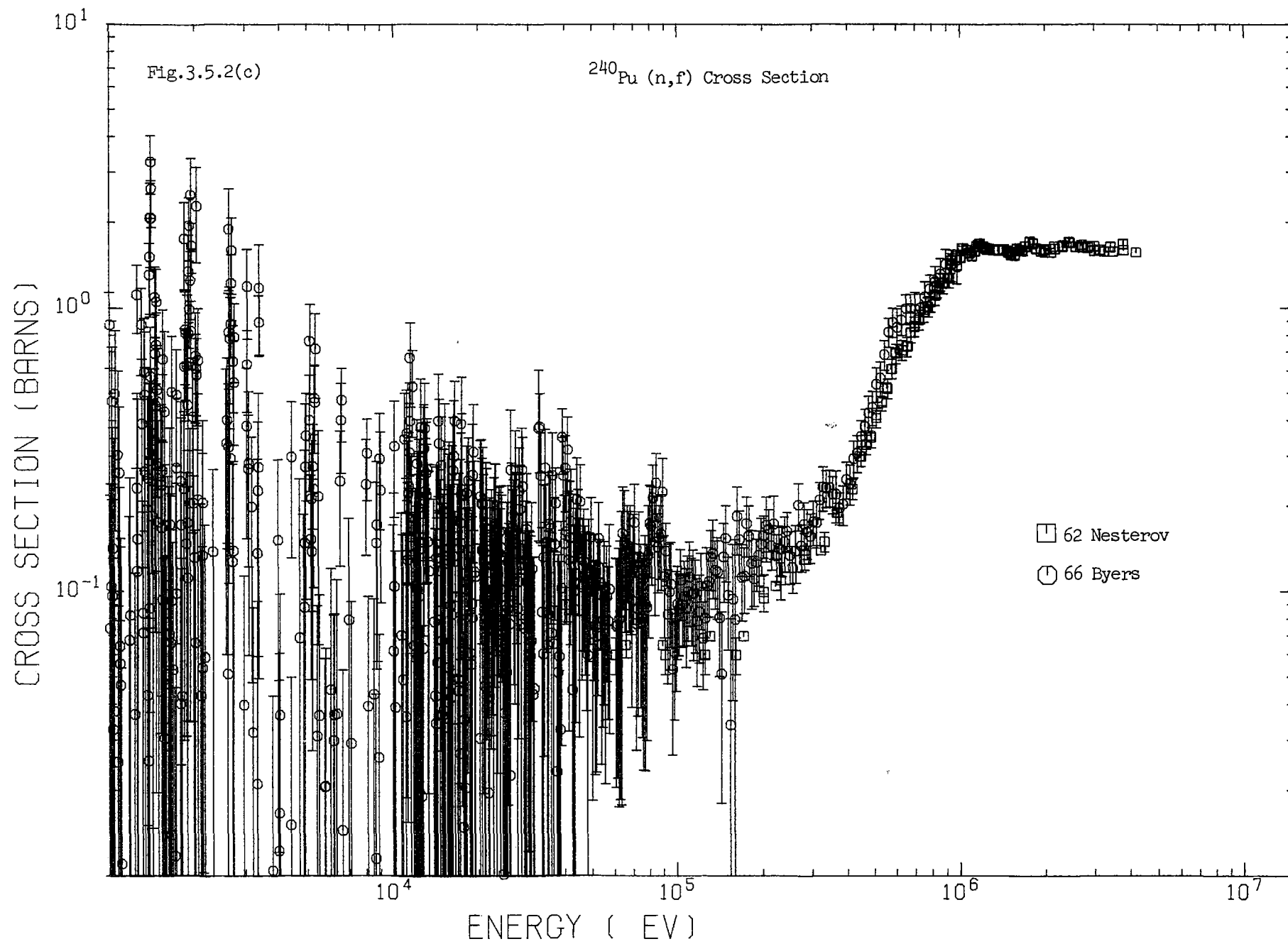


Fig.3.5.2(d)

^{240}Pu (total)

83

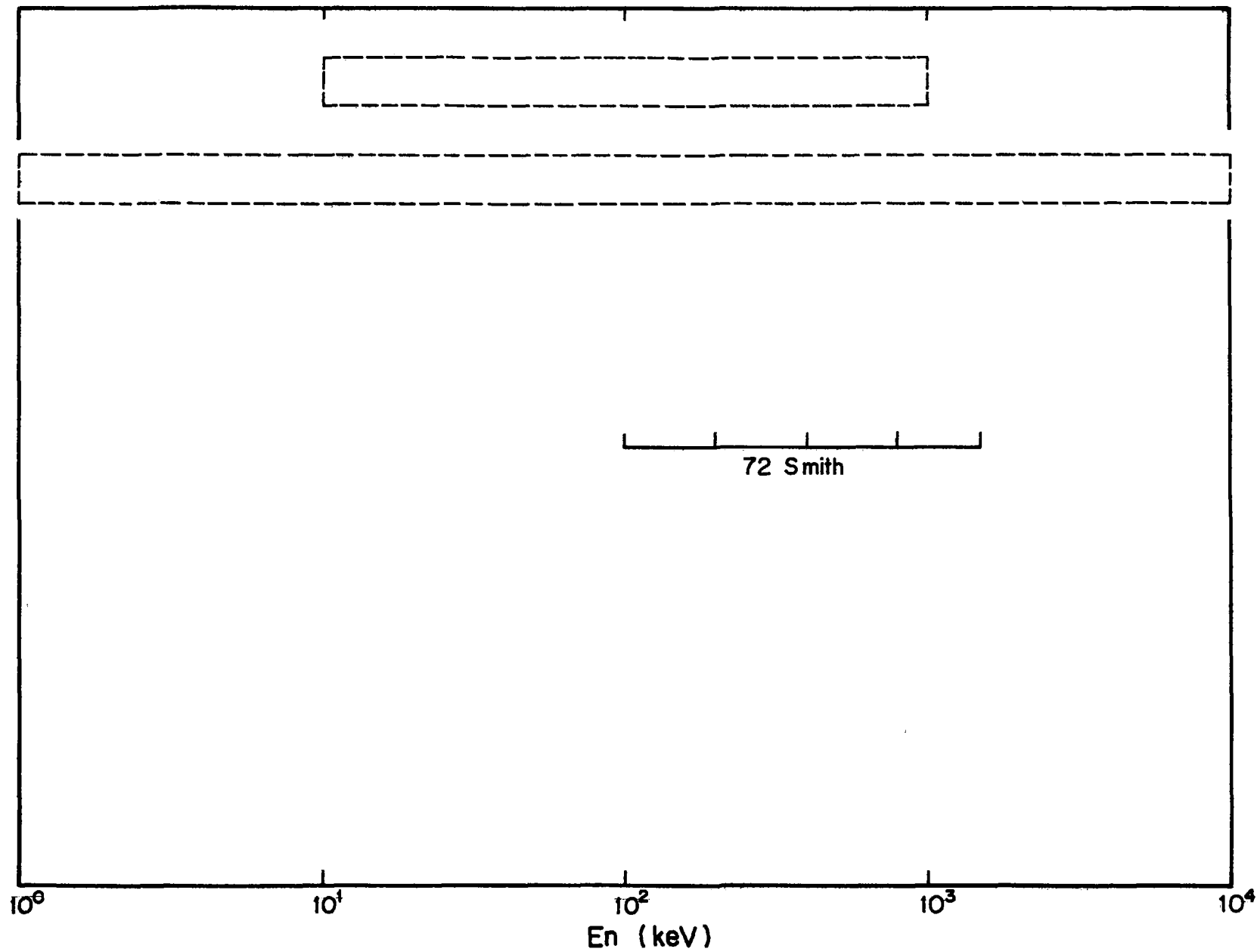


Fig.3.5.2(e) $^{240}\text{Pu} (n, \gamma)$

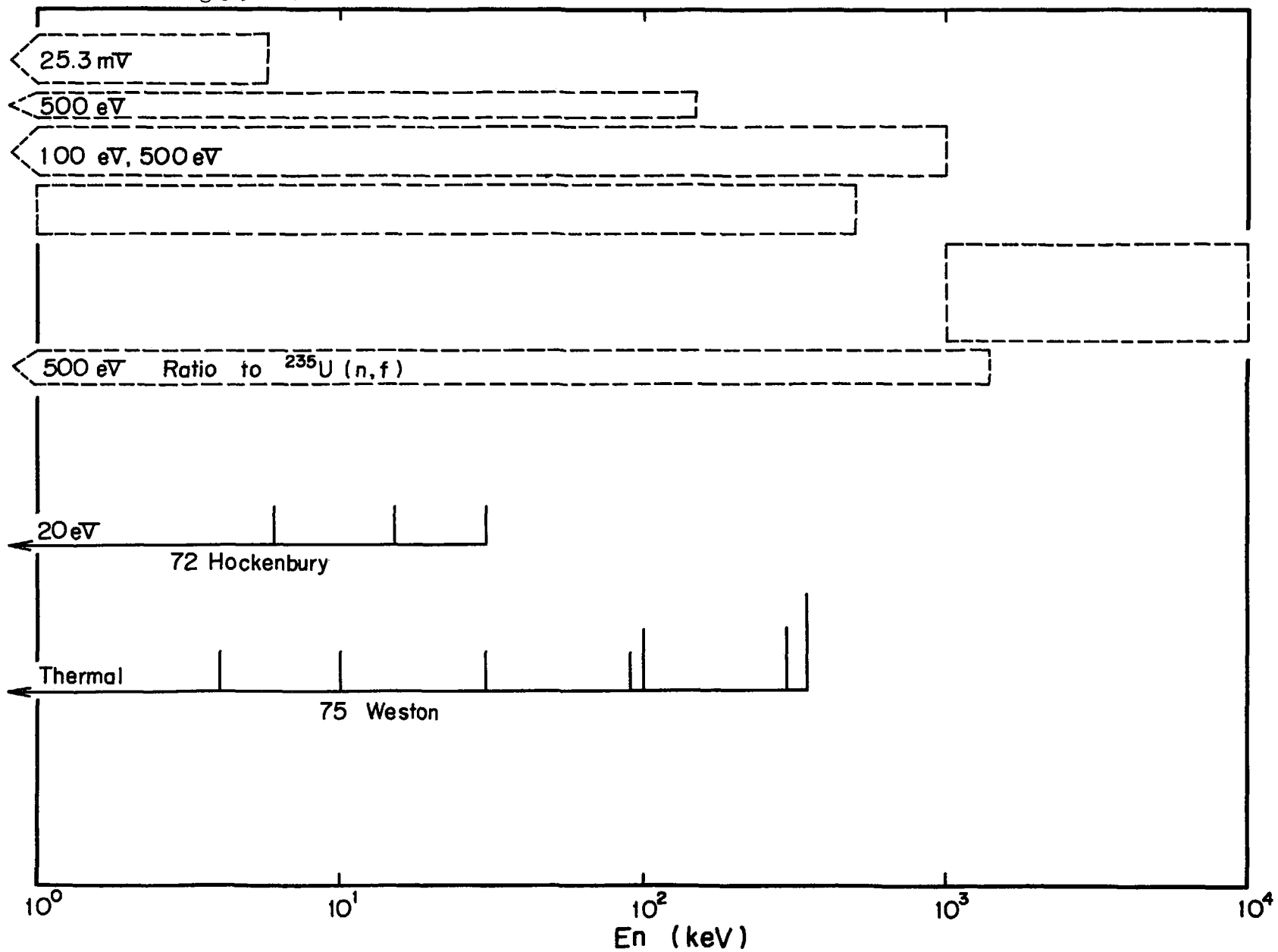


Fig.3.5.2(f)

^{240}Pu (n,f) ratio to ^{235}U (n,f)

85

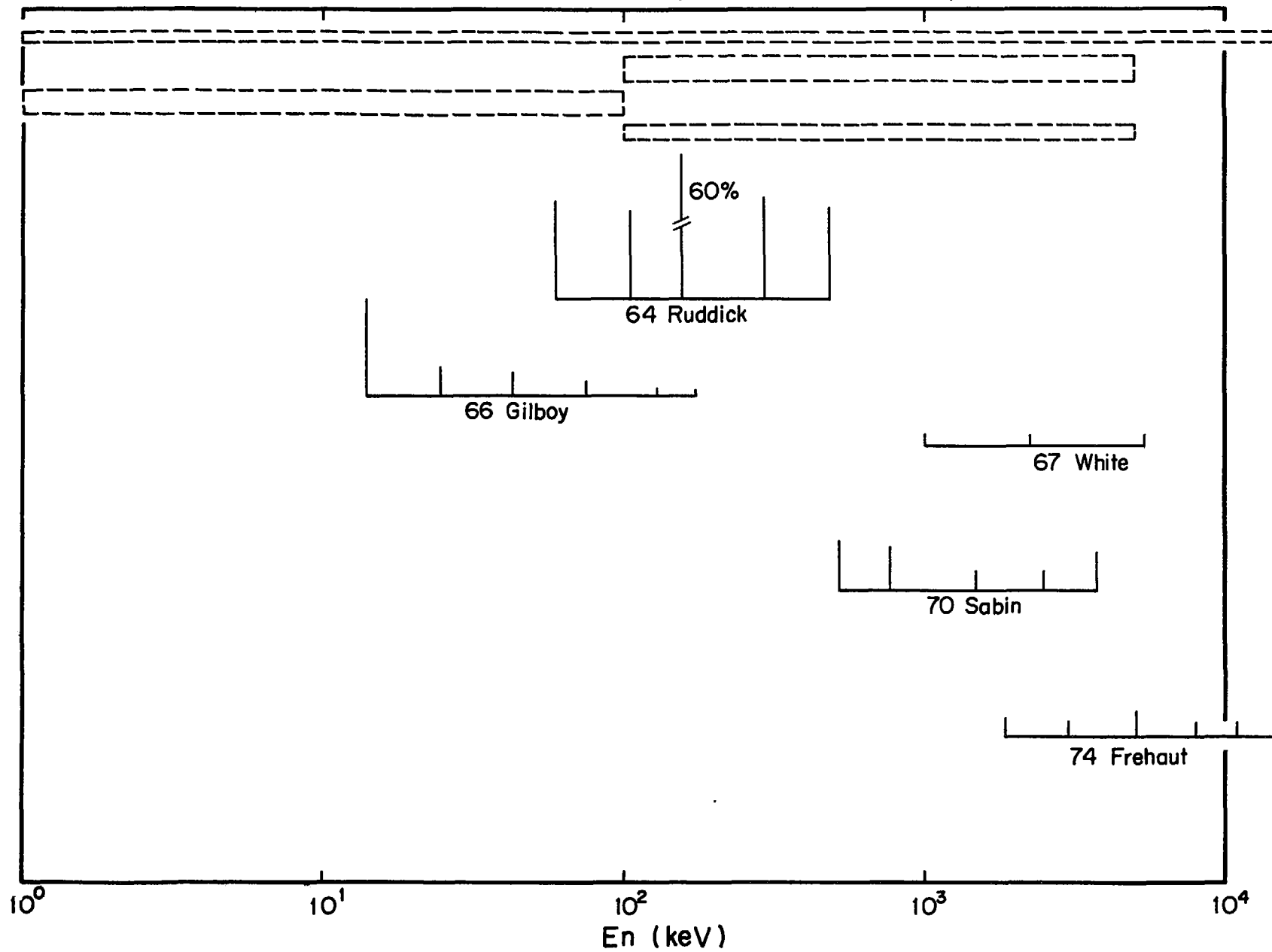


Fig.3.5.2(g)

^{240}Pu (n,f)

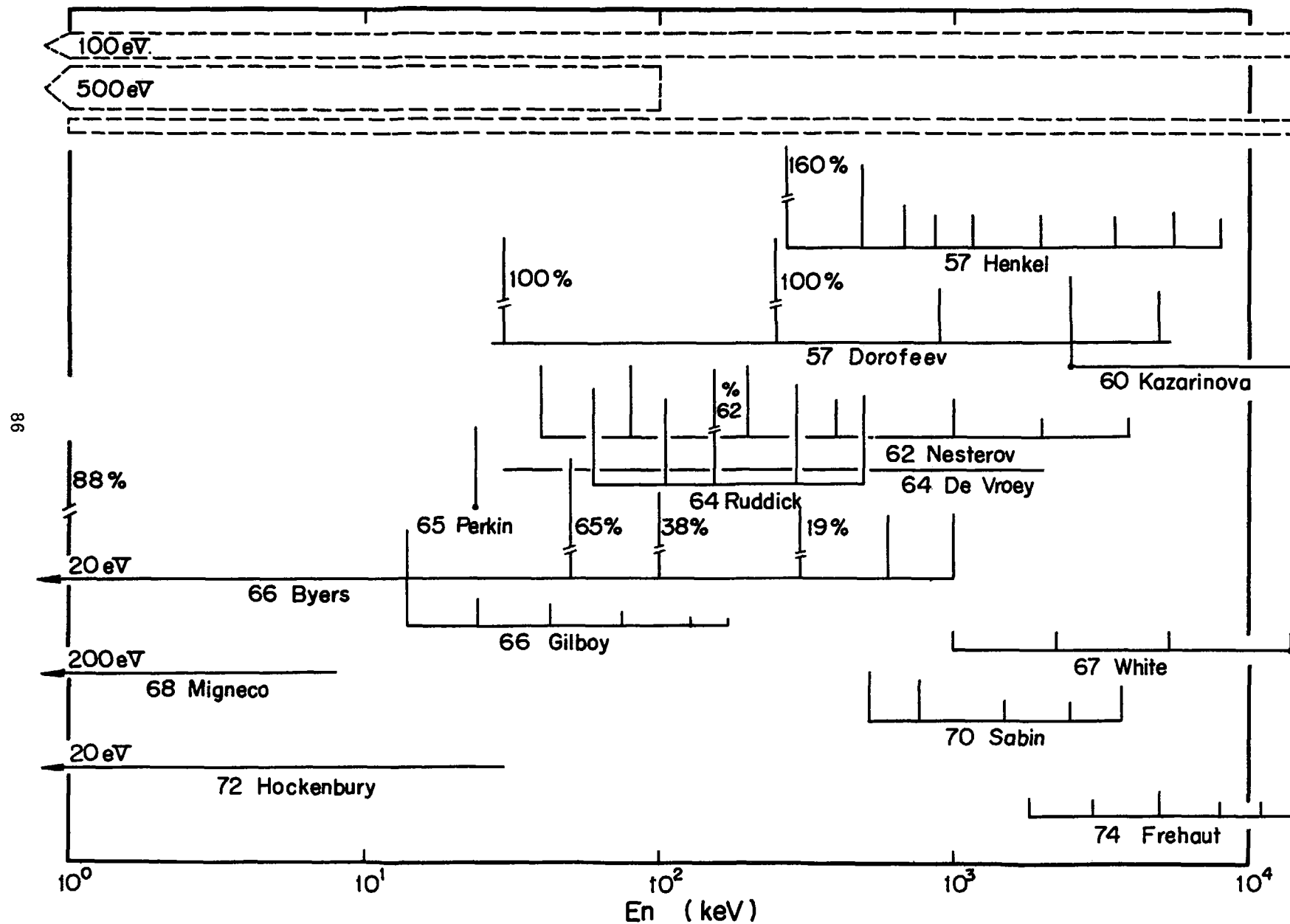


Fig.3.5.2(h)

$^{240}\text{Pu} \text{ (n,n')}$

87

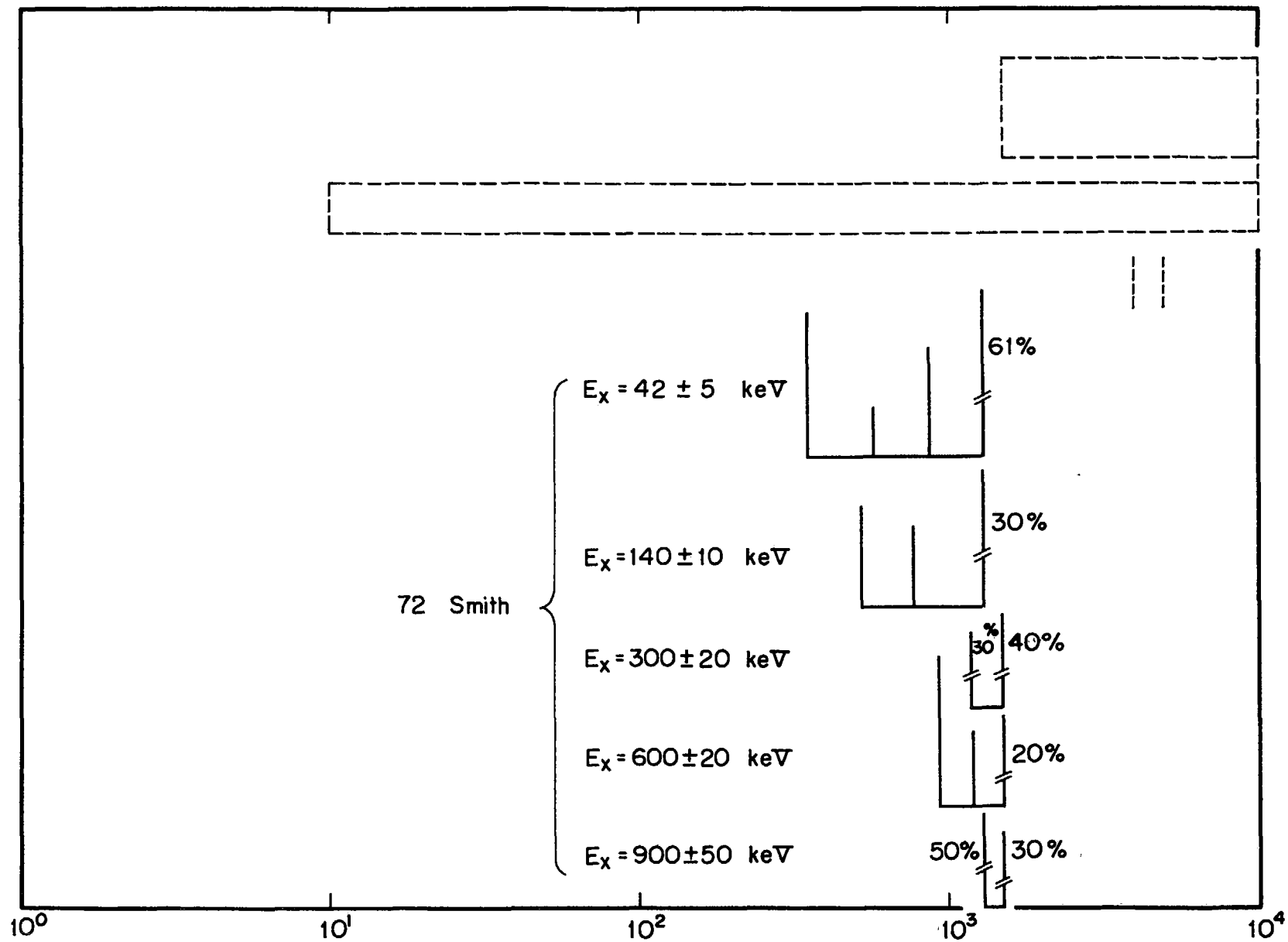


Fig.3.5.2(1)

^{240}Pu (Neutrons Emitted per Fission)

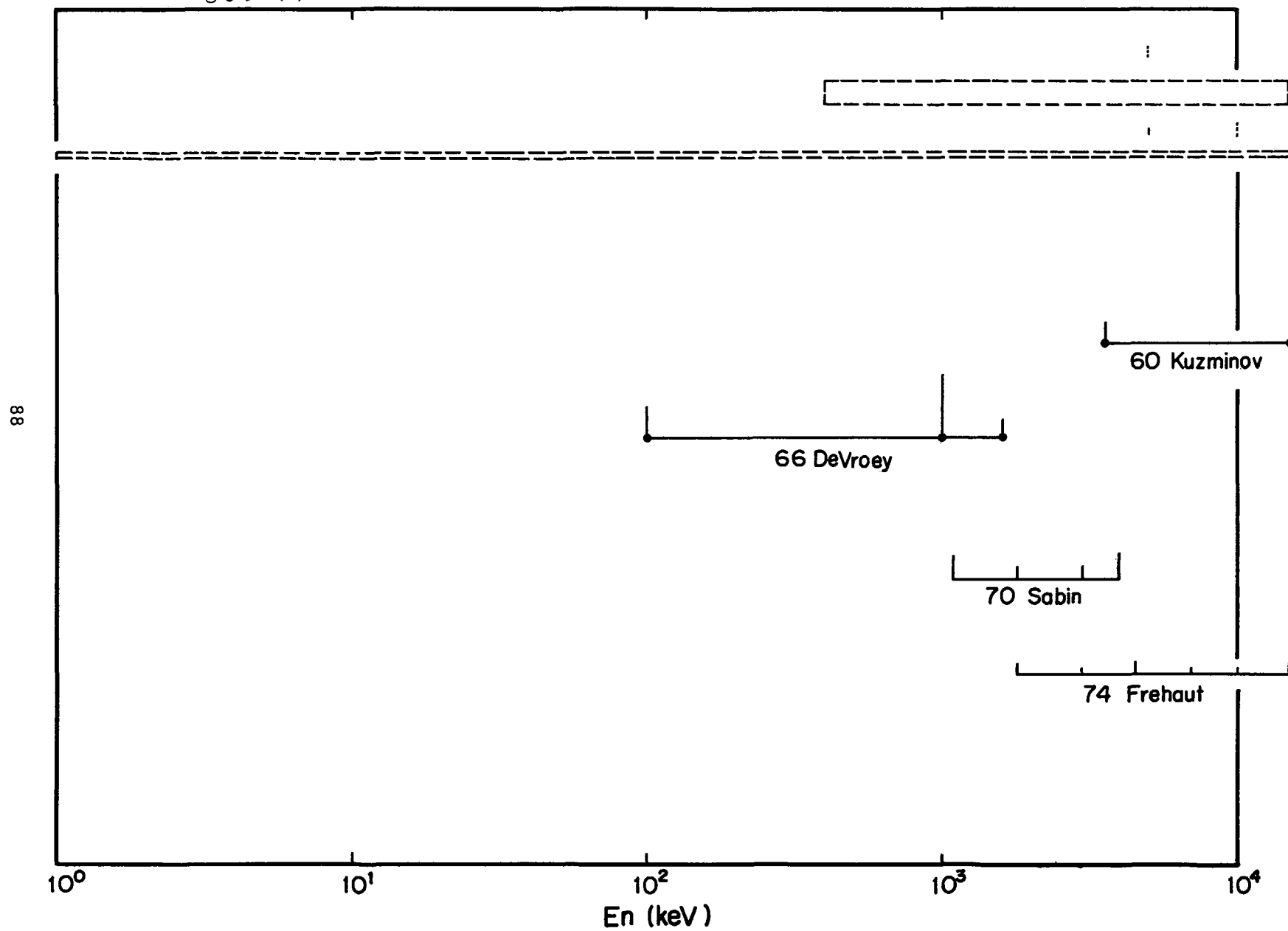
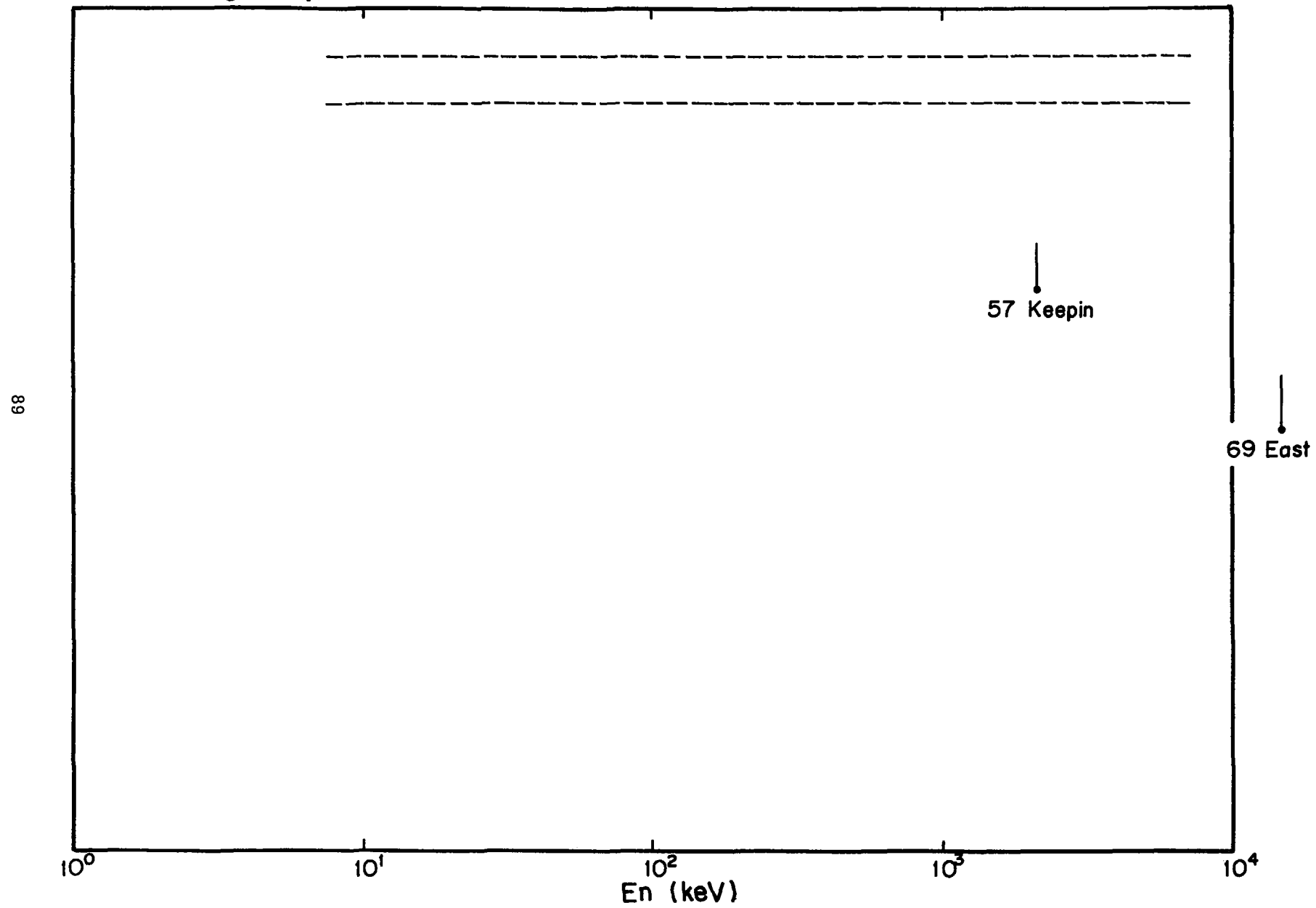


Fig.3.5.2(j) ^{240}Pu (Delayed Neutrons Emitted per Fission)



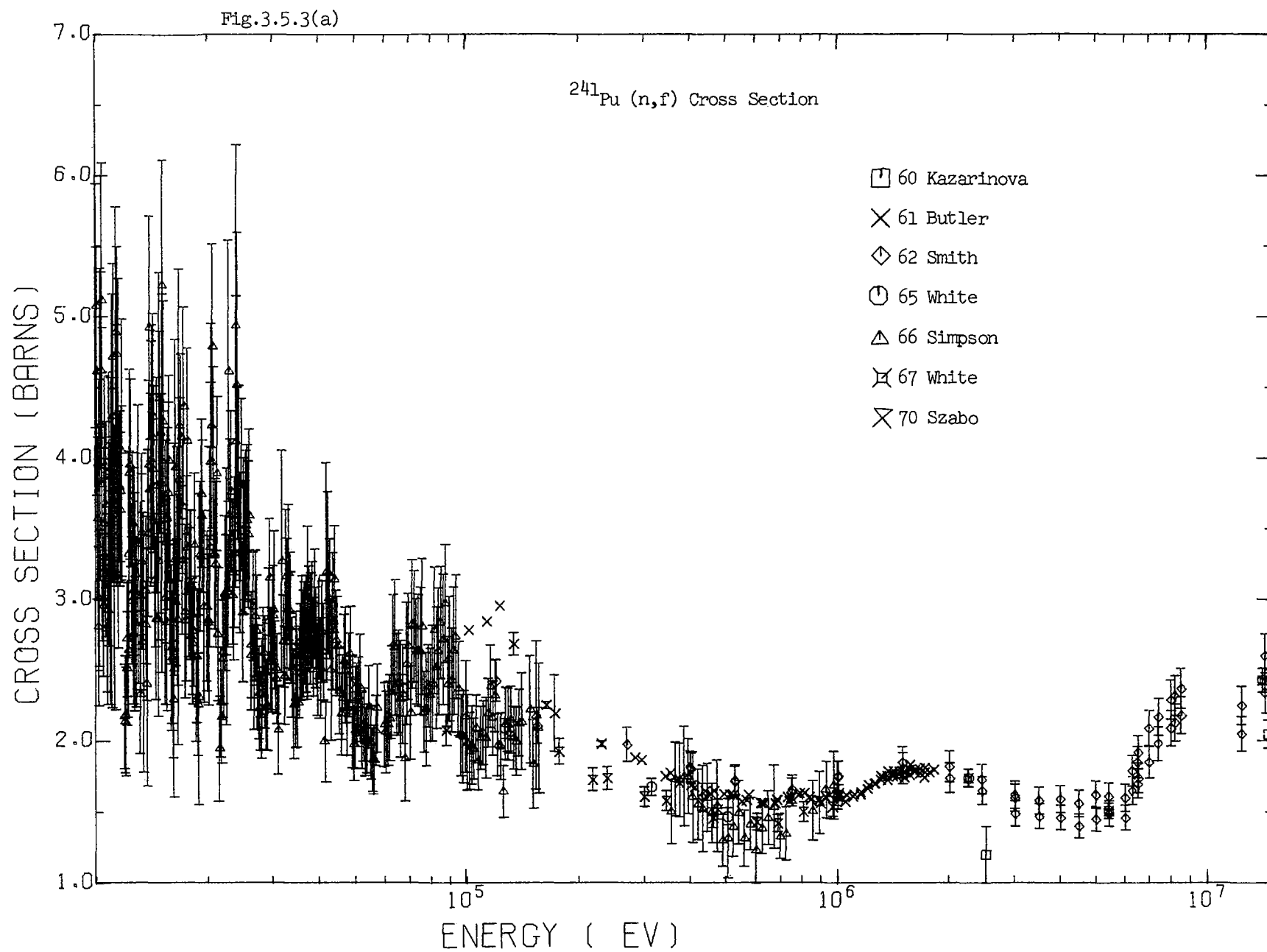
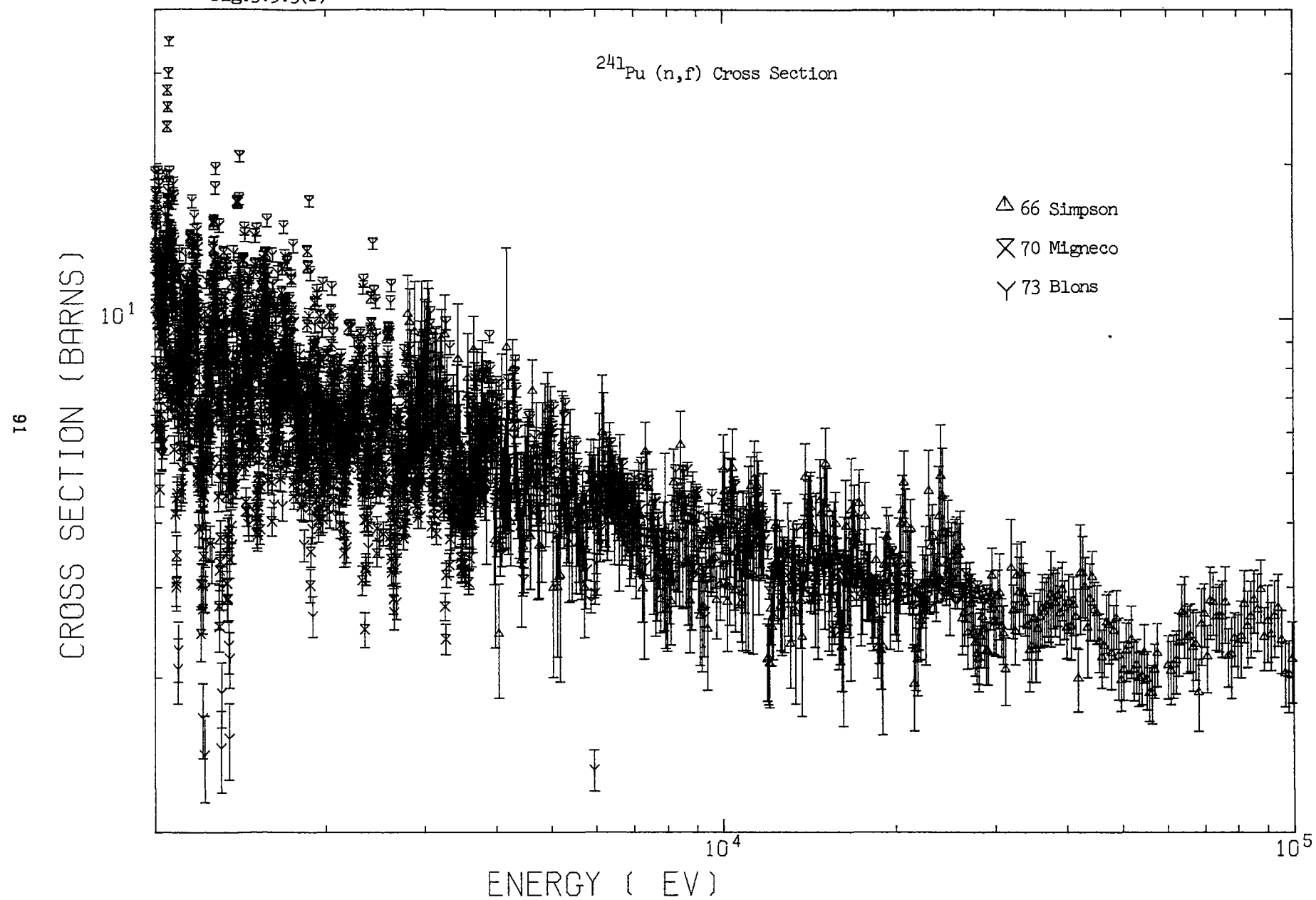


Fig.3.5.3(b)



^{241}Pu (total)

Fig.3.5.3(c)

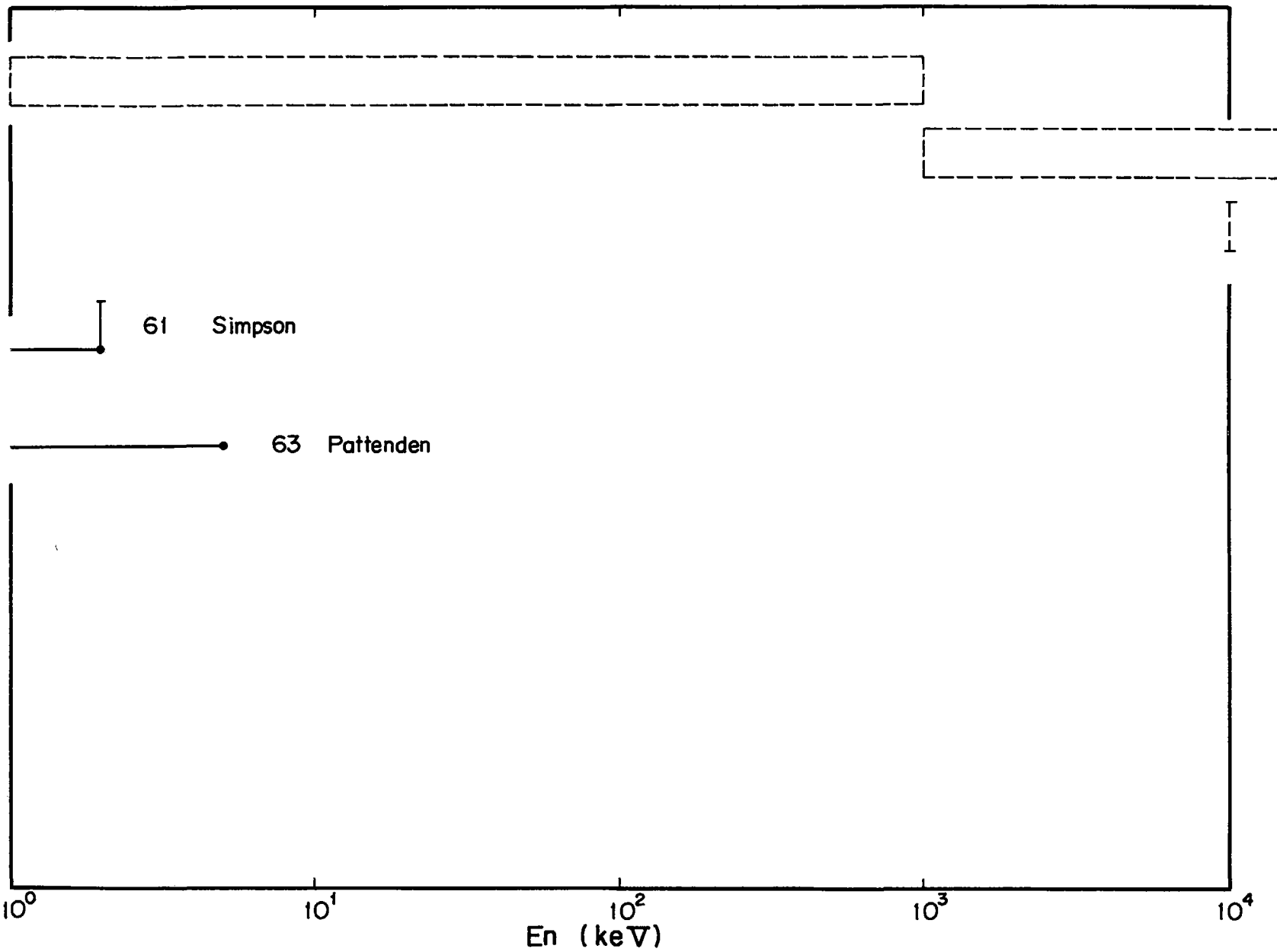
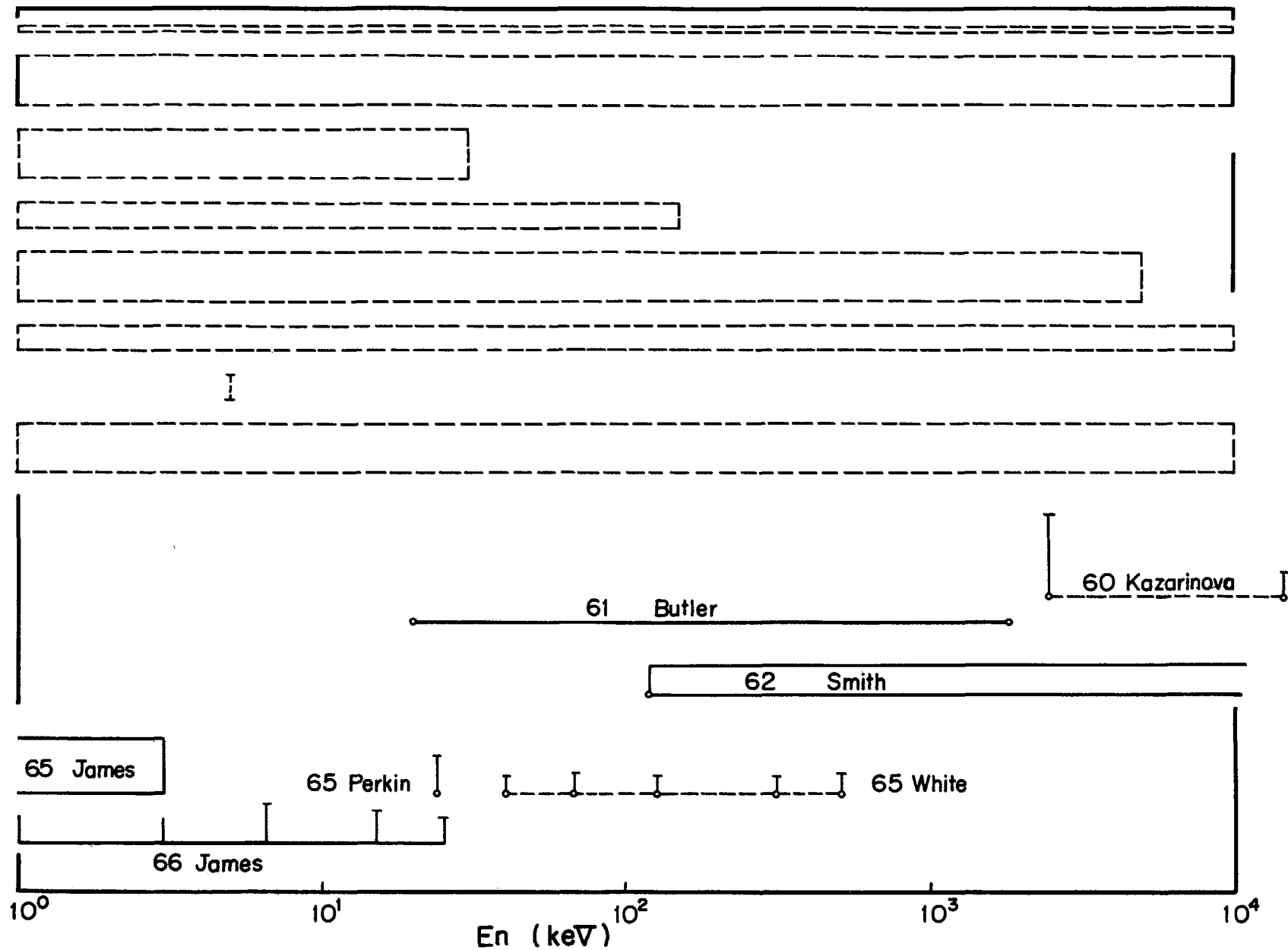


Fig.3.5.3(d)-1

$^{241}\text{Pu} (n,f)$

88



^{241}Pu (n,f) (continue)

Fig.3.5.3(d)-2

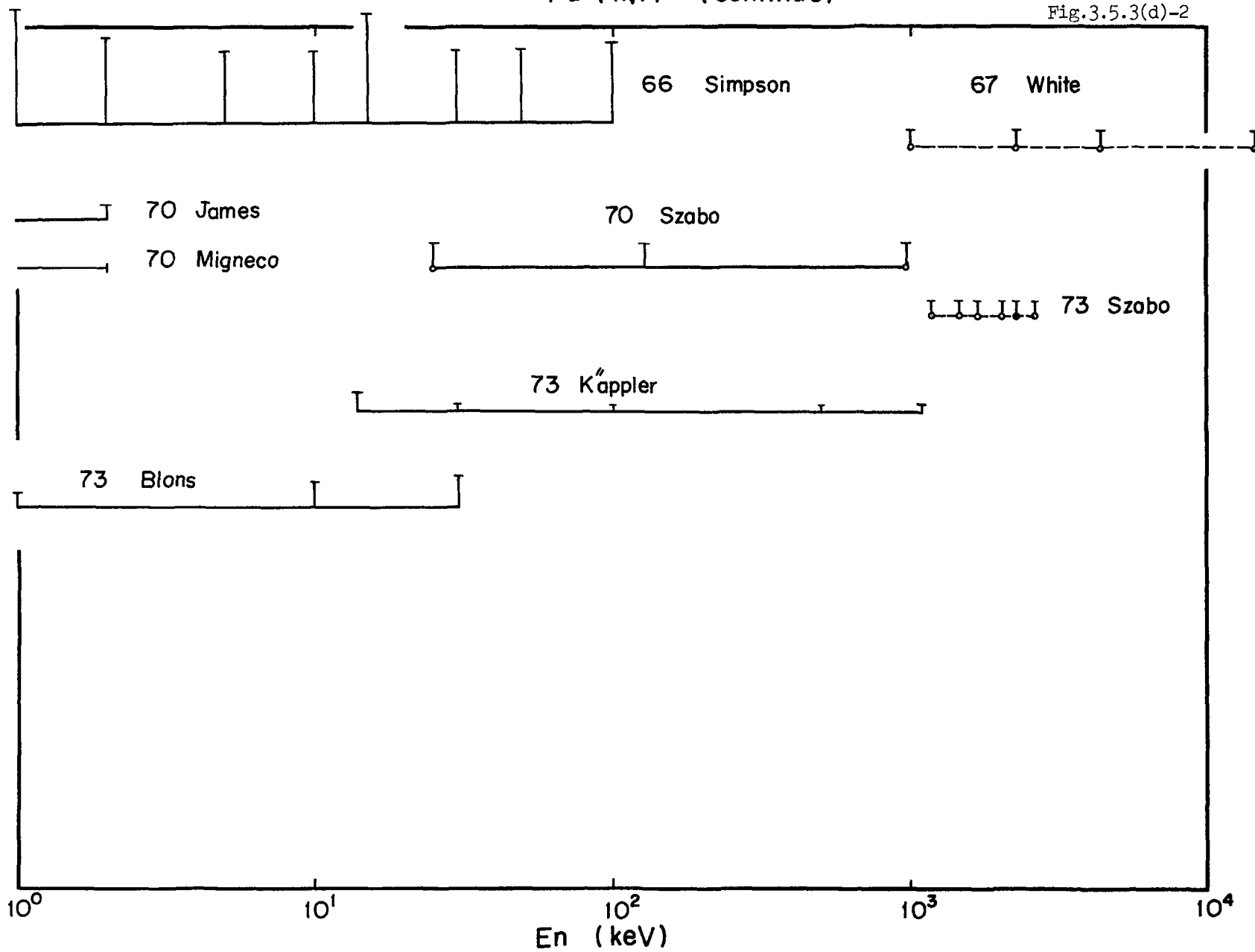


Fig.3.5.3(e)

^{241}Pu (ν_p)

95

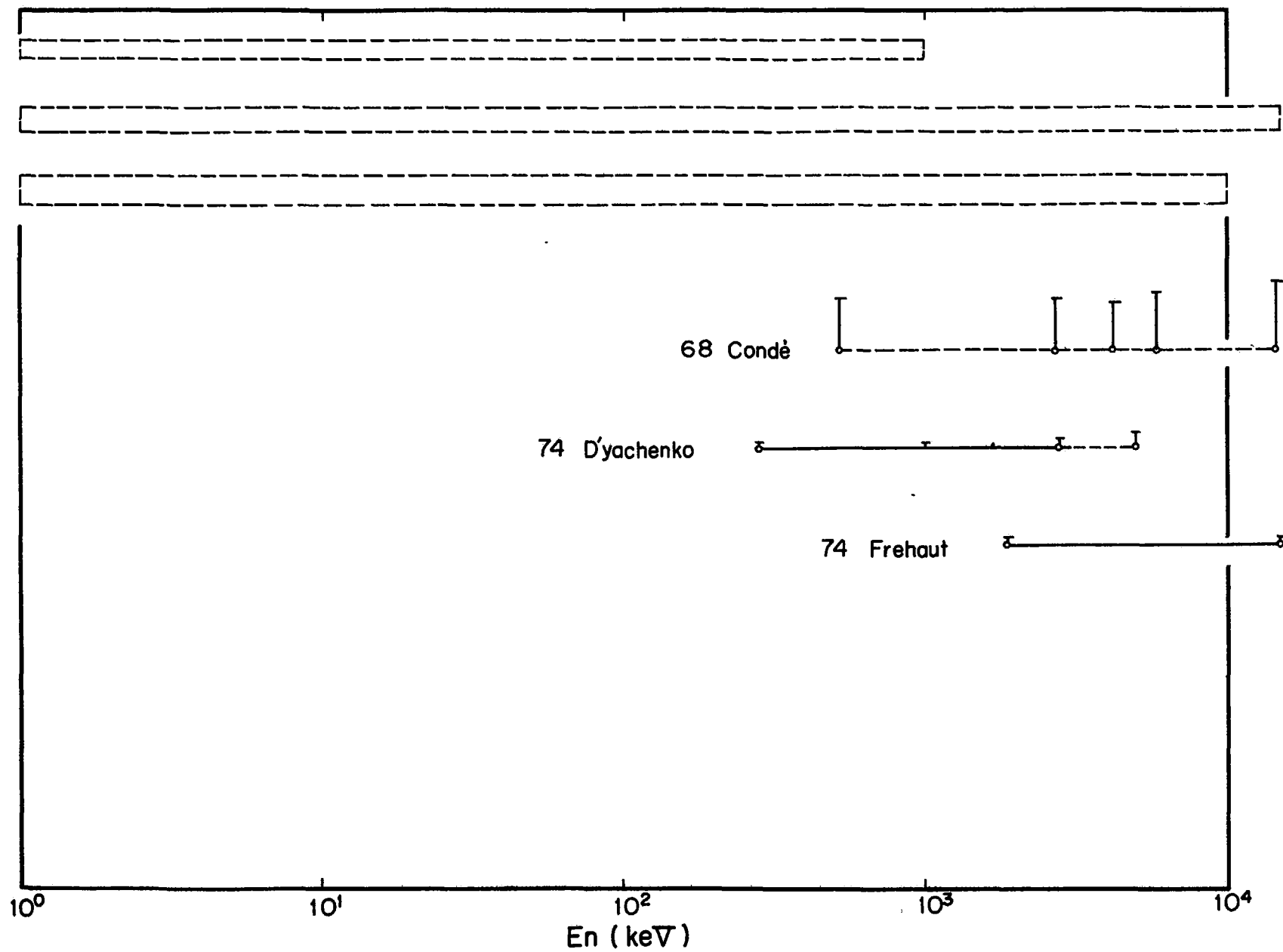
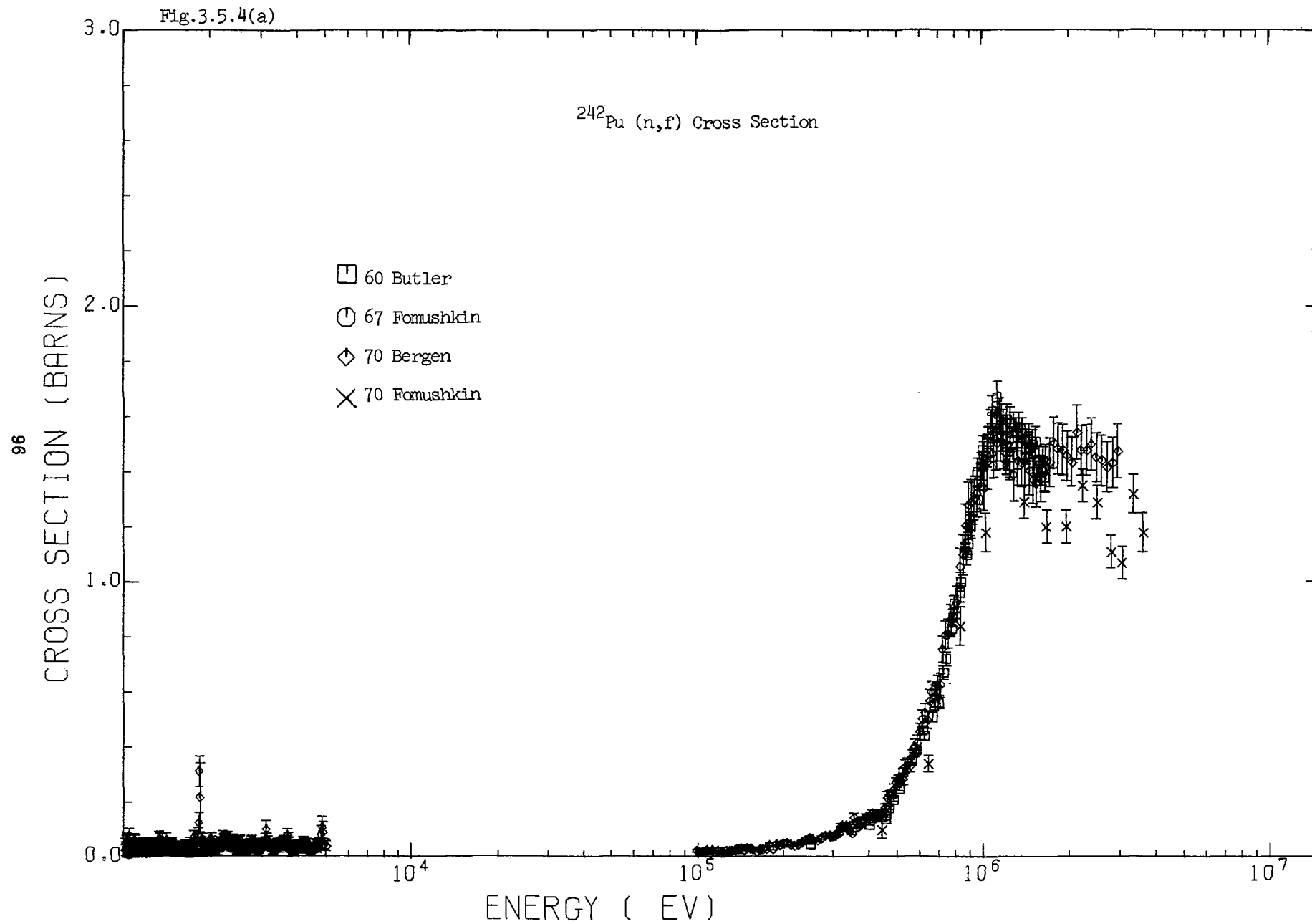
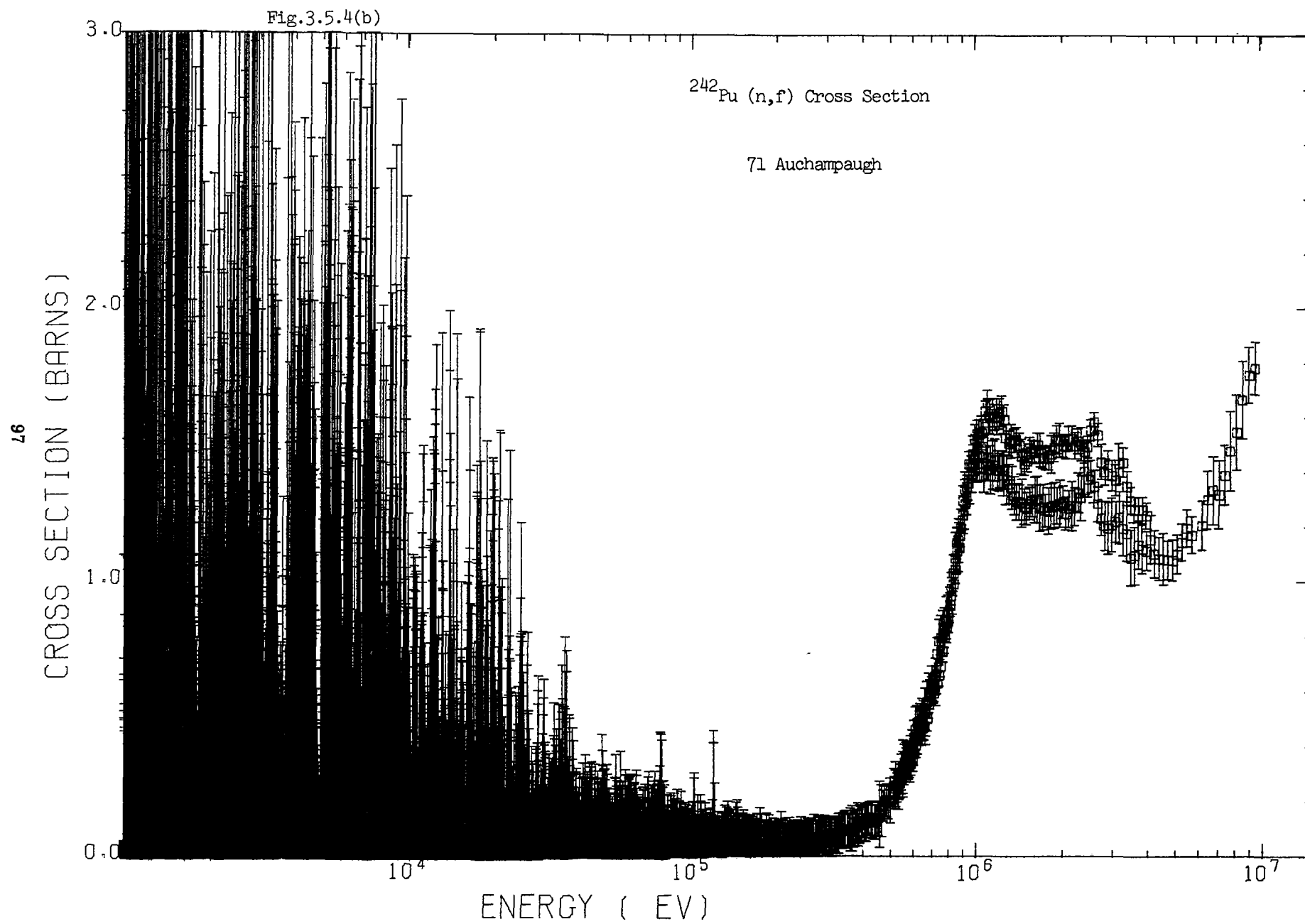
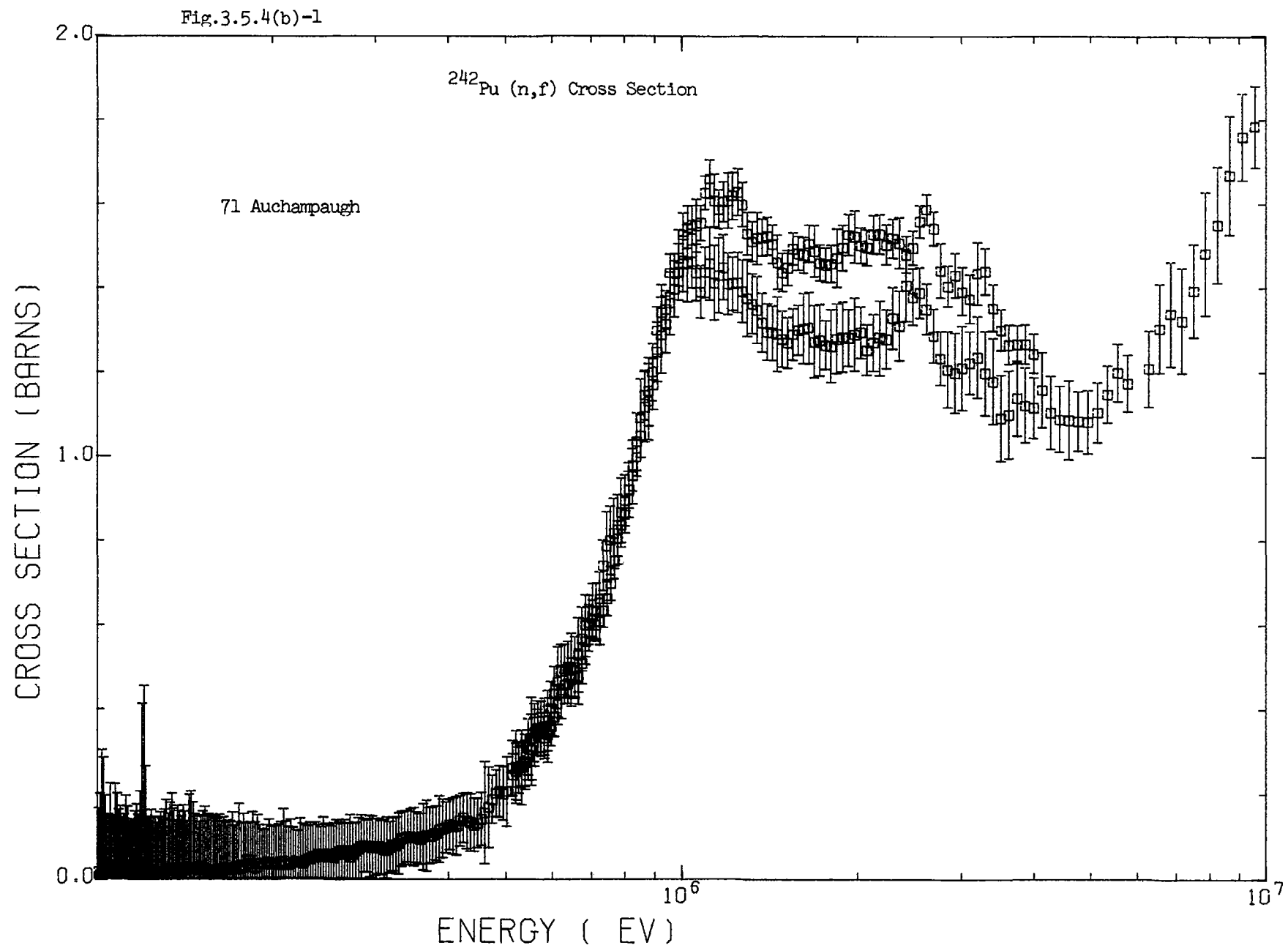


Fig.3.5.4(a)







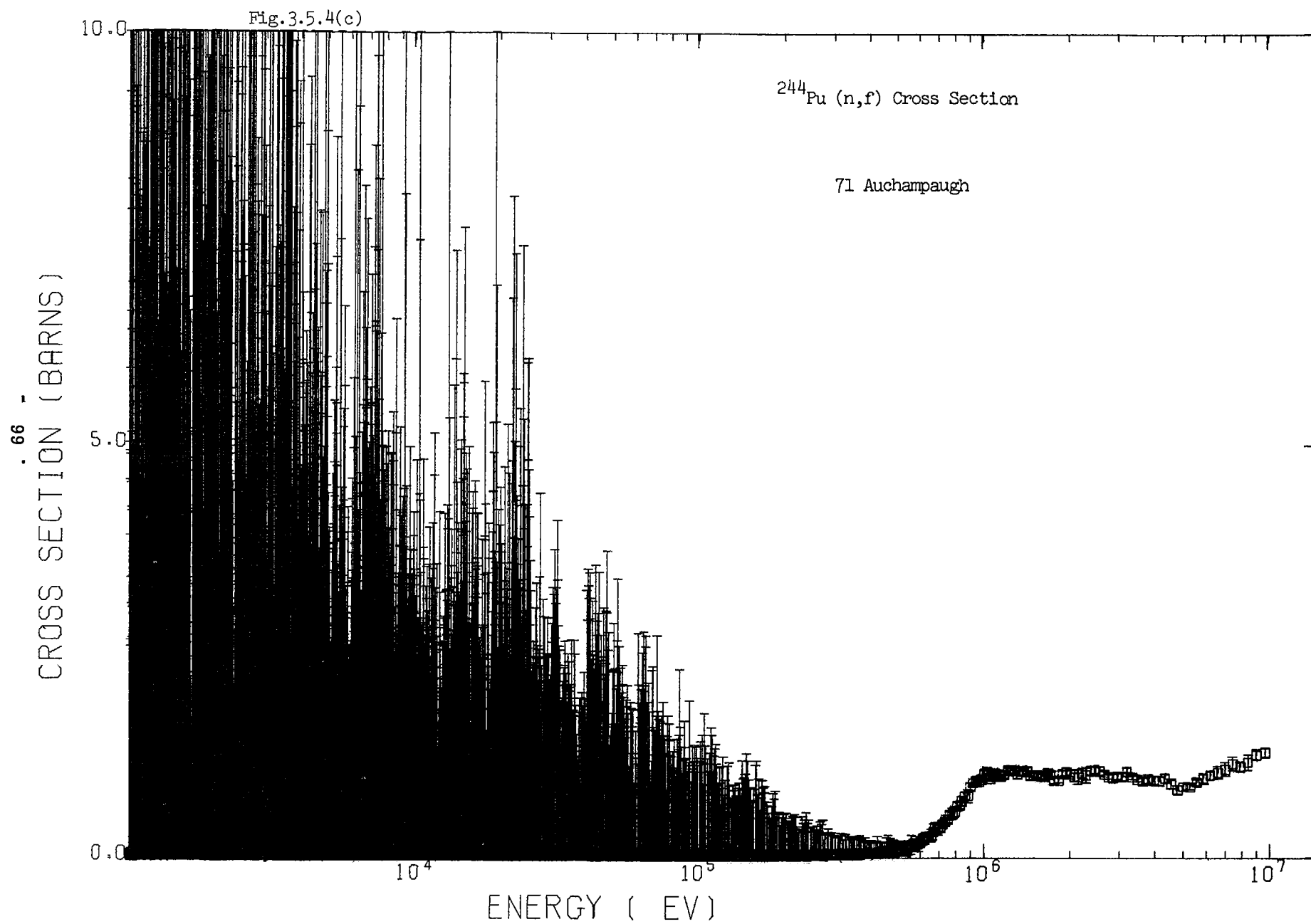


Fig.3.5.4(d) ^{242}Pu (n,f)

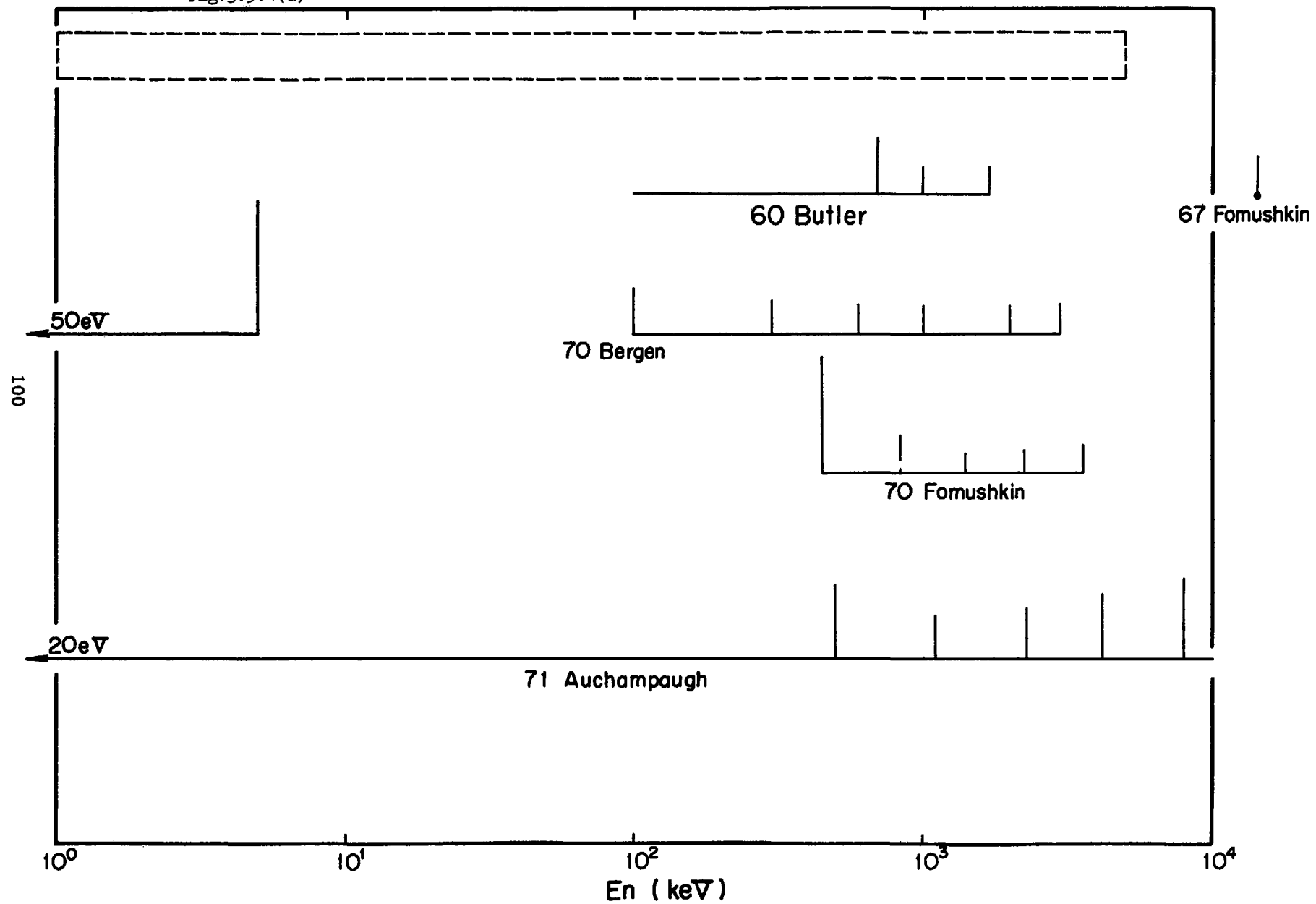


Fig.3.5.4(e)

$^{242}\text{Pu} \text{ (n, } \gamma \text{)}$

25.3 mV

500 eV

67 Bell

20 eV

73 Poortmans

101

10^0

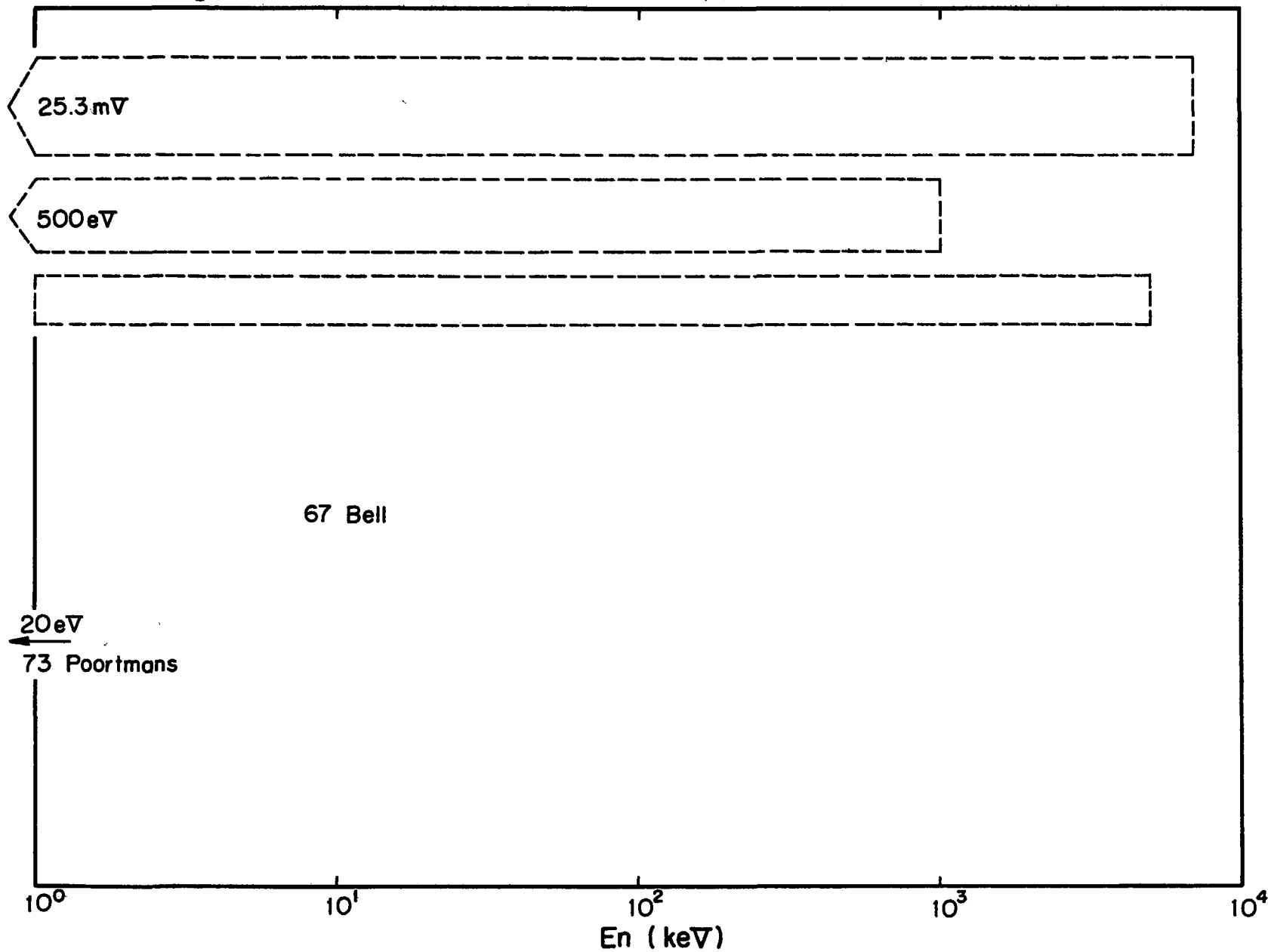
10^1

10^2

10^3

10^4

En (keV)



References for Review on ^{238}Pu , ^{240}Pu , ^{242}Pu , ^{243}Pu and ^{244}Pu Data

57 Dorofeev

Dorofeev, G.A., Dobrynin, Y.P.,
J. Nucl. Energy 11 ('57) 217

57 Henkel

Henkel, R.L., Nobles, R.A., Smith, R.K.,
AECD-4256 ('57)

57 Keepin

Keepin, G.R., Wimet, T.F., Zeigler, R.K.,
J. Nucl. Energy 6 ('57) 1,
Phys. Rev. 107 ('57) 1044

60 Butler *

60 Kazarinova

Kazarinova, M.I., Zamuyatin, Yu.S., Golbachev, V.M.,
Atom. Energiya 8 ('60) 139

60 Kuzminov

Kuzminov, B.D.,
AEC-Tr-4710 ('60)

62 Nesterov

Nesterov, V.G., Smirenkin, G.N.,
J. Nucl. Energy 16 ('62) 51,
Atom. Energiya 9 ('60) 16,
J. Exptl. Theoret. Phys. 35 ('58) 532

63 Butler

Butler, D.K., Sjoblom, R.K.,
Bul. Amer. Phys. Soc. 8 ('63) 369

64 DeVroey

DeVroey, M., Ferguson, A.T.G., Starfelt, N.,
AERE-PR/NP7 P.1 ('64)

64 Ruddick

Ruddick, P., White, P.H.,
J. Nucl. Energy 18 ('64) 561

65 Perkin

Perkin, J.L., White, P.H., Fieldhouse, P., Axton, E.J.,
Cross, P., Robertson, J.C.,
J. Nucl. Energy 19 ('65) 423

66 Byers

Byers, D.H., Diven, B.C., Silbert, M.G.,
LA-3586 ('66)

66 DeVroey

DeVroey, M., Ferguson, A.T.G., Starfelt, N.,
J. Nucl. Energy 20 ('66) 191

66 Gilboy

Gilboy, W.B., Knoll, G.F.,
KFK-450 ('66)

66 Vorontnikov

Vorontnikov, P.E., Dubrovina, S.M., Otroshchenko, G.A.,
Shigin, V.A.,
Sov. J. Nucl. Phys. 3 ('66) 348

67 Barton

Barton, D.M., Koontz, P.G.,
Phys. Rev. 162 ('67) 1070

67 Bell

Bell, C.I.,
Phys. Rev. 158 ('67) 1127

67 Fomushkin

Fomushkin, E.F., Gutnikova, E.K., Zamyatnin, Yu.S., Maslennikov,
B.K., Belov, V.N., Surin, V.M., Nasyrov, F., Pashkin, N.F.,
Sov. J. Nucl. Phys. 5 ('67) 689

67 Stubbins

Stubbins, W.F., Bowman, C.D., Auchampaugh, G.F., Coops, M.S.,
Phys. Rev. 154 ('67) 1111

67 White

White, P.H., Warner, G.P.,
J. Nucl. Energy 21 ('67) 671

67 Young

Young, T.E., Simpson, F.B., Berreth, J.R., Coops, M.C.,
Nucl. Sci. Eng. 30 ('67) 355

68 Ermagambetov

Ermagambetov, S.B., Smirenkin, G.N.,
Sov. J. Atom. Energy 25 ('68) 1364

68 Migneco

Migneco, E., Theobald, J.P.,
Nucl. Phys. A112 ('68) 603

69 East

East, L.V., Keepin, G.R.,
"Physics and Chemistry of Fission" P.647. IAEA ('69)

69 Ermagambetov

Ermagambetov, S.B., Smirenkin, G.N.,
JETP Letters 9 ('69) 309

70 Bergen

Bergen, D.W., Fullwood, R.R.,
LA-4420 P.123 ('70),
Nucl. Phys. A163 ('71) 577

70 Cramer

Cramer, J.D., Britt, H.C.,
Nucl. Sci. Eng. 41 ('70) 177

70 Drake

Drake, D.M., Bowman, C.D., Coops, M.S., Hoff, R.W.,
LA-4420 P.101 ('70)

70 East

East, L.V., Auguston, R.H., Menlove, H.O., Masters, C.F.,
Trans. Am. Nucl. Soc. 13 ('70) 760

70 Ermagambetov

Ermagambetov, S.B., Smirenkin, G.N.,
Sov. J. Atom. Energy 29 ('70) 1190

70 Fomushkin

Fomushkin, E.F., Gutnikova, E.K.,
Sov. J. Nucl. Phys. 10 ('70) 529,
INDC (CCP)-7/U

70 Sabin-1

Sabin, M.V., Khokhlov, Yu.A., Zamyatnin, Yu.S., Paramonova,
I.N.,
Sov. J. Atom. Energy 29 ('70) 938

70 Sabin-2

Sabin, M.V., Khokhlov, Yu.A., Zamyatnin, Yu.S., Paramonova,
I.N.,
"Second International Data for Reactors" Vol.2 P.157
IAEA ('70),
INDC (CCP) - 15/U ('70)

70 Young

Young, T.E., Reeder, S.D.,
Nucl. Sci. Eng. 40 ('70) 389

71 Androsenko

Androsenko, Kh.D., Smirenkin, G.N.,
Sov. J. Nucl. Phys. 12 ('71) 142

71 Auchampaugh

Auchampaugh, G.F., Farrel, J.A., Bergen, D.W.,
Nucl. Phys. A171 ('71) 31,
BNL-50276 P.132 ('70)

72 Hockenbury

Hockenbury, R.W., Moyer, W.R., Block, R.C.,
Nucl. Sci. Eng. 49 ('72) 153

72 Krick

Krick, M.S., Evans, A.E.,
Nucl. Sci. Eng. 47 ('72) 311
Evans, A.E., Thorpe, M.M., Krick, M.S.,
USNDC-3 P.127 ('72),
Nucl. Sci. Eng. 50 (1973) 80

72 Shpak

Shpak, D.L., Blokhin, A.I., Ostapenko, Yu.B., Smirenkin, G.N.,
JETP Letters 15 ('72) 228

72 Smith

Smith, A.B., Lambropoulos, P.P., Whalen, J.F.,
Nucl. Sci. Eng. 47 ('72) 19,
IAEA-153 P.477

73 Poortmans

Poortmans, F., Rohr, G., Theobald, J.P., Weigmann, H.,
Vanpraet, G.J.,
Nucl. Phys. A207 ('73) 342

73 Silbert-1

Silbert, M.G., Berreth, J.R.,
Nucl. Sci. Eng. 52 ('73) 187
Silbert, M.G.,
LA-5024

73 Silbert-2

Silbert, M.G., Moat, A., Young, T.E.,
Nucl. Sci. Eng. 52 ('73) 176
Moat, A.,
AWRE-013/72
Silbert, M.G.,
LA-4674, LA-4108-MS

74 Frehaut

Frehaut, J., Mosinski, G., Bois, R., Soleilhac, M.,
CEA-R-4626 ('74)

75 Weston

Weston, L.W., Todd, J.H.,
Proceedings of the Conference on Nuclear Cross Sections
and Technology, DA7. Washington 1975

*
60 Butler

Butler, D.K.,
Phys. Rev. 117 (1960) 1305

References for Review on ^{241}Pu Data

60 Kazarinova

Kazarinova, M.I., Zamyatin, Yu.S., Gorbachev, V.M.,
Atom. Energ. 8 (1960) 139
Sov. Atom. Energy 8 (1961) 125

61 Butler

Butler, D.K., Sjoblom, R.K.,
Phys. Rev. 124 (1961) 1129

61 Simpson

Simpson, O.D., Schuman, R.P.,
Nucl. Sci. Eng. 11 (1961) 111

62 Smith

Smith, H.L., Smith, R.K., Henkel, R.L.,
Phys. Rev. 125 (1962) 1329

63 Pattenden

Pattenden, N.J., Bardsley, S.,
ANL-6797 (1963) 369

64 Craig

Craig, D.S., Westcott, C.H.,
Can. J. Phys. 42 (1964) 2384

65 James

James, G.D.,
Nucl. Phys. 65 (1965) 353

65 Perkin

Perkin, J.L., White, P.H., Fieldhouse, P., Axton, E.J.,
Cross, P., Robertson, J.C.
J. Nucl. Energy 19 (1965) 423

65 White

White, P.H., Hodgkinson, J.G., Wall, G.J.,
IAEA Symposium on Physics and Chemistry of Fission,
Salzburg, (1965) Vol. 1, 217

66 James

James, G.D.,
ANL-7320 (1966) 16

66 Simpson

Simpson, O.D.,
LA-3586 (1966) 72

67 White

White, P.H., Warner, G.P.,
J. Nucl. Energy 21 (1967) 671

68 Conde

Conde, H., Hansen, J., Holmberg, M.,
J. Nucl. Energy 22 (1968) 53

70 James

James, G.D.,
Conf. on Nuclear Data for Reactors, Helsinki, (1970),
Vol. 1, 267

70 Migneco

Migneco, E., Theobald, J.P., Wartena, J.A.,
Conf. on Nuclear Data for Reactors, Helsinki, (1970),
Vol. 1, 437

70 Szabo

Szabo, I., Filippi, G., Huet, J.L., Leroy, J.L., Marquette,
J.P.,
CONF-701002 (1970) 257

71 Kolar

Kolar, W., Carraro, G.,
Conf. on Neutron Cross Section and Technology, Knoxville,
(1971) 707

72 Weston

Weston, L.W., Todd, J.H.,
Trans. A.N.S. 15 (1972) 480

73 Blons

Blons, J.
Nucl. Sci. Eng. 51 (1973) 130

73 Kappler

Kappler, F., Pfletschinger, E.
Nucl. Sci. Eng. 51 (1973) 124

73 Szabo

Szabo, I., Leroy, J.L., Marquette, J.P.,
Conf. on Neutron Physics, Kiev, (1973), Vol. 3, 27

74 D'yachenko

D'yachenko, N.P., Kolosov, N.P., Kuz'minov, B.D., Sergachev,
A.I., Surin, V.M.,
Sov. Atom. Energy 36 (1974) 406

74 Frehant

Frehant, J., Mosnski, G., Bois, R., Soleilhac, M.,
CEA-R-4626 (1974)

3.6 Americium

There are many requests in WREND 74 for the data of the capture and fission cross sections, and the number of neutrons per fission. Experimental data, however, are found for only the fission cross section, except for the data of the formation of the spontaneously fissioning isomers using $(n,2n)$ and (n,γ) reactions. These data are not counted in Fig. 1 (c). Formation of ^{242}Am ($T = 16.01$ h) through $^{241}\text{Am}(n,\gamma)$ reaction was measured by 71 Ivanova with activation method. The absorption cross section of ^{241}Am was obtained by 75 Weston. These data seem to be valuable for estimation of the capture cross section of ^{241}Am . An interesting experiment is a measurement of ^{242}Cm ($T = 163$ days) production cross section by Wiltshire et al.¹³⁾. For the application field, such experiments as this integral measurement may be efficient to estimate the data of the capture cross section.

3.6.1 Americium-241

There are many experiments for measurements of $^{241}\text{Am}(n,f)$ cross section. These were performed before 1970. No measurements could be found recently. The data are shown in Figs. 3.6.1 (a) and (b).

There are very large systematic differences between 67 Seeger and 70 Shpak, in particular, in sub-threshold region (see Fig. 3.6.1 (a)). The former data were measured by the underground nuclear explosion technique. As the authors mentioned in their paper, there may be some systematic errors. However, the latter data are so scarce below 100 keV and they could not be standard. Therefore, more measurements must be needed. These experiments would be useful for investigation of the sub-threshold resonance structures.

In Fig. 3.6.1 (b), the data by 68 Bowman and 70 Iyengar are transcribed from the graphs in the literatures. Hence, there are much ambiguities for these data points. Taking this fact into account, there are still large discrepancies between a set of 70 Shpak and 70 Fomushkin and a set

of 55 Nobles, 68 Bowman and 70 Iyengar. It is natural to say that the former set is superior, but no structures can be expected in the plateau region.

Comparison between the requested accuracies and the experimental errors is illustrated in Fig. 3.6.1 (c). The accuracy of 10% may be satisfied in MeV region, except for the systematic errors in the experimental data.

3.6.2 Americium-242

There are two measurements for the fission cross section of ^{242m}Am . One is the underground nuclear explosion experiment (67 Seeger) and the other is the experiment with linear accelerator (68 Bowman). The data are shown in Fig. 3.6.2 (a). The two data sets agree roughly with each other. However, the assigned errors are very large for the data by 67 Seeger. Moreover, as mentioned before, there are some systematic errors in 67 Seeger below 100 keV. Therefore, the data do not satisfy the requested accuracy (see Fig. 3.6.2 (b)).

Browne¹¹⁾ reported that, as a future plan of the cross section measurements at Livermore, they design to measure the fission cross section of ^{242m}Am with a high-purity sample. This aim is to improve the measurement of 68 Bowman. It may be expected that the present status of the data will be improved.

3.6.3 Americium-243

There are four data sets of the fission cross sections. They are shown in Fig. 3.6.3 (a). The data by 69 Boca are transcribed from the graph in the literature. A data by 67 Fomushkin at 1 MeV is an average value with the neutron fission spectrum. Hence, the data by 61 Butler and by 70 Seeger are only comparable with each other. Some systematic deviations are found in the graph. The latter experiment was performed with the underground nuclear explosion technique. Since no data have been obtained

in the region from 10 keV to 100 keV, nobody can say whether the connection between the data below 10 keV and above 100 keV will be well established or not. However, the data in low energy region seem to be large. The uncertainty is also large for the low energy data.

Glover et al.¹⁴⁾ measure the integral cross section of ^{243}Am leading to the production of ^{244}Cm . This may be useful for estimation of the capture cross section.

$^{241}\text{Am}(n,f)$

Ref.	Energy Range	Data
55 Nobles	0.5 MeV - 7 MeV	E. G.
	$^{235}\text{U}(n,f)$ standard. Gas scintillator. Data presented in BNL-325, 2nd edition. Values are relatively small.	
60 Protopopov	14.6 MeV	E.
	Ion chamber. One data point. Small value.	
61 Kazarinova	2.5 MeV, 14.6 MeV	E.
	Long counter.	
67 Fomushkin	fission spectrum	E. T. G.
	Relative measurements with $^{238}\text{U}(n,f)$ and $^{237}\text{Np}(n,f)$ of Pankratov's. Data obtained with ionization chamber and glass plate detector.	
67 Fomushkin	14.5 MeV	E. T. G.
	Relative measurements with $^{238}\text{U}(n,f)$ and $^{237}\text{Np}(n,f)$ of Pankratov's. Data obtained with ionization chamber and glass plate detector. Fragment distributions are also measured.	
67 Seeger	20 eV - 1 MeV	E. T. G.
	Underground nuclear explosion (Petrel). Relative values to the $^{235}\text{U}(n,f)$ and $^6\text{Li}(n,\alpha)$ data. Average values are also given.	
68 Bowman	0.5 MeV - 6 MeV	E. G.
	Linear accelerator. $^{239}\text{Pu}(n,f)$ used as a flux monitor.	

$^{241}\text{Am}(n, f)$

Ref.	Energy Range	Data
69 Iyer	14 MeV Relative value to $^{238}\text{U}(n, f)$. One data point.	E. T. Solid state track detector.
70 Shpak	8 keV - 3.3 MeV Relative values to $^{239}\text{Pu}(n, f)$.	E. T. G. Glass detector.
70 Fomushkin	450 keV - 3.6 MeV Relative values to $^{235}\text{U}(n, f)$. distribution is also measured.	E. T. Dielectric detectors. Fragment
70 Iyengar	320 keV - 2.1 MeV Relative values to $^{235}\text{U}(n, f)$. Data are relatively small.	G. Solid state track detector.

$^{241}\text{Am}(n, \gamma)$

67 Flerov-1	0 MeV - 6.5 MeV Data for excitation of 14 ms spontaneously fissioning isomer $^{242\text{m}}\text{Am}$. Mica fission fragment detector.	E. G.
69 Boca	300 keV - 4 MeV Excitation function of spontaneously fissioning isomer $^{242\text{m}}\text{Am}$. Data are a little higher than those of 67 Flerov-1, due to an improved estimation of geometrical factors.	G.

$^{241}\text{Am}(n,\gamma)$

Ref.	Energy Range	Data
71 Ivanova	fission spectrum	T.
Data for ^{242}Am ($T_{1/2} = 16.01$ h) formation. Activation method.		

$^{241}\text{Am}(\text{absorption})$

75 Weston	10 eV - 250 keV	E. T.
Average values are presented. Total energy detector.		

$^{241}\text{Am}(n,n')$

72 Belov	14.7 MeV	T.
Data for formation of spontaneously fissioning isomer.		

$^{241}\text{Am}(n,2n)$

72 Belov	14.7 MeV	T.
Data for formation of spontaneously fissioning isomer.		

$^{242}\text{Am}(n,f)$

67 Seeger	20 eV - 1 MeV	E. T. G.
Underground nuclear explosion (Petrel). Relative values to the $^{235}\text{U}(n,f)$ and $^6\text{Li}(n,\alpha)$ data. Average values are also given.		

$^{242}\text{Am}(n,f)$

Ref.	Energy range	Data
68 Bowman	0.02 eV - 6 MeV	E. G.
Linear accelerator. $^{239}\text{Pu}(n,f)$ is used as a flux monitor.		

$^{243}\text{Am}(n,f)$

61 Butler	0.3 MeV - 1.7 MeV	E. T. G.
Relative values to $^{235}\text{U}(n,f)$. Back-to-back gas scintillation counter.		

67 Fomushkin	fission spectrum	E. T.
Relative values to $^{238}\text{U}(n,f)$ and $^{237}\text{Np}(n,f)$. Ionization chambers and glass plate detectors are used.		

67 Fomushkin	14.5 MeV	E. T. G.
Relative values to $^{238}\text{U}(n,f)$ and $^{237}\text{Np}(n,f)$. Graphs for the angular distributions of fragments are presented.		

70 Seeger	50 eV - 3 MeV	E. T. G.
Underground nuclear explosion (Pommard). Relative values to Davey's evaluation of $^{235}\text{U}(n,f)$ above 100 keV.		

$^{243}\text{Am}(n,\gamma)$

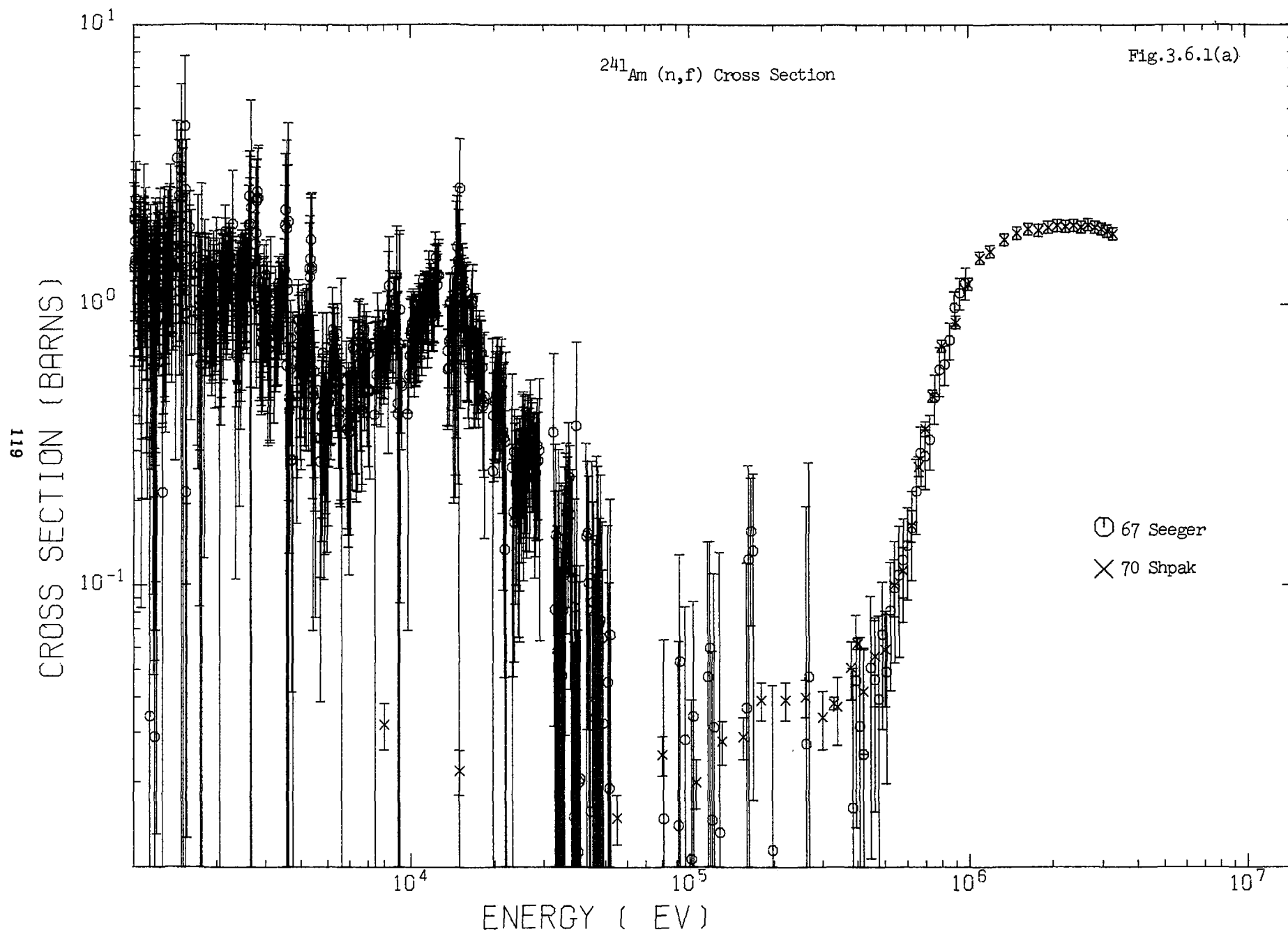
69 Boca	0.3 MeV - 4 MeV	E. T. G.
Excitation function of 0.6 ms spontaneously fissioning isomer. Ratio of isomer cross section to the prompt fission cross section is also presented in graph.		

$^{243}\text{Am}(n,n')$

Ref.	Energy Range	Data
72 Belov	14.7 MeV	T. Cross section for formation of spontaneously fissioning isomer.
72 Gangrsky	3 MeV - 7.6 MeV	T. Average cross section for formation of spontaneously fissioning isomer.

$^{243}\text{Am}(n,2n)$

65 Linev	14 MeV	E. Cross section for formation of spontaneously fissioning isomer of $T_{1/2} = 13.5 \pm 1.2$ ms.
67 Flerov-2	8 MeV - 14.4 MeV	E. T. G. Excitation function of spontaneously fissioning isomer. ($T_{1/2} = 14.0 \pm 1.0$ ms)
72 Belov	14.7 MeV	T. Cross section for formation of spontaneously fissioning isomer.
72 Gangrsky	threshold - 7.6 MeV	T. Average cross section for formation of spontaneously fissioning isomer.



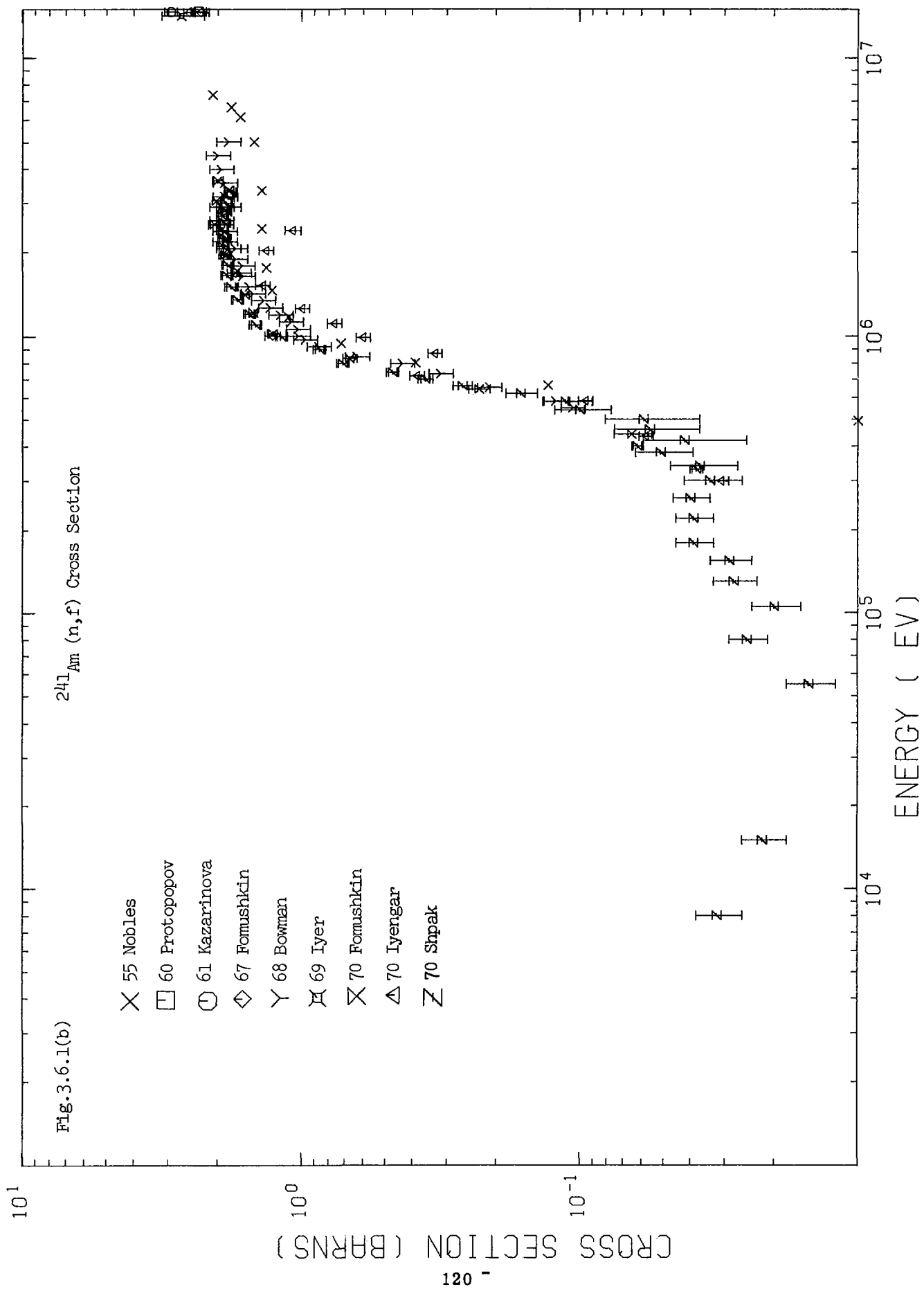
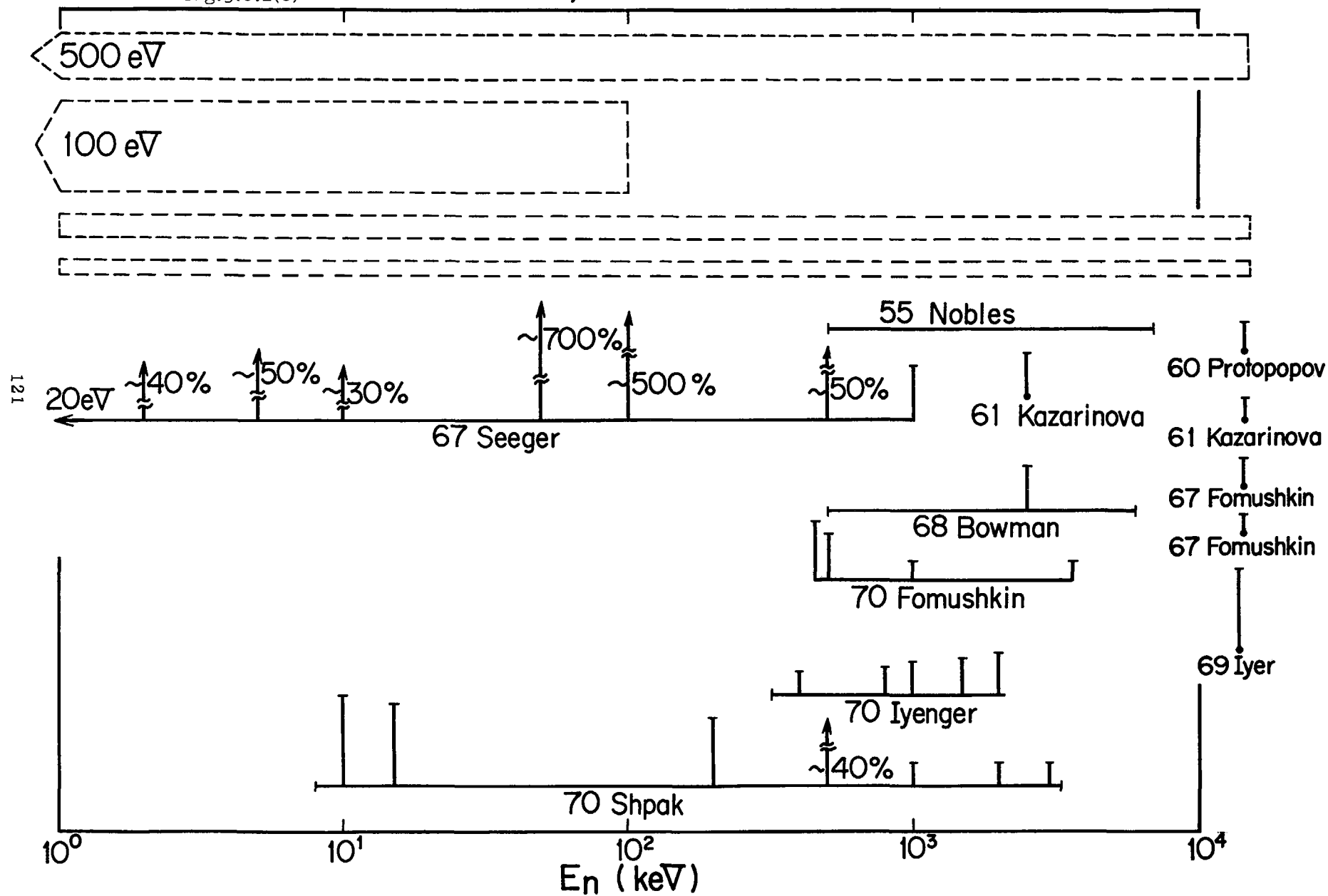


Fig. 3.6.1(c)

$^{241}\text{Am} (n, f)$



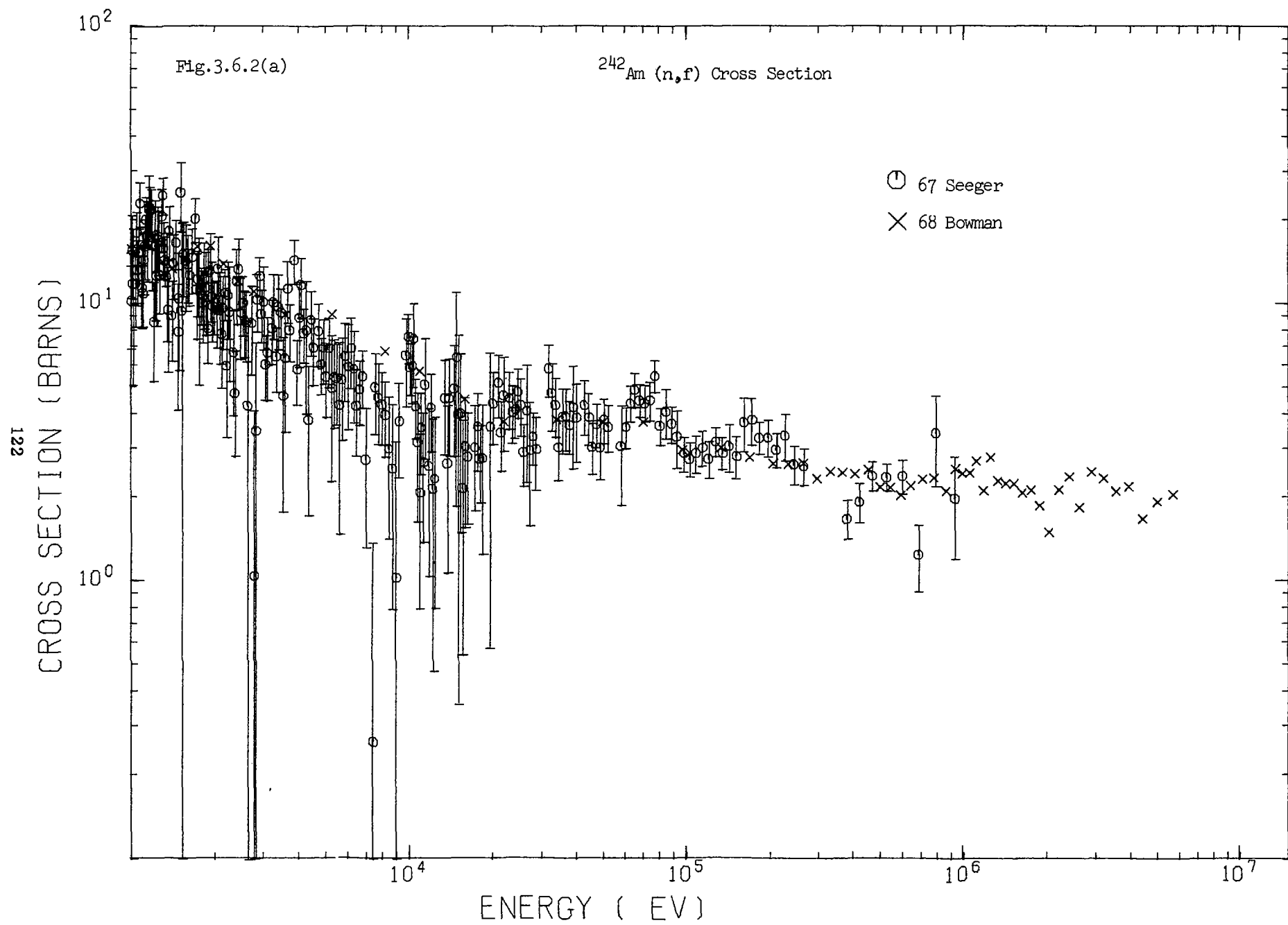
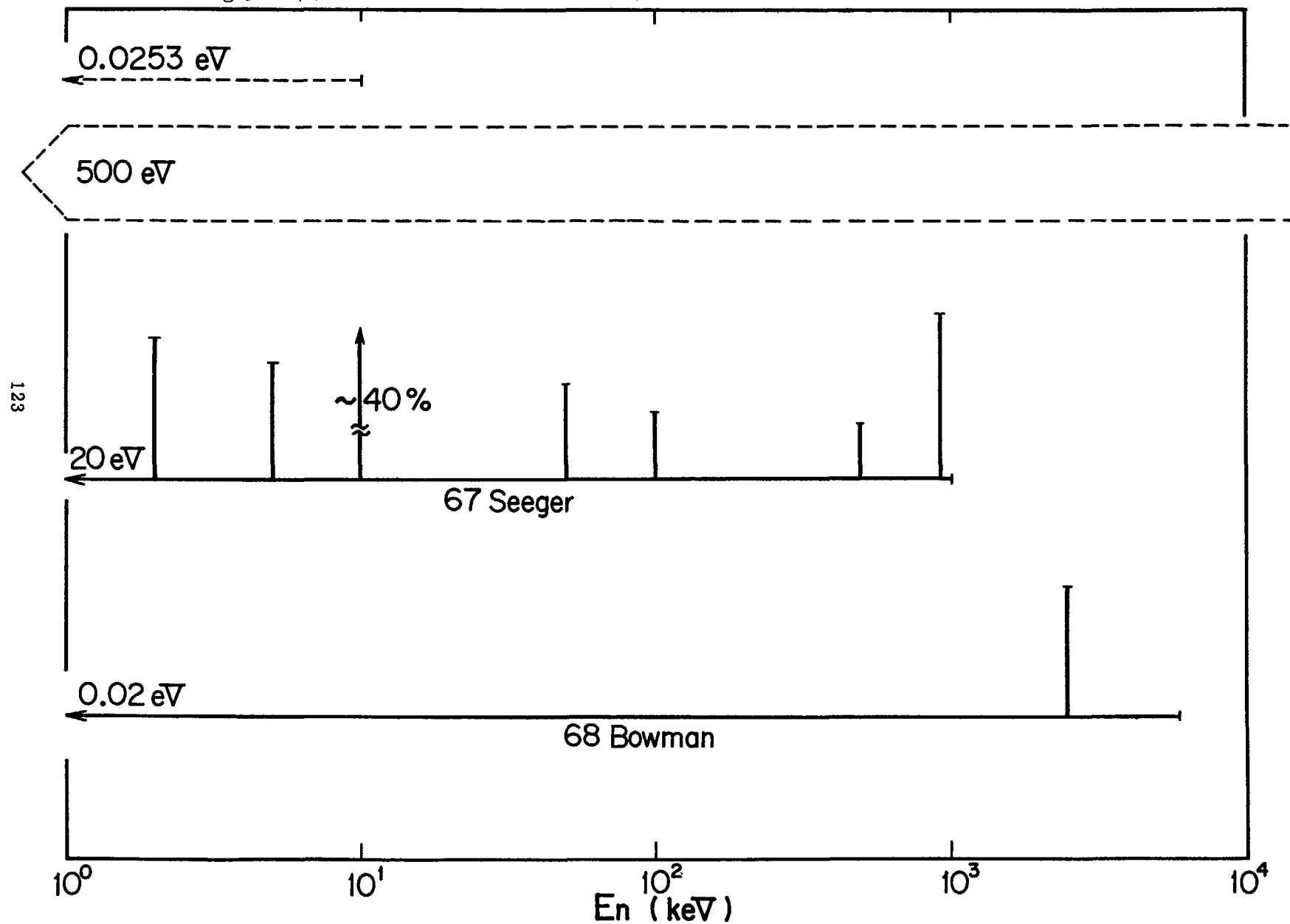


Fig.3.6.2(b)

$^{242}\text{Am} (n, f)$



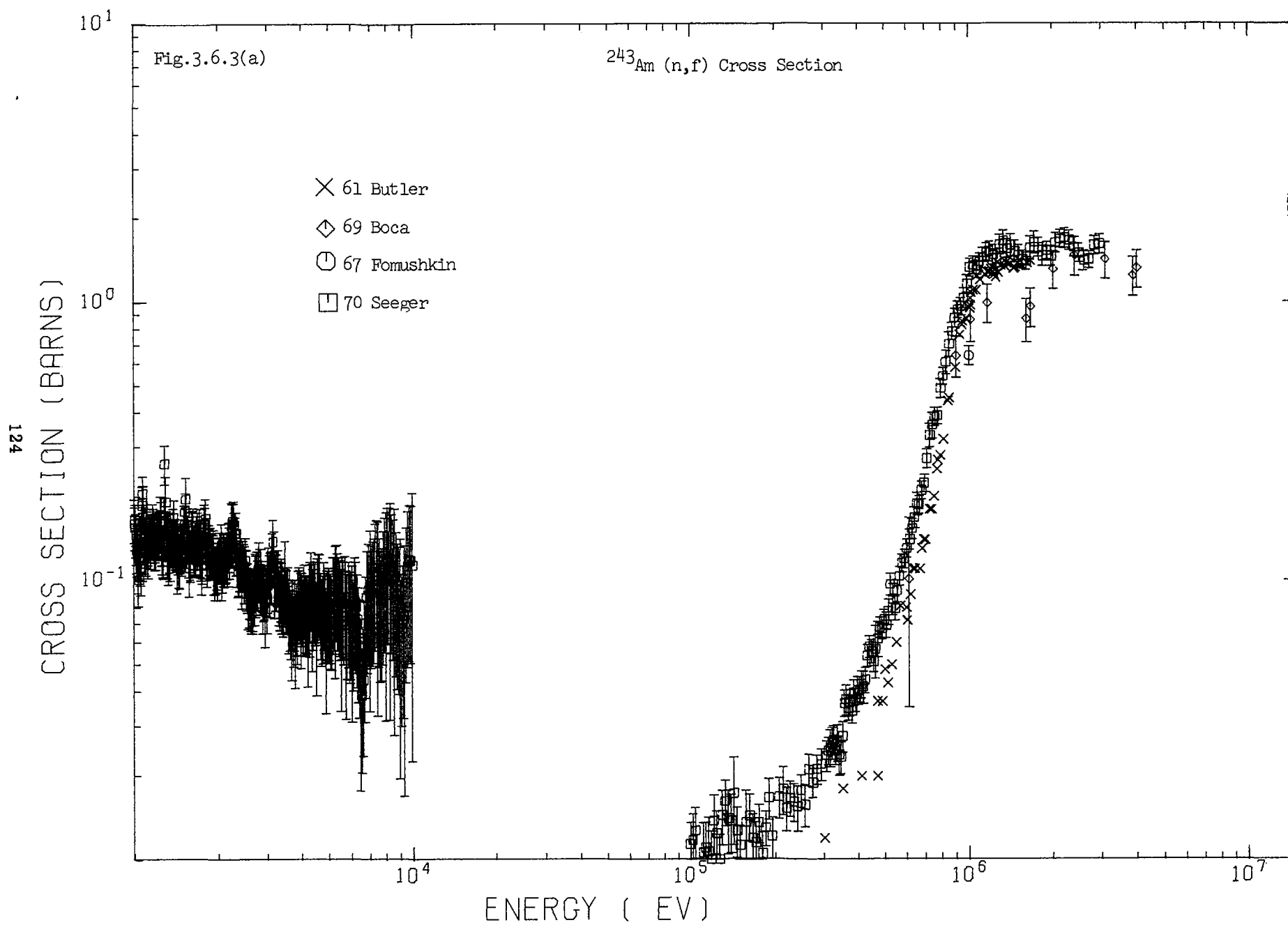
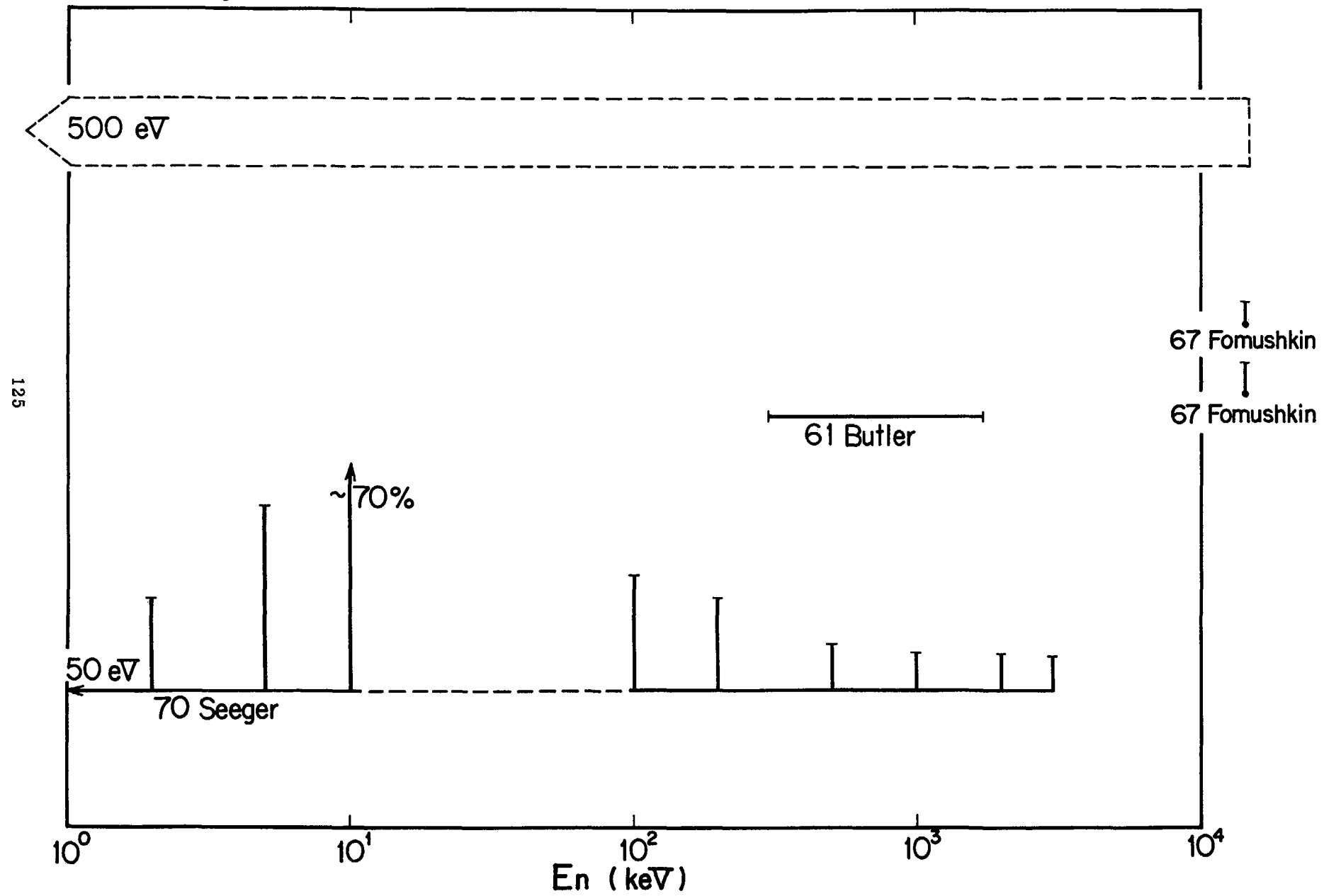


Fig.3.6.3(b)

$^{243}\text{Am} (n,f)$



References for Review on Am Data

55 Nobles

Nobles, R.A., Henken, R.L., Smith, R.K.,
Phys. Rev. A99 (1955) 616,
BNL-325, 2nd ed.

60 Protopopov

Protopopov, A.N., Selitskii, Yu.A., Solovev, S.M.,
Sov. Atom. Energy 6 (1960) 36

61 Butler

Butler, D.K., Sjoblom, R.K.,
Phys. Rev. 124 (1961) 1129

61 Kazarinova

Kazarinova, M.I., Zamyatin, Yu.S., Gorbachev, V.M.,
Sov. Atom. Energy 8 (1961) 125

65 Linev

Linev, A.F., Markov, B.N., Pleve, A.A., Polikanov, S.M.,
Nucl. Phys. 63 (1965) 173

67 Flerov-1

Flerov, G.N., Pleve, A.A., Polikanov, S.M., Tretyakova, S.P.,
Boca, I., Sezon, M., Vilcov, I., Vilcov, N.,
Nucl. Phys. A102 (1967) 443

67 Flerov-2

Flerov, G.N., Pleve, A.A., Polikanov, S.M., Tretyakova, S.P.,
Martalogu, N., Poenaru, D., Sezon, M., Vilcov, I., Vilcov, N.
Nucl. Phys. A97 (1967) 444

67 Fomushkin

Fomushkin, E.F., Gutnikova, E.K., Zamyatnin, Yu.S.,
Maslennikov, B.K., Belov, V.N., Surin, V.M., Nasyrov, F.,
Pashkin, N.F.,
Sov. J. Nucl. Phys. 5 (1967) 689

67 Seeger

Seeger, P.A., Hemmendinger, A., Diven, B.C.,
Nucl. Phys. A96 (1967) 605
LA-3586 (1966)

68 Bowman

Bowman, C.D., Auchampauch, G.F., Fultz, S.C., Hoff, R.W.,
Phys. Rev. 166 (1968) 1219

69 Boca

Boca, I., Martalogu, N., Sezon, M., Vilcov, I., Vilcov, N.,
Flerov, G.N., Pleve, A.A., Polikanov, S.M., Tretyakova, S.P.,
Nucl. Phys. A134 (1969) 541

69 Iyer

Iyer, R.H., Sampathkumar, R.,
Nucl. Phys. and Solid State Phys. Symposium, (1969) 289
BARC 474 (1970)

70 Fomushkin

Fomushkin, V.F., Gutnikova, E.K.,
Sov. J. Nucl. Phys. 10 (1970) 529
INDC (CCP) 7U28 (1970) 28

70 Iyengar

Iyengar, K.N., Iyer, R.H., Kapoor, S.S., Nadkarni, D.M.,
Sagu, M.L.,
Nucl. Phys. and Solid State Phys. Symposium, (1970) 67

70 Seeger

Seeger, P.A.,
LA-4420 (1970)

70 Shpak

Shpak, D.L., Ostapenko, Ju.B., Smirenkin, G.N.,
INDC (CCP) 8 (1970) 4

71 Ivanova

Ivanova, N.I., Kobzev, A.N., Krylov, N.G., Lbov, A.A.,
Martynov, N.P., Trikanov, A.E., Shelamkov, A.I.,
Sov. Atom. Energy 30 (1971) 452

72 Belov

Belov, A.G., Gangrsky, Yu.P., Dalkhsuren, B., Kucher, A.M.,
Nagy, T., Nadkarni, D.M.,
JINR-E15-6807 (1972)

72 Gangrsky

Gangrsky, Yu.P., Nad', T., Vinnai, I., Kovach, I.,
Sov. Atom. Energy 31 (1972) 874

75 Weston

Weston, L.W., Todd, J.H.,
Contributed paper for this Advisory Group Meeting

3.7 Curium

The requests were made for the total, capture and fission cross sections of the curium isotopes from ^{242}Cm to ^{248}Cm , and for the number of neutrons per fission of ^{242}Cm and ^{244}Cm . The experimental data, however, are found only for the fission cross section of these isotopes. The Livermore linac group has planned the measurements¹¹⁾ for the fission cross section of ^{243}Cm , ^{245}Cm and ^{247}Cm .

3.7.1 Curium-242 and -243

In spite of the requests for the data of capture and fission cross sections for both isotopes and for the number of neutrons per fission for ^{242}Cm , there are only data of the fission cross sections by 67 Fomushkin at 14.5 MeV for ^{242}Cm and by 70 Fullwood for ^{243}Cm . The aim of the former experiment was to investigate a systematic property of the fission cross sections for the heavy nuclei. The latter experiment was performed by using the intense neutrons from the underground nuclear explosion.

3.7.2 Curium-244

Many measurements on the fission cross section have been performed for this isotope. Three experiments, 68 Fullwood, 69 Fullwood and 71 Moore were those with the underground nuclear explosion technique. In these experiments, sub-threshold fission was observed. Below about 5 keV, the cross sections show some strong intermediate resonance structures. Some data by 68 Fullwood and by 71 Moore are transcribed from the graphs and are shown in Fig. 3.7.2 (a) with the data by 67 Fomushkin and 70 Barton. Fig. 3.7.2 (b) shows the data by 71 Moore.

Above the threshold, the data show a structure near 1.0 MeV. The data by 70 Barton (or 68 Koontz) agree well with the data by 71 Moore which are about 20% smaller than those by 68 Fullwood. At 14 MeV, a datum by 70 Barton is smaller than those by 67 Fomushkin. In order to satisfy the requests, these systematic deviations must be reduced.

The fission to capture ratio was obtained by 70 Keyworth with the underground nuclear explosion technique in the energy region from 100 eV to 5 keV. The data are given in the averaged form within the energy interval of 100 eV. These may be useful to estimate the capture cross section.

3.7.3 Curium-245,-246,-247 and -248

For these isotopes, the fission cross sections were measured by 71 Moore with the underground nuclear explosion technique and the average cross sections were obtained with the fast reactor spectrum by 73 Fomushkin.

The data for ^{245}Cm by 71 Moore are shown in Fig. 3.7.3 (a). In this experiment, ^6Li (n, α) cross section below 100 keV and ^{235}U (n,f) cross section above 100 keV were used as the standard. Owing to this difference of the standard cross sections, a little fault is found at 100 keV.

The comparisons between the requested accuracies and the experimental errors above 10 keV are shown in Figs. 3.7.3 (b) through 3.7.3 (e). The data for ^{245}Cm shown in Fig. 3.7.3 (a) may satisfy the request above 10 keV. Below 10 keV, however, the experimental errors are too large to compare with the requests.

$^{242}\text{Cm}(n,f)$

Ref.	Energy Range	Data
67 Fomushkin	14.5 MeV	E. T.
	$^3\text{H}(d,n)$ He. Glass plate fragment detectors. Relative method using $^{238}\text{U}(n,f)$ and $^{237}\text{Np}(n,f)$.	

 $^{243}\text{Cm}(n,f)$

70 Fullwood	100 keV - 3 MeV	E. G. T.
	Underground nuclear explosion (Pommard). Uncorrelated error is 6.3 to 30%. Correlated error is about 6 %.	

 $^{244}\text{Cm}(n,f)$

67 Fomushkin	14.5 MeV	E. T.
	Fission spectrum $^3\text{H}(d,n)$ He. Glass plate fragment detectors and ionization chambers. Relative values to $^{238}\text{U}(n,f)$ and $^{237}\text{Np}(n,f)$ data.	
68 Fullwood	20 eV - 2 MeV	E. T. G.
	Underground nuclear explosion. Solid state detectors. Relative values to $^6\text{Li}(n,\alpha)$ and $^{235}\text{U}(n,f)$ data. Errors are estimated about 30% or more.	
68 Koontz	1.0 MeV - 14.9 MeV	E. T.
	Solid State detectors. Relative values to $^{235}\text{U}(n,f)$ data. Preliminary results.	

$^{244}\text{Cm}(\text{n},\text{f})$

Ref.	Energy Range	Data
69 Fullwood	40 eV - 3 MeV	G.
Underground nuclear explosion (Physics 6). Solid state silicon detectors at 55° and 90°. Systematic deviation exists above 0.6 MeV.		
70 Barton	1.0 MeV - 14.9 MeV	T.
Revision of 68 Koontz. Data are given at 1.0, 1.5, 3.0 and 14.9 MeV.		
71 Moore	20 eV - 3 MeV	E. G.
Underground nuclear explosion (Physics 8). Si p-n junction detectors. Relative values to $^6\text{Li}(\text{n},\alpha)$ and $^{235}\text{U}(\text{n},\text{f})$ data.		
73 Fomushkin	Fast reactor spectrum	T.
Spectrum close to fission neutron spectrum. Dielectric silicate glass detectors.		

$^{244}\text{Cm}(\text{fission to capture ratio})$

70 Keyworth	100 eV - 5 keV	G.
Underground nuclear explosion (Physics 8). Resonance analysis. Intermediate structure of resonances are suggested.		

$^{245}\text{Cm}(\text{n},\text{f})$

71 Moore	20 eV - 3 MeV	E. G.
Underground nuclear explosion (Physics 8). Si p-n junction detectors. Relative values to $^6\text{Li}(\text{n},\alpha)$ and $^{235}\text{U}(\text{n},\text{f})$ data.		

$^{245}\text{Cm}(n,f)$

Ref.	Energy Range	Data
73 Fomushkin	Fast reactor spectrum	T.
	Spectrum close to fission neutron spectrum.	Dielectric silicate glass detectors.

$^{246}\text{Cm}(n,f)$

71 Moore	80 eV - 3 MeV	E. G.
	Underground nuclear explosion (Physics 8).	Si p-n junction detectors. Relative values to $^6\text{Li}(n,\alpha)$ and $^{235}\text{U}(n,f)$ data.
73 Fomushkin	Fast reactor spectrum	T.
	Spectrum close to fission neutron spectrum.	Dielectric silicate glass detectors.

$^{247}\text{Cm}(n,f)$

71 Moore	20 eV - 2 MeV	E. G.
	Underground nuclear explosion (Physics 8).	Si p-n junction detectors. Relative values to $^6\text{Li}(n,\alpha)$ and $^{235}\text{U}(n,f)$ data.
73 Fomushkin	Fast reactor spectrum	T.
	Spectrum close to fission neutron spectrum.	Dielectric Silicate glass detectors.

$^{248}\text{Cm}(n,f)$

Ref.	Energy Range	Data
71 Moore	20 eV - 3 MeV	E. G.
	Underground nuclear explosion (Physics 8). detectors. Relative values to $^6\text{Li}(n,\alpha)$ and $^{235}\text{U}(n,f)$ data.	Si p-n junction
73 Fomushkin	Fast reactor spectrum	T.
	Spectrum close to fission neutron spectrum. silicate glass detectors.	Dielectric

Fig.3.7.1(a)

$^{242}\text{Cm} (n,f)$

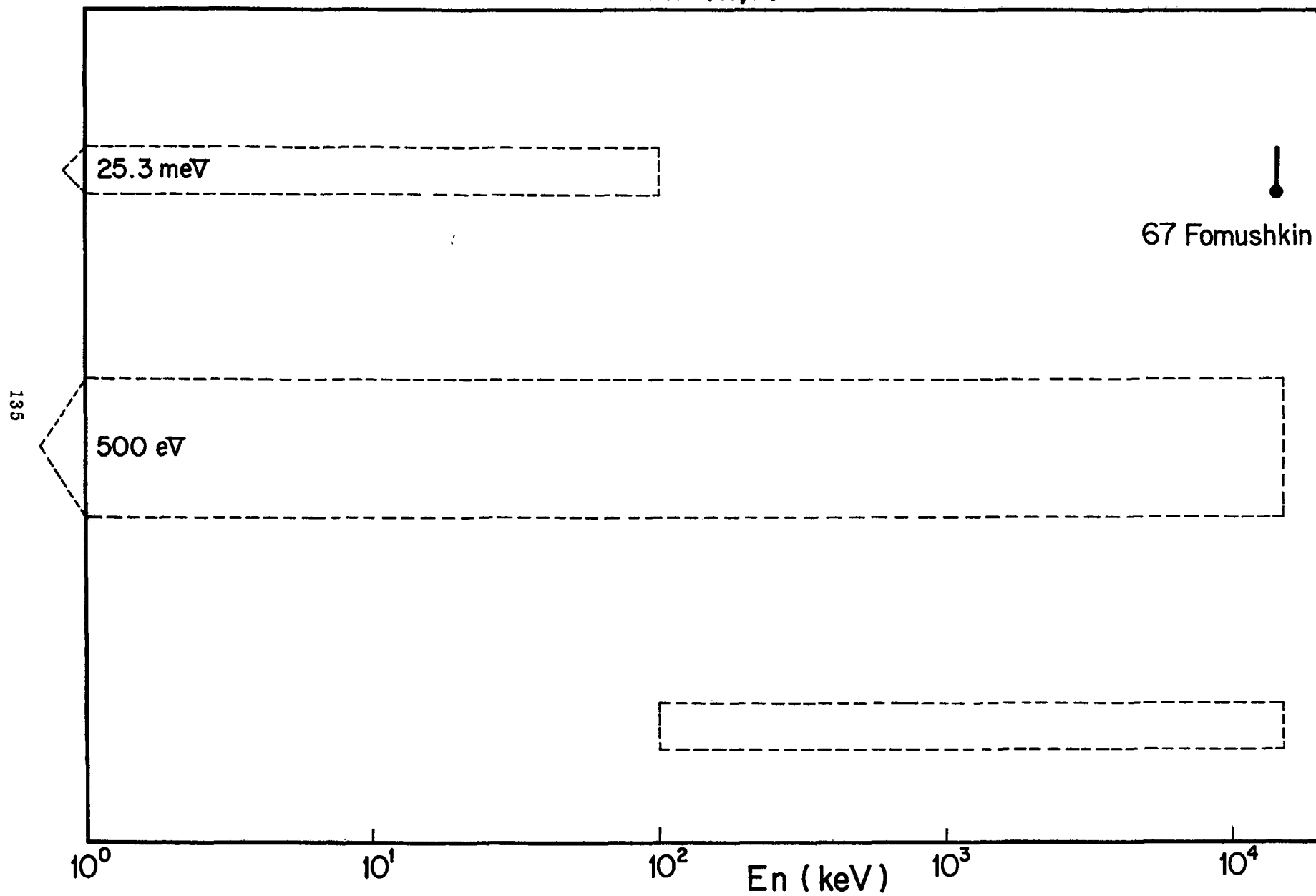


Fig.3.7.1(b)

$^{243}\text{Cm} (n,f)$

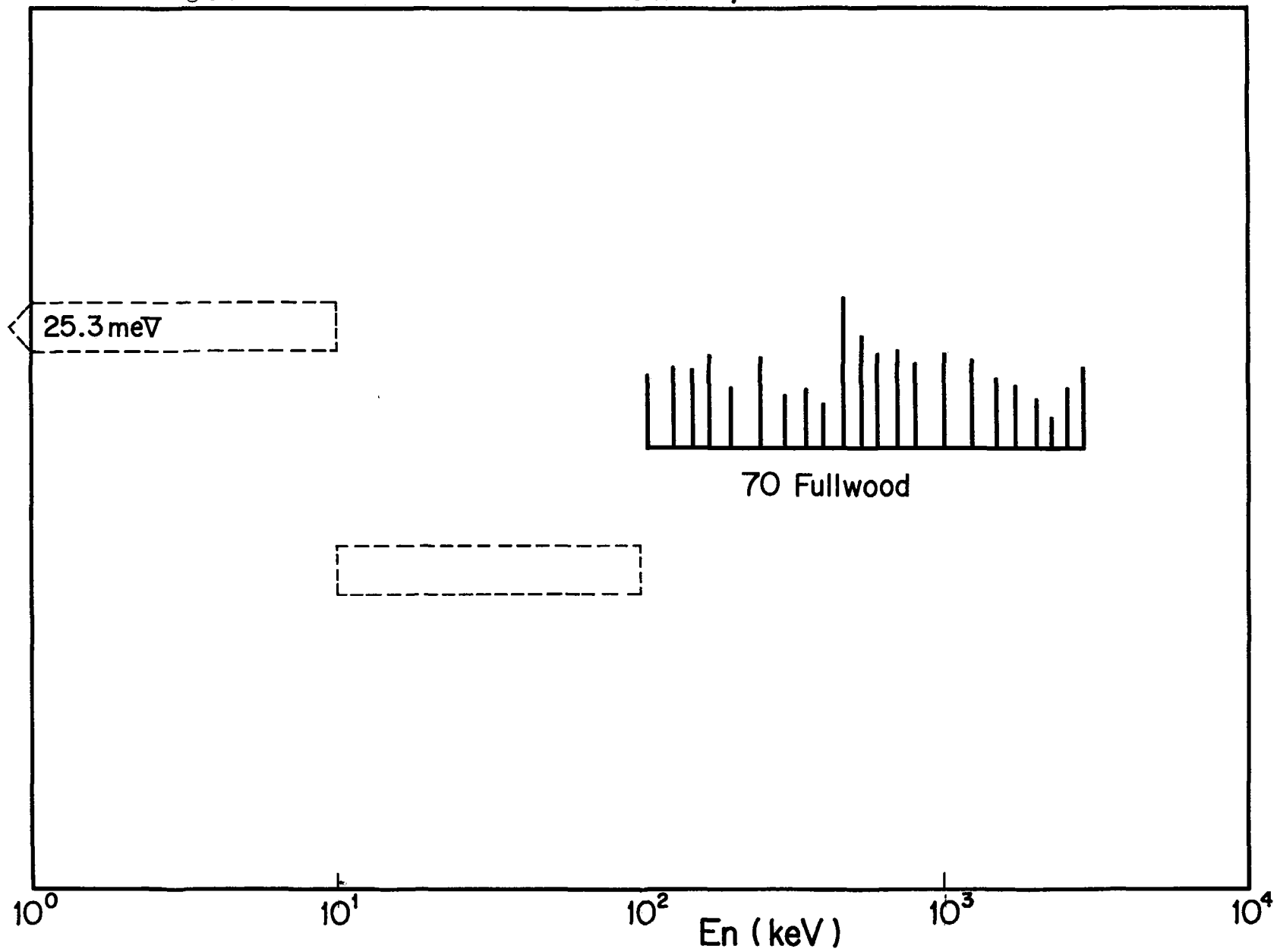


Fig.3.7.2(a)

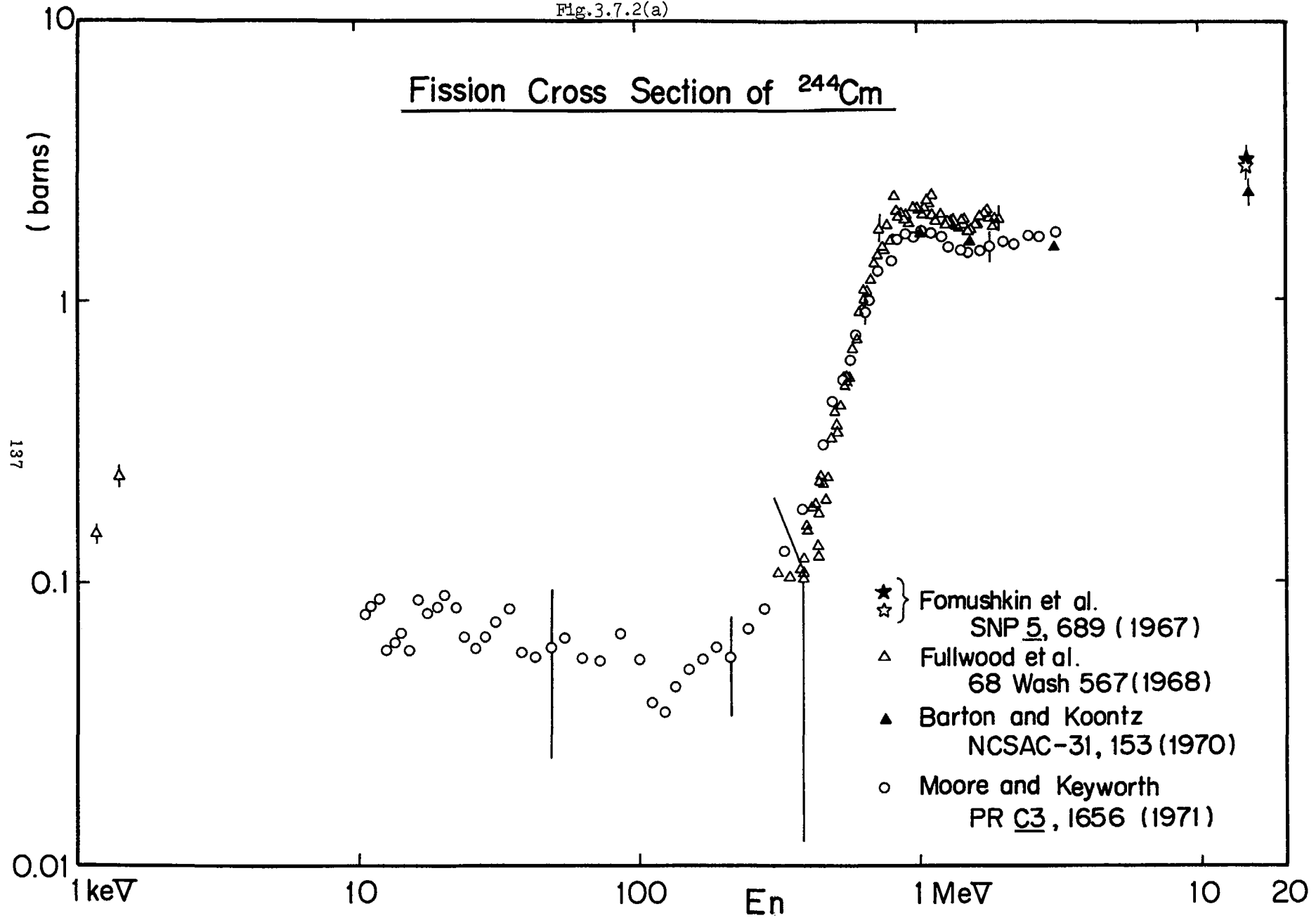


Fig. 3.7.2(b)

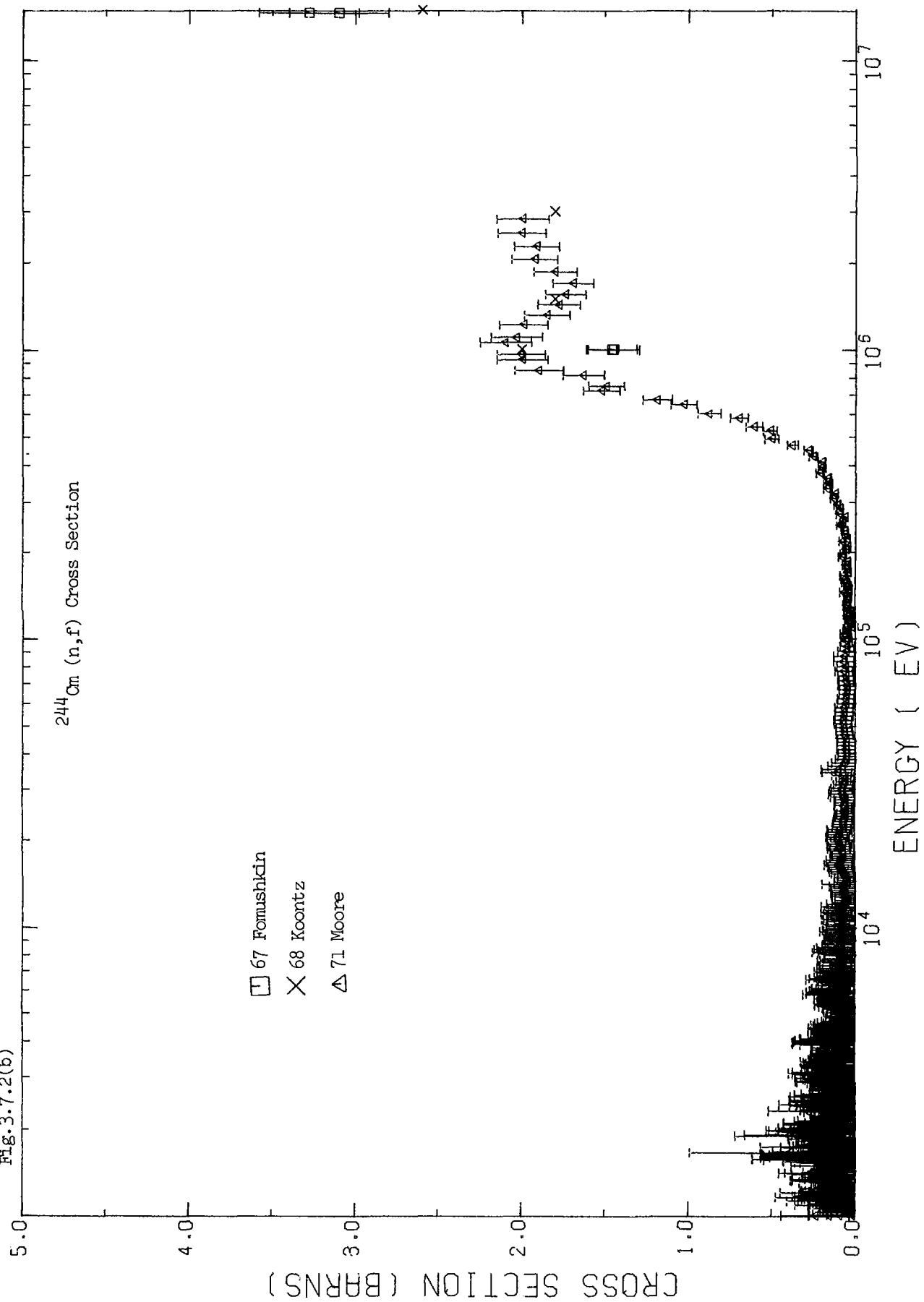


Fig.3.7.2(c)

$^{244}\text{Cm} (n,f)$

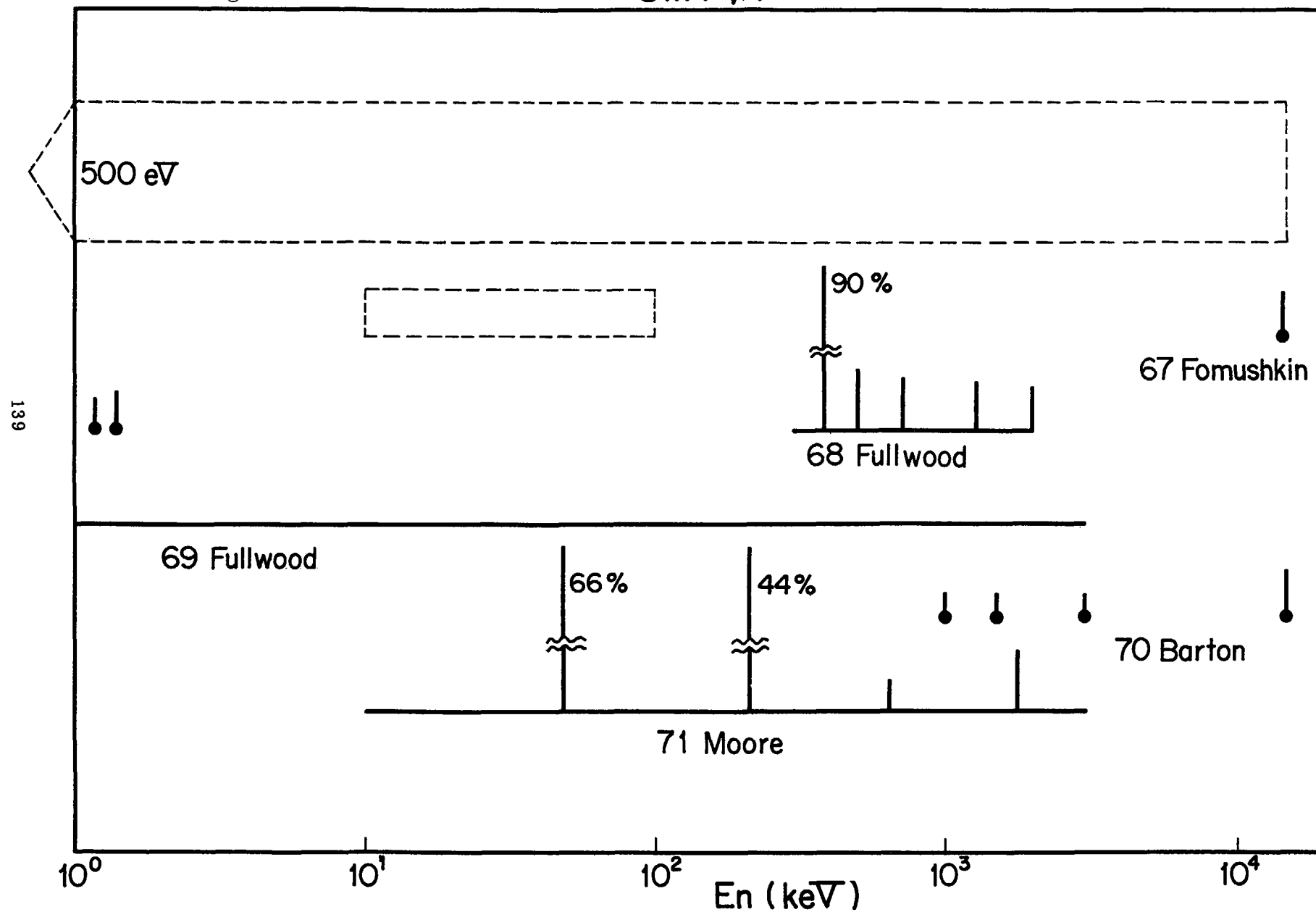


Fig.3.7.3(a)

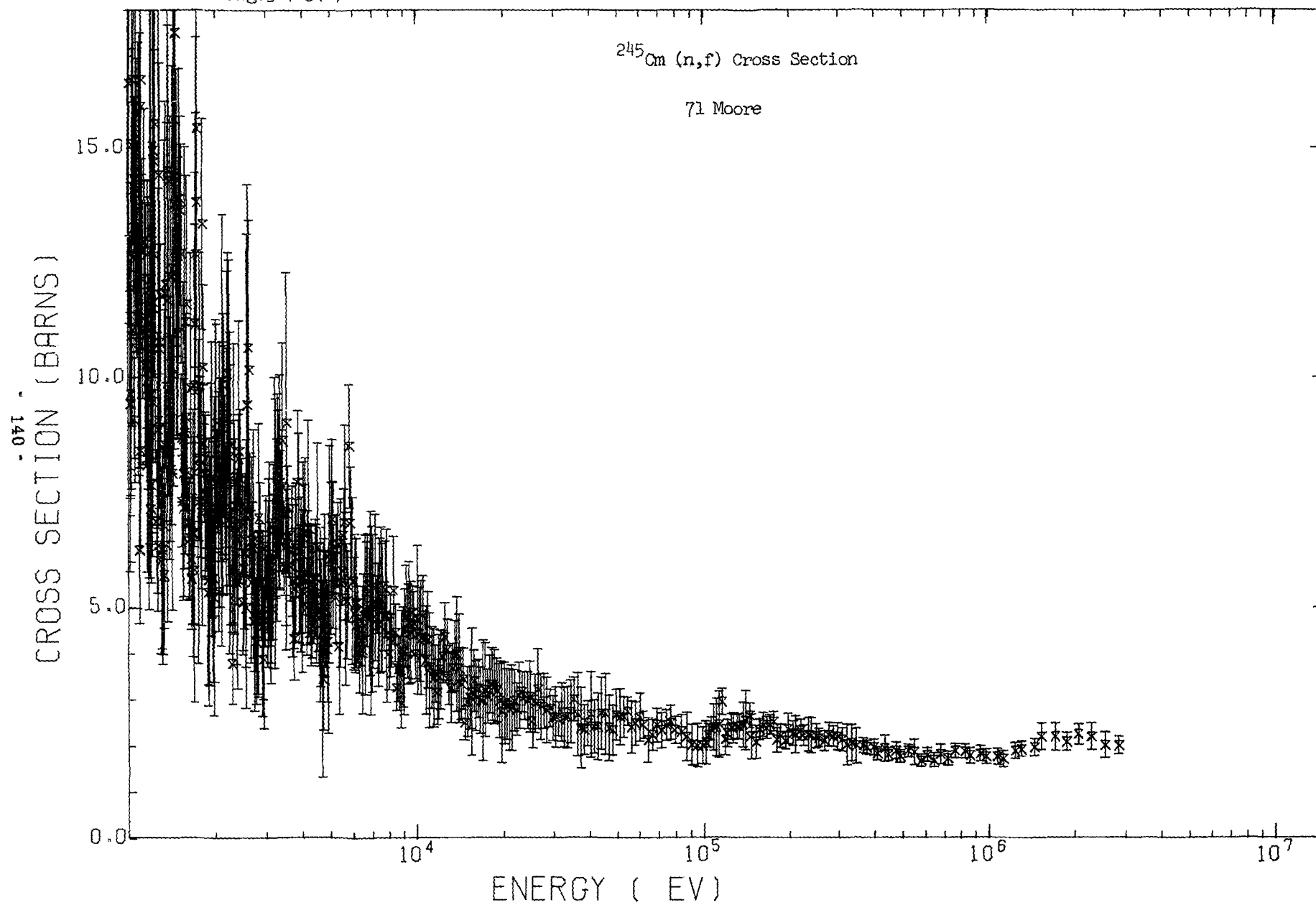


Fig.3.7.3(b)

$^{245}\text{Cm}(n,f)$

25.3 meV

71 Moore

10^0

10^1

10^2

En (keV)

10^3

10^4

Fig.3.7.3(c)

$^{246}\text{Cm (n,f)}$

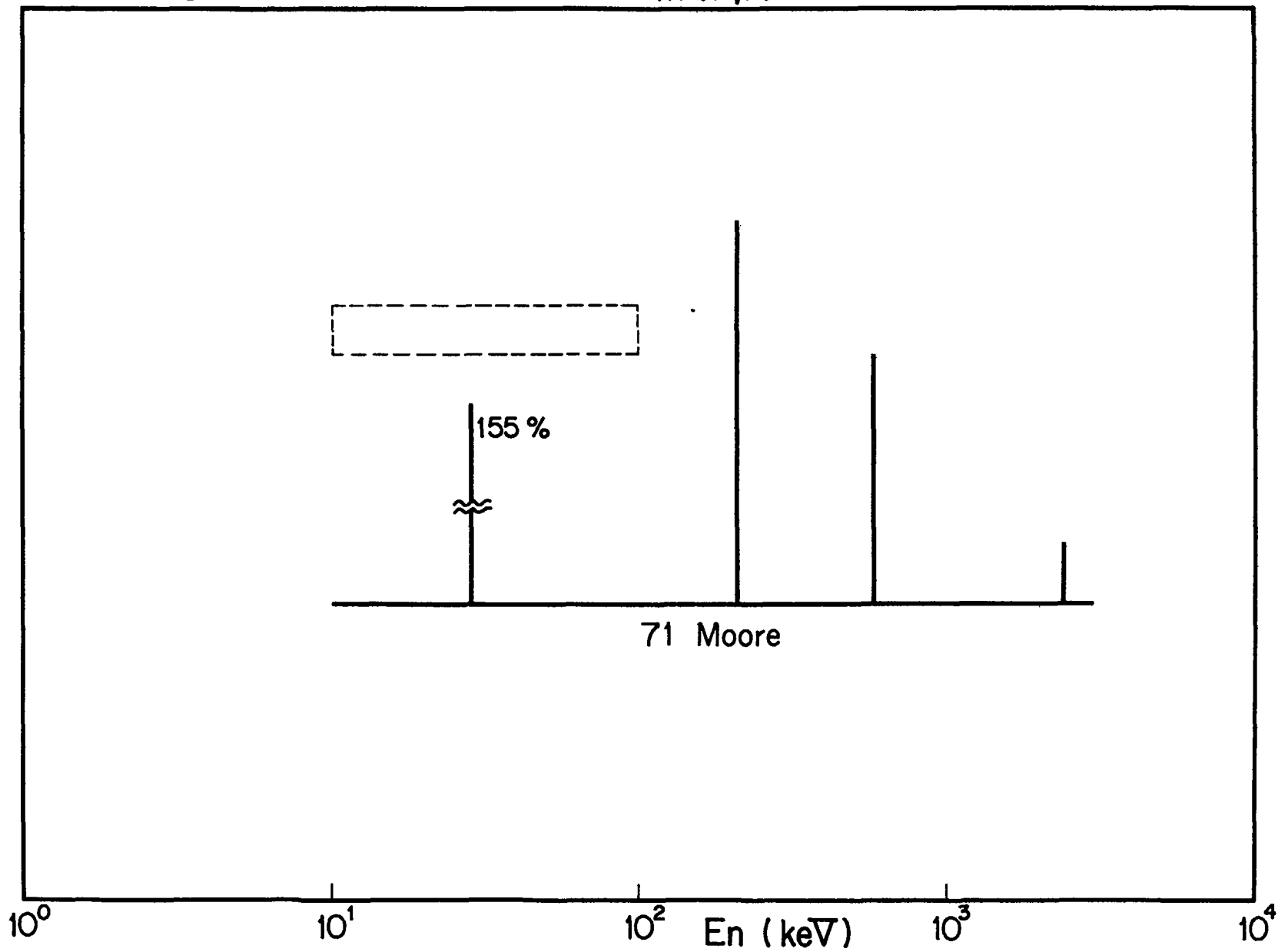


Fig.3.7.3(d)

$^{247}\text{Cm (n,f)}$

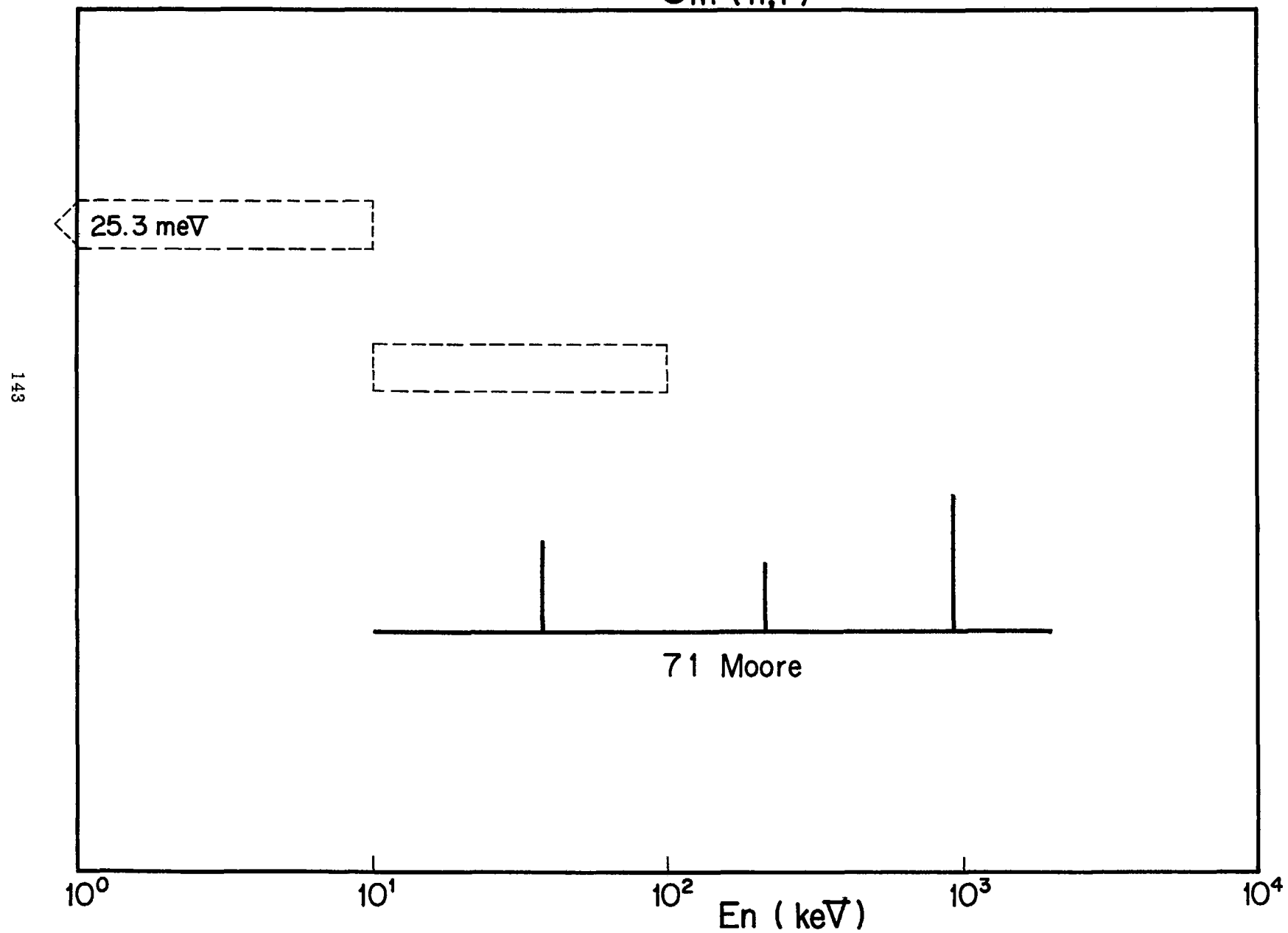
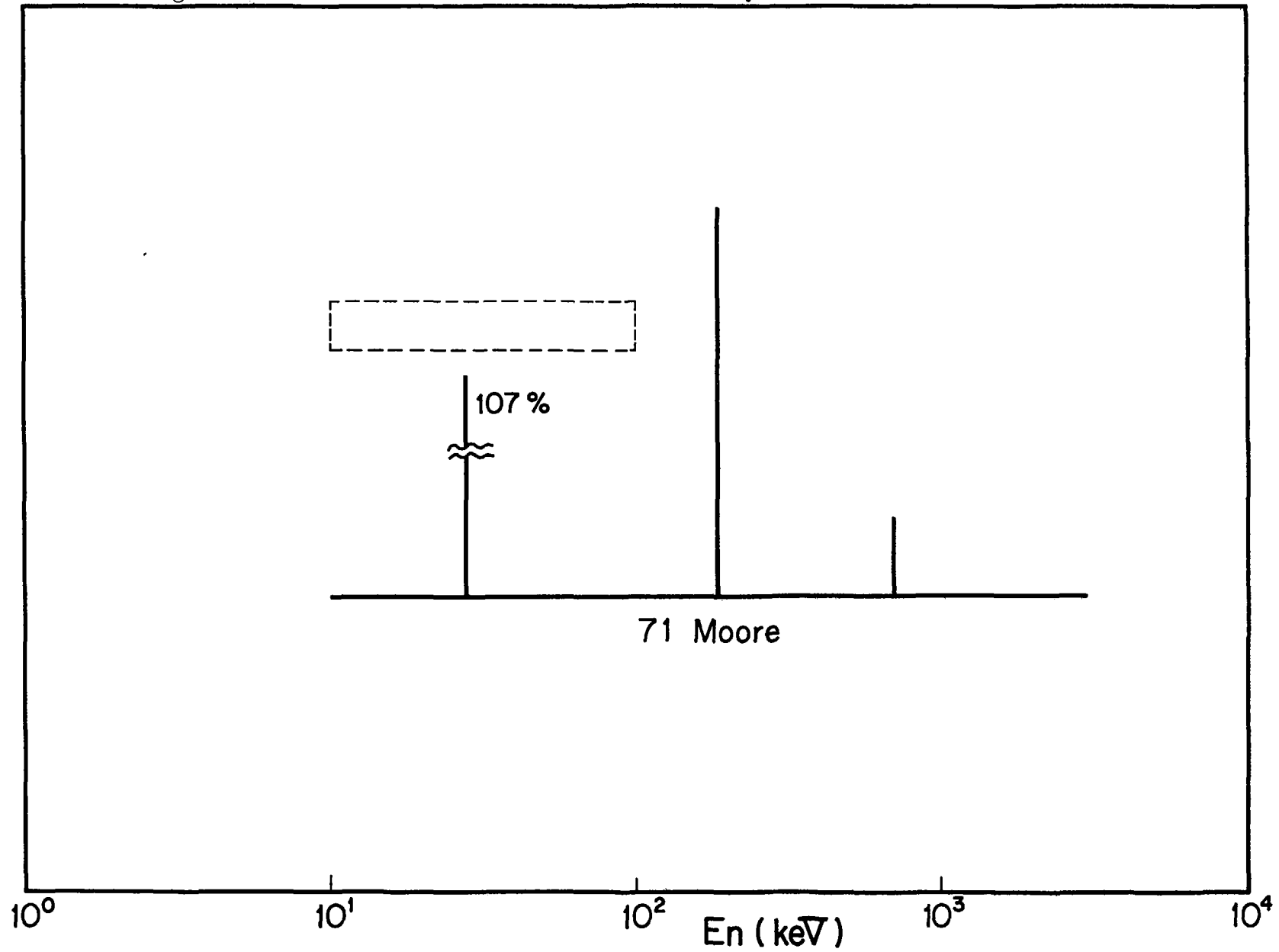


Fig.3.7.3(e)

$^{248}\text{Cm} (n,f)$



References for Review on Cm Data

67 Fomushkin

Fomushkin, E.F., Gutnikova, E.K., Zamyatnin, Yu.S.,
Maslennikov, B.K., Belov, V.N., Surin, V.M., Nasyrov, F.,
Pashkin, N.F.,
Sov. J. Nucl. Phys. 5 (1967) 689

68 Fullwood

Fullwood, R.R., McNally, J.H., Shunk, E.R.,
Conf. on Neutron Cross Sections and Technology, Washington,
(1968) 567

68 Koontz

Koontz, P.G., Barton, D.M.,
Conf. on Neutron Cross Sections and Technology, Washington,
(1968) 597

69 Fullwood

Fullwood, R.R., McNally, J.H., Shunk, E.R.,
WASH-1136 (1969) 110

70 Fullwood

Fullwood, R.R., Dixon, D.R., Loughheed, R.W.,
LA-4420 (1970) 157

70 Barton

Barton, D.M., Koontz, P.G.,
NCSAC-31 (1970) 153

70 Keyworth

Keyworth, G.A., Moore, M.S.,
BNL-50276 (1970) 136

71 Moore

Moore, M.S., Keyworth, G.A.,
Phys. Rev. C3 (1971) 1656

73 Fomushkin

Fomushkin, E.F., Gutnikova, E.K., Maslennikov, B.K.,
Korochkin, A.M.,
Sov. J. Nucl. Phys. 17 (1973) 12

3.8 Berkelium

The requested data for Bk-isotopes are the total and capture cross sections of ^{249}Bk only. No requests have been made for the fission cross section. Existing experimental data, however, are only the fission cross section of ^{249}Bk . The data were obtained by 70 Vorotnikov-1, 70 Vorotnikov-2 and 72 Fomushkin. The numerical data by 70 Vorotnikov-2 are given in the literature of 72 Vorotnikov.

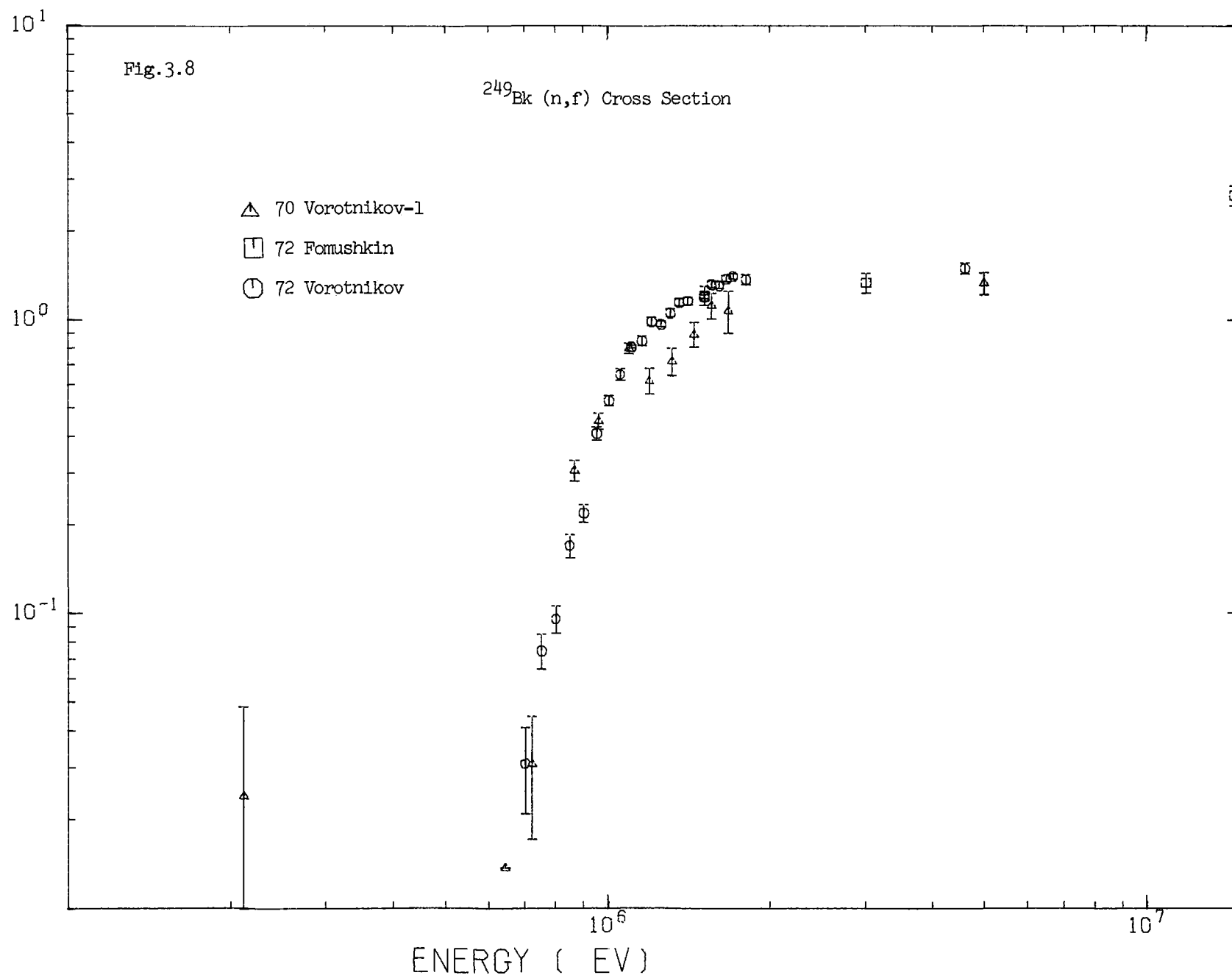
In 70 Vorotnikov, the fission fragments were detected with the glass plate detectors at angles 0° , 30° , 60° and 90° . Uncertainty of the cross section was about 15%. The plateau value and the threshold energy were 1.3 ± 0.2 b and 1.0 MeV, respectively. The data show some structures near 1.25 MeV (see Fig. 3.8).

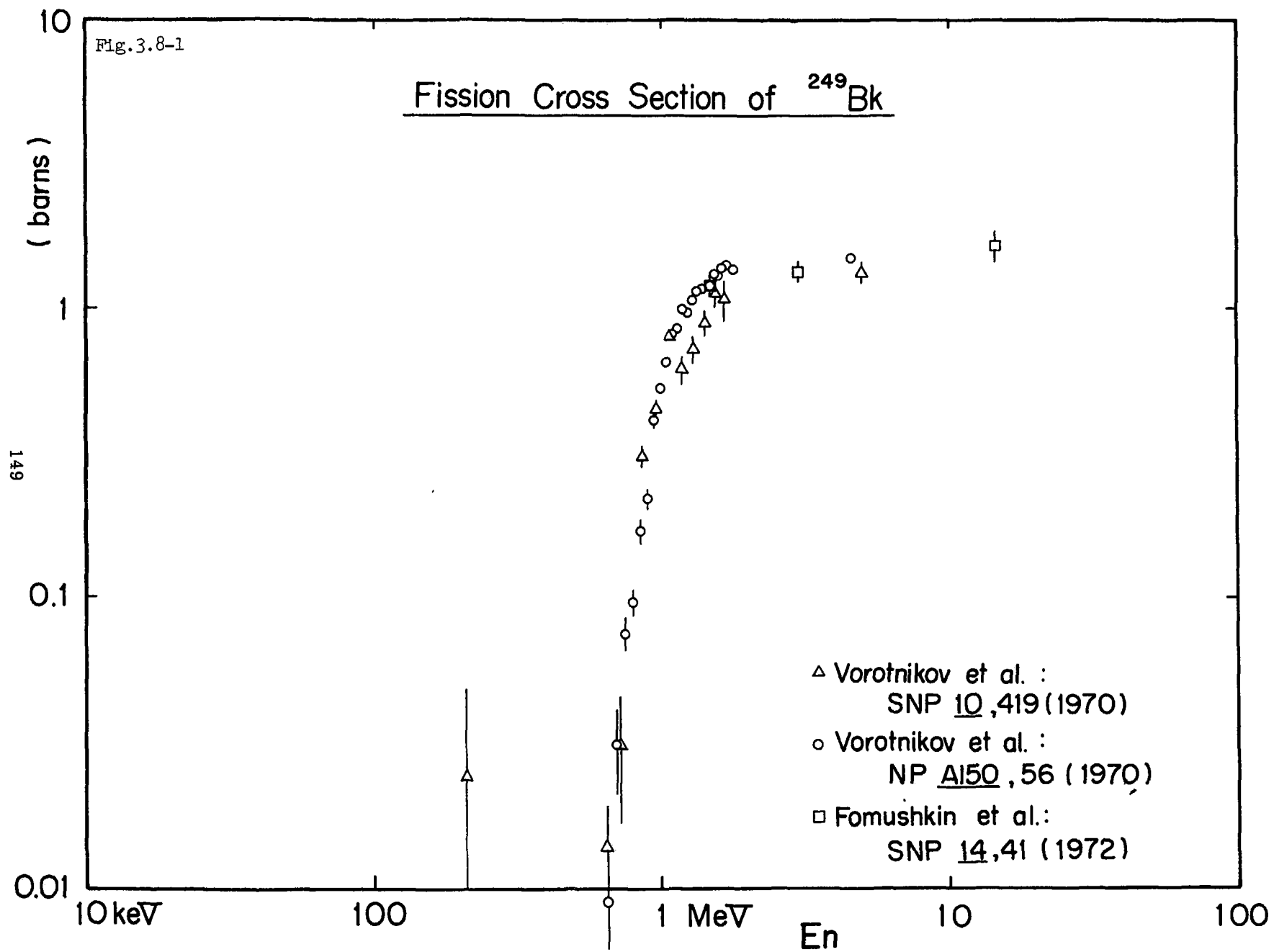
Improvements of the experimental techniques were tried by 70 Vorotnikov-2 to obtain more precise data than those by 70 Vorotnikov-1. The energy resolution was improved from 50 keV to 40 keV. The amount of the sample was increased from 0.2 μg to 1.2 μg . The uncertainty was reduced by about 5%. In this experiment, no structures were observed near 1.2 MeV. The plateau value and the threshold energy were modified to the values of 1.4 ± 0.15 b and 1.07 MeV, respectively.

The relative measurement to the fission cross section of ^{235}U was carried out by 72 Fomushkin. The data obtained by this experiment were shown in Fig.3.8 with the data by 70 Vorotnikov-1 and 72 Vorotnikov. Below 2 MeV, the data by 72 Vorotnikov are naturally better than those by 70 Vorotnikov-1. Above 2 MeV, however, more efforts may be needed for the measurements of the fission cross section.

^{249}Bk (n,f)

Ref.	Energy Range	Data
70 Vorotnikov-1	0.2 MeV - 5 MeV	G.
	$^3\text{H(p,n)}$, $^7\text{Li(p,n)}$ and $^2\text{H(d,n)}$ sources. Neutron flux monitored by a long counter. Glass plate detectors. Absolute values with 15% errors.	
70 Vorotnikov-2	0.6 MeV - 4.6 MeV	G.
	$^3\text{H(p,n)}$, $^7\text{Li(p,n)}$ and $^2\text{H(d,n)}$ sources. Neutron flux monitored by a long counter. Glass plate detectors. Absolute values with 10% errors. Fragment angular distribution also measured.	
72 Vorotnikov	0.65 MeV - 4.6 MeV	T.
	Same technique as 70 Vorotnikov-2 is used. Corrections are made for half-life of β -decay and for the background due to ^{249}Cf .	
72 Fomushkin	1.5 MeV - 14.5 MeV	T.
	Fast reactor spectrum $^3\text{H(d,n)}$, $^3\text{H(p,n)}$ and fast reactor neutrons. Dielectric detectors. Silicate glass detectors. Relative values to $^{235}\text{U(n,f)}$ and $^{238}\text{U(n,f)}$ data. Fragment angular distributions are also measured.	





References for Review on Bk Data

70 Vorotnikov-1

Vorotnikov, P.E., Dubrovina, S.M., Otroshchenko, G.A.,
Chistyakova, L.V., Shigin, V.A., Shubko, V.M.,
Sov. J. Nucl. Phys. 10 (1970) 419

70 Vorotnikov-2

Vorotnikov, P.E., Dubrovina, S.M., Kosyakov, V.N., Chistyakov,
L.V., Shigin, V.A., Shubko, V.M.,
Nucl. Phys. A150 (1970) 56

72 Vorotnikov

Vorotnikov, P.E., Dubrovina, S.M., Kosyakov, V.N., Otroshchenko,
G.A., Chistyakov, L.V., Shigin, V.A., Shubko, V.M.,
INDC(CCP) 31 (1972) 1

72 Fomushkin

Fomushkin, E.F., Gutnikova, E.K., Maslov, A.N., Novoselov,
G.V., Panin, V.I.,
Sov. J. Nucl. Phys. 14 (1972) 41

3.9 Californium

The requested data for Cf-isotopes are the total cross section of ^{250}Cf , the capture cross section of ^{250}Cf , ^{251}Cf , ^{252}Cf and ^{253}Cf , and the fission cross section of ^{249}Cf , ^{250}Cf and ^{252}Cf . The measured data, however, are only those on the fission cross section of ^{249}Cf and ^{252}Cf .

3.9.1 Californium-249

The fission cross section of ^{249}Cf is required in the energy region from 10 keV to 100 keV with 10% accuracy. The measured data covering this energy region are those by 73 Silbert with the underground nuclear explosion technique. Main purpose of this experiment was to investigate the fission cross section in the resonance energy region. However, the data were presented up to 3 MeV. The overall systematic error was assigned as 6%, relative to the reference data.^{18.19.23)} The data are shown with the other data in Fig. 3.9.1 (a). The data by 72 Vorotnikov are transcribed from the graph in the literature. Excluding this data set, there are still systematic differences between four data sets.

The experiment by 74 Fursov is a continuation of a study reported by 72 Fursov. These data were obtained relative to $^{239}\text{Pu}(n,f)$ cross section. Hence, the small difference between these data and those by 73 Silbert may be owing to the normalization of the cross sections, as well as the detector position in 73 Silbert. Above 1 MeV, averaged value of the data by 74 Fursov is about 9% larger than 1.7 b by 73 Silbert, and in the region from 2 to 3 MeV, the former is about 2.02 b which is about 5% larger than that by 73 Silbert. These values, however, are smaller than those expected by the systematics.²⁴⁾

3.9.2 Californium-252

The measurements on the fission cross section of this isotope were performed by 71 Moore with the underground nuclear explosion technique.

The data were obtained relative to the fission cross section of ^{235}U above 100 keV and to the ^6Li (n, α) cross section below 100 keV (Fig. 3.9.2 (a)).

In this experiment, the threshold energy was given as 900 ± 50 keV, and the barrier constant was about 1.5 MeV. Using these constants, the average fission width was estimated as 35 meV. The s-wave neutron strength function and fission resonance integral were calculated by using these parameters as well as the observed resonance parameters below 1 keV. They are 1.6×10^{-4} and 65 ± 6 barns, respectively. Above threshold, the cross section reveals so called saw-tooth structure.

$^{249}\text{Cf}(n,f)$

Ref.	Energy Range	Data
70 Vorotnikov	400 keV - 600 keV	
	Average cross section is presented.	
71 Fomushkin	14.5 MeV	T.
	Relative value to $^{235}\text{U}(n,f)$. Polycarbonate dielectric film detector. Fission fragment anisotropy is also shown.	
71 Fomushkin	fast reactor spectrum	T.
	Relative value to $^{235}\text{U}(n,f)$. Silicate glass detector is used.	
72 Fursov	0.5 MeV - 5.02 MeV	E. T. G.
	Relative values to $^{239}\text{Pu}(n,f)$. Cylindrical glass fragment detectors. Angular anisotropy of fission fragments is also shown.	
72 Vorotnikov	0.16 MeV - 1.6 MeV	G.
	Neutron flux monitored by a boron counter. Fission fragment glass detectors are used.	
73 Silbert	13 eV - 3 MeV	E. T. G.
	Underground nuclear explosion (Physics-8). Relative values to $^{235}\text{U}(n,f)$ and $^6\text{Li}(n,\alpha)$. Silicon semiconductor fission fragment detector. Average values are also given.	
74 Fursov	0.5 MeV - 7 MeV	E. T. G.
	Relative values to $^{239}\text{Pu}(n,f)$. Cylindrical glass detector is used for fission-fragment detection.	

$^{249}\text{Cf}(n,f)$

75 Fomushkin 0.25 MeV - 5.15 MeV T.
Relative values to $^{235}\text{U}(n,f)$. Dielectric track detector.

$^{252}\text{Cf}(n,f)$

71 Moore 20 eV - 5 MeV G.
Underground nuclear explosion (Physics-8). Relative values
to $^{235}\text{U}(n,f)$ and $^6\text{Li}(n,\alpha)$. Solid state detector.

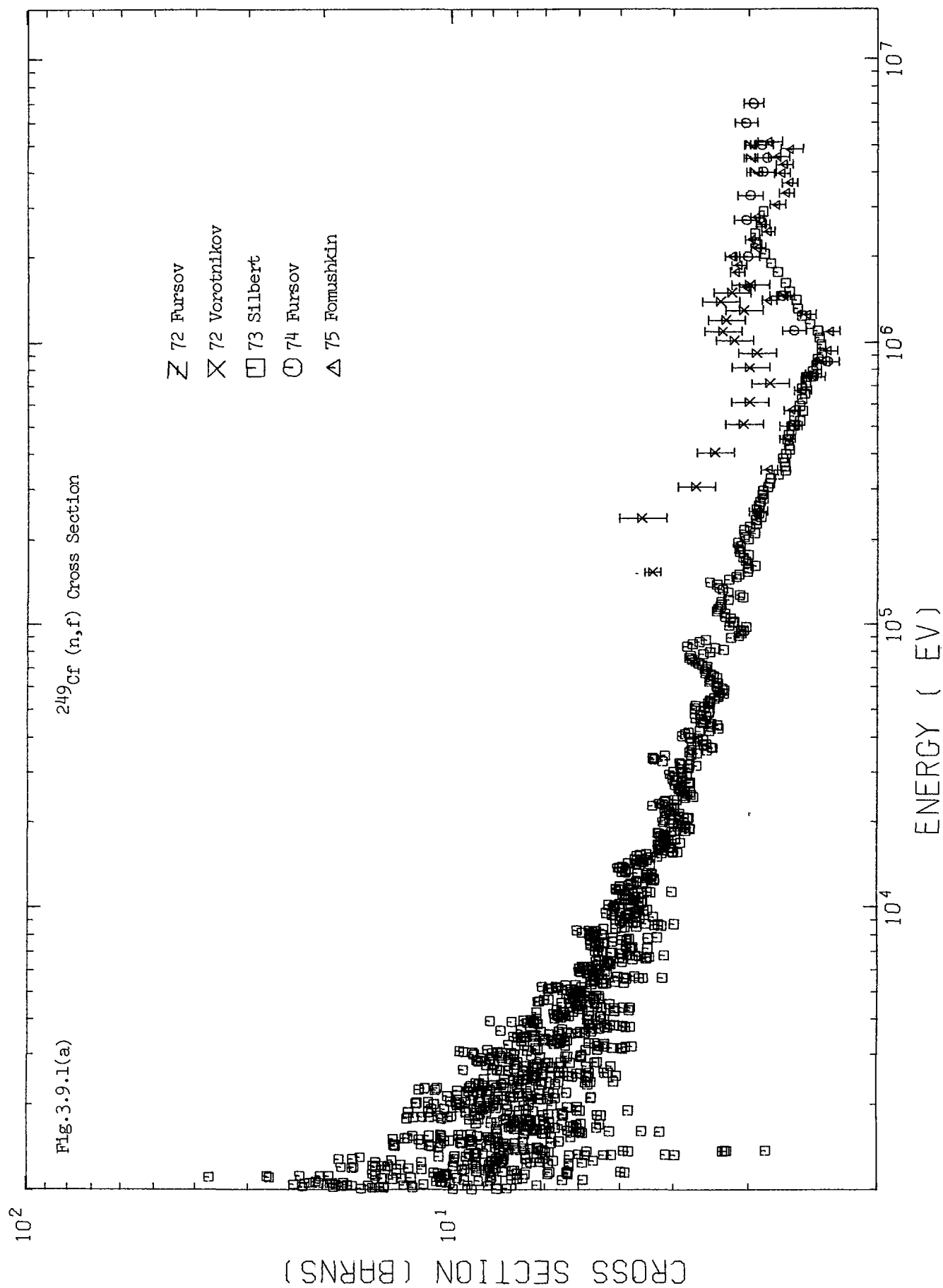
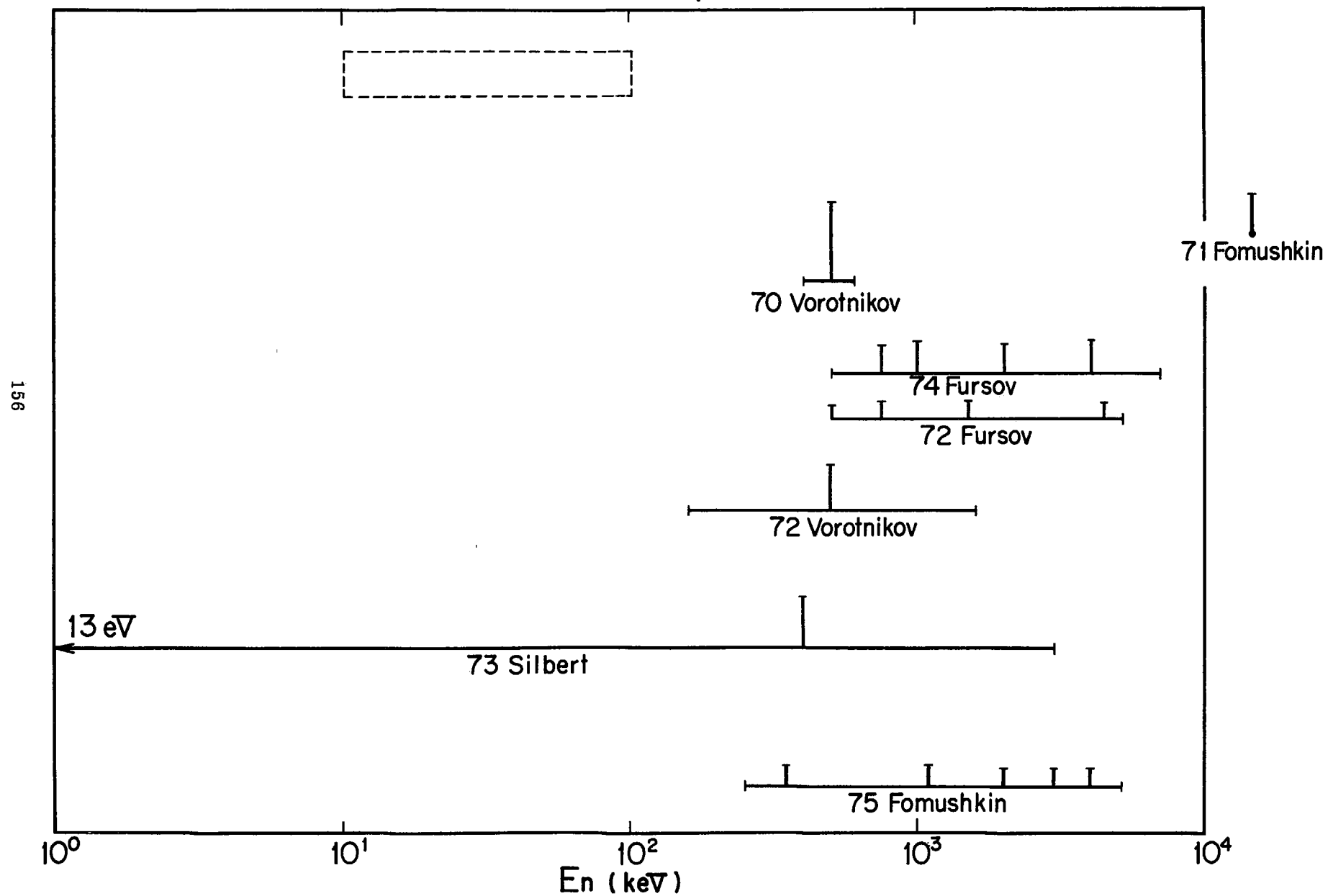


Fig.3.9.1(b)

$^{249}\text{Cf} (n,f)$



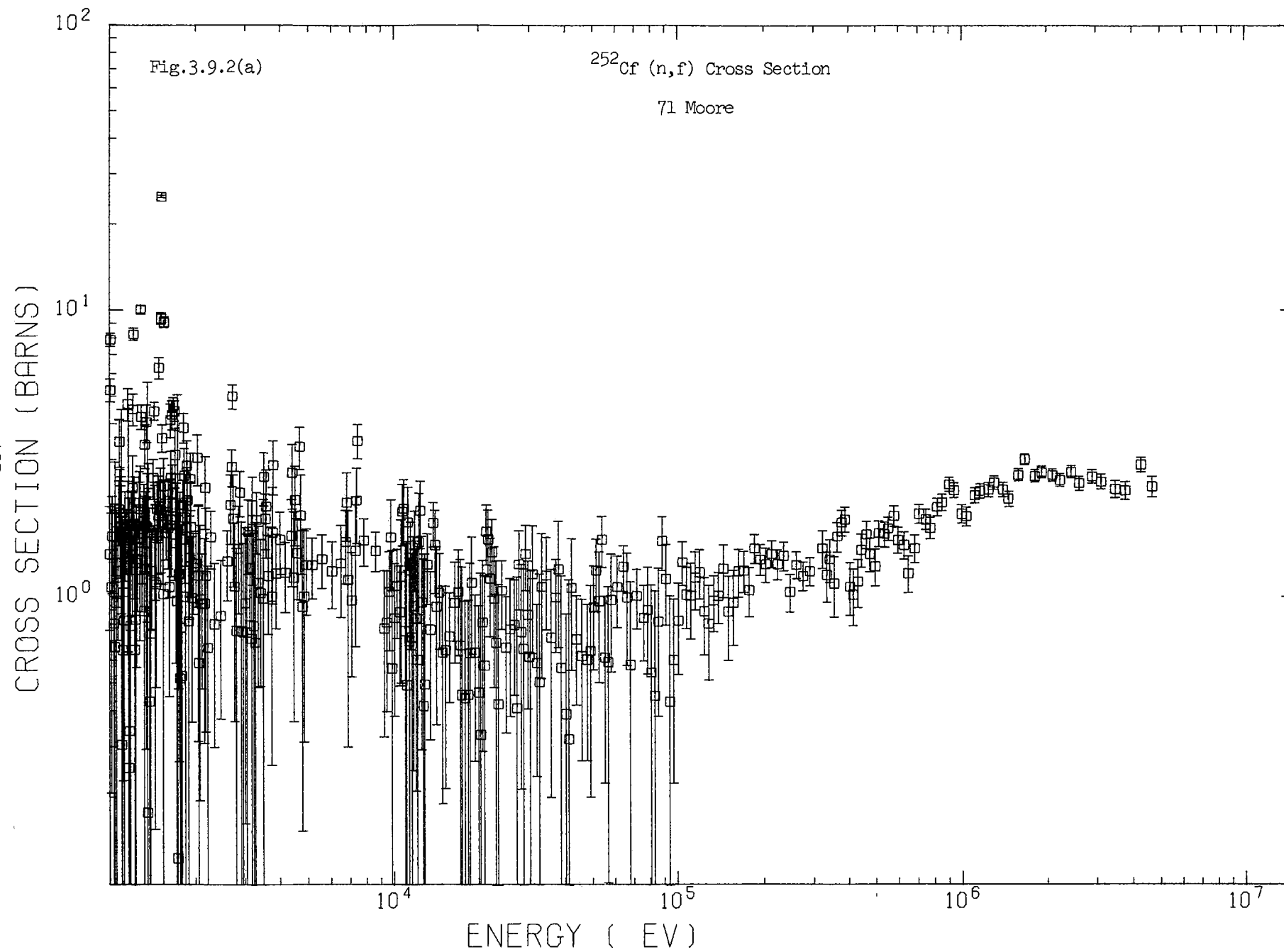


Fig.3.9.2(b)

$^{252}\text{Cf} (n, f)$

158

20 eV

71 Moore

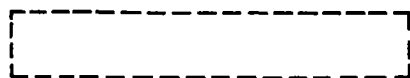
10^0

10^1

10^2
 $E_n \text{ (keV)}$

10^3

10^4



References for Review on Cf Data

70 Vorotnikov

Vorotnikov, P.E., Dubrovina, S.M., Otroshchenko, G.A.,
Chistyakov, L.V., Shigin, V.A., Shubko, V.M.,
Sov. J. Nucl. Phys. 10 (1970) 419

71 Fomushkin

Fomushkin, E.F., Gutnikova, E.K., Maslov, A.N., Novoselov,
G.V., Panin, V.I.,
Yad. Fiz. 14 (1971) 73
Sov. J. Nucl. Phys. 14 (1972) 41

71 Moore

Moore, M.S., McNally, J.H.,
Phys. Rev. C4 (1971) 273

72 Fursov

Fursov, B.I., Androsenko, Kh.D., Ivanova, V.I., Nesterov,
V.G., Smirenkin, G.N., Chistyakov, L.V., Shubko, V.M.,
Sov. Atom. Energy 32 (1972) 205

72 Vorotnikov

Vorotnikov, P.E., Gokhberg, B.M., Dubrovina, S.M., Kosyakov,
V.N., Otroshchenko, G.A., Chistyakov, L.V., Shigin, V.A.,
Shubko, V.M.,
Sov. J. Nucl. Phys. 15 (1972) 20

73 Silbert

Silbert, M.G., Nucl. Sci. Eng. 51 (1973) 376,
LA-5042 (1972)

74 Fursov

Fursov, B.I., Ivanov, V.I., Smirenkin, G.N.,
Sov. J. Nucl. Phys. 19 (1974) 25

75 Fomushkin

Fomushkin, E.F., Gutnikova, E.K., Novoselov, G.F.,
INDC (CCP) 65 U (1975) 6

4. Summary and Conclusion

The present status of the experimental data were surveyed from Pa to Cf. For Es and Fm isotopes, no experimental data could be found in this survey. In spite of the technical difficulties, many data have been measured and accumulated for many isotopes. In particular, the fission cross sections have been measured in the wide energy range for ^{234}U , ^{236}U , ^{237}Np , ^{238}Pu , ^{240}Pu , ^{241}Pu , ^{242}Pu , ^{241}Am , ^{244}Cm and ^{249}Cf . Though some discrepancies exist among different data sets, these data may be utilizable in the application field.

There may be two causes concerning the discrepancies between the different data sets. One is due to the technical problems, and the other is due to the difference of the reference data such as the standard cross sections, decay constants and so on. On the former, there are much uncertainties of which causes are undetectable or for which the corrections are difficult. Because of very high activity, the isotope composition in the sample is changeable during the measurements. Though the estimation of the impurity is important, it is not so easy and it becomes a serious cause of the uncertainty. Most experimentalists have surely endeavoured to improve these difficulties.

Effect of the angular dependence of the fission cross sections may be a cause of the discrepancy. In some experiments, two data sets were obtained at two different directions to the neutron beam, and significant differences were observed. Therefore, the angular distribution of the fission cross section should be taken into account, instead of 4π times the cross section at an angle.

There have been many experiments using the underground nuclear explosion technique. The data obtained by these measurements seem to have rather large uncertainties. Notwithstanding highly intense neutron source, it is hopeless defect that the measurements cannot be repeated. Highly intense neutron source should be developed, but the nuclear explosion

must be avoided.

The uncertainty of the data is closely dependent on the uncertainty of the reference data. Half-lives or decay constants of the active isotopes are key factors to estimate the target thickness and background impurity. Therefore, a part of the discrepancies between the data sets may be due to the difference of these data.

Since the existing experimental data are very valuable, they must be utilizable not only for the proper nuclear physics but also in the data application fields. In this sense, the numerical data should be released as quickly as possible. These data had better be compiled at the four data centers in a suitable format. The compiled data should be returned to the original authors to confirm the entry and to check the data. It is important to keep good communication between the authors and the centers, in order to utilize the data effectively.

Except for the fission cross section, the present status of the data is very poor. Since the capture cross sections for many nuclides have been requested, more efforts should be made to measure the capture cross section. Weston et al.¹⁵⁾ measured the absorption cross section, instead of the capture cross section. If the direct measurements were difficult, such indirect and safe method as this measurement should be developed. The method by Cramer et al.^{3,4,5)} in the fission cross section measurements is a clever technique. In addition to the development of the experimental technique, theoretical method as well as the systematic trends^{6,24,25)} of the data should be investigated to estimate any unknown nuclear data.

References

- 1) WRENDA 74, World Request List for Nuclear Data Measurements,
IAEA (1974)
- 2) CINDA 74, An Index to the Literature on Microscopic Neutron Data,
IAEA (1974)
- 3) Cramer, J.D., Britt, H.C., Nucl. Sci. Eng. 41 (1970) 177
- 4) Gavron, A., Britt, H.C., Konecny, E., Weber, J., Wilhelmy, J.B.,
Phys. Rev. Letters 34 (1975) 827
- 5) Wilhelmy, J.B., Britt, H.C., Gavron, A., Konecny, E., Weber, J.,
LA-UR-75-288, Submitted to Conf. of Nuclear Cross Sections and
Technology, Washington D.C., (1975)
- 6) Walsh, R.L., Boldeman, J.W., Ann. Nucl. Sci. Eng. 1 (1974) 353
- 7) Bertram, W.K., Boldeman, J.W., Walsh, R.L., Caruana, J.,
Paper presented to 3rd National Soviet Conf. on Neutron Physics, Kiev,
(1975)
- 8) Blyumkina, Yu.A., Bondarenko, I.I., Kuznetsov, V.F., Nesterov, V.G.,
Okolovitch, V.N., Smirenkin, G.N., Usachev, L.N., Nucl. Phys. 52
(1964) 648
- 9) Walsh, R.L., Boldeman, J.W., AAEC/TM 574 (1971)
- 10) Tsukada, K., Private Communication.
- 11) Browne, J.C., Private Communication. Contribution to this meeting.
- 12) Nishi, T., Fujiwara, I., Imanishi, N., Private Communication.
Contribution to this meeting.
- 13) Wiltshire, R.A.P., Willis, H.H., Rogers, F.J.G., Glover, K.M.,
Cunninghame, J.G., Sweet, D.W., AERE-R 7363 (1973)
- 14) Glover, K.M., Wiltshire, R.A.P., Rogers, F.J.G.,
UKNDC (75) P71 (1975) 51,
NEANDC (E) 162U Vol. 8 (1975) 51,
INDC (UK) - 25/U (1975) 51

- 15) Weston, L.W., Todd, J.H., Measurement of the Neutron Capture Cross Sections of the Actinides, submitted to the Conf. on Nuclear Cross Sections and Technology, Washington D.C., (1975). This paper is referred to as 75 Weston in this review.
- 16) Gwin, R., Weston, L.W., Todd, J.H., Ingle, R.W., Weaver, H., A Direct Comparison of Different Experimental Techniques for Measuring Neutron Capture and Fission Cross Section for ^{239}Pu , submitted to the Conf. on Nuclear Cross Sections and Technology, Washington D.C., (1975)
- 17) Weston, L.W., Todd, J.H., Trans. Am. Nucl. Soc. 15 (1972) 480
- 18) Davey, W.G., Nucl. Sci. Eng. 26 (1966) 149
- 19) Davey, W.G., Nucl. Sci. Eng. 32 (1968) 35
- 20) Davey, W.G., Nucl. Sci. Eng. 44 (1971) 345
- 21) Henkel, R.L., LA-2122 (1957)
- 22) Matsunobu, H., Private Communication
- 23) Schwartz, S., Strömberg, L.G., Bergström, A., Nucl. Phys. 63 (1965) 593
- 24) Smith, H.L., Smith, R.K., Henken, R.L., Phys. Rev. 125 (1962) 1329
- 25) Sikkeland, T., Ghiorso, A., Nurmia, M.J., Phys. Rev. 172 (1968) 1232

Status of Transactinium Isotope Evaluated

Neutron Data in the Energy Range

10^{-3} eV to 15 MeV

S. Yiftah, Y. Gur and M. Caner
Department of Nuclear Engineering
Technion-Israel Institute of Technology
Haifa, Israel

and

Israel Atomic Energy Commission
Soreq Nuclear Research Centre
Yavne, Israel

Abstract

Large amounts of transactinium elements will be produced in the next 25 years in thermal power reactors, fast breeders, test reactors, special purpose reactors, thermonuclear explosions and improved heavy-ion accelerators. To be able to evaluate, predict, compute and judge the effects and uses of these elements, the nuclear community needs fully evaluated nuclear data to be used as nuclear input to all computations and evaluations. The sixteen transactinium elements and two hundred isotopes known to-date are divided into three groups, and eight main application areas are mentioned from which needs can be derived for measurements and evaluations. Existing evaluations are tabulated and analysed, and following a WRENDA minus CINDA descriptive equation, nine main conclusions and recommendations are derived, amongst which a "world transactinium nuclear data evaluation program" and other specific items for IAEA future actions in this field.

1. INTRODUCTION
=====

Large amounts, in some cases tons and hundreds of kilograms, of transactinium elements will be produced, whether we like it or not, in

the next 25 years in thermal power reactors, fast power reactors, test reactors and special-purpose reactors. These elements will affect the behavior and operation of the reactors, the cost of the power produced, the content and disposal of the radioactive waste. Some of these elements will be used in space missions, cardiac pacemakers, artificial hearts, various industries, and remote unattended sources of power.

On the other hand, improved heavy-ion accelerators capable of accelerating ions of all elements up to uranium will enable the production of new and heavier translawrencium and transkurchatovium elements and enlarge the periodic table.

Finally, the intense neutron bursts of especially designed underground thermonuclear explosions will again serve to produce, instantly, several of the Transactinium isotopes.

To be able to evaluate, predict, compute and judge the effects of these new elements, optimise their production, optimise their beneficiary effects on reactors, evaluate their uses in different applications, minimise their contamination effects, minimise or cancel their long-term radioactive effect in nuclear wastes, the nuclear community needs fully evaluated nuclear data to be used as nuclear input to all these computations and evaluations.

2. SIXTEEN TRANSACTINIUM ELEMENTS AND TWO HUNDRED ISOTOPES

Actinium being element number 89, sixteen transactinium elements are known to date, from 90 to 105. The sixteen transactinium elements include three naturally* occurring elements, thorium, protactinium and uranium,

* Evidence for the occurrence of Plutonium-244 in nature has been obtained in 1971 in the U.S.A. Minute amounts of Pu-244 were found in the natural "as mined" bastnasite ore, a rare earth fluorocarbonate mineral.

eleven man-made transuranium elements, from neptunium (No. 93) to lawrencium (No. 103), that complete the fourteen elements of the actinide series, in which the filling of the 5f electron shell takes place, and two translawrencium elements, kurchatovium (No. 104) and hahnium (? , No. 105) that continue the periodic table below hafnium and tantalum.

The sixteen transactinium elements, together with predicted locations of new elements, are shown on a conventional form of the periodic table in figure 1⁽¹⁾.

It is seen that the actinides can be considered to be a "heavy rare-earth-like" series of elements analogous to the light rare-earth series, the lanthanides, in which the 4f electron shell is filled, an idea conceived by Seaborg in 1944 which was the key to the discovery of several of these elements. Some of the names reflect the actinide-lanthanide analogy. The actinide Americium versus the lanthanide Europium; Curium after Pierre and Mary Curie, by analogy with Gadolinium, after the Finnish rare-earth chemist, J. Gadolin; berkelium after Berkeley, California, analogous to terbium, derived from Ytterby, Sweden, where so many of the early rare-earth minerals were found.

Figure 1 also shows a possible "super-actinide" family, starting with element No. 122 which can again be considered as a superheavy-rare earth-like series of elements, resulting from the filling of the 14 - member 6f subshell of electrons.

It can be noted in Fig. 1 that all the transactinium elements known today, with the exception of Ku (No. 104) and Ha (No. 105), belong to the actinide series.

About 200 isotopes of the 16 transactinium elements are known to date. Only 72 isotopes, or about a third, have half-lives higher than one day. Out of these last 72 isotopes again a third, 24 isotopes, have evaluated neutron data reported in CINDA 75⁽²⁾. These last 24 isotopes

include the 5 main fissile and fertile isotopes (Th-232, U-233, U-235, U-238, Pu-239) not subject to discussion in the program of the present meeting.

Numerically speaking, we have then 48 (72 - 24) transactinium isotopes with half-lives higher than one day that do not have any evaluated data, at least any that are reported in the last issue of CINDA, published April 1975.

Several questions arise.

- 1) Are available evaluations not reported in CINDA 1975?
- 2) Are the evaluations fairly recent and do they contain all experimental information? Do some of these evaluations need updating?
- 3) Does the nuclear community need evaluations not existing today?
With what priorities?
- 4) Are these needs world-known, documented and coordinated, and related directly to specific applications?
- 5) Are evaluations needed for isotopes having half-lives shorter than one day?
- 6) Can a consensus be reached as to what evaluations are needed, with what priorities, and also on a coordinated international "division of labor" on performing the needed evaluations within a specified period of time?
- 7) Do enough experimental measurements exist which can form the basis, together with theoretical model calculations and systematics, of the needed evaluations?

This list of questions, which can probably be extended, will be dealt with during the whole of this meeting, and presumably also after the meeting.

This paper is an attempt to give partial answers to some of the above questions.

3. THREE GROUPS OF TRANSACTINIUM ELEMENTS

The sixteen transactinium elements known to date can be divided into three groups, as shown in Table I.

Group I - 5 elements, 90 - 94, thorium to plutonium.

Group II - 6 elements, 95 - 100, americium to fermium.

Group III - 5 elements, 101 - 105, mendelevium to hahnium.

Group I , (90 - 94), includes the main fissile and fertile isotopes that form the basis of the present nuclear technology. Thorium, protactinium and uranium are naturally occurring. Neptunium and plutonium were discovered in 1940 - 1941, when the whole present nuclear technology was born. The five elements of this group include 82 known isotopes of which 37 have half-lives higher than one day. For 19 of these 37 isotopes evaluations exist.

Group II , (95 - 100), includes six elements which were discovered by the three basic methods of transactinium elements productions, the first two yielding neutron-rich and the third neutron-deficient nuclides:

(a) Multiple neutron capture as a result of intense neutron bombardment over long periods of time in different types of nuclear reactors (power reactors, test reactors, special-purpose reactors).

(b) Refinement of the thermonuclear explosion method where suitable targets are subjected to intense bursts of neutrons in a very short period of time (milliseconds).

Fluxes and integrated fluxes for transactinium nuclides production by successive neutron capture are shown on Table II.

(c) Bombardment with heavy ions, from heavy-ion accelerators.

Of the six elements of group II, one, americium, was discovered (1945) as a result of irradiation of plutonium with neutrons in a nuclear reactor (method a). Three, curium, berkelium and californium were discovered, respectively, by bombardment of plutonium with helium ions (1944), bombardment of americium with helium ions (1949) and bombardment of curium with helium ions (1950) (method c). Einsteinium and fermium, on the other hand, were discovered unexpectedly in 1952 in investigations of the coral bottom of the Bikini atoll after the first hydrogen bomb test (method b).

The six elements of group II include eighty known isotopes, of which thirty-four have half-lives higher than one day. For only five of these (Am-241, Am-243, Cm-243, Cm-244, Cf-252) evaluations exist.

Group III, (101-105), includes five elements, all of which were discovered by bombardment with heavy ions. Medeleevium (101) was discovered in 1955 by bombardment of einsteinium with helium ions. Nobelium (102) was discovered in 1958 by bombardment of curium with carbon ions. Lawrencium (103) was discovered in 1961 by bombardment of californium with boron ions. Kurchatovium (104) was discovered in 1964 by bombardment of californium with carbon ions and also curium with oxygen-18 ions. Hahnium (105) was discovered in 1970 by bombardment of californium with nitrogen-15 ions and also berkelium with oxygen-16 and oxygen-18 ions.

The five elements of group III include 33 known isotopes, of which only one, mendelevium - 258, has a half-life of more than one day, actually 53 days. This surprisingly long half-life for this group may make it possible eventually to isolate the element mendelevium in macroscopic quantities. Three other isotopes, Md - 257 has a half-life of 5.1 hours, Md - 256 77 minutes, Md - 259 57 minutes. All the others have half-lives of seconds or less.

Table I
The Three Groups of Transactinium Elements

Group	No.	Atomic number	Element	Number of known isotopes	Known isotopes with $T_{1/2} > 1d$	No. of isotopes evaluated (CINDA 75)	Isotopes Evaluated (CINDA 75)
I	1	90	Thorium (Th)	20	7	1	232
	2	91	Protactinium (Pa)	18	6	2	231, 233
	3	92	Uranium (U)	15	9	7	232, 233, 234, 235, 236, 237, 238
	4	93	Neptunium (Np)	14	6	3	237, 238, 239
	5	94	Plutonium (Pu)	15 (82)	9 (37)	6 (19)	236, 238, 239, 240, 241, 242
II	6	95	Americium (Am)	13	4	2	241, 243
	7	96	Curium (Cm)	13	10	2	243, 244
	8	97	Berkelium (Bk)	9	5		
	9	98	Californium (Cf)	16	8	1	252
	10	99	Einsteinium (Es)	14	5		
	11	100	Fermium (Fm)	15 (80)	2 (34)	(5)	

Group	No.	Atomic number	Element	Number of known isotopes	Known isotopes with $T_{1/2} > 1d$	No. of isotopes evaluated (CINDA 75)	Isotopes Evaluated (CINDA 75)
III	12	101	Mendelevium (Md)	10	1		
	13	102	Nobelium (No)	9			
	14	103	Lawrencium (Lr)	6			
	15	104	Kurchatovium (Ku)	5			
	16	105	Hahnium (Ha)	3 (33)			
			Totals	195	72	24	

It is clear from the above and from glancing at Table I that the main evaluation work to be done is in group II.

4. MAIN NEEDS FOR TRANSACTINIUM NUCLEAR DATA

If it is obvious that the main reason for the big effort to produce transactinium elements and to discover new ones has been to increase our understanding of atomic and nuclear structure, it should be as clear that a big effort in measuring transactinium cross sections and performing complete nuclear data evaluations for these isotopes has been and will be motivated by the needs of actual specific applications.

After sketching the large-scale panorama of the 200 known isotopes of the transactinium elements, it is therefore logical to introduce the dimension of actual applications.

Table II

Fluxes and Integrated Fluxes for Transactinium NuclidesProduction by Successive Neutron Capture

Method		flux $\phi(\text{n cm}^{-2} \text{sec}^{-1})$	Irradia- tion time Δt	Integrated flux $\phi \Delta t(\text{n cm}^{-2})$	Remarks
Power Reactors	typical PWR	1.5×10^{13}	1 year	4.7×10^{20}	thermal neutrons relatively
	typical BWR	3×10^{13}	1 year	9.45×10^{20}	
	typical HWR	0.5×10^{14}	1 year	1.58×10^{21}	
Special Reactors	HFIR*	3×10^{15}	1 year	9.45×10^{22}	higher capture cross- section
	Savannah* (thermal high-flux mode operation)	6×10^{15}	1 year	1.89×10^{23}	
Thermonuclear Explosion		$>10^{31}$	$<10^{-6} \text{ sec}$	10^{25}	fast neutrons relatively lower σ_{γ}
Cosmological Nucleosynthesis Production	s Process	$\sim 10^{16}$	$\sim 10^3 \text{ year}$	$10^{26} - 10^{27}$	
	r Process	$\gtrsim 10^{27}$	1-100 sec	$>10^{27}$	

* Production of Cf-252 requires neutron flux densities of at least $3 \times 10^{15} \text{ n cm}^{-2} \text{sec}^{-1}$. The flux value for HFIR is the central region perturbed flux (with Pu-242 target material, for instance).

In five reactor experiments performed at SRL for testing and adjustment of their consistent transplutonium multigroup cross section set (see below), integrated fluxes of between 2.47×10^{20} and $1.22 \times 10^{23} \text{ n/cm}^2$ have been reported (with exposure times ranging from 165 to 850 days).

Of course the main applications are the uses of the main fissile and fertile isotopes in thermal power reactors and nuclear explosives, which form the basis of the whole present nuclear technology.

For the purpose of this meeting and in order to gain perspective, we mention the following eight main areas from which needs can be derived for nuclear data measurements and evaluations for a large number of the trans-actinium isotopes.

a) The nuclear fuel charge for fast reactors: plutonium produced as by-product from thermal power reactor operation, will consist of maybe 50 % of the higher plutonium isotopes ^{240}Pu , ^{241}Pu , ^{242}Pu . A typical 1000 MWe fast power reactor core contains 3 tons of plutonium. Half of this plutonium, that is 1.5 tons, will consist of ^{240}Pu , ^{241}Pu and ^{242}Pu . If the plutonium has been stored for a few years, waiting for the fast reactors, there is an appreciable buildup of ^{241}Am because of the 15-years half-life of ^{241}Pu . The presence of ^{241}Am in the fuel implies that ^{242}Am and ^{242}Cm will be produced during reactor operation. These facts and figures illustrate the major importance of fully evaluated nuclear data of these actinide isotopes for the study, design, statics and dynamics of fast reactors (3-7), right from the very beginning.

(b) Long burn-Up Fuels (up to 100,000 MWD/T) of fast reactors will accumulate relatively large amounts of transplutonium elements, as these increase with the burn-up.

The effect of these elements on the behavior of fast reactors should and would be carefully studied if the necessary nuclear data become available.

(c) Long-lived actinides contained in the radioactive wastes* of thermal reactors, fast reactors and reprocessing plants could possibly be transmuted into fission products or other elements thereby helping solve the radioactive waste problem. This "actinide wastes recycle" requires a neutron source which might be the same reactor producing the wastes or a specially designed burner reactor or even a fusion reactor (23,24).

* See Appendix

Evaluated data are needed to predict in advance the amount and nature of actinide wastes that will be generated and to analyse and test the proposed recycle schemes, much before we have any proven technology for separating and recycling actinides.

(d) The alpha-particle-emitting ^{238}Pu , ^{242}Cm and ^{244}Cm are being and will be widely used as heat sources in auxiliary electrical power systems for satellites, space probes, cardiac pacemakers, artificial hearts, and remote unattended applications. One interesting example occurred in 1967 on the moon. The surveyor V spacecraft landed on the moon and performed a chemical analysis of the lunar surface. The analysis was done using a 100 mCi ^{242}Cm alpha-particle source produced by neutron irradiation of ^{241}Am . As energy markers for the detection equipment, the 6.4 MeV alpha-particle of a small ^{254}Es source was used (1).

The ^{238}Pu , having a specific power output of 0.5 W/g which drops very slowly because of its long half-life of 86 years, is used in high power radionuclide batteries in remote locations and in very low power batteries for cardiac pacemakers.

^{238}Pu can be produced in a reactor in two ways, by irradiating either ^{237}Np or ^{241}Am . The two ^{238}Pu production chains which emphasize the cross sections significant to the production process are shown in figure 2 (8).

(e) Californium - 252 constitutes the most intense, compact source of neutrons known. The spontaneous fission decay (3% of its nuclei) of about 2 mg (1 Curie) of ^{252}Cf yields 4.4×10^9 neutrons per second. 1 gram of ^{252}Cf emits over 10^{12} fission neutrons per second. ^{252}Cf , which has a half life of 2.65 years, is and will be widely used in various fields including cancer radiotherapy, neutron radiography, neutron activation analysis and hydrology.

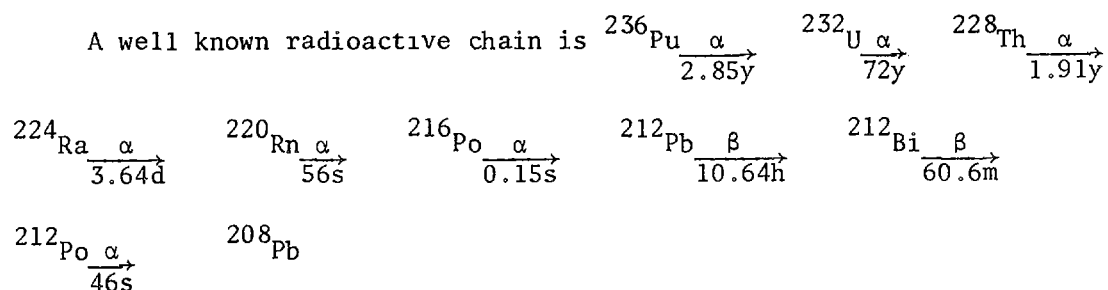
The ^{252}Cf production chain showing the cross sections significant to the production process is shown in figure 3 (8).

(f) Starting materials for production of useful actinides

We have already mentioned ^{241}Am and ^{237}Np as starting materials for the production of ^{238}Pu . ^{241}Am is extracted from stored reactor plutonium. During storage, ^{241}Pu is converted by beta decay into ^{241}Am at the rate of about 5% per year. ^{244}Cm is produced mainly by special irradiation of reactor plutonium where ^{239}Pu , ^{240}Pu and ^{241}Pu fission or are converted into ^{242}Pu . After separation of the fission products ^{242}Pu becomes the starting material for irradiation and conversion into ^{244}Cm via ^{243}Pu and ^{243}Am . ^{244}Cm and ^{242}Cm can also be formed from ^{241}Am by successive neutron capture. ^{252}Cf is formed from ^{244}Cm after eight consecutive neutron captures. Under neutron irradiation, ^{252}Cf yields einsteinium and in a second step, fermium.

^{257}Fm decays predominantly by alpha particle emission with a half-life of about 100 days which makes it a convenient isotope to study. ^{257}Fm is the heaviest isotope both in atomic number and mass number which is available in sufficient quantity to obtain reliable counting statistics. The 380 microseconds half-life of ^{258}Fm leads to the conclusion that nuclei heavier than ^{257}Fm cannot effectively be produced in nuclear reactors.

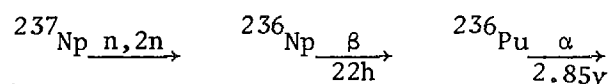
(g) Radioactive contamination chain ^{236}Pu , ^{232}U , ^{228}Th



It is seen that all nuclides following ^{228}Th are short lived. Many of these are powerful gamma emitters, and raise important contamination problems due to ^{232}U in spent reactor fuel, ^{236}Pu in ^{238}Pu heat sources, ^{236}Pu in recycled Pu for thermal and fast reactors, ^{232}U in ^{233}U . Materials contaminated with surprisingly small amounts of this radioactive chain require remote handling behind shielding.

Diffusion cascades can be contaminated by spent reactor fuel containing ^{232}U . Members of the chain are formed and deposited on process surfaces.

^{238}Pu made by irradiating ^{237}Np in a reactor is accompanied by ^{236}Pu formed by the (n,2n) reaction.



and is therefore unsuitable for cardiac pacemakers. For this application the alternative route of ^{238}Pu production via ^{241}Am should be used.

Cross section requirements for the production of ^{232}U and ^{236}Pu are the (n,2n) cross section of ^{237}Np , ^{232}U , ^{233}Pa and ^{232}Th with an accuracy of 10% (5% for ^{232}Th), $^{236}\text{U}(n,\gamma)$ with an accuracy of 5%, $^{237}\text{U}(n,\gamma)$, with an accuracy of 10% and (n, α) of ^{232}U and ^{236}Pu with an accuracy of 10%.

(h) Criticality of actinide elements

The applications of ^{238}Pu and ^{244}Cm as heat sources, as well as applications of americium and other actinides require knowledge of the criticality limits, especially the effects of moderating materials. It has been calculated, for instance, that the critical mass of ^{238}Pu is about half that of ^{239}Pu .

For criticality evaluations one needs to know the ^{238}Pu and ^{244}Cm (n,f), $\bar{\nu}$, (n, γ), (n,n'), (n,n) to an accuracy of about 5% and the americium isotopes cross sections to an accuracy of maybe 10%.

These requirements become more important if one takes into account the large amounts of actinide isotopes to be produced in the future. One such estimate, for illustration purposes, is given in Table III ⁽⁹⁾.

Table III

Annual Production of Actinide Isotopes - 1987 ⁽⁹⁾

	<u>U.S. (tonnes/year)</u>	<u>World (tonnes/year)</u>
Fission Products	160	430
U-236 (in U-235 & U-238)	22	60
Np - 237	2.3	6.3
Pu - 238	0.6	1.6
Pu - 239	40	110
Pu - 240	13	36
Pu - 241	6.7	18
Am - 241	0.9	2.5
Pu - 242	1.5	4.1
Cm - 242	0.03	0.08
Am - 243	0.6	1.7
Cm - 244	0.1	0.3

5. EXISTING EVALUATIONS

To find evaluations of transactinium nuclides one should first look at the big evaluated nuclear data files of the various countries and laboratories working with actinides, that is

- 1) ENDF/B-IV, U.S.A.
- 2) UKNDL, United Kingdom
- 3) KEDAK, Germany
- 4) LLL, Lawrence Livermore Laboratory, U.S.A.
- 5) SRL, Savannah River Laboratory, U.S.A.

Table IV

Actinide Evaluations

No.	Nuclide	Half-Life $T_{1/2}$	ENDF/ B-IV	UKNDL	KEDAK (1)	LLL (2)	SRL (3)	OTHER
1	Pa-231 *	3.25×10^4 y			+(1970)			GA-7462 (1967)
2	Pa-233 *	27d	+(1970)					GA-7462 (1967)
3	U-232 *	72y			+(1970)			
4	U-234 *	2.44×10^5 y	+(1967)		+(1970)	+(1972)		
5	U-236 *	2.342×10^9 y	+(1971)		+(1970)	+(1972)		
6	U-237 *	6.75d			+(1970)	+(1972)		
7	U-239	23.5m				+(1972)		
8	Np-237 *	2.14×10^6 y	+(1973)		+(1970)	+(1973)		
9	Np-238 *	2.12d			+(1970)			
10	Np-239 *	2.35d						
11	Pu-236 *	2.85y			+(1970)			
12	Pu-238 *	87.8y	+(1967)	+(1967)	+(1974)	+(1972)		
13	Pu-240 *	6540y	+(1974)	+(1970)	+(1972)	+(1972)		
14	Pu-241 *	15y	+(1973)	+(1970)	+(1973)	+(1972)		
15	Pu-242 *	3.87×10^5 y	+(1967)		+(1973)		+(1975)	
16	Pu-243	4.96h					+	
17	Am-241 *	433y	+(1966)		+(1970)			
18	Am-242	16.02h				+		
19	Am-242 ^m	152y				+(1972)		see re- mark NO. 4
20	Am-243 *	7370y	+(1966)				+(1975)	

No.	Nuclide	Half-Life $T_{1/2}$	ENDF/ B-IV	UKNDL	KEDAK ⁽¹⁾	LLL ⁽²⁾	SRL ⁽³⁾	OTHER
21	Cm-242	163d			+(1970)			
22	Cm-243*	28y						
23	Cm-244*	17.9y	+(1967)				+	
24	Cm-245	8.5×10^3 y				+(1974)	+	
25	Cm-246	4.76×10^3 y					+	
26	Cm-247	1.54×10^7 y					+	
27	Cm-248	3.5×10^5 y					+	
28	Bk-249	311d					+	
29	Cf-249	352y					+	
30	Cf-250	13.1y					+	
31	Cf-251	~ 900y					+	
32	Cf-252	2.63y				+(1974)	+	
33	Cf-253	17.8d					+	
34	Es-253	20.47d						

Remarks:

* The 19 nuclides marked by an asterisk have evaluations listed in CINDA 75.

A second reference to study would be CINDA 75⁽²⁾, the Computer Index of Neutron Data, which contains bibliographical references to measurements, calculations, reviews and evaluations of neutron cross-sections and other microscopic neutron data. CINDA is published yearly on behalf of the USA National Neutron Cross-Section Center, the USSR Nuclear Data Centre, the NEA Neutron Data Compilation Centre and the IAEA Nuclear Data Section. In the future, it will apparently be published once every two years.

Table IV lists the actinide evaluations known to the authors to be

included in five evaluated files as well as those listed in CINDA 75. The year after the sign + indicates the date of the evaluation. Where there is no mention of the year-authors could not ascertain the evaluation date. This omission can easily be corrected later.

Another paper prepared for the present meeting entitled "A Survey of Cross Section Evaluation Methods for Heavy Isotopes" ⁽¹⁰⁾ gives details of the nuclear models and the formalisms used in the thermal, resolved resonances, unresolved resonances and fast energy ranges, in some recent evaluations.

- (1) The KEDAK column includes evaluations of Pa-231, U-232, U-234, U-236, U-237, Np-237, Np-238, Pu-236, Pu-238, Am-241 and Cm-242 done by B. Hinkelmann ⁽¹¹⁾, and evaluations of Pu-238, Pu-240, Pu-241 and Pu-242 done by M. Caner and S. Yiftah ^(12, 13, 14).
- (2) Lawrence Livermore Laboratory ⁽¹⁵⁾. LLL revisions in the evaluations: σ_f of U-234 revised 1974; σ_f and $\sigma_{n,3n}$ of U-236 revised 1974; σ_f , $\sigma_{n,\gamma}$ and σ_{el} of Pu-238 revised Jan. 1975 ⁽¹⁵⁾.
- (3) Savannah River Laboratory ⁽¹⁶⁾.
- (4) A partial evaluation of fission and capture cross sections from 0 to 5 MeV has been done in Saclay, France. The results are given in a multigroup form adapted to thermal reactor study. These cross sections are now checked with irradiated fuel analysis ⁽¹⁷⁾.

Examining Table IV some general remarks are in order.

It can be seen clearly that ENDF/B-IV includes evaluations of 11 actinides of which only three have been performed after 1972 (similarly KEDAK includes evaluations of 14 actinides of which only four have been performed after 1972). It has been therefore recognised (see also Raman's review paper A-1) that the ENDF/B-IV data files for Americium, Curium, Berkelium and Californium are inadequate or nonexistent. New actinide evaluations are underway at SRL, Hanford

(Schenter) and LLL (Howerton). These are shown in table IV and will be included in ENDF/B-V, for which a file of Actinide Nuclear Data is currently being prepared. This file will also include evaluated decay data by Dr. Reich.

The LLL (Lawrence Livermore Laboratory) library does not contain resonance parameters.

The SRL (Savannah River Laboratory) library is more than an evaluated library of the 15 nuclides in the production chain from ^{242}Pu through ^{253}Es . Actually the process has gone one step further and an evaluated consistent transplutonium multigroup cross section set has been obtained (16,18).

The data are currently in a format similar to the HAMMER format and consist of resolved and unresolved resonance parameters (up to 10 keV) and smooth 84-group cross sections that span the energy range from 0 to 10 MeV with a thermal cutoff at 0.625 eV. The 30-group THERMOS structure is used for the thermal region and the 54-group MUFT structure is used for the epithermal region. The 84-group sets have also been collapsed to 37 groups (12 thermal and 25 epithermal groups) which may be used to reduce computer time. The data have been tested through comparison of measured and calculated production yields in thermal and near thermal neutron spectra. Available data above 10 keV have been included, but have been neither evaluated nor tested. The data is being put, along with some additional actinides, into the ENDF/B format and will probably be made available through the National Neutron Cross Section Center, Brookhaven.

Generally, the concentrations of actinide nuclides predicted with the newly-formulated consistent set are within $\pm 10\%$ of the experimentally-measured concentrations.

Table V (18) lists the values of the 2200 m/s fission and capture cross sections, the g-factor which is a convenient measure of the departure from $1/v$ dependence and the resonance integrals I_c and I_f with a thermal cutoff of 0.625 eV. For two group calculations the thermal value used should be the product of the 2200 m/s cross section and the g-factor.

Table V

Characteristic Cross Sections from the SRL					
Multigroup Data Sets (18)					
Isotope	σ_c^{2200} (barns)	σ_f^{2200} (barns)	g-factor	I_c ≥ 0.625 eV (barns)	I_f ≥ 0.625 eV (barns)
^{242}Pu	18.7	0	1.0	1,280	4.74
^{243}Pu	87.4	180	1.0	264	541
^{243}Am	74.4	0	1.015	2,159	3.4
^{244}Cm	10.0	1.5	0.995	585	17.1
^{245}Cm	383	2161	0.971	104	766
^{246}Cm	1.4	0.17	1.0	119	10.0
^{247}Cm	58.0	72.3	1.0	500	761
^{248}Cm	2.89	0.11	1.0	251	14.7
^{249}Bk	1600	0	1.0	4,000	0
^{249}Cf	495	1720	0.969	777	1863
^{250}Cf	1701	0	1.0	11,000	0
^{251}Cf	2849	4801	1.0	1,600	5400
^{252}Cf	20.4	32.0	1.0	43.5	110
^{253}Cf	12.0	1100	1.0	12.0	2000
^{253}Es	155	0	1.0	7,300	0

Another general remark concerning Table IV is the following: while some nuclides have been evaluated only once and appear in only one of the big evaluated data files, others have evaluations in two, sometimes three, of the big files. In this case several problems arise: what are the differences between the evaluations and between the multigroup sets obtained from them? Will physics and other parameters of the reactors calculated using the different files be different? How big is the difference?

To shed some light on these problems a comparative analysis of the various evaluated files should be performed. The results of the analysis can then be used as a tool for the detailed examination of discrepant data.

Examples of comparative analyses of this type are given in references (19-22).

Generally speaking, it seems reasonable to assume that most evaluations performed before 1972 should be reevaluated, taking into account new experimental measurements and better theoretical model calculation techniques.

6. WREND A - CINDA = ?

As is well known, since 1972 a World Request List for Nuclear Data Measurements (WREND A) is issued annually by the IAEA Nuclear Data Section on behalf of the U.S.A. National Neutron Cross Section Center, Brookhaven, the European (NEA) Neutron Data Compilation Centre, Saclay, the IAEA Nuclear Data Section, Vienna and the USSR Nuclear Data Center, Obninsk. WREND A 74 was the first edition to be printed from the computerized data request file maintained by the IAEA Nuclear Data Section.

IAEA also publishes CINDA, the Computer Index of Neutron Data, the last issue being the two volume CINDA 75. CINDA contains bibliographical references to measurements, calculations, reviews and evaluations.

In principle, if the two IAEA publications, WREND A and CINDA, are complete and up-to-date, the complicated - sophisticated equation of

$$\text{WREND A} - \text{CINDA} = \text{NUNDA}$$

should constitute a guide for the needed and unavailable nuclear data.

The first conclusion of just looking at the equation and glancing at the two recent issues of WREND A and CINDA is that there is some

assymetry. While CINDA contains also evaluations of nuclear data, WRENDA lists only measurements.

We recommend therefore to add to WRENDA the "quantity" EVALUATION and put under this heading evaluation requests recommended by the present panel and in future by Member States, This way WRENDA will become also a World Request List for Evaluated Nuclear Data.

Another assymetry is in the opposite direction. WRENDA rightly lists, in much detail, the accuracies required of the various requests. When one looks up a measurement report listed in CINDA, he finds, usually, listed explicitly, the uncertainties attached to the measurements. Not so if one looks up evaluated data listed in CINDA. Also the main big evaluated nuclear data files do not contain uncertainties.

It has been recommended before that evaluations should contain rough estimates of the uncertainties in the recommended data. We agree with this opinion and further suggest that in the future these estimates be included in the "general information" section of the evaluated data files.

As examples of recent requests in WRENDA, we mention the requests of G.A. Cowan, Los Alamos Scientific Laboratory, for the fission cross section of 12 isotopes in the energy range 10-100 keV with an accuracy of 10% and priority 1. The 12 isotopes are: Fm-257, Fm-255, Es-253, Cf-252, Cf-250, Cf-249, Cm-248, Cm-247, Cm-246, Cm-245, Cm-244, Cm-243. Some of these cross sections are needed to evaluate Cf production, while the cross section of Cm-243 is needed to evaluate Cm-244 production.

As another example we mention the requests of G. Dessauer of the Savannah River Laboratory for the capture cross section of 13 isotopes in the energy range 25.3 meV to 10 keV with an accuracy of 10% and priority 1 or 2. The 13 isotopes are: Cf-253, Cf-252, Cf-251, Cf-250, Bk-249, Cm-248, Cm-247, Cm-246, Cm-245, Cm-243, Cm-242, Am-242 (152 year isomer), Am-241. G. Dessauer also requests the total cross section of

several californium, berkelium, curium and americium isotopes in the same energy range with an accuracy of 10 - 20% and priorities 1 or 2.

As a third example, again a large bundle of requests, we mention the requests of R. Yumoto and H. Matsumobu of Japan, for the fission and capture cross sections of 22 isotopes, from Pu-243 to Cf-254, in the energy range from thermal to 10 MeV, with accuracies of 5 - 20%. Fourteen of the isotopes requests have priority 1 and eight priority 2. These requests are motivated by reactor burnup calculations and estimation of trans-uranium nuclide build-up in spent fuel, and neutron shielding of spent-fuel transport cask.

The WRENDA definition of priorities is the following:

Priority 1 - Nuclear data which satisfy the criteria of priority 2 and which have been selected for maximum practicable attention, taking into account the urgency of nuclear energy programme requirements.

Priority 2 - Nuclear data which will be required during the next few years in the applied nuclear energy program.

Priority 3 - Nuclear data of more general interest and data required to fill out the body of information needed for nuclear technology.

The above accuracies of 10 - 20% can be compared with much greater ones, in the range of 2% - 1% and even as great as 0.1%, requested for $\bar{\nu}$ in the spontaneous fission of Cf-252, and for the energy spectrum of Cf-252 neutrons, as illustrated in the following short tables.

7. Conclusions

(1) Because of their major importance as fuel for fast reactors the higher plutonium isotopes Pu-240, Pu-241 and Pu-242 (together with Pu-239 and U-238) should have at all times exact reliable up-to-date evaluations, to be revised and updated at regular intervals of two to three years. The accuracy of the higher plutonium isotopes should not be less than that of ^{239}Pu and ^{238}U .

(2) The main evaluation work to be done is in the four elements of Group II, americium, curium, berkelium and californium. Group I elements have been extensively evaluated. Group III elements have extremely short half-lives and exist in minute atom quantities. For Einsteinium and Fermium, the heaviest elements of Group II, few requests and relatively few measurements exist. The four elements, americium, curium, berkelium and californium combine some of the major application needs of long burnup fuels, long-lived actinides in radioactive wastes, heat sources in auxiliary electrical power systems for space^{*}, medical uses and remote unattended applications^{*}, and the multiple uses of californium-252, together with its production chain.

(3) The four elements, americium, curium, berkelium and californium have 51 known isotopes of which 27 have half-lives of more than one day.

The complete nuclear data evaluations of these 27 isotopes should constitute "the world transactinium nuclear data evaluation program" to be sponsored and coordinated on an international basis by the International Atomic Energy Agency.

(4) From the point of view of applications, it seems that out of the 27 nuclides of the "world program" the following 14 nuclides are the most important: Am-241, Am-242^m, Am-243, Cm-242, Cm-244, Cm-245, Cm-246, Cm-247, Cm-248, Bk-249, Cf-249, Cf-250, Cf-251 and Cf-252.

If further priorities are necessary, first priority should be assigned to the evaluation of the following 6 isotopes: Am-241, Am-243, Cm-242, Cm-244, Cm-245 and Cf-252.

(5) In general, it is advisable that two separate evaluations be done of each nuclide, these two to be critically compared and analysed in

^{*} together with Pu-238

various ways, in order to discover inconsistent and discrepant data and to improve future evaluations.

(6) Comparative critical analysis of different nuclear data files and evaluations should be sponsored by the International Atomic Energy Agency for the benefit of all users.

(7) At the present stage of nuclear technology and applications on one hand, and the relatively important world-wide nuclear data measurement programs on the other, it is reasonable to consider, in general, that the half-life of a good reliable nuclear data evaluation should not be more than three years. All evaluations should be checked for revisions or complete reevaluation -- at least at three-year intervals.

(8) WRENDa, the world request list for nuclear data measurements should become a world list for evaluated and measured nuclear data. Users should specifically request nuclear data evaluations needed. The requests should be well documented and related to specific applications.

(9) All evaluations should contain at least rough estimates of the uncertainties in the recommended data. These estimates should be included in the "general information" section of evaluated data files.

References

- (1) G.T. Seaborg, "Annual Reviews of Nuclear Science", Vol. 18, p. 96, 136 (1968).
- (2) CINDA 75, Vol. 2, IAEA, Vienna (1975).
- (3) D. Saphier and S. Yiftah, Proceedings, International Symposium on Physics of Fast Reactors, Tokyo, Vol. III, pp. 1491 - 1512 (1973).
- (4) S. Yiftah, Physics of Fast and Intermediate Reactors, Vol. II, IAEA, pp. 257 - 270 (1962).

- (5) G. Shaviv and S. Yiftah, Nucl. Appl. 3, 4, 213 (1967).
- (6) D. Ilberg, D. Saphier and S. Yiftah, Nucl. Technol. 24, 111 (1974).
- (7) D. Ilberg, D. Saphier and S. Yiftah, Trans. Amer. Nucl. Soc. 21, 463 (1975).
- (8) R.W. Benjamin, DP-1324, SRL (1973).
- (9) T.M. Snyder, CONF-660303, Book 2, 1025 (1966).
- (10) M. Caner and S. Yiftah, paper presented for IAEA TND Advisory Group Meeting (Nov. 1975).
- (11) B. Hinkelmann, KFK-1186 (1970).
- (12) M. Caner and S. Yiftah, INDC (ISL)-2/L, IA-1301 (revised Jan. 1975).
- (13) M. Caner and S. Yiftah, IA-1243 (1972), IA-1275 (1973) and IA-1276 (1973).
- (14) M. Caner, S. Yiftah, B. Shatz and R. Meyer, Proceedings, International Symposium on Physics of Fast Reactors, Tokyo, Vol. II, pp. 683 - 702 (1973).
- (15) R.J. Howerton, Livermore, U.S.A., private communication.
- (16) R.W. Benjamin, Savannah, U.S.A., private communication.
- (17) H. Tellier, Saclay, France, private communication.
- (18) R.W. Benjamin, V D. Vandervelde, T.C. Gorrel and F.J. McCrosson, DP-MS-74-61, presented at the Conference on Nuclear Cross Sections and Technology, Washington D.C. (March 1975).
- (19) S. Yiftah, (also: D. Ilberg and S. Yiftah), "Neutron Nuclear data evaluation", IAEA-153 and IAEA Technical Report Series No. 146 (1973).
- (20) S. Yiftah, Y. Gur, M. Segev and L. Gitter, Proceedings, International Symposium on Physics of Fast Reactors, Tokyo, Vol. III, pp. 1479 - 1490 (1973).
- (21) M. Segev, S. Yiftah, Y. Gur and L. Gitter, Nuclear Science and Engineering, 55, pp. 103 - 104 (1974).
- (22) M. Caner and S. Yiftah, Analysis and Comparison of Plutonium-238 Nuclear Data, accepted for publication in Nuclear Science and Engineering (1975).

- (23) H.C. Clairborne, Neutron-Induced Transmutation of High-Level Radioactive Wastes, ORNL-TM-3964 (Dec. 1972).
- (24) S. Raman, C.W. Nestor, Jr., and W.T. Dabbs, A Study of the $^{233}\text{U} - ^{232}\text{Th}$ Reactor as a burner for Actinide Wastes, presented at the Conference on Nuclear Cross Sections and Technology, Washington D.C. (March 1975).

Table VI

Cf-252 $\bar{\nu}$ spontaneous fission

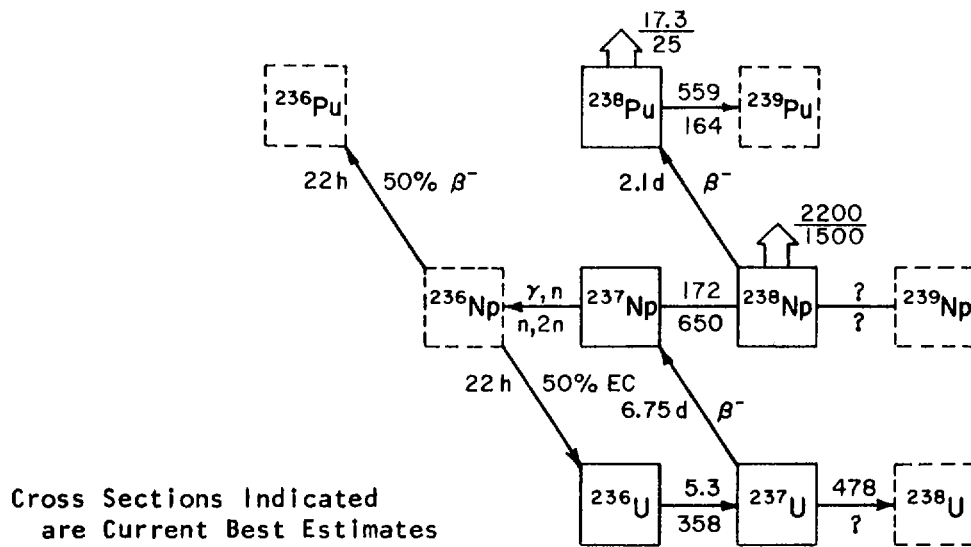
Accuracies requested

U.S.A.	0.25%	primary standard
Canada	0.5%	to resolve discrepancies
France	0.3%	to resolve discrepancies
U.S.S.R.	0.1%	for 1% in keff and 1.6% in breeding ratio of fast breeders.

Table VII

Cf-252: energy spectrum of spontaneous fission
neutrons Accuracies requested

U.S.A.	1%, 5%
U.K.	2%
France	2%



Numbers Above Arrows are Thermal Cross Sections; Those Below the Arrows are for Resonance Integrals.

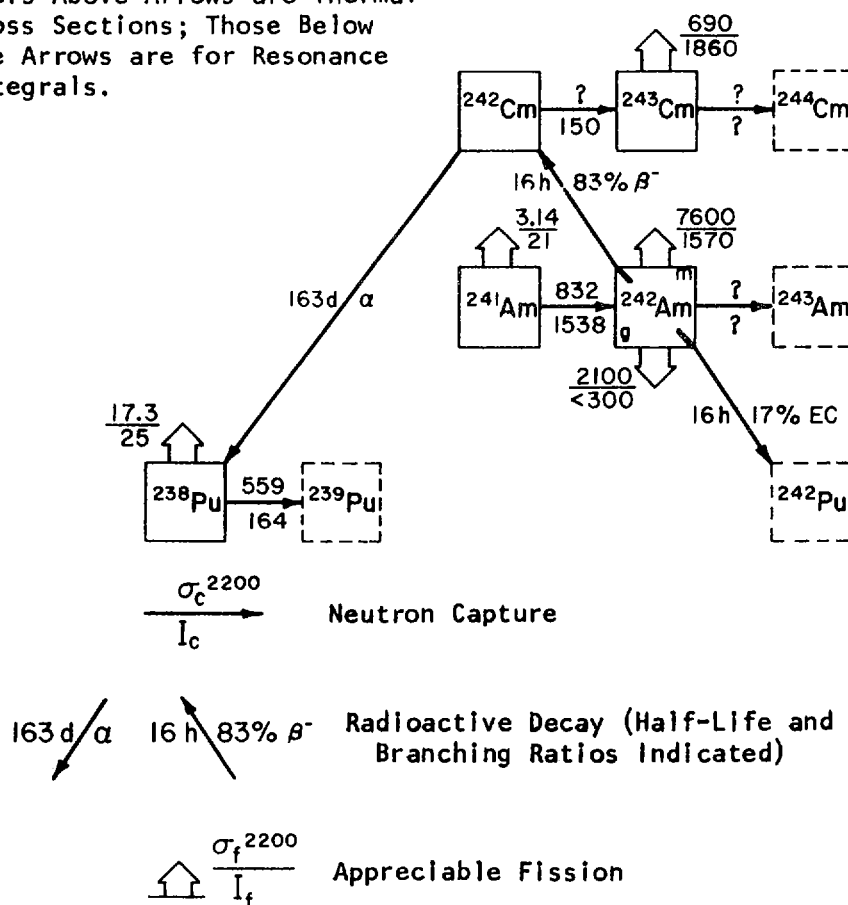


FIGURE 2. The ^{238}Pu Production Chains (8)

FBR oxide fueled sodium cooled fast breeder
equilibrium fuel cycle
· annual fuel replacement 34.4 t HM/GWe a (load factor 0.8)
burnup of core 70 000 MWD/t heavy metal, averaged
burnup of core and blanket 34000 MWD/t HM

Actinide Nuclide Concentration in Spent Fuels 150 Days after
Reactor Discharge
(Grams/T HM)

Nuclide	Half-life $T_{1/2}$	LWR		LWR Pu-recycle		FBR core+blanket 34 GWD/T
		34 GWD/T	45 GWD/T	1 recycle	2 recycle	
U-234	247000 Y	119	389	105	108	0.9
U-235	7.10E+8 Y	7560	8210	6890	7070	2330
U-236	2.39E+7 Y	4580	6450	3600	3580	330
U-238	4.51E+9 Y	942000	927000	941000	942000	864000
Np-237	2.13E+6 Y	500	769	376	368	271
Pu-238	88.9 Y	180	304	237	260	30
Pu-239	24400 Y	5270	5260	5360	5360	75800
Pu-240	6760 Y	2200	2310	2610	2650	22100
Pu-241	14.6 Y	1050	1160	1440	1490	2210
Pu-242	380000 Y	380	488	966	1230	627
Am-241	433 Y	47.2	51.5	79.9	85.5	220
Am-242M	151 Y	1.0	1.1	2.2	2.4	2.5
Am-243	7650 Y	105	155	462	686	36.8
Cm-242	163 D	5.8	4.7	14.7	16.3	2.7
Cm-243	32.0 Y	0.1	0.1	0.3	0.4	0.2
Cm-244	18.1 Y	34.4	60.0	273	456	1.9
Cm-245	8260 Y	2.3	4.4	24.2	42.0	0.04
Cm-246	4710 Y	0.3	0.6	4.8	8.8	
Total						
Trans- Uranium elements		9776	10568	11850	12655	101302

Contribution from the NEA
Neutron Data Compilation Centre

February 1975

The Transactinides in the Main

Evaluated Neutron Data Files

Abstract

The transactinium elements for which data are contained in the principal evaluated neutron data files are tabulated. A detailed listing of all transactinium isotope nuclear data types contained in the main evaluated neutron cross-section libraries is given.

THE TRANSACTINIDES IN THE MAIN
EVALUATED NEUTRON DATA FILES

Z	S	Isotope	UKNDL '73	ENDF/B-IV	KEDAK	ENDL	SPENG
91	Pa	Pa-233	X	X			
92	U	U-234	X	X		X	
		U-236	X	X		X	
		U-237				X	
		U-239	X			X	
		U-240	X			X	
93	Np	Np-237		X		X	
94	Pu	Pu-238	X	X		X	
		Pu-240	X	X	X	X	X
		Pu-241	X	X	X	X	X
		Pu-242	X	X	X		
95	Am	Am-241	X	X			
		Am-242				X	
		Am-243	X	X			
96	Cm	Cm-244	X	X			

DATA TYPES FOR TRANSACTINIDES IN THE MAIN
EVALUATED NEUTRON CROSS-SECTIONS LIBRARIES

	Pa-233		U-234			U-236			U-237	U-239	
	U.K.	ENDF IV	U.K.	ENDF IV	ENDL	U.K.	ENDF IV	ENDL	ENDL	U.K.	ENDL
<u>NEUTRON DATA</u>											
Nu-bar	X	X	X	X	X	X	X	X	X	X	X
Radioactive Decay Data		X		X			X				
Branching Ratios				X			X				
Fission Yield											
Delayed Neutrons											
Prompt Neutrons											
Resonance Data		X		X			X				
Total	X	X	X	X	X	X	X	X	X	X	X
Elastic	X	X	X	X	X	X	X	X	X	X	X
Non-elastic	X	X								X	
Total Inelastic		X	X	X	X	X	X	X	X		X
(n,2n)	X	X	X	X	X	X	X	X	X	X	X
(n,3n)		X	X	X	X	X	X	X	X	X	X
(n,4n)											X
Fission	X	X	X	X	X	X	X	X	X	X	X
Inelastic to discrete levels and/or to cont.	X	X	X	X	X	X	X	X	X	X	X
Capture	X	X	X	X	X	X	X	X	X	X	X
Absorption											
Transport											
Alpha											
Eta											
Angular Distributions	X	X	X	X	X	X	X	X	X	X	X
Energy Distributions	X	X	X	X	X	X	X	X	X	X	X
<u>PHOTON DATA</u>											
Multiplicities					X			X	X		X
Photon Production					X			X	X		X
Photon Angular Distribution					X			X	X		X
Continuum Energy Spectra					X			X	X		X

DATA TYPES FOR TRANSACTINIDES IN THE MAIN
EVALUATED NEUTRON CROSS-SECTIONS LIBRARIES

	U-240		Np-237		Pu-238			Pu-240				
	U.K.	ENDL	ENDF IV	ENDL	U.K.	ENDF IV	ENDL	U.K.	ENDF IV	KED.	ENDL	SPENG
<u>NEUTRON DATA</u>												
Nu-bar	X	X	X	X	X	X	X	X	X	X	X	X
Radioactive Decay Data			X			X			X			
Branching Ratios			X			X			X			
Fission Yield			X									
Delayed Neutrons									X			X
Prompt Neutrons									X			
Resonance Data			X			X			X	X		X
Total	X	X	X	X	X	X	X	X	X	X	X	X
Elastic	X	X	X	X	X	X	X	X	X	X	X	X
Non-elastic	X				X			X		X		
Total Inelastic		X	X	X		X	X		X	X	X	X
(n,2n)	X	X	X	X	X	X	X	X	X	X	X	X
(n,3n)	X	X	X	X	X	X	X	X	X		X	
(n,4n)		X										
Fission	X	X	X	X	X	X	X	X	X	X	X	X
Inelastic to discrete levels and/or to cont.	X	X	X	X	X	X	X	X	X	X	X	X
Capture	X	X	X	X	X	X	X	X	X	X	X	X
Absorption										X		
Transport										X		
Alpha										X		
Eta										X		
Angular Distributions	X	X	X	X	X	X	X	X	X	X	X	X
Energy Distributions	X	X	X	X	X	X	X	X	X	X	X	
<u>PHOTON DATA</u>												
Multiplicities		X	X	X			X		X		X	
Photon Production		X	X	X			X		X		X	
Photon Angular Distribution		X	X	X			X		X		X	
Continuum Energy Spectra		X	X	X			X		X		X	

DATA TYPES FOR TRANSACTINIDES IN THE MAIN
EVALUATED NEUTRON CROSS-SECTIONS LIBRARIES

	Pu-241					Pu-242			Am-241	
	U.K.	ENDF IV	KED.	ENDL	SPENG	U.K.	ENDF IV	KED.	U.K.	ENDF IV
<u>NEUTRON DATA</u>										
Nu-bar	X	X	X	X	X	X	X	X	X	X
Radioactive Decay Data		X					X			X
Branching Ratios							X			X
Fission Yield		X								X
Delayed Neutrons		X			X					
Prompt Neutrons		X								
Resonance Data		X	X				X	X		X
Total	X	X	X	X	X	X	X	X	X	X
Elastic	X	X	X	X	X	X	X	X	X	X
Non-elastic	X		X					X		
Total Inelastic		X	X	X	X	X	X	X	X	X
(n,2n)	X	X	X	X	X	X	X	X		
(n,3n)	X	X	X	X		X	X	X		
(n,4n)				X						
Fission	X	X	X	X	X	X	X	X	X	X
Inelastic to discrete levels and/or to cont.	X	X	X	X	X	X	X	X	X	X
Capture	X	X	X	X	X	X	X	X	X	X
Absorption			X					X		
Transport			X					X		
Alpha	X		X					X		
Eta			X					X		
Angular Distributions	X	X	X	X		X	X	X	X	X
Energy Distributions	X	X	X	X		X	X	X	X	X
<hr/>										
<u>PHOTON DATA</u>										
Multiplicities				X						
Photon Production				X						
Photon Angular Distribution				X						
Continuum Energy Spectra				X						

DATA TYPES FOR TRANSACTINIDES IN THE MAIN
EVALUATED NEUTRON CROSS-SECTIONS LIBRARIES

	Am-242	Am-243		Cu-244	
	ENDL	U.K.	ENDF IV	U.K.	ENDF IV
<u>NEUTRON DATA</u>					
Nu-bar	X	X	X	X	X
Radioactive Decay Data			X		X
Branching Ratios			X		X
Fission Yield			X		
Delayed Neutrons					
Prompt Neutrons					
Resonance Data			X		X
Total	X	X	X	X	X
Elastic	X	X	X	X	X
Non-elastic					
Total Inelastic	X	X	X	X	X
(n,2n)	X				X
(n,3n)	X			X	X
(n,4n)	X				
Fission	X	X	X	X	X
Inelastic to discrete levels and/or to cont.	X	X	X	X	X
Capture	X	X	X	X	X
Absorption					
Transport					
Alpha					
Eta					
Angular Distributions	X	X	X	X	X
Energy Distributions	X	X	X	X	X
<u>=====</u>					
<u>PHOTON DATA</u>					
Multiplicities	X				
Photon Production	X				
Photon Angular Distribution	X				
Continuum Energy Spectra	X				

Theoretical calculation of Transactinium Isotope Nuclear Data
for Evaluation Purposes

J.E. Lynn

U.K.A.E.A., A.E.R.E., Harwell, Didcot, Oxfordshire, U.K.

Abstract

The use of theoretical methods to calculate transactinium nuclear data is discussed. The review concentrates on the attempts to estimate theoretically the differential neutron cross sections, averaged over local resonance phenomena in the neutron energy range between 1 KeV and 20 MeV. The applications of the optical model and the statistical model computer calculations is outlined, and a summary of calculated transactinium nuclide cross sections is tabulated. The review estimates that present-day theoretical calculations of cross sections for transactinium nuclides may at best have an uncertainty of 25 percent.

1. INTRODUCTION

There are very many (at least 50) transactinium nuclides for which nuclear data are required, but for most of these much of the required data is not at present measurable. The only hope for providing reasonable values for the evaluated files of such data in the near future lies in the exploitation of nuclear theory.

In this connection nuclear theoretical methods apply basically to the estimation of cross-sections and some related quantities (such as perhaps $\bar{\nu}$ and the fission neutron spectrum); they certainly do not appear to have any possibility in the foreseeable future of playing a useful role in improving data on nuclear half-lives. In the cross-section area too some data requirements cannot usefully be provided by nuclear theory. This applies particularly to the cross-section requirements for thermal reactor systems. Thermal neutron cross-sections depend mainly on the detailed positions and parameters of the nearest few least-bound and unbound levels of the compound nuclear system, and the properties of such levels, which may be at the hierarchy position of the order of one million in the nuclear level system, cannot be predicted in detail, but only in a statistical fashion. If some experimental cross-section data are available at low neutron energies however, then nuclear theory provides the rigorous formalism necessary for interpolation or extrapolation to other neutron energies. This aspect of nuclear theory is not reviewed here.

In the cross-section requirements for fast reactors nuclear theory can play a more generally useful role. The nature of the fission neutron spectrum, which is only partially moderated in fast reactor systems, indicates that cross-sections up to several MeV neutron energy can be important. The moderation of the spectrum limits the interest in some of these cross-sections, particularly radiative capture, to energies below a few MeV, but there are some cross-sections, important for the generation of new nuclear species, such as $(n,2n)$ and $(n,3n)$, which are

important at energies of several MeV. The important feature of nearly all these cross-sections of the very heavy nuclei is that individual resonance features in the cross-section are obscured by the very wide energy interval of the incident neutron spectrum and therefore "statistical" nuclear reaction theories can be employed for their estimation. The main exception to this statement is the requirement of cross-section data for calculating quantities like the Doppler temperature coefficient of reactivity. Here knowledge of the detailed resonance fine structure of fertile materials, and possibly of the narrow intermediate resonance structure of fissile nuclei, is required. Such requirements are ignored in the present review, however, which concentrates on the attempts to estimate theoretically the differential neutron cross-sections, averaged over local resonance phenomena, for a neutron energy range of perhaps 1 keV to about 20 MeV.

It is not claimed that this review is complete; it is based mainly on the contributions sent to me for the purposes of this Advisory Group Meeting. Earlier theoretical work on cross-sections required for fast reactors was reported at the Nuclear Data for Reactors Conferences at Paris and Helsinki (see refs. [1] to [8]), and work prior to that time has been carried out by Wilmore [9] and Moldauer and his associates [10], for example. Most of this earlier work was concerned with the cross-sections of the major fissile and fertile nuclei and is therefore outside the scope of this Advisory Group.

2. MODELS FOR THE CALCULATION OF NEUTRON CROSS-SECTIONS

Since the whole subject of theoretical nuclear models for the calculation of nuclear data is to be discussed at a Consultants' Meeting at Trieste in December, 1975, the summary of nuclear models given in this section is little more than a catalogue of the methods that have been used specifically for the transactinium data presented in this review.

Two general classes of model are in use. One is the optical model [11] and its more sophisticated variants including deformed potential wells and coupled channels [12]. The second is the statistical model of decay of the compound nucleus basically due to Hauser and Feshbach [13].

2.1 Optical models

2.1.1 Spherical optical model

The optical model is used for calculations of total cross-sections $\sigma_{n,T}$, and elastic scattering $\sigma_{n,n}$, including the angular distributions $\partial \sigma_{n,n} / \partial \omega$, (by summing the calculations of shape elastic scattering and compound elastic scattering that result from the application of the optical model concept). It is also used for calculating the compound nucleus formation cross-section $\sigma_{n,CN}$, which is the starting quantity for calculating various partial reaction cross-sections by the Hauser-Feshbach formalism and for the transmission coefficients for inelastic scattering to discrete low-lying states also required by the Hauser-Feshbach theory. The optical model parameters (of which there are several in the more elaborate versions of the model) are generally obtained by fitting to well-known total cross-section and/or elastic scattering data of a nucleus such as ^{238}U . The parameters for other nuclei can be obtained by extrapolation or interpolation in a physically reasonable way. The optical potential normally employed in these calculations has a Woods-Saxon [14] radial dependence for the real part with a depth having a linear dependence on neutron energy, and a gaussian surface term for the imaginary part. The spin-orbit term is of the usual Thomas form [15] with radial dependence related to the derivative of the real potential.

A common computer programme that has been used for spherical optical model calculations on transactinium nuclei is ABACUS-2 written by Auerbach et al [16]. This has been tested by Auerbach and Moore [17] on ^{238}U and ^{232}Th and found to give reasonable fits to total, elastic scattering and inelastic scattering data to low-lying levels. This code has been employed particularly on transactinium data evaluation by Caner and Yiftah [18-21] but with different optical model parameters from those of ref. [17]. Another set of spherical optical model parameters that has been commonly used is that of Moldauer [22]; this set represents a fit over a wide range of mass numbers and is therefore suited for extrapolations to unmeasured nuclei. The Moldauer set has been used particularly by Gardner [23] in calculations of cross-section data on ^{239}U and by Smith et al [24] in applications to ^{240}Pu .

2.1.2 Coupled channel calculations

The coupled channel variants of the optical model, as well as giving a physically more reliable basis for extrapolation of total and elastic scattering cross-sections to other nuclei, also have the great advantage of providing estimates of the inelastic scattering to certain collective states (particularly the members of the rotational band built on the ground state of even target nuclei) which are greatly under-estimated at higher neutron energies (above about 1.5 MeV) by the statistical model. For the transactinium nuclei the computer codes for such calculations generally allow quadrupole and hexadecapole deformation terms, and in other ways the optical potential generally has the features mentioned above for the more elaborate of the spherical optical model calculations. General descriptions of the formalism for coupling the rotational channels are given by Tamura [25].

One of the principal computer programmes for carrying out coupled channel calculations has also been written by Tamura [26]; this is the JUPITOR-1 code which has been used for example by Jary et al [27] in an analysis of experimental data on ^{238}U . Another common coupled channel computer programme is 2-PLUS written by Dunford [28]. This has been used by the Argonne group [24].

2.2 Statistical models

The Hauser-Feshbach model starts from the assumption that the reaction cross-sections it treats are controlled fully by the compound nucleus mechanism. A particular reaction cross-section is then given by a statistical division of the compound nucleus formation cross-section:

$$\sigma_{n,c} = \sigma_{n,CN} \frac{T_{(c)}}{\sum_{c'} T_{(c')}} \quad (1)$$

the $T_{(c')}$ being a transmission coefficient for entrance or exit to each channel c' . Strictly speaking, this formula is to be applied to every state of total angular momentum, J , and parity, π , and since the compound nucleus formation cross-section is itself proportional to the transmission coefficient $T_{(n)}$ for the state J^π , we have

$$\sigma_{n,c}^{J^\pi} = \pi \lambda^2 g(J) \frac{T_{(n)} T_{(c)}}{\sum_{c'} T_{(c')}} \quad (2)$$

This formally simple equation has received important modifications since it was first established, one being the recognition of the role played by

statistical fluctuation effects in the compound nucleus levels governing the transmission coefficients [29,30], and another being the interference effects of these levels [29,31,32]. The second effect is particularly important for the estimation of compound elastic scattering at higher energies where there is considerable overlap, and is generally treated by the use of Moldauer's formula [32]. The fluctuation effect tends to be important at lower energies, where few particle channels are open; at higher energies the departures from equation (2) due to fluctuations are small (except for elastic scattering) and are completely swamped by other uncertainties in the estimation of the transmission coefficients.

At these higher energies the quantities that are of major importance in determining cross-sections for reactions involving several, or a 'continuum' of exit channels are the level densities, once the reaction thresholds and barriers are specified. In spite of this fact there is still a great deal of ignorance about the detailed dependence of nuclear level densities on energy and, especially, on angular momentum. As far as the transactinium nuclei are concerned, direct experimental data at lower energies are limited to the first MeV of excitation in many of the even nuclei, and to the first few hundred keV in many odd-A nuclei, while scarcely anything is known about the odd nuclei save for one or two of the actinium isotopes. At higher excitation energies the slow neutron resonances provide data for many of these nuclei at spot energies ranging from about 5 to 7 MeV and for very limited angular momentum values. Interpolation and extrapolation from these data have to be provided semi-empirically or from nuclear models. Level densities governing the fission reaction are in even worse shape. Such level densities are on a more abstract plane, being the density of states of intrinsic excitation of the compound nucleus as it passes over a potential energy barrier at an extended deformation. Such densities can only be calculated from a nuclear model or inferred from the characteristics of fission cross-sections themselves. To further complicate this matter it is now known that there are two such barriers in the actinides with a certain degree of interplay between them.

2.2.1 Statistical model codes

There are several computer programmes in existence for the calculation of cross-sections from the statistical model. They vary, normally, in the physical treatment given to certain reaction channels, notably those corresponding to radiative capture and fission. One of the most commonly used codes is NEARREX [10]. Fluctuations are treated in this on the assumption that in each neutron channel the level partial widths are distributed according to the Porter-Thomas distribution [33]. Level overlap is treated by putting the Moldauer Q-parameter in as input data. Radiation transmission coefficients are treated within the context of the strong-coupling dipole model (in which all partial transition strengths are assumed to be proportional only to the cube of the transition gamma-ray energy). Fission transmission coefficients are treated on an empirical basis as a linear function of the incident neutron energy. NEARREX has been used by the Argonne group of course (see ref. [24]), and by Caner and Yiftah in their work on plutonium isotopes [18-21]. Generalised statistical model codes which treat cascading decays through multiple gamma-ray or neutron transitions on the basis of statistical theory are available; examples are CASCADE due to Poenitz [60] and EVAPF used in my own work [35].

2.2.2 Level density laws adopted for statistical model calculations

Information on the dependence of nuclear level density on excitation energy is required for all calculations of the radiation transmission

coefficient for the statistical model, and, as stated above, for all calculations of neutron inelastic scattering to the 'continuum', i.e. where specific information on individual residual nucleus levels is not available. The commonest level density formulation employed in the work reviewed in this article is that due to Gilbert and Cameron [34]. This is a composite formula, adopting a constant temperature form,

$$\rho(E) = C e^{E/\theta} \quad (3a)$$

in the lower energy range, and an independent-particle form at higher energies:

$$\rho(U, J^\pi) = \frac{(2J+1)e^{-(J+\frac{1}{2})^2/2\sigma^2}}{4 \sqrt{2\pi} \cdot \sigma^3} \cdot \rho(U) \quad (3b)$$

$$\rho(U) = \frac{\sqrt{\pi}}{12} \cdot \frac{e^{2\sqrt{aU}}}{a^{1/4} U^{5/4}} \quad (3c)$$

$$\sigma^2 = 0.0888 \text{ atA}^{2/3} \quad (3d)$$

$$t = \sqrt{U/a} \quad (3e)$$

$$a = \pi^2 \tilde{\rho}_s / 6 \quad (3f)$$

The effective excitation energy U is adjusted from the true excitation energy E according to the odd or even nature of the nucleus (see below). The predominant parameter here is a , and this is related to the density $\tilde{\rho}_s$ of single-particle states around the Fermi energy of the nucleus, the width of the averaging function for this density being of the order of the temperature, t . The parameter σ is also related to this as well as to the spin distribution of these single-particle states; the numerical coefficient adopted in equation (3d) comes in fact from a gross assessment of the spins of all the bound single-particle levels and is not expected to be an accurate value for individual nuclei. The correction to the true excitation energy to give the effective excitation energy is

$$U = E - P(Z) - P(N), \quad (3g)$$

the P -functions being zero for odd values of proton and neutron number. The energy of demarcation between the regimes of equations (3a) and (3c), denoted by E_x in ref. [34], is defined by equality of value and slope of the level density from the two formulae for the particular parameters stipulated for each individual nuclide. While the parametrisation of Gilbert and Cameron has been used unchanged in the work of Jary et al [27], modification of these parameters has been made in my own work [35] in the light of new experimental data, while a simplified form of equation (3c) has been used in references [18] to [21]. Thus care has to be taken in comparing the level density parameters quoted in different pieces of work.

In addition to the modification and extension of the level density parameters from the Gilbert and Cameron values, ref. [35] also modifies the very low-energy component of the level density behaviour in order to allow a crude reproduction of the "energy gap" feature of even and odd- A nuclei. With the simple representation

$$\rho(E, J) = (2J + 1) \exp \left[\frac{-(J + \frac{1}{2})^2}{2\sigma^2} \right] \cdot \rho_{\text{eff}}^{(0)} \quad (4)$$

up to 1 MeV, the parameters $\text{eff}(0) \approx 0.5 \text{ MeV}^{-1}$, $\sigma \approx 4$ for even nuclei, and $\text{eff}(0) \approx 1.25 \text{ MeV}^{-1}$, $\sigma \approx 4.5$ for odd-A nuclei are recommended. The parameters used for the constant temperature zone immediately above 1 MeV (or from zero in the case of odd nuclei) are given in Table 1. For the independent-particle model parameters used at still higher energies reference is made to Table 5 of ref. [35]. It should be noted that the temperatures quoted in Table 1 were largely chosen as a result of fitting the neutron capture cross-section of ^{238}U up to 3 MeV as evaluated by Sowerby et al [40], using a giant dipole resonance model (GDR) for the estimation of the radiation transmission coefficient [52].

2.2.3 Fission barrier level densities

The fission reaction tends to be the least satisfactorily treated in calculational work to provide nuclear data on the transactinium nuclei. Some treatments are wholly empirical as in the original NEARREX code. Many rely on the Hill-Wheeler [36] transmission formula for a single-humped barrier, with an adjustable channel weighting, N_F , and barrier height, E_F , and penetrability parameters $\hbar\omega_F$ adjusted to fit available fission cross-section data:

$$T_{(F)} = \frac{N_F}{1 + \exp \left[\frac{2\pi(E_F - E)}{\hbar\omega_F} \right]} \quad (5)$$

This is the treatment, for example, used by Caner and Yiftah [20] for ^{241}Pu , a separate set of parameters being used for each spin and parity component of the cross-section. More systematic treatments are possible for even nuclei. The calculations for ^{240}Pu [18] set up a rotational band, each member of which has a weighting N_F equal to 2, on each possible K value (projection of total angular momentum on the cylindrical symmetry axis of the fissioning nucleus).

Such treatments generally cope with fission cross-section data in the region of, or below, the fission barrier energy E_F , provided there are some fission cross-section data available to allow adjustment of the parameters. The main reason for such treatments is to provide a quantification for the fission competition entering the calculation of other cross-sections. At higher neutron energies the variation of density of the fission channels with excitation energy has to be taken into account in some way, although this has been avoided in some empirical treatments; for example Miyamoto et al [37] in calculations of the fission cross-section and $(n, \infty n)$ cross-sections of ^{239}Np and ^{233}Pa employ the shape of the ^{237}Np fission cross-section adjusted in size at 3 MeV neutron energy according to a linear dependence on $Z^{4/3}/A$. Nearly all calculations that employ the barrier level density do so through an empirical adjustment of parameters to measured fission cross-section data (e.g. Murata [38], Jary [39]), but do so for each individual nucleus treated. What is really required is a systematic treatment that will allow extrapolation to nuclei for which few or no measured data are available.

Two attempts along these lines have been made. The first [35] has obtained the barrier level density by adjustment, on the basis of the double-humped barrier model, to a few well-measured cross-sections up to neutron energies of about 3 MeV. For odd-A compound nuclei these are the fission cross-sections of ^{246}Cm [41], ^{238}U [40] and ^{232}Th [42]; for odd-A nuclei the fission cross-sections of ^{237}Np [43-45] and ^{241}Am [46] were chosen; for even-nuclei the cross-sections were those of ^{235}U and ^{239}Pu (as evaluated in ref. [40]). The level density parameters found and

suggested for universal use through the transactinium series of nuclei are given in Table 2. It is to be noted that these densities must be used in conjunction with level density parameters for normal deformation as given in ref. [35] (and Table 1 here).

These densities at barrier A (the inner peak of the double-humped barrier) are a factor of 4 or 5 higher (at the same equivalent excitation) than the normal level density, and the barrier B density is about a factor of 2 higher (although this is less certain because the evidence rests mainly on the cross-sections of Th and Pa which show a great deal of vibrational structure rather than smooth quasi-plateaux in their energy variation). This is attributed [47] to deficiencies in nuclear shape symmetries at the barrier deformations; this gives rise to extra member states in the rotational bands built on the intrinsic independent quasi-particle states. Using this hypothesis to augment the density of states calculated numerically from an independent quasi-particle model, Gavron et al [48] have calculated barrier level densities which can be used to reproduce fairly well the fission probabilities measured in a range of $^3\text{He}(d,F)$ and $(^3\text{He},tF)$ reactions up to several MeV above the barrier. This is the second attempt to provide a systematic approach to the problem of calculating fission cross-sections and other data that depend heavily on fission competition.

2.2.4 Fission barrier parameters

The work of ref. [35] on deduction of barrier level densities implies a knowledge of fission barrier parameters. For the nuclei employed in that survey these were determined by detailed fitting of neutron-induced fission cross-sections and other data (in particular (t,pF) and (d,pF) reactions leading to fission of ^{236}U and ^{240}Pu) below and up to the barrier energies. For the even nuclei studied in this fitting procedure, physically reasonable models of the low-lying discrete channel structure were adopted, and for all nuclei the detailed effect of coupling of class-I and class-II states across the double-humped barrier, as described in ref. [49], was taken into account. This coupling is particularly important for the analysis of fission probability data on even compound nuclei, for which the fission barriers lie below the neutron separation energy. With the barrier level densities then fixed, an analysis of all available fission data on the transactinium nuclei was carried out to determine the barrier parameters of as many as possible of these nuclei. The final results cannot be taken to be unique, however, because of the number of parameters involved (at least 4: V_A , $\hbar\omega_A$, V_B , $\hbar\omega_B$). The penetrability parameters in general were fixed to the values determined in the best fits to the key cross-sections. The outer barrier height (V_B) is generally the least well-determined parameter. A semi-quantitative indication of its value in Pu, Am and Cm nuclei has been determined from analysis of excitation curves for the formation of spontaneously fissioning isomers [50,51] and this was used as a guide in the survey of ref. [35]. In the Th nuclei it appears that the outer barrier is comparable to or even slightly higher than the inner barrier (but see Section 3.5 below); this is inferred from the low magnitude of fission cross-sections of these nuclei. The detailed barrier parameters are given in Table 11 of ref. [35]. The general trend of inner barrier heights is shown in Fig. 1, and this can be used for rough extrapolation to nuclei for which no measured fission data are available.

2.2.5 Level densities for calculations at higher energies

For the estimation of cross-sections at neutron energies above a few MeV, the Gilbert-Cameron level density parameters have often been used (e.g. refs. [27,39]) and barrier densities have been fitted by adjustment

to measured fission cross-sections. Again this approach leaves little scope for extending calculations to nuclei for which no data are available; the adjusted parameters seem to vary too erratically from one nucleus to another.

I have attempted to extend the scheme of ref. [35] to higher energies. For normal nuclear deformations the level density parameters of Table 5 of ref. [35] have been adopted (where a value of the transition energy E_{IP} from constant temperature to Fermi-gas form is not quoted the neutron separation energy has been used). The barrier densities have been taken by adjustment to the fission cross-sections of ^{238}U , ^{235}U , ^{239}Pu and ^{237}Np up to 20 MeV neutron energy. Where $(n, \infty n\text{F})$ begin to contribute to the fission cross-section the already established parameters of ref. [35] are used. The extended barrier level density parameters are given in Table III.

3. CALCULATED DATA AND UNCERTAINTIES

The complete set of calculated data submitted to me for the purposes of this Panel plus some other recent work that seems relevant is summarised in Table IV. Much of this work has been devoted to nuclei for which a considerable amount of experimental data exists, and the role of theory is a comparably minor one, filling the gaps in this body of information. Also much of the work of making theoretical fits to experimental data fulfils the important role of ascribing values to important parameters (such as the optical model parameters) that must be known in order to extend the theoretical treatment to other nuclei. To fulfil this aspect of course models with systematic trends are required, rather than those with specific applicability to individual nuclei. Overall comments on various features of the calculations are given below.

3.1 Compound nucleus formation cross-section

This is one of the important qualities that comes out of the optical model calculations, and here I comment on its consistency and likely error in estimation.

A direct comparison of calculations of the compound nucleus formation cross-section comes from the work of Wilhelmy et al [53]. This is given in the form of calculations of the fission cross-section of ^{237}Np (calculated as the compound nucleus formation cross-section multiplied by fission probability as determined from the $^{238}\text{U}(^3\text{He}, \text{tF})$ reaction). Four calculations are shown (see Fig. 2) corresponding to compound nucleus formation cross-sections from optical model calculations by Wilmore and Hodgson [54], Andreev et al [55], Auerbach and Moore [17] and Mani et al [56]. The spread in these values is of the order of 25% or more, and gives the impression that the accuracy of estimation of this important quantity from spherical optical model calculations can hardly be better than $\pm 15\%$ (roughly speaking, in standard deviation terms).

Coupled channel calculations, particularly for even nuclei, ought to give a rather better-based account of the compound nucleus cross-section, if only because they give a realistic yield of the semi-direct inelastic scattering to the first rotational levels of the target nucleus, which can still be some hundreds of mb at neutron energies of a few MeV. However, there is obviously greater freedom in fitting the model to the available data, so in practice Benzi et al [57] consider that there is still considerable uncertainty in determining the compound nucleus formation cross-section from this model.

In view of this uncertainty, simplified methods of calculating this important quantity are still relatively valid. In ref. [35] the

calculation is performed by taking the measured s- and p-wave neutron strength functions, as experimentally determined at low neutron energies for ^{238}U , to be typical of the values for even and odd orbital angular momenta respectively. These values are taken unchanged for all neutron energies. This procedure gives a compound nucleus formation cross-section of the order of 2.8 b between about 0.1 MeV and 3 MeV. At higher energies this calculated value gradually increases, so it is assumed to remain constant at 2.8 b indefinitely. Gardner [23] uses the spherical optical model calculation but applies an energy-dependent reduction factor to allow for semi-direct inelastic scattering. Experimental evidence on the magnitude of this cross-section is not much more accurate than the theoretical estimates. For example Batchelor et al [58] give values of the non-elastic scattering cross-section varying from 2.6 to 3.4 b with a standard error of about 10% for ^{238}U and ^{232}Th in the energy range 3 MeV to 7 MeV (where compound elastic scattering is small). With due allowance for semi-direct inelastic scattering this supports the above estimate of 2.8 b within this degree of error.

3.2 Radiative capture cross-sections

Radiative capture is one of the most difficult to measure among the cross-sections of major importance, and therefore more effort has been put into the theoretical estimation of this quantity than of other cross-sections. It is also most sensitive to the broadest variety of theoretical concepts and their parametrisation. It depends not only on the magnitude of the compound nucleus formation cross-section but is also strongly sensitive to inelastic scattering and fission competition, to the detailed model of the radiation mechanism and the level density of the compound nucleus. A typical calculation (capture cross-section of ^{238}U due to Jary et al [27]) is shown in Fig. 3. It agrees well with evaluated experimental data up to a few hundred keV and is still within 30% at 1 MeV but thereafter there is increasing discrepancy.

In ref. [35] a deliberate attempt was made to adjust the important parameters for the radiative capture process to the ^{238}U capture cross-section up to higher neutron energies (~ 3 MeV) and simultaneously fit as much other data as possible (such as the gamma-ray spectrum in thermal neutron capture and the spectrum of inelastically scattered neutrons). The fit to the ^{238}U data is shown in Fig. 4 both for a detailed Hauser-Feshbach calculation, in which inelastic scattering to discrete known levels is properly taken into account, and for a calculation on a more statistical basis, in which continuum level density formulae are used. With the use of the GDR model for the radiation mechanism, and a temperature for low-lying level densities of 0.5 MeV the fit at higher energies is seen to be good. It is believed that this model can be applied reasonably well to the bulk of the transactinium nuclei. Its application to the common fissile nuclei (^{233}U , ^{235}U , ^{239}Pu) is satisfactory, without any further adjustment of parameters; the worst case, ^{235}U , is shown in Fig. 5. To 1 MeV the discrepancy with data is no worse than about 25%.

The other main body of data for testing capture models comprises the total radiation widths of low energy neutron resonances. The experimental data on capture widths have to be treated with a considerable degree of caution. These widths are notoriously difficult to measure with great accuracy; for example, that for neutron capture by ^{238}U has received a great deal of attention by several groups, and the most reliable sets of data still contain systematic differences of the order of 5%, while in the case of ^{240}Pu capture the consensus of experimental values has changed suddenly by nearly 30% in the last few years. Radiative widths for capture by fissile nuclei are much more difficult to measure, and it is difficult to believe that these widths are known to a much greater degree of accuracy

than 25%. The agreement of the model with the data appears to lie generally within this degree of accuracy (see Table 9 of ref. [35]). There do appear to be some systematic deviations however. Thus, the model appears to be over-predicting the widths for plutonium nuclei by about 10% and for americium nuclei by perhaps 20%. This last figure is perhaps a fair assessment of the uncertainty to be attached to the model.

3.3 Inelastic scattering

Probably a similar, or slightly greater ($\sim 30\%$), degree of uncertainty should be attributed to the calculation of inelastic scattering to discrete states at the lower neutron energies. The detailed calculation depends on knowledge of the neutron strength functions in both the entrance and exit channels, and these fall within the general uncertainty of calculation of compound nucleus formation cross-sections using the optical model (see Section 3.1). The kind of difference in estimating such cross-sections from different variants of the optical model is shown in Fig. 6 from ref. [24].

At the higher neutron energies this particular comparison is distorted by the effect of the deformed optical model in introducing a semi-direct component. The extent and magnitude of this component at still higher energies is indicated in Fig. 7 from ref. [59]; at the highest energies on this figure the contribution to the cross-sections from pure compound nucleus processes (Hauser-Feshbach theory) is very much smaller than the experimental data. The existence of the semi-direct excitation of the rotational states of even nuclei implies an additional uncertainty in the theoretical treatment of the cross-sections at lower energies; a correlation is expected between the reduced neutron widths for the entrance channel and the exit channel [5] and, if properly taken into account, this could increase the estimate of the inelastic scattering cross-section by up to 50%, depending on the magnitude of the imaginary component of the optical potential.

3.4 Fission cross-sections

For the calculation of fission cross-sections at low energies the main uncertainties are the detailed ordering of the fission channel states, especially for the cross-sections of even targets, and the characteristics of vibrational resonances, especially for nuclei of lower charge than Pa. The uncertainties associated with the vibrational resonances for these light nuclei also extend to energies considerably above the fission barrier. The semi-empirical model developed in ref. [35] seems to be reasonably satisfactory for the higher charge nuclei, however, in giving agreement with a wide range of experimental data. Overall this model can probably allow the estimation of fission cross-sections to better than 20%, and should allow the calculation of fission competition against other reactions proceeding through the compound nucleus mechanism to within about 30%.

The treatments of fission for individual nuclei that are to be found in most of the references in Table IV serve to quantify the fission competition factors required for the calculation of other cross-sections of the nucleus treated. The value of this approach is that for very many transactinium nuclei some fission cross-section or fission probability data are available and it is experimental information on other cross-sections that is lacking. The accuracy of such treatments should generally be similar to or better than that of the generalised approach of ref. [35].

3.5 Multiple-stage neutron evaporation and fission reactions

In most of the work reviewed in this paper it is assumed that the principal mechanism leading to nuclear reactions initiated by neutrons is

the compound nucleus one. However, above a few MeV in neutron bombarding energy, mechanisms variously classed as direct, pre-equilibrium, and so on, become of comparable, or even predominant, importance relative to compound nucleus formation, and this implies that many kinds of cross-section can no longer be treated adequately by the methods outlined above. This statement does not apply fully to multi-stage particle reactions, and there have been a number of more or less successful attempts to calculate the cross-sections of $(n, \gamma n)$ and $(n, \gamma n f)$ reactions up to energies of about 20 MeV. Jary [39] for instance calculates $(n, 2n)$ and $(n, 3n)$ cross-sections after determining the total fission transmission coefficient by fitting to known fission cross-sections.

The main systematic treatment of such cross-sections is my own extension to the work of ref. [35]. For such calculations the spectrum of excitation after each neutron evaporation must be determined and multiplied by the fission probability, or probability of further neutron emission, and then integrated. This is done numerically by the computer programme EVAPS, a simplified version of EVAPF, a cascade calculation based on statistical evaporation theory. Typical results for $(n, 2n)$ and $(n, 3n)$ cross-sections are shown in Fig. 8. While its application to higher charge nuclei, as in this figure, seems to work quite well, for lighter charge nuclei it seems to overestimate the fission cross-section quite considerably. This may be due to a basic uncertainty in modelling the fission barrier for such nuclei; Müller and Nix [61] have carried out calculations that indicate that the inner barrier A is considerably lower than the outer barrier B in the Th nuclei and that the outer barrier B is itself further split. With level densities at barrier B lower than at A this picture would give a reduction in fission cross-sections.

Apart from this deficiency fission cross-sections at the onset of multiple chance fission, particularly of second-chance fission, show too steep a rise. This may be due to the neglect of pre-equilibrium neutron emission processes in the calculation of such cross-sections, and indicates another deficiency in theoretical method that has yet to be improved.

3.6 Other reactions

Cross-sections for other neutron reaction processes can be and have been treated by theoretical methods with more or less success. As an example the cross-section for the $(n, \gamma n')$ process on ^{238}U has been studied by a number of authors. The reaction could be important as another source of low energy neutrons in fast breeder reactor systems. The results have been controversial but the latest attempt using the computer programme EVAPF and the parameters of ref. [35] indicate that the cross-section is virtually negligible (see Fig. 9).

Isomeric ratios provide another example of possible quantities to calculate by such cascade programmes as EVAPF, but the present indications are that a considerably more detailed theoretical understanding of the low-lying level structure will be required before much confidence can be placed in such calculations.

4. GENERAL CONCLUSIONS

Overall, my assessment of the degree of confidence that can be placed in the models used at the present time for calculating cross-sections of a statistical or 'integral' character (i.e. capture, summed inelastic scattering, etc.) for the transactinium nuclei is that the estimates may carry ~25% error (in the sense, very roughly, of one standard deviation). The possible error in the calculation of a cross-section of more specific character (e.g. inelastic scattering to a single residual state, radiative

capture populating an isomeric state) is likely to be rather worse than this. While this is certainly much poorer than the degree of accuracy attainable with very careful experimental techniques, it is certainly a useful and acceptable degree of accuracy for many nuclei for which differential cross-section measurements have not been made, or for which the existing measurements are very suspect for one reason or another.

It is plain from the account given above that there are many deficiencies in the basic nuclear reaction theory required for such calculations. At present indeed nuclear reaction theory should be regarded as a framework for linking many different kinds of experimental data, many at first sight apparently unrelated to the required neutron cross-sections, to deduce the basic parameters and suggest the correct mechanism or model for the calculation required. This framework should be extended to connect as many different kinds of data as possible.

Improvements in models and parametrisation are required in many directions. For total cross-sections, elastic scattering, compound nucleus formation and neutron transmission coefficients the coupled channel version of the optical model requires further exploration. Of particular importance here is the correct assessment of the magnitude of the imaginary component of the potential; once this is known with a fair degree of certainty it will lead to further insight into the question of correlations among reduced widths for different channels. More detailed nuclear structure considerations will need to be brought into the optical model treatment of odd-A and odd target nuclei, so that the treatment of channel coupling can be done with confidence. The importance of efficient numerical procedures and computer programmes is also to be stressed here.

Formally, the Hauser-Feshbach theory has received a great deal of attention of late [66,67], and while a complete mathematically rigorous proof of its statement is still lacking, it is now well understood in microscopic terms and prescriptions for treatment of level interference within its framework are now quite precise. Most uncertainty in the application of the Hauser-Feshbach theory now rests in the provision of its principal physical parameters.

Level density formulations in particular provide a great area of uncertainty. Virtually all the calculations surveyed in this report have used an empirical choice of the basic level density parameters although the basic form is generally governed by theory. This empiricism is particularly marked for the level densities at barrier deformations, because for these there is not even a direct experimental datum from which the level density parameter can be inferred. Many attempts are now being made to calculate level densities from basic single particle level schemes, as, for example, the work of ref. [48] (see also refs. [64], [65]). It is to be hoped that these can ultimately be pushed to real quantitative success. For this to be achieved it will be necessary for the fundamental researches on the detailed single particle level structure of heavy nuclei to be pursued vigorously, particularly for the highly deformed fission isomer nuclei; here the difficult and exotic experimental work of such groups as that of Vandenbosch [68] and Pedersen [69] has an importance transcending that of pure scientific interest.

There is still considerable ignorance on the detailed mechanism of radiative capture. The simplest form of the valency neutron model seems to work well for high energy transitions in certain groups of light nuclei, the giant dipole resonance model seems to give a reasonably good overall account of the magnitude of radiation widths and shapes of radiation spectra with only modest adjustments from the theoretically expected parameters, while the simple strong-coupling dipole model gives a surprisingly

consistent account of radiation widths for a minimum of adjustable parameters. A fundamental reconciliation or merging of all these models still has to be achieved before radiative capture phenomena in the unknown regions beyond plutonium can be calculated with real confidence.

Finally, the calculation of cross-sections at higher neutron energies than a few MeV deserves a great deal of extra attention. In this region it is known that reactions of various degrees of 'directness' often predominate over strictly compound nucleus processes, but the methods of treating these are still often unsatisfactory for the quantitative requirements of nuclear data. In particular, unified treatments that do not attempt to break the reaction down into strictly direct or strictly compound nucleus components need to be developed.

REFERENCES

- [1] GOLDMAN, D. T., Nuclear Data for Reactors (Proc. Conf. Paris, 1966) 1, IAEA, Vienna (1967) 339.
- [2] DUNFORD, C. L., Ibid. p.429.
- [3] WILMORE, D., Ibid. p.443 (abstract only).
- [4] FRANCIS, N. C., LUBITZ, C. R., REYNOLDS, J. T. and SLAGGIE, E. L., Ibid. Vol. 2, p.267.
- [5] LYNN, J. E., Nuclear Data for Reactors (Proc. Conf. Helsinki, 1970) 1, IAEA, Vienna (1970) 93.
- [6] FRICKE, M. P., LOPEZ, W. M., FRIESENHAHN, S. J., CARLSON, A. D., and COSTELLO, D. G., Ibid. Vol. 2, p.281.
- [7] CANER, M. and YIFTAH, S., Ibid. Vol. 2, p.735.
- [8] PRINCE, A., Ibid. Vol. 2, p.825.
- [9] WILMORE, D., UKAEA Rep. AERE-R 5053.
- [10] MOLDAUER, P. A., ENGELBRECHT, G. A. and DUFFY, G. J., Argonne Report ANL-6978 (1964).
- [11] FESHBACH, H., PORTER, C. W. and WEISSKOPF, V. F., Phys. Rev. 96 (1954) 448.
- [12] CHASE, D. M., WILKES, L. and EDMONDS, A. R., Phys. Rev. 110 (1958) 1080.
- [13] HAUSER, W. and FESHBACH, H., Phys. Rev. 87 (1952) 366.
- [14] WOODS, R. D. and SAXON, D. S., Phys. Rev. 95 (1954) 577.
- [15] THOMAS, L. H., Nature 117 (1926) 514.
- [16] AUERBACH, E. H., Brookhaven Report BNL-6562 (1964).
AUERBACH, E. H. et al., USAEC Report KAPL-3020 (1964).
- [17] AUERBACH, E. H. and MOORE, S. O., Phys. Rev. 135 (1964) B895.
- [18] CANER, M. and YIFTAH, S., Israel Atomic Energy Commission Report IA-1243 (1972).
- [19] CANER, M. and YIFTAH, S., Israel Atomic Energy Commission Report IA-1275 (1973).
- [20] CANER, M. and YIFTAH, S., Israel Atomic Energy Commission Report IA-1276 (1973).
- [21] CANER, M. and YIFTAH, S., Israel Atomic Energy Commission Report IA-1301 (1975).
- [22] MOLDAUER, P. A., Nucl. Phys. 47 (1963) 65.
- [23] GARDNER, D. G., Lawrence Livermore Report UCID-16679 (1975).
- [24] SMITH, A. B., LAMBROPOULOS, P., WHALEN, J. F., Nucl. Sci. Eng. 47 (1972) 19.
- [25] TAMURA, T., Rev. Mod. Phys. 37 (1965) 679.
- [26] TAMURA, T., Oak Ridge Report ORNL-4152 (1967).
- [27] JARY, J., LAGRANGE, Ch. and THOMET, P. Paper at National Soviet Conference on Neutron Physics, Kiev (1975).
- [28] DUNFORD, C. L., Atomics International Report NAA-SR-11706 (1966).
- [29] LANE, A. M. and LYNN, J. E., Proc. Phys. Soc. A70 (1957) 557.

- [30] DRESNER, L., Neutron Interactions with the Nucleus (Proc. Conf. New York, 1957) USAEC Report TID-7547, p.71.
- [31] THOMAS, R. G., Phys. Rev. 97 (1955) 224.
- [32] MOLDAUER, P. A., Revs. Mod. Phys. 36 (1964) 1079.
- [33] PORTER, C. E. and THOMAS, R. G., Phys. Rev. 104 (1956) 483.
- [34] GILBERT, A. and CAMERON, A. G. W., Can. J. Phys. 43 (1965) 1446.
- [35] LYNN, J. E., UKAEA Rep. AERE-R 7468 (1974).
- [36] HILL, D. L. and WHEELER, J. A., Phys. Rev. 89 (1953) 1102.
- [37] MIYAMOTO, K., OHTA, M., OHSAWA, T., Mem. Faculty Eng. Kyushu Univ. 33 (1973) 47.
- [38] MURATA, T., Communication to this Panel.
- [39] JARY, J., Paper at National Soviet Conference on Neutron Physics, Kiev (1975).
- [40] SOWERBY, M. G., PATRICK, B. H. and MATHER, D., Ann. Nucl. Sci. and Eng. 1 (1974) 409.
- [41] BAYBARZ, R. D., BERRETH, J. R., SIMPSON, F. B., BROWN, W. K., ENNIS, M. E., FULLWOOD, R. R., KEYWORTH, G. A., McNALLY, J. H., MOORE, M. S. and THOMPSON, M. C., Los Alamos Report LA-4566 (1971).
- [42] LAMPHERE, R. W., Physics and Chemistry of Fission (Proc. Conf. Salzburg, 1965), IAEA, Vienna, 1965, Vol. 1, p.63.
- [43] BROWN, W. K., DIXON, D. R. and DRAKE, D. M., Nucl. Phys. A156 (1970) 609.
- [44] STEIN, W. E., SMITH, R. K. and SMITH, H. L., Neutron Cross-Sections and Technology (Proc. Conf. Washington, 1968) NBS special publication 299, Vol. 1, p.627.
- [45] MUIR, D. W. and VEESER, L. R., Nuclear Cross-Sections and Technology (Proc. Conf. Knoxville, 1971) USAEC report CONF 710301, Vol. 2, p.292.
- [46] SEEGER, P. A., HEMMENDINGER, A. and DIVEN, B. C., Nucl. Phys. A96 (1967) 605.
- [47] BJØRNHOLM, S., BOHR, A. and MOTTELSON, B., Physics and Chemistry of Fission (Proc. Conf. Rochester, 1973) IAEA, Vienna, Vol. 1, p.367.
- [48] GAVRON, A., BRITT, H. C., KONECNY, E., WEBER, J. and WILHELMY, J. B., Phys. Rev. Letts. 34 (1975) 827.
- [49] LYNN, J. E. and BACK, B. B., J. Phys. A7 (1974) 395.
- [50] BRITT, H. C., BURNETT, S. C., ERKKILA, B. H., LYNN, J. E. and STEIN, W. E., Phys. Rev. C4 (1971) 1444.
- [51] BRITT, H. C., BOLSTERLI, M., NIX, J. R. and NORTON, J. L., Phys. Rev. C7 (1973) 801.
- [52] BRINK, D. M., D.Phil. Thesis, Oxford (unpublished) (1955).
- [53] WILHELMY, J. B., BRITT, H. C., GAVRON, A., KONECNY, E. and WEBER, J., Nuclear Cross-Sections and Technology (Proc. Conf. Washington, 1975).
- [54] WILMORE, D. and HODGSON, P. E., Nucl. Phys. 55 (1964) 673.
- [55] ANDREEV, M. F., GLADKOV, V. V., ZAVGORODNII, V. A., SEROV, V. I. and SURIN, V. M., Sov. J. Nucl. Phys. 17 (1973) 243.
- [56] MANI, G. S., MELKANOFF, M. A., IORI, I., Saclay Report CEA-2380 (1963).
- [57] BENZI, V., FABBRI, F. and REFFO, G., Critique of Nuclear Models and their validity in Evaluation of Nuclear Data (Proc. EANDC Topical Discussion, Tokyo, 1974) Japan Atomic Energy Research Institute Report JAERI-M 5984 (1975).
- [58] BATCHELOR, R., GILBOY, W. B. and TOWLE, J. H., Nucl. Phys. 65 (1965) 236.
- [59] GUENTHER, P. and SMITH, A., Nuclear Cross-Sections and Technology (Proc. Conf. Washington, 1975). Also private communication for this Panel.
- [60] POENITZ, W., Karlsruhe Report KFK 523 (1966).
- [61] MÖLLER, P. and NIX, J. R., Physics and Chemistry of Fission (Proc. Conf. Rochester, 1973) IAEA, Vienna, Vol. 1 (1974) p.103.
- [62] LYNN, J. E., Nuclear Energy Agency Nuclear Data Committee Paper EANDC(UK)157AL.
- [63] THOMET, P., Paper at National Soviet Conference on Neutron Physics, Kiev (1975).

- [64] DØSSING, T. and JENSEN, A. S., Nucl. Phys. A222 (1974) 493.
 [65] HUIZENGA, J. R., BEHKAMI, A. N., ATCHER, R. W., SVENTEK, J. S.,
 BRITT, H. C. and FREIESLEBEN, H., Nucl. Phys. A223 (1974) 589.
 [66] ENGELBRECHT, C. A. and WEIDENMÜLLER, H. A., Phys. Rev. C8 (1973) 859.
 TEPEL, J. W., HOFMANN, H. M. and WEIDENMÜLLER, H. A., Phys. Lett. 49B
 (1974) 1.
 HOFMANN, H. M., RICHERT, J., TEPEL, J. W. and WEIDENMÜLLER, H. A., To
 be published.
 [67] MOLDAUER, P. A., Phys. Rev. C11 (1975) 426.
 [68] VANDENBOSCH, R., RUSSO, P. A., SLETTEN, G. and MEHTA, M.,
 Phys. Rev. C8 (1973) 1080.
 [69] KALISH, R., HERSKIND, B., PEDERSEN, J., SHACKLETON, D. and
 STRABO, L., Phys. Rev. Letts. 32 (1974) 1009.
 [70] PEARLSTEIN, S., Journal of Nuclear Energy 27 (1973) 81.

TABLE I. Level density parameters for the actinides at
 intermediate excitation energies. Constant
 temperature forms of type

$$\rho(E, J^{\pi}) = (2J + 1) \exp[-(J + \frac{1}{2})^2 / 2\sigma^2].$$

$Ce^{E/\theta}$ are assumed.

Type	Energy Range	C (MeV ⁻¹)	θ (MeV)	σ
Even	1 MeV - E_{IP}	0.225	0.5	5.3
Odd-A	1.2 - E_{IP}	0.9	0.5	6.1
Odd	0 - E_{IP}	3.75	0.5	6.1

TABLE II. Barrier level density parameters employed for actinide nuclei. Level densities take the form

$$\rho_F(E, J, \pi) = (2J + 1) e^{-(J + \frac{1}{2})^2 / 2\sigma^2} \cdot C_F e^{E/0_F}$$

Type	Energy range (MeV)	C_A	θ_A	C_B	θ_B	σ
Even	1.0 - 2.5	0.02135	0.3005			5.7
	2.5 - 2.8	1.435×10^{-4}	0.1877			6.0
	2.8 - $\gtrsim 5$	1.6	0.5			6.3
	1.0 - 1.4			0.02135	0.3005	5.7
	1.4 - 2.0			0.198	0.576	5.7
	2.0 - 3.05			0.00965	0.308	6.0
	3.05 - $\gtrsim 5$			0.4265	0.5	6.3
Odd-A	0 - $\gtrsim 3$	6.8	0.48	3.4	0.48	6.4
Odd	0 - ~ 2	11.5	0.36	5.75	0.36	6.4
	~ 2 - $\gtrsim 5$	54.5	0.5	27.2	0.5	6.4
Suggested: no data analysed beyond ~ 2						

TABLE III. Barrier level density parameters for higher excitation energies (relative to barrier potential). Notation as in Table II, σ taken to be 6.3.

Type	Energy range (MeV)	C_A (MeV ⁻¹)	Θ_A (MeV)	C_B (MeV ⁻¹)	Θ_B (MeV)
Even	2.8 - 7.5 7.5 - 10.9	1.72 19.47	0.506 0.605		
	3.05- 7.2 7.2 - 8.9 8.9 - 10.9			0.426 0.94 8.55	0.50 0.531 0.61
	10.9 - 13.0 13.0 - 15.0 15.0 - ~20	74.0 191.5 1.25 x 10 ⁴	0.653 0.686 0.849	29.2 80.5 5.4 x 10 ³	0.653 0.686 0.849
Odd-A	4.0 - 6.5 6.5 - 9.0 9.0 - 16.0 16.0 - ~20	14.2 50.0 835 1.32 x 10 ⁴	0.528 0.587 0.719 0.821	7.1 25.0 417 6.8 x 10 ³	0.528 0.587 0.719 0.821
Odd	2.0 - 6.5 6.5 - 11.5 11.5 - ~20	104.5 1.19 x 10 ³ 2.52 x 10 ⁴	0.5 0.673 0.82	52.2 590 1.26	0.5 0.673 0.82

TABLE IV. Summary of calculations on transactinium nuclide cross-sections

Target	Cross-section	Energy Range	Reference	Remarks
^{232}Th	$\sigma_{n,\text{capt}}$	0.01 - 5 MeV	M. Ohta, T. Ohsawa, K. Miyamoto, Y. Kawamara, cont. to Panel	Optical model calculation (for compound nucleus cross-section). Hauser-Feshbach with fluctuation and interference corrections. Gilbert-Cameron level density parameters. Calculations made with inelastic scattering competition to discrete levels below 0.6 MeV (i) only, (ii) plus continuum with $a = 10.41 \text{ MeV}^{-1}$, (iii) plus continuum with $a = 29.44 \text{ MeV}^{-1}$. Presumably SCD model used for radiation trans. coeff.
^{231}Pa	$\sigma_{n,F}$	0.4 - 6 MeV	[53]	Calculated from multiplication of compound nucleus formation cross-section calculated from optical model parameters with fission probability measured from $^3\text{He}(d,F)$ and $(^3\text{He},tF)$ reactions. Note discrepancy (up to range of 50%) in C.N. cross-section from different optical model parameters. Fission probabilities can also be calculated from level density calculation (independent quasi-particle model with pairing correlation and rotational state enhancement at barriers).

TABLE IV. Continuation sheet 1

Target	Cross-section	Energy Range	Reference	Remarks
^{233}Pa	$\sigma_{n,T}$ $\sigma_{n,n}$ $\sigma_{n,n'}$ $\sigma_{n,\text{capt}}$ $\sigma_{n,2n}$ $\sigma_{n,3n}$ $\sigma_{n,F}$	0.02 - 15 MeV 0.02 - 15 MeV threshold-9MeV 0.02 - 0.7 MeV threshold-13MeV threshold-15MeV 0.4 - 13 MeV	[37]	Optical model. Simple Hauser-Feshbach. Pearlstein method [70] for $(n, \times n)$. Fission cross-section from systematic variation at $E_n = 3$ MeV. $Z^{4/3}/A$, with shape of ^{231}Pa $\sigma_{n,F}$ below $E_n = 3$ MeV and shape of ^{237}Np $\sigma_{n,F}$ above $E_n = 3$ MeV.
^{237}U	$\sigma_{n,F}$ $\sigma_{n,2n}$ $\sigma_{n,3n}$	2 - 20 MeV 2 - 20 MeV 2 - 20 MeV	[39]	Barrier level density taken to have independent-particle form with arbitrary multiplicative factor K_1 and parameter $a_F = a(1 + K_2/(E^* - \Delta))$ where a is Gilbert-Cameron value, K_2 adjustable. Parameters fixed from adjustment to $^{238}\text{U}(n,F)$, $^{235}\text{U}(n,F)$; $\sigma_{n,F}$ agrees with $^{236}\text{U}(t,pF)$ (Cramer and Britt) but factor 2 below $^{237}\text{U}(n,F)$ data of McNally at 2 MeV. Note K_1 parameter varies irregularly with N .
^{237}U	$\sigma_{n,T}$ $\sigma_{n,n}$ $\sigma_{n,n'}$ to discrete states up to 0.555 MeV $\sigma_{n,\text{capt}}$.01 - 0.7 MeV .01 - 0.7 MeV threshold-1MeV .01 - 0.7 MeV	M. Caner, M. Segev and S. Yiftah, pre-publication	Optical model and statistical theory calculation (ABACUS-NEARREX). Optical model parameters from ^{241}Pu evaluation.

TABLE IV. Continuation sheet 2.

Target	Cross-section	Energy Range	Reference	Remarks
^{238}U	$\sigma_{n,n'}$ to discrete states at 0.045, 0.148, 0.308 MeV	threshold-3MeV	[59]	Theoretical estimate (Moldauer theory) compared with data; agreement good (within ~10%).
^{238}U	$\sigma_{n,\text{capt}}$	0.01 - 3 MeV	M. Ohta et al. Cont. to this Panel	See under ^{232}Th . Option (ii) gives best fit to data.
^{238}U	$\sigma_{n,T}$ $\partial\sigma_{nn}/\partial\omega$ $\sigma_{n,\text{capt}}$ $\sigma_{n,n'}$ to discrete states up to 1.168 MeV $\sigma_{n,F}$ $\sigma_{n,2n}$ $\sigma_{n,3n}$.003 - 20 MeV 2 - 15.5 MeV .003 - 3 MeV 2 - 20 MeV threshold-20MeV threshold-20MeV	J. Jary, Ch. Lagrange P. Thomet, Kiev Neutron Physics Conf. 1975 more details in [39] more details in [63] more details in [63]	Optical model parameters adjusted to reproduce s_0 , s_1 , R' , $\sigma_{n,T}$, $\partial\sigma_{nn}/\partial\omega$ (deformed potential, coupled channel method employed). For inelastic scattering to continuum, const. temp. level density employed ($T = 0.41$, $C = e^{0.15/0.41}$, no J-dependence). Fission barrier $V_A = 6.25$ MeV, $\hbar\omega_A = 1.05$ MeV, $V_B = 5.93$, $\hbar\omega_B = 0.5$, fixed parameters, barrier level density fitted by adjustment to $\sigma_{n,F}$ data. $\sigma_{n,\text{capt}}$ too high (up to ~50%) above a few 100 keV; GDR model used. $\sigma_{n,n'}$ - reasonable agreement for lower levels, tendency to be too low for higher levels (worst case .826, over 100%) $\sigma_{n,2n}$ calculations use Gilbert and Cameron level density parameters, single-hump barrier parameters - reasonable agreement (within ~20%) except above 14 MeV for (n,2n).

TABLE IV. Continuation sheet 3.

Target	Cross-section	Energy Range	Reference	Remarks
^{239}U	$\sigma_{n,F}$ $\sigma_{n,2n}$ $\sigma_{n,3n}$	2 - 20 MeV 2 - 20 MeV 2 - 20 MeV	[39]	See remarks on barrier parameters under ^{237}U , ref. [39]. Agreement with $^{238}\text{U}(t,pF)$ data (Cramer and Britt) at 2 MeV quite good.
^{239}U (23.5m) ^{239m}U (.78 μ s)	$\sigma_{n,T}$ $\sigma_{n,n}$ $\sigma_{n,n'}$ $\sigma_{n,capt}$ $\sigma_{n,F}$	10^{-5} - 2.5MeV 10^{-5} - 2.5MeV threshold- 2.5 MeV 10^{-5} - 2.5MeV 10^{-5} - 2.5MeV	D. G. Gardner, UCID-16679 (1975)	Compound nucleus formation cross-section calculated from Moldauer (1963) optical model parameters. No direct reaction included but reduction in σ_{CN} made to allow for this. Gilbert-Cameron level density parameters. GDR model. Single-humped fission barrier with $V_F = 5.7$ MeV, $\hbar\omega = 0.5$ MeV, 20 discrete fission channels to 0.7 MeV, continuum of fission channels with level density parameters increased by 15% (over Gilbert-Cameron) (causes factor 2 increase at $E_n = 25$ MeV, none at 0.5 MeV).
^{232}Np	$\sigma_{n,F}$	0.1 - 3.0 MeV	[53]	See remark under ^{231}Pa
^{233}Np	$\sigma_{n,F}$	0.1 - 4.5 MeV	[53]	See remark under ^{231}Pa
^{234}Np	$\sigma_{n,F}$	0.1 - 6.0 MeV	[53]	See remark under ^{231}Pa

TABLE IV. Continuation sheet 4.

Target	Cross-section	Energy Range	Reference	Remarks
^{235}Np	$\sigma_{n,F}$	0.1 - 6.5 MeV	[53]	See remark under ^{231}Pa
^{236}Np	$\sigma_{n,F}$	0.1 - 4.5 MeV	[53]	See remark under ^{231}Pa
^{237}Np	$\sigma_{n,F}$	0.5 - 8 MeV	[53]	See remark under ^{231}Pa
^{238}Np	$\sigma_{n,F}$	0.1 - 5 MeV	[53]	See remark under ^{231}Pa
^{239}Np	$\sigma_{n,\text{capt}}$	0.01 - 3 MeV	M. Ohta et al, cont. to this Panel	See under ^{232}Th
^{239}Np	$\sigma_{n,T}$ $\sigma_{n,n}$ $\sigma_{n,n'}$ $\sigma_{n,\text{capt}}$ $\sigma_{n,2n}$ $\sigma_{n,3n}$ $\sigma_{n,F}$	0.02 - 15 MeV 0.02 - 15 MeV threshold-9MeV 0.02 - 1 MeV threshold-13MeV threshold-15MeV 0.4 - 15 MeV	[37]	Optical model. Simple Hauser-Feshbach Perlstein method for $(n, \times n)$ Fission cross-section from systematic variation at $E_n = 3$ MeV v. $Z^{4/3}/A$, with shape of cross-section of ^{237}Np .

TABLE IV. Continuation sheet 5.

Target	Cross-section	Energy Range	Reference	Remarks
^{238}Pu	$\sigma_{n,T}$	0.001 - 15MeV	[21]	Calculated with spherical optical potential (ABACUS-2)
	$\sigma_{n,n}$	0.001 - 15MeV		Calculated with spherical optical potential (ABACUS-2)
	$\sigma_{n,\text{capt}}$	0.001 - 15MeV		Calculated with Hauser-Feshbach (NEARREX), SCD model and simple Fermi gas law.
	$\sigma_{n,F}$	0.001-0.004MeV		Calculated with Hauser-Feshbach (NEARREX). Fission transmission coefficient computed from Hill-Wheeler formula (eq. 5) with $N_F = 20$ for each J^π value; $E_F = 0.7$ MeV, $\hbar\omega_F = 0.586$ for $J^\pi = \frac{1}{2}^+$, 0.741 for other J^π values.
	$\sigma_{n,n'}$ to 20 discrete states			
^{239}Pu	$\sigma_{n,F}$	2 - 20 MeV	[39]	See remarks on barrier parameters under ^{237}U , ref. [39]
	$\sigma_{n,2n}$	2 - 20 MeV		Adjustment of K_1, K_2 to give agreement (within about 5%) with Sowerby et al evaluation. $\sigma_{n,2n}$ agrees with limited data to within about 30% except near threshold.
	$\sigma_{n,3n}$	2 - 20 MeV		One data point for $\sigma_{n,3n}$ (near threshold) disagrees.
^{240}Pu	$\sigma_{n,T}$	0.1 - 1.5MeV	[24]	Calculations compared with measured data.
	$\partial\sigma_{n,n}/\partial\omega$	0.1 - 1.5MeV		Optical model parameters for spherical and deformed (coupled-channel) well determined. Fission competition introduced, predominantly in $J^\pi = \frac{1}{2}^+$ channel below 700 keV, but with $J^\pi = \frac{1}{2}^-, 3/2^-$ channels about 600 keV.
	$\sigma_{n,n'}$ to states at 0.042, 0.140, 0.3, 0.6, 0.9 MeV			

TABLE IV. Continuation sheet 6.

Target	Cross-section	Energy Range	Reference	Remarks
^{240}Pu	$\sigma_{n,T}$	0.001-15MeV	[18]	Calculated with spherical optical potential (ABACUS-2)
	$\sigma_{n,n}$	0.001-15MeV		Calculated with spherical optical potential (ABACUS-2)
	$\sigma_{n,capt}$	0.001-1.3MeV		Calculated with Hauser-Feshbach (NEARREX), SCD model and simple Fermi gas law ($a = 29.76 \text{ MeV}^{-1}$)
	$\sigma_{n,F}$	0.001-0.004MeV		Calculated with Hauser-Feshbach. Fission transmission coefficients calculated for single hump barrier and Hill-Wheeler formula with assumption that all possible K-bands with 2-fold degeneracy are present. $E_F = .81 \text{ MeV}$, $\chi\omega_F = .635 \text{ MeV}$ for best fit. Agrees with data up to E_F
	$\sigma_{n,n'}$ for states at 0.042, 0.140, 0.3, 0.6, 0.9 MeV	threshold - 1.5 MeV		
^{240}Pu	$\sigma_{n,T}$ $\sigma_{n,n}$ $\sigma_{n,F}$	4 - 15 MeV 4 - 15 MeV 4 - 15 MeV	T. Murata, private communication for this Panel	Optical model calculation with $^{238}\text{U}+n$ parameters Neutron-fission branching ratio from Vandenbosch and Huizenga expression, $E_F = 0.71 \text{ MeV}$, for 1st chance fission. Level density parameters a_n , a_F varied to reproduce experimental fission cross-section in energy range 3-7 MeV and at 14 MeV; a_n increase asymptotically to 23 MeV^{-1} , a_F decreases asymptotically to 27.3 MeV^{-1}

TABLE IV. Continuation sheet 7.

Target	Cross-section	Energy Range	Reference	Remarks
^{241}Pu	$\sigma_{n,T}$ $\sigma_{n,n}$ $\sigma_{n,\text{capt}}$ $\sigma_{n,F}$ $\sigma_{n,n'}$ to discrete states at 0.04, 0.092, 0.163 MeV	0.001-15 MeV 0.001-15 MeV 0.001-0.5 MeV 0.0001-0.035 MeV threshold-15 MeV	[20]	As under ^{240}Pu , ref. [18] Fermi gas level density parameter $a = 29.62 \text{ MeV}^{-1}$ Fission transmission coefficient computed with channel nos. varying from 1 to 5 for various J^π and divided into energy ranges. $E_F(2^+) = -0.097 \text{ MeV}$, $E_F(3^+) = 0.0013 \text{ MeV}$, other $E_F = 0.0$
^{242}Pu	$\sigma_{n,T}$ $\sigma_{n,n}$ $\sigma_{n,\text{capt}}$ $\sigma_{n,F}$ $\sigma_{n,n'}$ for 17 discrete states	0.001-15 MeV 0.001-15 MeV 0.001-1.2 MeV	[19]	As under ^{240}Pu , ref. [18] Fermi gas level density parameter $a = 27.95 \text{ MeV}^{-1}$ Fission barrier parameters are $E_F = 0.87 \text{ MeV}$, $\hbar\omega_F = 0.509 \text{ MeV}$
^{241}Am	$\sigma_{n,F}$	0.5 - 7 MeV	[53]	See remark under ^{231}Pa
^{242m}Am	$\sigma_{n,F}$	0.1 - 4.5 MeV	[53]	See remark under ^{231}Pa
<u>In Progress</u>				
^{236}Pu to ^{244}Pu	$\sigma_{n,F}$ $\sigma_{n,n}$	2 - 20 MeV threshold - 20 MeV	J. Jary, Ch. Lagrange	

TABLE IV. Continuation sheet 8.

Target	Cross-section	Energy Range	Reference	Remarks
^{241}Am to ^{243}Am	$\sigma_{n,\text{capt}}$ $\sigma_{n,n'}$ $\sigma_{n,F}$ $\sigma_{n,\alpha n}$	0.001-3MeV threshold- 20MeV 0.001-20MeV threshold- 20MeV	J. E. Lynn	
^{242}Cm to ^{246}Cm	$\sigma_{n,\text{capt}}$ $\sigma_{n,n'}$ $\sigma_{n,F}$ $\sigma_{n,n}$	0.001-3MeV threshold- 20MeV 0.001-20MeV threshold- 20MeV	J. E. Lynn	

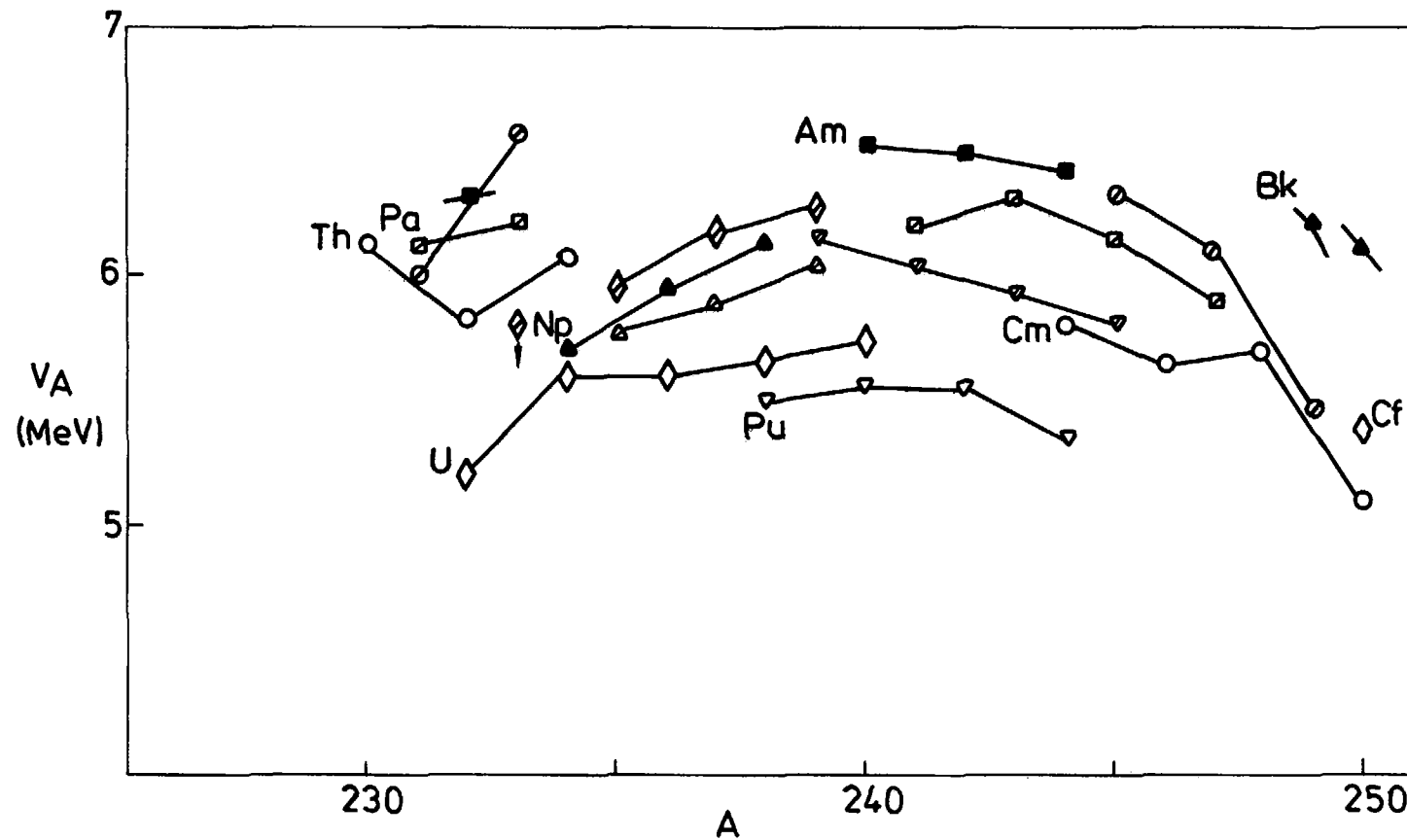


FIG.1. INTERMEDIATE BARRIER HEIGHTS AS A FUNCTION OF MASS NUMBER. OPEN SYMBOLS DENOTE EVEN NUCLEI, HATCHED DENOTE ODD-MASS, BLACK DENOTE ODD NUCLEI ; \circ - Th, Cm ; \square - Pa, Am ; \diamond - U, Cf ; Δ - Np, Bk ; ∇ - Pu

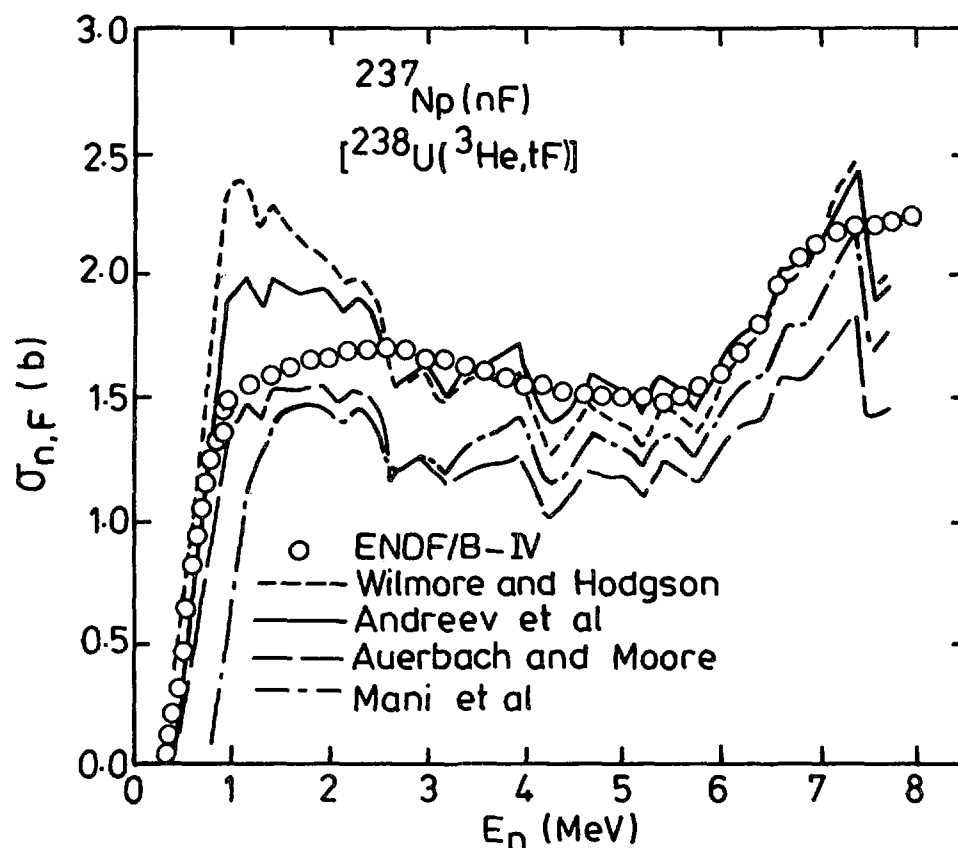


FIG. 2. COMPARATIVE CALCULATIONS OF FISSION CROSS-SECTION OF ^{237}Np FROM REF. [53]. DIFFERENCES ARE DUE TO DIFFERENT COMPOUND NUCLEUS FORMATION CROSS-SECTIONS EMPLOYED.

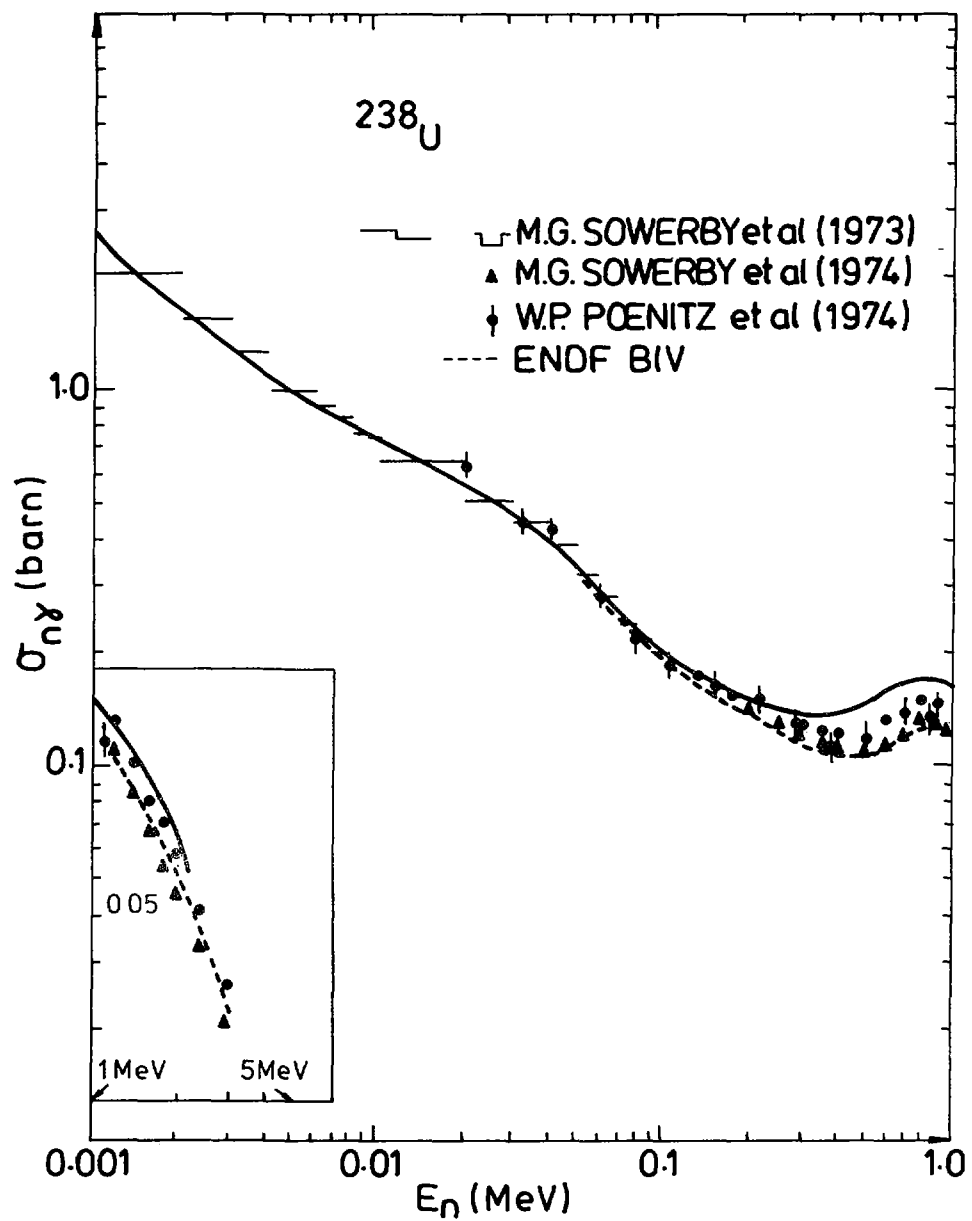


FIG. 3. CALCULATED CAPTURE CROSS-SECTION OF ^{238}U FROM REF. [27] COMPARED WITH EVALUATED DATA.

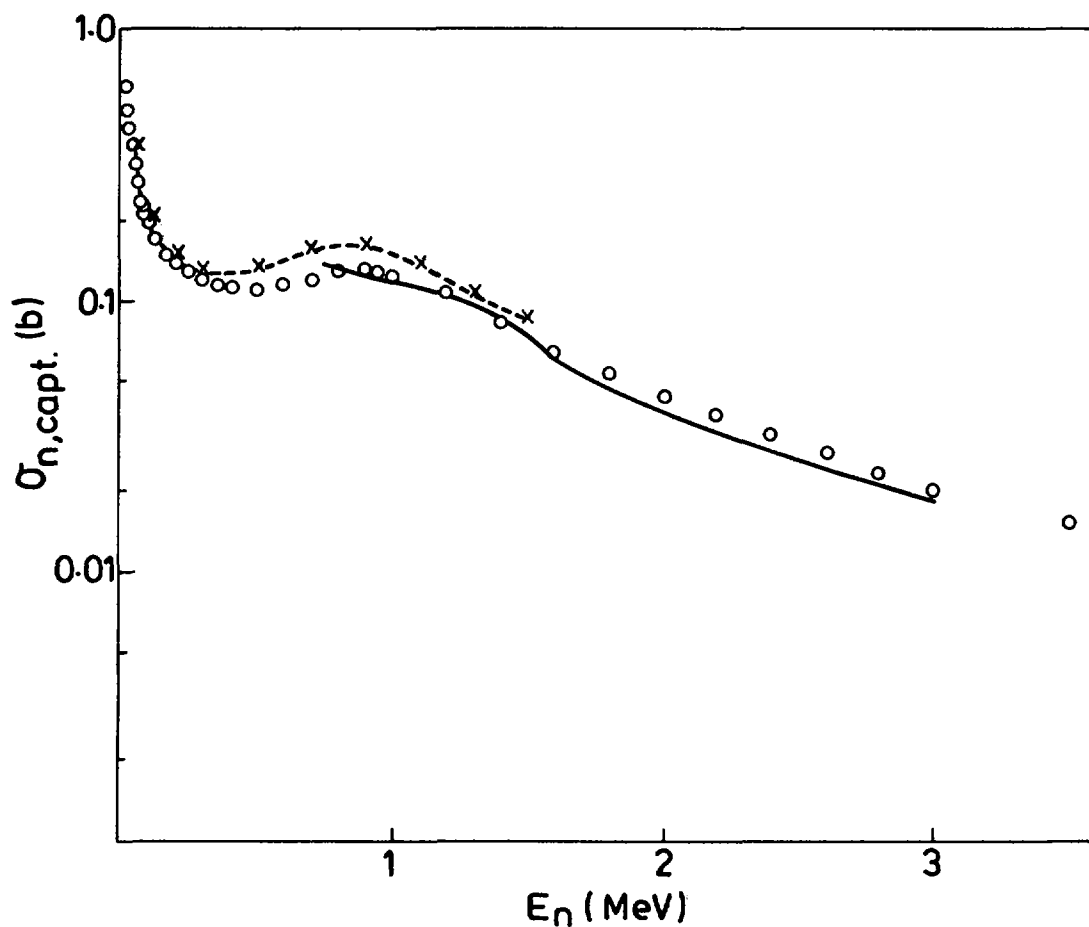


FIG. 4. CALCULATED CAPTURE CROSS SECTION OF ^{238}U FROM REF.[35], COMPARED WITH EVALUATED DATA, x-x-x DETAILED HAUSER-FESHBACH, — STATISTICAL HAUSER-FESHBACH

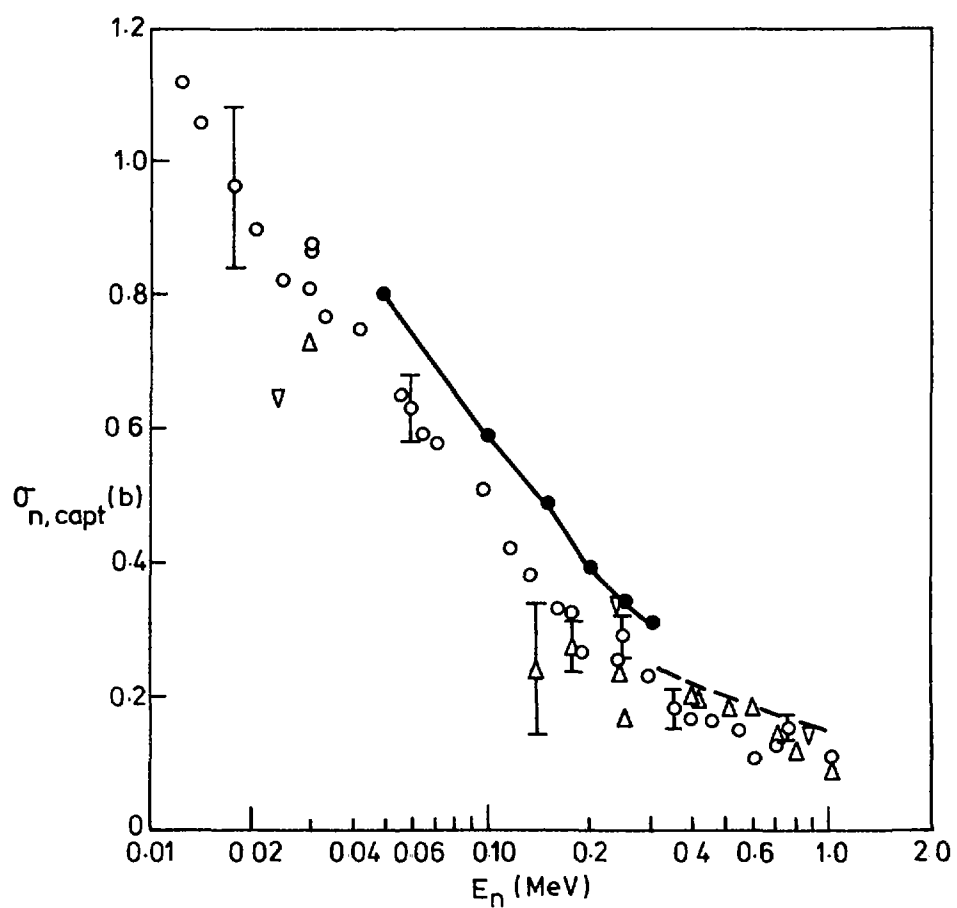


FIG. 5. CALCULATED CAPTURE CROSS-SECTION OF ^{235}U FROM REF. [35], COMPARED WITH DATA ,
 — DETAILED HAUSER-FESHBACH ,
 ----- STATISTICAL THEORY.

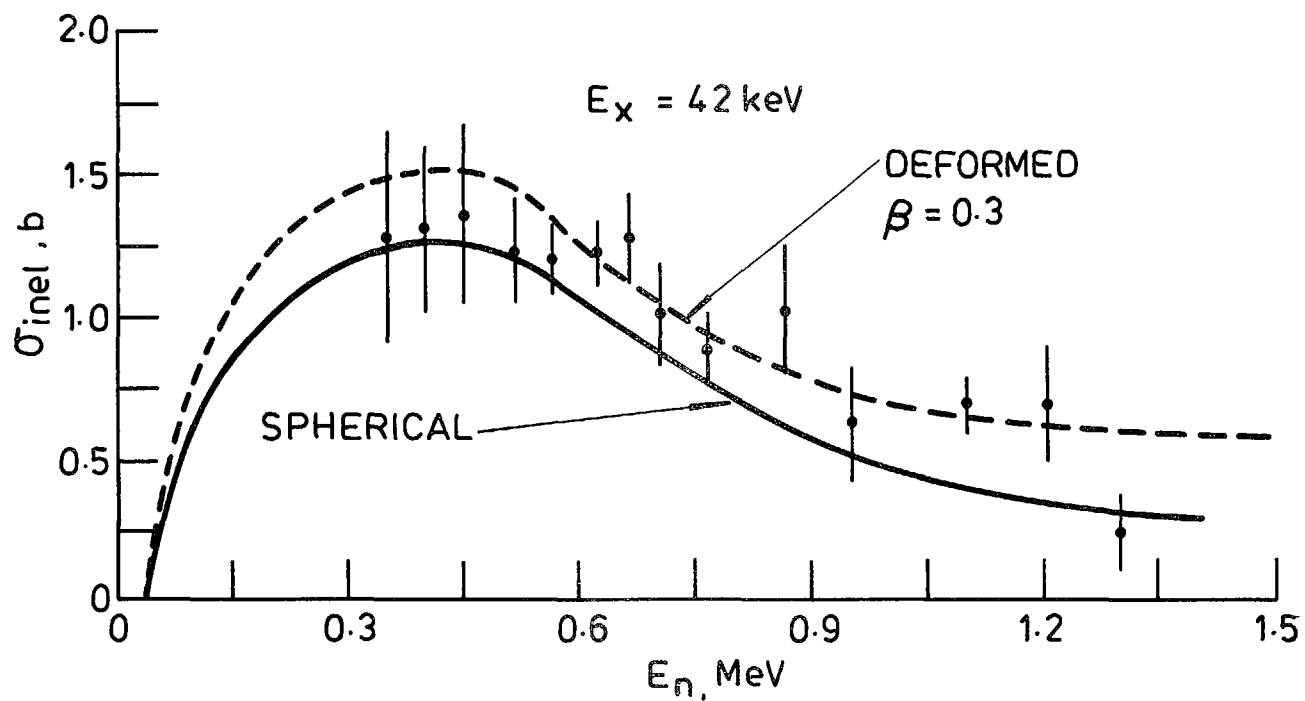


FIG. 6. INELASTIC SCATTERING CROSS-SECTION TO FIRST ROTATIONAL STATE OF ^{240}Pu , CALCULATED FOR SPHERICAL OPTICAL POTENTIAL (—) AND DEFORMED OPTICAL POTENTIAL (-----)

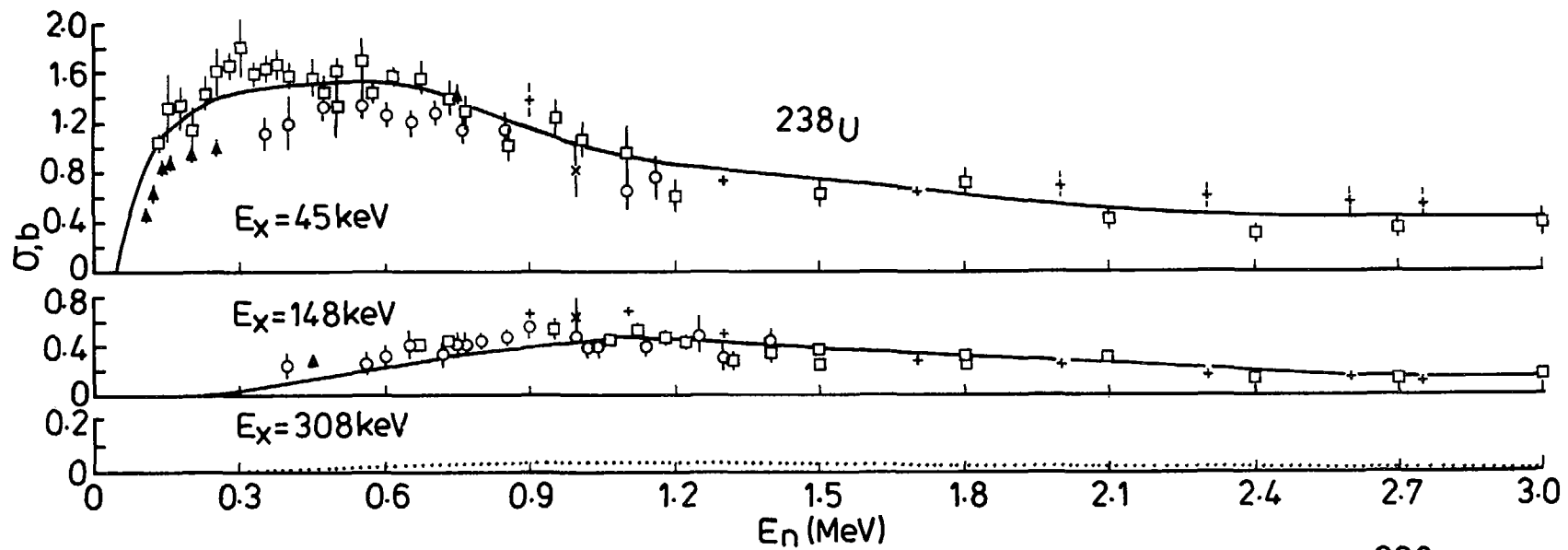


FIG. 7. INELASTIC SCATTERING CROSS-SECTION TO ROTATIONAL STATES OF ^{238}U CALCULATED FROM COUPLED-CHANNEL OPTICAL MODEL AND COMPARED WITH DATA[59]

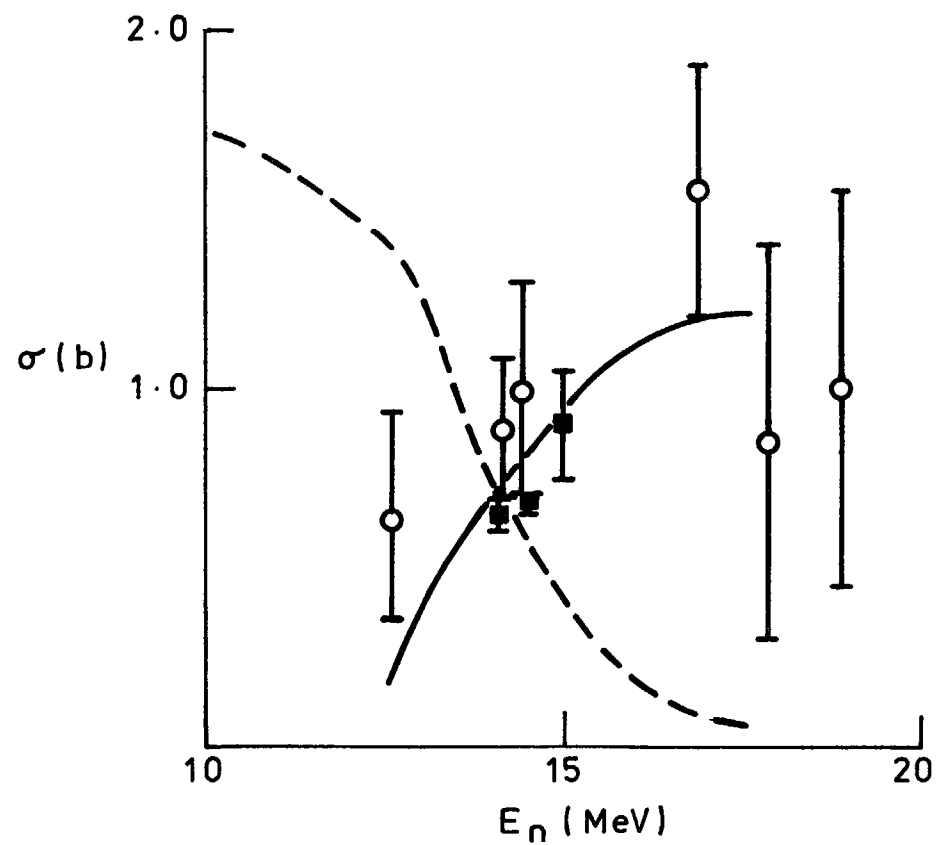


FIG.8 (n,xn) CROSS-SECTIONS OF ^{238}U — $\sigma_{n,2n}$ CALCULATION, ■, $\sigma_{n,2n}$, DATA; — $\sigma_{n,3n}$ CALCULATION, ○ $\sigma_{n,3n}$ DATA.

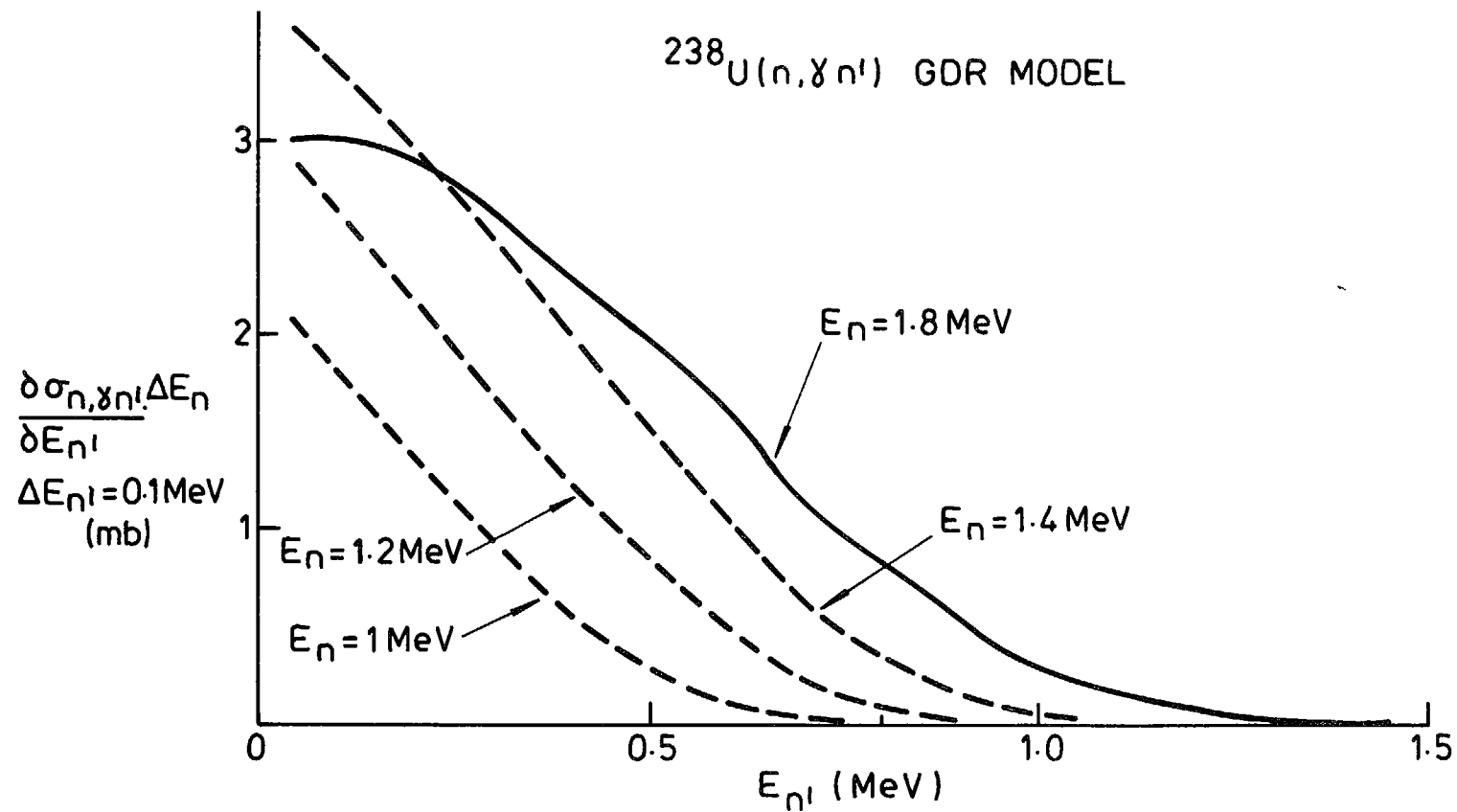


FIG. 9. CALCULATED $(n, \gamma n')$ CROSS-SECTION OF ^{238}U USING PARAMETERS OF REF. [35]. DIAGRAM FROM REF. [62].

A SURVEY OF CROSS SECTION EVALUATION METHODS FOR HEAVY ISOTOPES*

M. Caner and S. Yiftah

Israel Atomic Energy Commission
Soreq Nuclear Research Centre
Yavne, Israel

Abstract

Abstract

Evaluation methods and neutron nuclear reaction theories for heavy isotopes are discussed. A compilation of the most recent evaluations of the transactinium isotopes discussed in this meeting is presented, with emphasis on the formalisms used.

In this paper we discuss evaluation methods and neutron nuclear reaction theories applicable to heavy isotopes. In Table I we present a compilation of the most recent evaluations of the transactinium isotopes discussed in the present meeting. The evaluations are examined in terms of the formalisms and models used in the different energy ranges.

The energy range of interest for neutron nuclear data for fast reactor calculations spans approximately 10 decades, from 10^{-3} to 15×10^6 eV (10^{-5} to 20×10^6 eV in ENDF/B-IV). It is convenient to subdivide this energy range into thermal, resolved resonances, unresolved resonances, and fast neutron ranges. The thermal range comprises the thermal energy (0.0253 eV) and can be defined as extending from 10^{-3} (or 10^{-5} eV) to 1 eV. The resolved resonances range is defined as the range spanned by the resonances for which a full set of parameters is available. (In some instances it overlaps the thermal range.) The unresolved resonances range extends from the last resolved resonance up to the vicinity of 10 - 100 keV. The fast neutron range extends up to 15 - 20 MeV; sometimes, the continuous cross section calculations in this range are extended downward to include the average cross sections in the unresolved resonances range.

Let us now discuss the formalisms used in the different ranges. In the thermal range the cross sections are calculated from resonance parameters and resonance theory formalisms. In some cases a negative resonance has to be postulated to fit the thermal values.

* Prepared for the International Atomic Energy Agency Advisory Group Meeting on Transactinium Isotope Nuclear Data (TND), Karlsruhe, 3-7 November, 1975 (contribution to topic B 5 b)

In the resolved resonances range the Breit-Wigner single-level formula [1] is most frequently used. For fissile nuclides, however, there are asymmetries in the fission cross sections due to level-level interference; the Breit-Wigner formula does not adequately describe the cross section between the resonances, and a multilevel formula is needed. The Reich-Moore [2] multilevel formalism is used most often: it has the advantage over the Adler formalism [3] in that the parameters are the same as those of the Breit-Wigner formula, with the addition of the interference sign, and they obey the same statistics. On the other hand, Doppler - broadened cross sections are calculated more easily in the Adler formalism. A compromise between the convenience of the Breit-Wigner formula and the accuracy of the multilevel formulas can be made as follows. Pointwise cross sections generated from the recommended multilevel parameters are used to calculate infinite dilution cross sections, and the Breit-Wigner parameters are used to calculate self-shielding factors; this approach is used in KEDAK. Another approach is given by the ENDF/B [4] option for using Breit-Wigner resonance parameters in conjunction with a tabulated smooth background cross section which accounts for the level-level interference.

In the unresolved resonances range, average cross sections are calculated using the Lane and Lynn formalism [5]. S-wave average parameters can be calculated from the resolved resonance parameters. P-wave parameters can be calculated from resolved p-wave parameters (if available), from systematics, or by fitting the experimental data or the optical model and statistical theory results.

In the fast neutron energy range the optical model and statistical theories are used.

By examining the experimental data at our disposal we can distinguish between a resolved and an unresolved inelastic scattering range. In the former we have complete information on the energies, spins and parities of the residual nucleus; in the latter, part of this information is missing. In the ENDF/B approach, an intermediate range is also present where inelastic scattering to both resolved levels and the continuum is present.

Spherical optical model calculations [6] are based on the solution of Schroedinger's equation for a spherically symmetric average nucleon-nucleus potential. The quantities obtained are the total cross section and the shape elastic scattering cross section, as well as the differential shape elastic cross sections.

Deformed (or coupled-channel) optical model calculations [7] are based on a non-spherical interaction potential. The quantities obtained are the total cross section, the shape elastic scattering cross section and the direct inelastic excitation curves for the lowest levels. Also calculated are the angular distributions of the above-mentioned scattering cross sections.

The Hauser-Feshbach statistical theory [8] can be used to split the compound nucleus cross section into partial cross sections - capture, fission and the inelastic excitation curves - in terms of transmission coefficients. This theory was refined by Moldauer [9] to include width fluctuation and resonance interference corrections. The transmission coefficients for the neutron channels are calculated with the optical model. The transmission coefficients for the fission channels are usually calculated with the Hill-Wheeler potential [10] (one-humped fission barrier); a more sophisticated approach [11] incorporates the double-humped fission barrier, based on the Strutinski model [12]. The radiative capture transmission coefficient is calculated using the Weisskopf dipole radiation model [1].

The statistical theory formalism of Pearlstein [13] can be used to split the (compound nucleus) cross section for emitting only neutrons into its components: (n, n') , $(n, 2n)$ and $(n, 3n)$ cross sections.

We now mention some recently developed formalisms applicable to heavy isotopes.

Sukhovitskij and Konshin [14] evaluated σ_{2n} and σ_{3n} for ^{238}U and ^{238}Pu . Their formalism is based on the compound nucleus model and statistical theory. It expresses the $A(n, 2n)$ and $A(n, 3n)$ cross sections in terms of the partial cross sections of the nuclei A to $A-3$. Their results for $^{238}\text{U}(n, 2n)$ agree with the experimental data better than those based on Pearlstein's model.

Jary [15,38] developed a statistical model for the calculation of $A(n, 2n)$, $A(n, 3n)$, $A(n, nf)$ and $A(n, 2nf)$ cross sections for heavy isotopes in terms of the partial reaction widths of the compound nuclei $A+1$ to $A-1$. The neutron widths were calculated with the deformed optical model; the capture widths with the Weisskopf electric dipole radiation formula; the fission widths were calculated with the Hill-Wheeler formula near threshold and with a fission level density formula high above threshold. Results for $(n, 2n)$, $(n, 3n)$ and (n, F) are presented for the uranium isotopes from ^{232}U to ^{239}U in the neutron energy range 2 to 15 MeV.

Igarasi et al. [16] calculated the $^{238}\text{U}(n, \gamma)$ cross section using the Axel-Brink [17] dipole radiation formula for $\langle \Gamma_{\gamma} \rangle$. It is not clear

at present if this formula has an advantage over the Weisskopf formula in the σ_γ calculation.

Lynn [39] made an analysis of neutron cross sections of the actinides from a few keV up to 3 MeV. The analysis is based on Hauser - Feshbach theory, the statistical model of level densities, the Axel - Brink [17] dipole radiation model, and a parametrization of the double-humped fission barrier. This report presents formalisms and parameters to be used in actinide evaluation work.

An examination of Table I, reveals that, of the 18 isotopes included, 11 were evaluated using optical model and statistical theory calculations (referred to in what follows as "theoretical calculations") and the other 7 were evaluated using systematic methods of varying degrees of sophistication. We checked the experimental data now available on the latter 7 isotopes in order to ascertain for which of them a theoretical calculation has become feasible. The data needed are: excited energy levels, their spins and parities; fission cross sections; average capture widths and average level spacings. Enough data for theoretical calculations are available for ^{234}U , ^{237}Np , ^{241}Am , ^{243}Am and ^{245}Cm , but not enough for ^{238}Np and ^{236}Pu .

The next point to be considered is: which isotopes, for which there are requests in WRENDIA [18], do not appear in this table? these isotopes are ^{239}U (σ_γ, σ_f requested), ^{239}Np (σ_γ requested) and ^{237}Pu (σ_γ, σ_f requested). However, there are not enough data available for any of these to perform theoretical calculations. Only preliminary evaluations, based on systematics and the limited experimental data, are possible.

It is hoped that this analysis will help pinpoint those isotopes for which new evaluations should be requested by the present panel.

References

1. BLATT, J.M., WEISSKOPF, V.F., Theoretical Nuclear Physics, Wiley, New York (1962)
2. REICH, C.W., MOORE, M.S., Phys. Rev. 111 (1958) 929.
3. ADLER, D.B., ADLER, F.T., ANL-6792 (1963) 695.
4. DRAKE, M.E., BNL-50274 (1970)
5. LANE, A.M., LYNN, J.E., Proc. Phys. Soc. A70 (1957) 557.
6. HODGSON, P.E., The Optical Model of Elastic Scattering, Oxford University Press, London (1963)
7. TAMURA, T., Rev. Mod. Phys. 37 (1965) 679.
8. HAUSER, W., FESHACH, H., Phys. Rev. 87 (1952) 366.
9. MOLDAUER, P., Rev. Mod. Phys. 36 (1964) 1079.

10. WHEELER, J.A., Fast Neutron Physics, Vol II, (MARION, J.B., FOWLER, J.L., Eds.), Wiley, New York (1963)
11. THOMET, P., JAERI - M 5984 (1975) 71.
12. STRUTINSKI, V.M., Nucl. Phys. A95 (1967) 420.
13. PEARLSTEIN, S., BNL 897 (1964)
14. SUKHOVITSKIJ, E. SH., KONSHIN, V.A., INDC (CCP) - 63/L (1975)
15. JARY, J., JAERI - M 5984 (1975) 76.
16. IGARASI, S., MORI, A., HARADA, K., JAERI - M5984 (1975) 103.
17. AXEL, P., Phys. Rev. 126 (1962) 671.
18. WRENDA 74, INDC (SEC) - 38/U (1974)
19. DRAKE, M.K., NICHOLS, P.F., GA-7462 (1967)
20. DRAKE, M.K., NICHOLS, P.F., GA-8135 (1967)
21. PARKER, K., AWREO-30/64 (1964)
22. DUNFORD, C.L. ALTER, H., NAA-SR-12271 (1967)
23. HOWERTON, R.J., Nucl. Sci. Eng. 46 (1971) 42.
24. CANER, M., YIFTAH, S., IA-1301 (1974); also: Nucl. Sci. Eng. (to be published).
25. DAVEY, W.G., Nucl. Sci. Eng. 44 (1971) 345.
26. THOMET, P., CEA-R-4631 (1974)
27. HUNTER, R.E., STEWART, L., HIRONS, T.J., LA-5172 (1973)
28. CANER, M., YIFTAH, S., IA-1243 (1972)
29. CANER, M., YIFTAH, S., SHATZ, B., MEYER, R., Proc. Int. Symp. Fast Reactor Phys., Tokyo (1973) 683.
30. CANER, M., YIFTAH, S., IA-1276 (1973)
31. CANER, M., YIFTAH, S., IA-1275 (1973)
32. SMITH, J.R., GRIMSEY, R.A., IN-1182 (1969)
33. GORDEEVA, L.D., SMIRENKIN, G.N., Sov. J. At. Energy 14 (1963) 562.
34. HINKELMANN, B., KFK 1186 (1970)
35. PRINCE, A., Proc. 2nd. Int. Conf. Nucl. Data for Reactors, IAEA (1970) Vol. II, 825.
36. PEARLSTEIN, S., BNL 982 (1966)
37. PRINCE, A., BNL 50168 (1969)
38. JARY, J., CEA-R-4647 (1975).
39. LYNN, J.E., AERE-R-7468 (1974).

Table I: Summary of TND evaluations *

Isotopes	File and/or reference	Latest data revision	Energy range (eV)	Thermal range	Resolved resonance range	Average resonance parameters	Fast neutron energy range	σ_{2n}, σ_{3n}	\bar{v}
^{231}Pa , ^{233}Pa , ^{232}U	Drake 67 [19]	1967	$10^{-3} - 15 \times 10^6$	pointwise xsect.	BW(100; 18; 75 eV)	$\ell=0,1$	$10^3 - 15 \times 10^6$ eV; SOM+HF; σ_γ calc. from $\langle \Gamma_\gamma \rangle$ without competing processes; σ_f, σ_n of ^{233}Pa taken from ^{231}Pa .	Pearlstein syst.[13]	
^{233}Pa	E4, Young 70 (unpub)	1974	$10^{-5} - 20 \times 10^6$	BW	BW (39 eV)	$\ell=0,1$	$10^4 - 20 \times 10^6$ eV; $\sigma_{2n}, \sigma_{3n}, \sigma_n^{E_j}$ from Drake 67 [19] other xsect.by systematics	taken from Drake 67 [19]	syst.
^{234}U	E4, Drake 67A [20]	1967	$10^{-5} - 20 \times 10^6$	pointwise xsect; BW	BW (370 eV)	$\ell=0,1$	σ_f from exp.; $\sigma_n, \sigma_{2n}, \sigma_{3n}$ from Parker 64 [21] other xsect. from systematics	taken from Parker 64 [21]	exp.

Table I:(cont.)

Isotopes	File and/or reference	Latest data revision	Energy range (eV)	Thermal range	Resolved resonance range	Average resonance parameters	Fast neutron energy range	σ_{2n}, σ_{3n}	$\bar{\nu}$
^{236}U	E4, Drake 67A [20] McCrosson 71 (unpub.)	1971	$10^{-5} - 20 \times 10^6$	pointwise xsect.; BW	BW(415 eV)	$\ell=0,1$	σ_f, σ_γ from exp.; $\sigma_n, \sigma_{n'}, \sigma_{2n}, \sigma_{3n}$ from Parker 64 [21]	taken from Parker 64 [21]	same as for ^{234}U [20]
^{236}U	Parker 64 [21]	1964	$10^3 - 15 \times 10^6$	-	-	-	σ_T, σ_n from ^{238}U ; $\sigma_{n'}, \sigma_{2n}, \sigma_{3n}$ by syst.; σ_f, σ_γ from exp.	syst.	
^{237}U	Caner 75 (to be pub.)	1975	$10^4 - 7 \times 10^5$	-	-	-	SOM + HFM; σ_f (I)	-	-
$^{238}\text{Pu},$ $^{242}\text{Pu},$ ^{244}Cm	E4, Dunford 67 [22]	1967	$10^{-5} - 20 \times 10^6$ (E4)	pointwise xsect.; BW	BW (200 eV)	$\ell=0,1$	DOM+HFM; σ_f (I)	Pearlstein syst. [13]	Howerton syst. [23]

Table I: (cont.)

Isotopes	File and/or reference	Latest data revision	Energy range (eV)	Thermal range	Resolved resonance range	Average resonance parameters	Fast neutron energy range	σ_{2n}, σ_{3n}	$\bar{\nu}$
^{238}Pu	Caner 74 [24]	1974	$10^{-3} - 15 \times 10^6$	pointwise xsect.; BW	BW(500 eV)	$\ell=0,1$	SOM+HFM; σ_f (I)	Pearlstein syst. [13]	Davey 71[25]
^{232}U , ^{236}U , ^{238}Pu , ^{240}Pu	Thomet 74 [11] [26]	1974	$3 \times 10^3 - 10^6$	-	-	$\ell=0,1$	DOM+HFM; σ_f (II)	-	-
^{240}Pu	E4, Pennington 74 (unpub.) Hunter 73 [27]	1974	$10^{-5} - 20 \times 10^6$	pointwise xsect.	BW(3910 eV)	$\ell=0,1$	exp.; σ_γ calc. with Lane-Lynn formula	similar to ^{239}Pu	exp.
^{240}Pu	K, Caner 72 [28] [29]	1972	$10^{-3} - 15 \times 10^6$	pointwise xsect.; BW	BW (3990 eV)	$\ell=0,1$	SOM+HFM; σ_f (I)	Pearlstein syst. [13]	exp.
^{241}Pu	K, Caner 73 [29] [30]	1973	$10^{-3} - 15 \times 10^6$	pointwise xsect.; RM	BW(160 eV) RM(61 eV) and pointwise xsect.(61eV)	$\ell=0,1$	SOM+HFM; σ_f (I)	Pearlstein syst. [13]	exp.

Table I: (cont.)

Isotopes	File and/or reference	Latest data revision	Energy range (eV)	Thermal range	Resolved resonance range	Average resonance parameters	Fast neutron energy range	σ_{2n}, σ_{3n}	$\bar{\nu}$
^{242}Pu	K, Caner 73A [29] [31]	1973	$10^{-3} - 15 \times 10^6$	pointwise xsect.; BW	BW (494 eV)	$\ell=0,1$	SOM+HFM; σ_f (I)	Pearlstein syst. [13]	syst.
^{237}Np	E4, Smith 69 [32]	1973	$10^{-5} - 20 \times 10^6$	pointwise xsect.	BW (130 eV)	$\ell=0,1$	exp. data and systematics	Pearlstein syst. [13]	exp. + Gordeeva syst. [33]
$^{231}\text{Pa},$ $^{232}\text{U},$ $^{234}\text{U},$ $^{236}\text{U},$ $^{237}\text{U},$ $^{237}\text{Np},$ $^{238}\text{Np},$ $^{236}\text{Pu},$ $^{238}\text{Pu},$ $^{241}\text{Am},$ ^{242}Cm	Hinkelmann 70 [34]	1970	$0.025 - 10^7$	thermal energy values	-	$\ell=0,1$	$\sigma_\gamma, \sigma_f, \sigma_{2n}, \bar{\nu}$ from exp. and syst.	σ_{2n} from exp. and Pearlstein syst. [13]	exp. + Howerton syst. [23]

Table I: (cont.)

Isotopes	File and/or reference	Latest data revision	Energy range (eV)	Thermal range	Resolved resonance range	Average resonance parameters	Fast neutron energy range	σ_{2n}, σ_{3n}	$\bar{\nu}$
^{241}Pu	E4, Hummel 73 (unpub.)	1974	$10^{-5} - 20 \times 10^6$	pointwise xsect.	BW (60 eV)	$l=0,1$	Fast neutron data based on Prince 70 [35]	syst.	
($^{238}\text{U},$ $^{239}\text{Pu},$ $^{240}\text{Pu},$ ^{241}Pu)	Prince 70 [35]	1970	$10^4 - 15 \times 10^6$	-	-	$l=0,1$	DOM+HFM	syst.	-
$^{236}\text{U},$ $^{237}\text{Np},$ $^{238}\text{Pu},$ $^{240}\text{Pu},$ $^{241}\text{Pu},$ $^{242}\text{Pu},$ $^{241}\text{Am},$ $^{243}\text{Am},$ ^{244}Cm	Pearlstein 66[36]	1966		thermal energy values	BW; RI	-	-	-	-

Table I: (cont.)

Isotopes	File and/or reference	Latest data revision	Energy range (eV)	Thermal range	Resolved resonance range	Average resonance parameters	Fast neutron energy range	σ_{2n}, σ_{3n}	$\bar{\nu}$
^{241}Am	E4, Smith 66 (unpub.)	1966	10^{-5} - 20×10^6	pointwise xsect.	BW (16 eV)	$\ell=0,1$; pointwise σ_f	syst. + exp.		exp. + syst.
^{243}Am	E4, Smith 66 (unpub.)	1966	10^{-5} - 20×10^6	BW	BW(16 eV)	$\ell=0$	syst. + exp.		syst.
^{245}Cm	LLL, Howerton 75 (private comm.)	1974	thermal- 20×10^6	pointwise xsect.	pointwise xsect.	-	SOM+ σ_{CE} correction; exp.+ syst.	syst.	Howerton syst.[23]
^{252}Cf	LLL, Howerton 75 (private comm.)	1974	thermal- 20×10^6	pointwise xsect.	pointwise xsect.	-	SOM; exp + syst.	syst.	Howerton syst.[23]
^{252}Cf	Prince 69 [37]	1969	0.0253- 15×10^6	thermal energy values	RI	-	DOM+HFM		syst.

* List of symbols and abbreviations

E4	:	ENDF/B-IV file
K	:	KEDAK file
LLL	:	Lawrence Livermore Laboratory file
BW(E_{\max})	:	Breit-Wigner resonance parameters (up to energy E_{\max})
RM	:	Reich-Moore multilevel resonance parameters
RI	:	resonance integrals
SOM	:	spherical optical model
DOM	:	deformed optical model
HF	:	Hauser-Feshbach theory
HFM	:	Hauser-Feshbach-Moldauer theory
σ_f (I)	:	fission cross section calculated with one-humped potential
σ_f (II)	:	fission cross section calculated with two-humped potential
exp.	:	experimental data
syst.	:	systematics
xsect.	:	cross section
unpub.	:	unpublished

The Experimental Investigation
of the Alpha Decay of Transactinium Isotopes.

(Status of Alpha Decay Data)

S.A. Baranov, A.G. Zelenkov, V.M. Kulakov
(Moscow, 1975)

Abstract

Current methods and existing experimental facilities to measure the energy spectrum of alpha radiation are described, and a list of recent publication containing compilation on alpha-decay data is given. The review concentrates on the presentation of the current status of alpha decay data of the transactinium isotopes. The values and uncertainties of the absolute energies and the relative intensities of alpha-groups are tabulated. Suggested "best values" of decay half-lives of some of the most often used long-lived transactinium isotopes are listed.

Translated by A. Lorenz
Nuclear Data Section. IAEA

INTRODUCTION

The investigation of alpha decay of transactinium isotopes has been conducted now for more than thirty years. The performance of these investigations has been determined by the following circumstances. Almost all of the isotopes of transactinium elements are alpha-unstable. For this reason the measurement of the alpha spectra gives the possibility to determine the isotopic composition of heavy element samples. On the other hand, the study on the systematics of alpha radioactivity performed in 1950 (Ref. 1), which allows one to predict the alpha decay energy and half-life of previously unknown isotopes, has given the possibility to successfully to identify isotopes obtained in the course of research investigations which were unknown until that time. The investigation of the fine structure of alpha decay from transactinium isotopes has been conducted intensively in the 1950 and 1960s. These investigations have given extensive information on the properties of excited levels of nuclei, which has been extensively used in the development of the unified nuclear model and the theory of alpha-

decay (Refs. 2, 3 and 4). The development of alpha-decay investigations has been closely related to the significant development of the means to produce isotopes of transactinium elements, primarily with the development of high flux research reactors and heavy ions accelerators, as well as the development of research methods. In this connection one should note the development of such instruments as the grid ionization chamber, the magnetic alpha spectrometer with double focusing, and semi-conductor detectors for alpha particles (Ref. 5).

The detail of the measurement of the alpha spectrum, and the accuracy with which the half-life is determined for a given nuclide depends on its properties (e.g. the magnitude of its half-life), the availability of isotopically clean samples, the quantity of a given isotope available for research, and how amenable it is to existing measurement methods. As a rule, the more detailed and accurate measurements are made on long-lived beta-stable isotopes obtained from nuclear reactors. Under these advantageous circumstances the half-life can be determined or measured with an accuracy of better than 1%, and for alpha spectra it is possible to measure up to 20 groups of fine structure for odd nuclei, and up to 10 groups of fine structure for even nuclei with a relative intensity of up to 10^{-5} %.

METHODS USED TO MEASURE THE ENERGY SPECTRUM OF ALPHA

RADIATION.

As indicated above three methods are used for the measurement of energy spectra of alpha radiation: the magnetic alpha spectrometer, and grid ionization chamber, and the semi-conductor detector for radiation (Ref. 5).

The main and most precise method to measure alpha spectra from most radioactive nuclei of transactinium elements is based on the deflection of charged particles in a magnetic field. This method has considerable advantages over other known methods. The photographic emulsions and semi-conductor detectors used to measure the alpha radiation, together with the alpha spectrometer, allows one to reduce the background of the whole instrumentation to approximately $10^{-6} - 5 \times 10^{-7} \alpha/10 \text{ keV}$ (Ref. 6). This type of measurement assembly has a very high resolution (the measured alpha line at half-height is approximately 1.5 - 3.0 keV (Ref. 6/8)). Thus most of the accurate measurements of alpha particle energies from transactinium isotopes have been measured by means of magnetic alpha spectrometers (Ref. 9-14). Some of these instruments are described below.

1. The magnetic alpha sector spectrometer (Berkeley, USA) (Ref. 2). This instrument has the following characteristics; double focusing, a maximum solid angle of $5 \times 10^{-4} / 4\pi$ the radius of the equilibrium orbit $\rho_0 = 35 \text{ cm}$. Also an assembly of semi-conductor detectors, connected to a multi-channel analyser, is distributed in the focal plane of this instrument. The resolution of this spectrometer is approximately 3 keV. This particular instrument was used in most experiments in which the alpha decay of nuclides has been measured.

2. The large magnetic spectrometer with double focusing (Moscow, USSR) (Ref. 10). The double focusing of the alpha particle beam has an angle of $\pi\sqrt{2}$. It has a solid angle of $8 \times 10^{-4}/4\pi$, a dispersion of $2.3 \times 10^{-4} E_0$, which corresponds to a magnitude of 1,35 keV/mm for alpha particles from ^{242}Cm . It weighs 90 t and has a maximum magnetic field of 3000 gauss. The stability of the magnetic field (with regard to the current) is 5×10^{-5} . The maximum clearance between poles is approximately 300 mm. The resolution capability of this alpha spectrometer (i.e. half-width at maximum) for alpha groups of a given isotope is 1.39 keV ($\Delta H\rho/H\rho = 0,01\%$) for a solid angle of approximately $10^{-4}/4\pi$. The large dimensions of this spectrometer ($\rho_0 = 1550$ mm) allows one to measure samples of active materials which weigh approximately 100 micro-grams and allows one to observe groups of alpha particles having half-lives of up to 2×10^{10} years.

3. Magnetic α -spectrometer of the Bureau International des Poids et Mesures (Sèvres, France) (Ref. 14).

The alpha-particle focusing angle is 180° . The solid angle is $4,4 \times 10^{-6}/4\pi$, the dispersion is 11 keV/mm, the weight is 8.5 tonnes, the maximum field is 10 Kgauss, the magnet current stability is $\pm 2 \times 10^{-5}$, the clearance between the magnet's poles is 70 mm, and the α -particle energy measurement range is 2300 to 10700 keV. The instrument was specially built to measure absolute α -particle energies.

Regardless of the apparent preference which is attributed to magnetic spectrometers for the investigation of the fine structure of α -decay, they are not always usable for this purpose because of the low alpha intensity. Because the solid angle in the case of double focusing is in the vicinity of 10^{-5} to $10^{-3}/4\pi$, in the cases where the quantity of the isotope being investigated (or its relative abundance in the sample) is too small to perform a spectral analysis, methods which have a stronger beam intensity must be used.

In the 1940's and 1950's, pulsed grid ionization chambers were widely used for alpha spectrum analyses (Ref. 5). In these detectors it is possible to use samples having a large surface area, and the solid angle of the apparatus is close to 2π ; but in the best of these instruments, a half-width of 15-50 keV (0.3 - 0.7 %) cannot be exceeded.

In the last ten years, semiconductor detectors have been extensively used for the measurement of alpha spectra (Refs. 5, 15). The solid angle for these detectors is also close to 2π , and the alpha half-width at maximum, as determined by the instrument, can be 11 - 15 keV ($\sim 0.25\%$).

Semiconductor detectors have a number of advantages over the pulsed grid ionization chambers; a better energy resolution capability, a lower background wise level, a faster response time, and higher stability.

It must be noted however, that the thickness and quality of the alpha-emitting sample is decisive in getting the best possible energy resolution in alpha spectrum measurements. The best results are obtained with samples obtained by the evaporation of the material in vacuum, or by the method of forward recoil desposition. The thickness of the sample should not exceed a few microgrammes per square centimeter.

For the accurate energy determination, and for the evaluation of the intensity of alpha-groups, it is sometimes useful to use the gamma or conversion electron spectra which accompany alpha decay, or the alpha-gamma coincidence technique.

Let us briefly consider the measurement of half-lives. Values which lie within the range from a few seconds to a few years can be measured directly from the gradual activity decrease, as registered by the detector. Shorter half-lives are measured by using the electronic technique of delayed coincidence, whereby two consecutive events are registered by the equipment.

In the case of long-lived isotopes the half-life is determined normally from the specific activity of the sample. The exact amount of the isotope under investigation is determined by gravimetry, coulomb (-metry) or isotope solution, and the decay rate is then measured by radiometric or calorimetric techniques. For the results to be reliable, a minimum degree of chemical and radiation contamination of the sample must be ascertained. Half-life measurements of long-lived isotopes can also be performed by the quantitative determination of the build-up of daughter decay-products, or by the comparison of the isotope sample with the spectrum of its radiation.

REVIEWS AND COMPILATIONS CONTAINING EXPERIMENTAL ALPHA- DECAY DATA.

A large number of alpha-decay reviews and compilations as well as tabulations of radioactive properties and decay schemes containing experimental alpha-decay data have been published in the course of the last thirty years. Inasmuch as the more recent publications usually include previously published data, it is justifiable to limit this review to the published compilations of the last few years.

1. B.S. Dzhelepov, L.K. Peker, and V.O. Sergeev. Decay Schemes of Radioactive Nuclei $A \geq 100$, Ak. Nauk USSR, 1963.

This compilation contains experimental data on the radioactive properties of heavy elements which were published and known to the authors prior to 1962. This compilation contains decay schemes, which, in addition to experimental values and quantized level characteristics, also include quantities predicted by the authors.

2. E.K. Hyde, I. Perlman, G.T. Seaborg. The Nuclear Properties of the Heavy Elements, Prentice-Hall, Inc., Englewood Cliffs N.Y. (1964).

This is a most complete survey of the methods of productions and nuclear properties of heavy elements. This work includes a detailed critical analysis of experimental results known at the time of writing. Decay schemes of heavy nuclei are shown, and the publication has an ample bibliography of research experiments.

3. C.M. Lederer, J.M. Hollander and I. Perlman. Table of Isotopes, Sixth Ed., John Wiley, New York (1967).

This tabulation contains detailed information on the radioactive properties of nuclei, which have been published before March 1966. The basic methods of production and the identification of radioactive isotopes are included. This publication includes nuclear decay schemes, the results of a large number of experiments and a broad bibliographic reference. A new edition of this publication is in preparation.

4. Yu. S. Zamiatin. Radioactive Decay and Level Schemes of Heavy Elements ($Z \geq 90$). Compilation published in "Nuclear Constants", Vol. 14, Atomizdat 1974.

This work contains new data on radioactive decay of transactinium isotopes, published before 1972. Experimental data on the fine structure of radiation spectra, decay schemes and level schemes with an indication of level characteristics and life times are given in the appendix. The bibliography lists 716 authors. In contrast to other tabulations, experimental values of alpha decay energies are normalized to the $E_{\alpha 0}$ values of 5304.6 ± 0.6 keV for ^{210}Po , 6112.9 ± 0.25 keV for ^{242}Cm , and 6632.73 ± 0.9 keV for ^{253}Es .

5. A. Rytz. Catalogue of recommended alpha Energy and Intensity Values. Atomic Data and Nuclear Data Tables 12, 479-498 (1973).

This tabulation contains experimental data on the most intensive alpha-decay groups ($\geq 5\%$). The uncertainties of measured fine structure energy groups, included in the table, do not exceed 5 keV. The tabulation contains the energy and intensity values of 339 alpha-groups of 161 alpha-active isotopes, which have been published before March 1973. The experimental values of alpha energies are normalized to common standards. The work proposes the use of recommended energy and relative intensities of alpha-particle groups, and includes an evaluation of probable uncertainties of the recommended values.

6. R. Vaninbroux. The Half-Lives of Some Long-lived Actinides: A Compilation. EUR-5194-e, CERN, 1974.

The work contains the results of half-life measurements of fourteen long-lived widely-used transactinium isotopes. The compilation includes the characteristics of the samples and of the measurement methods. "Best Values" of measured half-lives are given as well as their probable uncertainties.

STATUS OF ALPHA DECAY DATA

An overwhelming number of experimental values of alpha-groups, listed in the compilations described above, is the result of relative energy measurements, whereby those measured in the 1950's and 1960's were normalized to non-standard energy values of a few alpha-emitters. It is evident in this connection, that a number of standard values, which would cover the energy range of the alpha groups, are of absolute necessity in order to calibrate alpha spectrometers so as to be able to determine absolute energy values.

As a result of the recommendation of the Nuclear Physics Congress (Paris, 1964), the Bureau International des Poids et Mesures (BIPM

Table I

Absolute values of alpha-group energies

Isotopes	Alpha-groups *	E_{α} , keV (absolute)
^{227}Th	α_0	6038.21 ± 0.15
	α_{61}	5977.92 ± 0.10
	α_{286}	5757.06 ± 0.15
^{228}Th	α_0	5423.33 ± 0.22
	α_{43}	5340.54 ± 0.15
^{232}U	α_0	5320.3 ± 0.14
	α_{58}	5263.54 ± 0.09
^{238}Pu	α_0	5499.21 ± 0.20
	α_{44}	5456.5 ± 0.4
^{240}Pu	α_0	5168.30 ± 0.15
	α_{45}	5123.43 ± 0.23
^{241}Am	α_{60}	5485.74 ± 0.12
	α_{103}	5442.98 ± 0.13
^{242}Cm	α_0	6112.918 ± 0.082
	α_{44}	6069.63 ± 0.12
^{244}Cm	α_0	5804.958 ± 0.050
	α_{43}	5762.835 ± 0.030
^{253}Es	α_0	6632.73 ± 0.050

* Note: the subscripts correspond to the energy (in KeV) of the level of the daughter nucleus.

at Sévres, France) established a programme in 1966 with the specific objective to measure the absolute values of alpha-particle energies emitted by alpha-active isotopes, including isotopes of the trans-actinium elements. The alpha spectrometer at BIPM (Ref. 14) was built in order to perform these absolute measurements.

Since 1969, the research group under the leadership of Dr. Rytz has measured the energies of the intensive groups of more than 20 nuclides (Refs. 16-18), including 18 groups of 9 transactinium isotopes (see table I). This table lists the alpha particle groups, the values of their energies and the magnitude of the uncertainty in the determination of the energy. The statistical uncertainties (standard deviation) of these measurements, according to the author's estimate, range between 30 and 400 eV; the systematic errors in most cases do not exceed 100 eV. The major source of error, according to the authors, is in the unsatisfactory quality of the emitters.

Between 1967 and 1971, the group under the direction of S.A. Baranov, has undertaken the relative measurement of the energies of the most intensive alpha-groups among 29 long-lived transactinium isotopes. All of these measurements were performed with the same method using the same instrumentation and equipment. The energy values of the basic alpha-groups of ^{240}Pu and ^{242}Cm were used as standards. Table II lists the results of these measurements (Refs. 19-21), and takes into account the latest absolute alpha-group energy measurements of the ^{240}Pu , and $E_{\alpha 0} = 6112.9 \text{ keV}$ for ^{242}Cm reported in references 16 and 17. This tabulation also lists the values of the relative intensities of the alpha-groups. The uncertainty in the measurement of the energy ranges between 0.6 and 1.8 keV, and depends on the sample quality of the emitter, the nature of the spectrum, the difference between the measured energy and the standard reference energy, as well as on the accuracy of the energy calibration of the spectrometer. The last column lists the difference between the energy values obtained by the two groups of investigators (see Table I). With the exception of the data for ^{228}Th , where the difference in $E_{\alpha 0}$ is 2.7 keV, Table II shows that the discrepancies lie, as a rule, within the range of experimental error.

In 1973, A. Rytz (Ref. 22) published a compilation of data on fine structure energies and intensities of the most intensive alpha-groups ($\geq 5\%$), for which the energy is measured to an accuracy not exceeding 5 keV. This table contains data on 68 alpha-emitting transactinium isotopes, and includes corrections to the measured energy values due to the latest absolute measurements of the energies of the standards. This compilation also gives recommended values for alpha-groups and probable experimental errors (standard deviations). An examination of this table shows that for the intensive groups of approximately 40 transactinium isotopes, the uncertainty of the measured energy does not exceed $\sim 2 \text{ keV}$.

Table II also lists the recommended values of the relative intensities (I_{α}) of the most intensive groups. Probable experimental errors (standard deviation) are given for some of the nuclides. An examination of available experimental data on fine structure group intensities (Refs. 23, 24) show that for 10 of the most widely investigated nuclides (^{230}U , $^{240,241}\text{Pu}$, $^{242-244}\text{Cm}$, $^{246,252}\text{Cf}$, ^{243}Am , ^{254}Es) the difference between the results on the most intensive groups, arrived at by various authors, lie within 1% of each other; and that for 13 nuclides ($^{228,230}\text{Th}$, $^{232,233,234,236}\text{U}$, ^{238}Pu , ^{241}Am , $^{240,246}\text{Cm}$, ^{249}Bk , ^{249}Cf , ^{256}Es) the differences lie with 1 to 2%.

Table II

Energy and Relative Intensity of Alpha-Groups

Element	Mass Number	Alpha-group	E_{α} (KeV)	Standard	Relative intensity * I_{α} , %	Difference in E_{α} between Table I and Table II (KeV)
Th	228	α_0	5420,6 \pm 1,0	^{240}Pu	72,4 \pm 1,0	-2,7
		α_{83}	5339,2 \pm 1,0		26,6 \pm 0,5	-1,3
	229	α_{101}	4978,5 \pm 1,2	^{240}Pu	3,17 \pm 0,04	
		α_{112}	4967,5 \pm 1,2		5,97 \pm 0,06	
		α_{180}	4901,0 \pm 1,2		10,20 \pm 0,08	
		α_{236}	4845,3 \pm 1,2		56,2 \pm 0,2	
		α_{268}	4814,6 \pm 1,2		9,30 \pm 0,08	
Pa	231	α_0	5058,1 \pm 1,0	^{240}Pu	11,7 \pm 0,1	
		α_{46}	5013,3 \pm 1,0		25,3 \pm 0,2	
		α_{73}	4986,4 \pm 1,0		1,60 \pm 0,05	
		α_{109}	4950,9 \pm 1,0		22,5 \pm 0,2	
		α_{327}	4736,1 \pm 1,0		8,35 \pm 0,08	
U	232	α_0	5320,8 \pm 1,0	^{240}Pu	68,6 \pm 0,8	+0,5
		α_{58}	5263,9 \pm 1,0		31,2 \pm 0,4	+0,4
	233	α_0	4824,2 \pm 1,2	^{240}Pu	84,4 \pm 0,5	
		α_{42}	4783,5 \pm 1,2		13,2 \pm 0,2	
Np	237	α_{86}	4788,1 \pm 1,5	^{240}Pu	51,3 \pm 0,8	
		α_{104}	4771,1 \pm 1,5		19,4 \pm 0,4	
		α_{109}	4766,1 \pm 1,5		16,8 \pm 0,4	

* The values of relative intensities of alpha-groups and their statistical errors were calculated on the basis of experimental results received by the authors. This table contains more information in comparison to that published in References 19-21.

I	2	3	4	5	6	7
Pu	236	α_0	5770,1 \pm 1,0	^{242}Cm	67,3 \pm 0,6	
		α_{49}	5721,9 \pm 1,0		32,7 \pm 0,4	
	238	α_0	5499,5 \pm 1,0	^{240}Pu	72,13 \pm 0,06	+0,3
		α_{44}	5456,0 \pm 1,0		27,87 \pm 0,03	-0,5
	239	$\alpha_{0+0,03}$	5156,2 \pm 0,8	^{240}Pu	73,3 \pm 0,7	
		α_{13}	5143,9 \pm 0,8		15,1 \pm 0,2	
		α_{52}	5106,1 \pm 0,8		11,5 \pm 0,2	
	240	α_0	-		73,4 \pm 0,8	
		α_{45}	-		26,5 \pm 0,4	
	241	α_{158}	4896,5 \pm 1,2	^{240}Pu	83,3 \pm 0,8	
		α_{202}	4853,5 \pm 1,2		12,3 \pm 0,3	
	242	α_0	4900,6 \pm 1,2	^{240}Pu	79,7 \pm 2,7	
		α_{45}	4856,3 \pm 1,2		20,2 \pm 1,1	
Am	241	α_{60}	5484,9 \pm 1,0	^{240}Pu	85,8 \pm 0,7	- 0,8
		α_{103}	5442,4 \pm 1,0		12,83 \pm 0,08	- 0,6
	243	α_{75}	5275,4 \pm 1,0	^{240}Pu	87,8 \pm 0,5	
		α_{118}	5233,5 \pm 1,0		10,73 \pm 0,01	

I	2	3	4	5	6	7
Cm	240	α_0	6290, $1 \pm 0,6$	^{242}Cm	71, $1 \pm 0,6$	
		α_{43}	6247, $3 \pm 0,6$		28, $9 \pm 0,3$	
	241	α_{145}	5938, $6 \pm 0,6$	^{242}Cm	71, $6 \pm 0,5$	
		α_{157}	5926, $0 \pm 0,6$		16, $3 \pm 0,2$	
		α_{200}	5884, $3 \pm 0,6$		11, $5 \pm 0,2$	
	242	α_0	-		74, $1 \pm 1,1$	
		α_{44}	-		25, $9 \pm 0,5$	
	243	α_{76}	5992, $2 \pm 1,0$	^{240}Pu	6, $5 \pm 0,2$	
		α_{286}	5785, $1 \pm 1,0$		73, $5 \pm 1,0$	
		α_{330}	5742, $2 \pm 1,0$		10, $6 \pm 0,3$	
	244	α_0	5805, $2 \pm 1,0$	^{240}Pu	76, $4 \pm 0,6$	+0,2
		α_{43}	5763, $3 \pm 1,0$		23, $6 \pm 0,2$	+0,5
	245	α_{170}	5362, $0 \pm 0,7$	^{244}Cm	93, $2 \pm 0,5$	
		α_{227}	5303, $8 \pm 1,0$		5, $0 \pm 0,1$	
Br	249	α_0	5437, $3 \pm 1,0$	^{242}Cm	5, $9 \pm 0,1$	
		α_{21}	5416, $8 \pm 1,0$		74, $9 \pm 0,5$	
		α_{48}	5389, $9 \pm 1,0$		17, $9 \pm 0,2$	
cf	249	α_0	6194, $0 \pm 0,7$	^{242}Cm	2, $15 \pm 0,07$	
		α_{55}	6139, $5 \pm 0,7$		1, $09 \pm 0,05$	

I	2	3	4	5	6	7
Cf	249	α_{252}	5946,2 \pm 1,0		3,93 \pm 0,09	
		α_{296}	5903,4 \pm 1,0		2,84 \pm 0,08	
		α_{350}	5849,5 \pm 1,0		1,03 \pm 0,05	
		α_{387}	5813,5 \pm 1,0		84,1 \pm 0,6	
		α_{441}	5759,7 \pm 1,0		4,02 \pm 0,09	
	250	α_0	6030,8 \pm 0,6	^{242}Cm	84,6 \pm 1,2	
		α_{42}	5989,1 \pm 0,6		15,1 \pm 0,4	
	251	α_{407}	5680,3 \pm 1,0	^{242}Cm	-	
	252	α_0	6118,3 \pm 0,5	^{242}Cm	84,1 \pm 0,4	
		α_{43}	6075,7 \pm 0,5		15,8 \pm 0,1	
Es	253	α_0	6631,3 \pm 1,5	^{242}Cm	90,5 \pm 0,7	-1,4
	254	α_{36}	6428,8 \pm 1,5	^{242}Cm	92,7 \pm 1,0	
	255	-	6299,5 \pm 1,5	^{242}Cm	-	
Fm	255	α_{107}	7015,8 \pm 1,8	^{242}Cm	92,9 \pm 1,4	

The differences between the measured values of I_α for alpha-groups having an intensity between 10 and 30 %, for those isotopes listed above, range from 2 to 8 %. For groups of lower intensities the differences are considerably larger. It must be noted that for some long-lived isotopes, characterized by a complex spectrum (^{235}U , ^{237}Np and ^{245}Cm), the difference between the measured values of the more intensive groups is very large (they are respectively 16, 18 and 13 %).

Table III lists "best values" of decay half-lives of some of the most often used long-lived transactinium isotopes, taken from the compilation of Vaninbroukx (Ref. 25), with the exception of the data for ^{239}Pu and ^{241}Pu . The probable errors of the listed values are also given in the Table. These have been obtained as a result of a critical analysis of results obtained during the last few years. In the case of a small number of high quality measurements, the uncertainty is evaluated at three standard deviations. The authors of this review have found it justifiable to replace the half-life values for ^{239}Pu and ^{241}Pu , because of the completion of some high quality measurements of these quantities since the publication of Vaninbroukx's paper (see footnotes to Table III). The analysis of the results of these last measurements has led to a substantial change of the recommended half-life value for ^{239}Pu and ^{241}Pu (by 0.8 and 1.4 % respectively), and allows for a notable reduction in

Table III

Suggested Values of Decay Half-Lives (Ref. 25)

Nuclide	Decay Half-life (years)
I	2
^{232}U	72 ± 2
^{233}U	$(1,592 \pm 0,003) \cdot 10^5$
^{234}U	$(2,446 \pm 0,007) \cdot 10^5$
^{235}U	$(7,038 \pm 0,020) \cdot 10^8$
^{236}U	$(2,34 \pm 0,02) \cdot 10^7$
^{238}U	$(4,468 \pm 0,010) \cdot 10^9$
^{238}Pu	$87,8 \pm 0,8$
^{239}Pu	$(2,41 \pm 0,01) \cdot 10^4$ *)
^{240}Pu	$(655 \pm 0,07) \cdot 10^3$
^{241}Pu	$14,7 \pm 0,4$ **)
^{242}Pu	$(3,87 \pm 0,05) \cdot 10^5$
^{244}Pu	$(8,2 \pm 0,1) \cdot 10^7$
^{241}Am	432 ± 4
^{252}Cf	$2,64 \pm 0,02$

* Derived on the basis of recent experimental values

F.L.Oetting, "Plutonium 1970 and other Actinides" *Proc. of the Symposium on Plutonium and other Actinides, Santa Fe, New Mexico, pp.154-162, 1970*) $T_{1/2} = 24065 \pm 50$ years; Reference 28: $T_{1/2} = 24060 \pm 38$ years; private communication from K.M. Glover: $T_{1/2} = 24115 \pm 80$ years; and preliminary results of Vaninbrouckx.

** Obtained on the basis of results of seven measurements performed since 1970, listed in report AERE-R-7906 (1974) by Wilkins, and of a private communication from K.M. Glover (1975).

the half-life error of ^{239}Pu (up to 0.4 %). Unfortunately, the probable error in the half-life of ^{241}Pu remains very large as before in view of the considerable discrepancies between the results of the recent measurements, which claim a high accuracy (ranging from 14.355 ± 0.007 to 15.02 ± 0.1 years).

An examination of Table III shows that the decay half-lives for ^{233}U , ^{234}U , ^{235}U , ^{238}U and ^{239}Pu are measured to an accuracy of 0.2 to 0.3 %. The measurement errors for the decay half-lives of ^{236}U , the other long-lived isotopes of Pu, ^{241}Am and ^{252}Cf , amount to ~ 1 %. This is due to a considerable difference of values, obtained by different authors, performed in different years using different techniques (e.g. radiometric and calorimetric) (Refs. 26, 27, 28). The considerable discrepancies between these values have a considerable effect on the uncertainties quoted by the authors.

An examination of the experimental values of the decay half-lives (Refs. 24 and 25) shows that the indicated situation is typical for most long-lived transactinium isotopes (i.e. the discrepancy between experimental half-life values for ^{230}Th is 9 %, for ^{232}Th 4 %, for ^{231}Pa 7 %, for ^{243}Am 7 %, for ^{243}Cm 10 %, for ^{245}Cm 12 %, and for ^{246}Cm 15 %). The discrepancies of the values for ^{228}Th , ^{237}Np , ^{242}Cm , ^{244}Cm and $^{249-251}\text{Cf}$ lie between 1 % and 3 %. The accuracy of decay half-lives of some nuclides measured by only one or two experimental groups are difficult to judge. The evaluation of the relative alpha-decay probability, for long-lived beta-unstable nuclei (e.g. ^{241}Pu , $^{242\text{m}}\text{Am}$ and ^{249}Bk) is also very difficult.

The existing situation of the status of decay half-life data cannot be considered satisfactory. As an example, according to Prof. Aten (see Review Paper A9) the half-life accuracy required to perform a quantitative analysis using alpha-decay activity is 0.01 %, an accuracy which is not available to-day. According to Dierckx (Review Paper A8) the determination of nuclear fuel composition and dosimetry considerations require a knowledge of the decay half-life of ^{238}Pu , ^{239}Pu , ^{240}Pu isotopes to an accuracy not exceeding 0.5 %, and that of ^{242}Pu to be less than 2 %. The accuracy of the decay half-life of ^{244}Cm must be better than 0.5 %, and for ^{242}Cm better than 0.1 %. Certainly the first task at hand is to eliminate the existing experimental half-life discrepancies for the ^{243}Cm , ^{245}Cm , ^{246}Cm and ^{243}Am isotopes. Vaninbroukx and Glover have indicated that their groups will perform new measurements of decay half-lives relative to ^{238}Pu , ^{239}Pu and ^{241}Pu , in the near future.

It is also necessary to systematically compile experimental decay half-life values and alpha-decay branching ratios, of at least all long-lived transactinium isotopes, and to perform a critical analysis of these results, obtained by different techniques and on different samples. Such an evaluation should certainly indicate those isotopes for which additional measurements must be performed. A list of such isotopes would most certainly include ^{243}Am as well as all long-lived Cm isotopes.

According to communication from A. Rytz, his group plans to conduct supplementary absolute measurements of alpha-group energies using the reconstructed instrument with the objective to eliminate the discrepancies between his and the data obtained by the group at the Technical University in Munich (Ref. 30). He proposes also to complete and update his own list of recommended energy values

and alpha radiation intensities. In this connection it will be necessary to perform a more detailed critical analysis of experimental data on relative intensities of fine structure alpha-decay groups and to perform additional measurements of alpha decay spectra on those nuclide in which there exist a significant discrepancy in existing experimental data (e.g. ^{235}U , ^{237}Np and ^{245}Cm).

To conclude, the authors would like to acknowledge Drs. Rytz, Vaninbroukx, Oetting, Dierckx, Aten and the group of K.M. Glover, who have sent us their contributions and informed us of their planned experiments.

REFERENCES

1. Perlman I., Ghiorso A., Seaborg G.T., Phys. Rev., 77, 26 (1950)
2. Perlman I., Rasmussen I., Handbuch der Physik, Band XLII (1957)
3. Bohr A., Fröman P.O., Mottelson B.R., Den. Mat. -fys. Medd., 29, No. 10 (1955)
4. Ellis Y.A., Schmorak M.R., Nuclear Data Sheets, B8-345 (1972)
5. Alpha-, beta and gamma- ray spectroscopy (ed. K. Siegban), North-Holland Publishing Company, Amsterdam, 1965.
6. Baranov S.A., Rodionov Yu.F., Kulakov V.M., Shatinskij V.M., Yadernaja Fizika, 4, 1108 (1966).
7. Baranov S.A., Kulakov V.M., Shatinskij V.M., Yadernaja Fizika, 7, 727, (1968).
8. Perlman I., Asaro F., Proc. of the Pehovoth Conference on Nuclear Structure (ed.H.I. Lipkin), Sess II., 100 (1958).
9. Walen R.J. Nucl. Instrum. and Methods, 1, 242, (1957).
10. Baranov S.A., Zelenkov A.G., Shtchepkin G. Ya., Beruchko V.V., Malov A.F., Izvestia Ak. Nauk, USSR, Seria Fizika 23, 1402 (1959).
11. Gol'din L.L., Tpetjakof E.F., Novikova G.I., Izvestia Akad. Nauk, USSR, Seria Fizika 20, 859 (1956).
12. Judd D.L., Bludman S.A., Nucl. Instrum. and Methods, 1, 46 (1957).
13. Dzhelepov B.S., Ivanov R.B., Hedovesov V.G., Tehulin V.G., Izvestia Akademii Nauk USSR, Seria Fizika 23, 782 (1959).
14. Rytz A., Grennberg B., Report on the progress of the construction of an absolute alpha spectrometer at the BIPM, France (Sevres), 1967.
15. Baranov S.A., Kulakov V.M., Experimental Methods and Techniques, 4, 5 (1969).
16. Grennberg B. and Rytz A., Metrologia, Vol. 7, No. 2, 65 (1971).

17. Gorman D.I., Rytz A., Michel H.V., C.R. Acad. Sc. Paris, 275 (1972).
18. Rytz A., Nucl. Instrum. and Methods., 112, 261 (1973).
19. Baranov S.A., Kulakov V.M., Shatinskij V.M., Yadernaja Fizika 7, 727 (1968).
20. Baranov S.A., Shatinskij V.M., Kulakov V.M., Yadernaja Fizika 10, 1110 (1969).
21. Baranov S.A., Shatinskij V.M., Kulakov V.M., Yadernaja Fizika 14, 1101 (1971).
22. Rytz A. Atomic Data and Nuclear Data Tables 12, No. 5, 479 (1973).
23. Lederer C.M., Hollander I.M., Perlman I., Table of Isotopes, Sixth Edition, John Wiley and sons, inc., New York-London-Sydney, 1967.
24. Zam'atun Yu.S., Radioactive Decay and Level Schemes of Heavy Elements ($Z \geq 90$). "Nuclear Constants", Vol. 14 Atomizdat, 1974.
25. Vaninbroukx R. The Half-Lives of Some Long-Lived Actinides: A. Compilation. EUR-5194-e, CBNM, 1974.
26. Hanna G.C. et al. Atomic Energy Rev. 7, 3 (1969).
27. Oetting F.L. Proc. of the Symposium on Thermodynamics of Nuclear Materials - IAEA, September 1967, Vienna, Austria pp 55-66, 1968.
28. Alexandrov B.M., et al, Izvestia Akademii Nauk, Seria Fizika 39, 482 (1975).
29. Kerrigan W.J. and Dorsett R.S., J. Inorg. Nucl. Chem. 34, 3603 (1972).
30. Huenges et al, Nucl. Inst. and Methods, 121, 307 (1974).

STATUS OF BETA- AND GAMMA-DECAY AND SPONTANEOUS-
FISSION DATA FROM TRANSACTINIUM ISOTOPE[†]

C. W. Reich

Idaho National Engineering Laboratory
Aerojet Nuclear Co.
Idaho Falls, Idaho U.S.A.

Abstract

Several categories of β - and γ -related decay data for the transactinium isotopes are assessed in the light of their potential use in applied areas. The status as of August, 1975, of these data is summarized for 142 transactinium nuclides with $228 \leq A \leq 257$ by the listing of experimental values and errors where known. Several useful compilations of transactinium-isotope decay data are discussed. Recent developments related to the yields and energy distributions of prompt and delayed neutrons from spontaneous fission are briefly treated. Comments and observations about the interrelation of the important nuclear-data activities of measurement, compilation and evaluation and needs assessment are given. The applications-oriented file of decay data prepared at our laboratory for ENDF/B is discussed. Finally, a summary by G. Rudstam of the status of the OSIRIS work on delayed-neutron energy spectra of individual precursors is included.

1. INTRODUCTION

In this paper, we review and summarize the current status of a broad range of categories of decay data for the transactinium nuclides ($Z \geq 90$). The selection of the specific types of decay data which are treated here was based on a consideration of their general importance for various applications of decay data. For each individual nuclide, measured values (and, where reported, their uncertainties) of these chosen decay parameters are listed. This compilation of measured values provides a convenient means of assessing the adequacy of the present data for use in specific applications. It should be emphasized that these values do not constitute a set of evaluated or "recommended" values.

[†] Work performed under the auspices of the U.S. Energy Research and Development Administration.

The inclusion of decay data in the subject matter of this meeting, the first one of international scope on the subject of transactinium-isotope nuclear data, provides another illustration of the increasing recognition of the importance of radioactive-nuclide decay data as one category of "Nuclear Data." While data from radioactive-decay studies have contributed much to the basic concepts of nuclear physics, their relevance to a number of applied problems is now becoming more widely appreciated. For example, decay data for fission products constituted a major topic for discussion at the IAEA Panel Meeting on Fission-Product Nuclear Data [1]. Also, the scope of the Evaluated Nuclear Data File (ENDF/B) has now been expanded to incorporate such data, partly in response to their obvious importance for the assessment of certain safety questions in nuclear reactors. The recently released Version IV is the first version of ENDF/B to contain a detailed set of decay data [2]. With the increasing interest in assessing the impact of radioactivity on the environment, attention is being focused not only on the monitoring of radioactive effluents associated with the operation of nuclear power plants but also on all aspects of the nuclear fuel cycle, including the management of the waste products and the safeguarding of the reprocessed fuel material. Among the components of such an assessment are the identification of the important radioactive nuclides and the establishment of a commonly accepted and utilized base of relevant, evaluated decay data. In some cases, this evaluation may point out the need for a vigorous program of experimental measurements to provide such data where they are either nonexistent or not of the required accuracy. Through its subject matter and organization, the present meeting represents, for the transactinium nuclides, one step toward the effective use of nuclear decay data in the solution of important problems of both an applied and a basic character.

1.1. Applications

To provide a framework for the discussion of the decay data to be treated, it is appropriate to point out some of the applications of such data. Since detailed discussions of the applications of these data appear in a number of papers presented at this meeting, we give here only a brief listing. In reactor-related applications, decay data are needed for the proper assessment of the impact of radioactivity on the environment from all components of the fuel cycle, from the mine through the reprocessing plant, and including the accounting for and safeguarding of the fissionable material. Important operational problems include not only monitoring of the effluents from the nuclear-power plants, but

also the storage and handling of the spent fuel. In long-term operation of fast reactors, there is a considerable build-up of transactinium isotopes, leading to the accumulation of a sizeable inventory of nuclides for which spontaneous fission is a significant decay mode; and the evaluation of the neutron source term in such systems following shutdown is an important problem.

Biomedical applications represent another area where decay data have an important impact. In calculations of the absorbed dose, for example, it is necessary to know not only the energy release in radioactive decay, but also the form in which this energy is emitted (e.g., conversion electrons, x-rays, β and γ radiation and α particles). To do this realistically requires a quite detailed knowledge of the decay scheme. In the quantitative assay of radioactivity to determine the amount of a given radioactive nuclide present, a knowledge of the nuclide half-life and the energies and absolute intensities of the radiations being measured in the analysis is necessary. Because of the widespread use of γ -ray spectroscopy employing Ge(Li) spectrometers to do such assays, the γ -ray absolute intensities represent a particularly important subset of decay data.

1.2. Special features of transactinium-nuclide decay data

Experimentally, the study of the decay properties of the transactinium nuclides is in many ways little different from that of any other class of nuclei. However, the decay of the transactinium nuclei exhibits a much richer variety of phenomena than is the case for the nuclides commonly encountered in the region below (and slightly above) the $Z=82$ magic number. For example, in addition to β^- and electron-capture (and β^+) decay, α -particle emission and spontaneous fission--with prompt and delayed neutron emission--occur. Furthermore, these nuclides frequently decay via two or three different, competing processes. The relative probabilities (branching ratios) of these decay modes are important.

Finally, internal conversion and its associated phenomena assume an important role in transactinium-nuclide decay data because of the large internal-conversion coefficients that result from the large Z -values and the generally lower energies of the γ -ray transitions. Consequently, the discrete electrons and the x-rays contain a significant fraction of the energy associated with the γ -decay process. Knowledge

of the conversion-electron spectrum may be important in its own right or for the determination of absolute γ -ray intensities for some applications.

Taken together, this increased variety of modes of decay provides the measurer with valuable additional information for gaining insight into the make-up of these nuclides, but it greatly complicates the problems of data compilation and evaluation, particularly when data for various applications are desired.

1.3. The role of theory in transactinium-nuclide decay data

1.3.1. Nuclear models for strongly deformed nuclei

The transactinium nuclides are all included in the general category of "strongly deformed" nuclei, in that their equilibrium shapes are characterized by relatively large axially symmetric deformations. Because of this, the coupling scheme which describes their elementary modes of motion assume a basic simplicity (see, e.g., [3]). For example, their energy-level schemes exhibit a number of striking features such as the existence of a well-developed rotational-band structure. The spins (and parities) of these observed rotational states can frequently be deduced from energy-spacing considerations alone. From such considerations and data on the within-band γ -ray intensities, one can extract multipolarity information concerning these transitions. Furthermore, the ordering and properties of the "single-particle" states in the strongly deformed nuclei can be calculated fairly simply [4], and such calculations are found to give a good description of many of the properties of these states, particularly of those that lie at fairly low ($\lesssim 0.5$ MeV) excitation energies. For these deformed nuclei, nuclear physicists with experience in nuclear-structure studies can frequently use these various calculational tools and arguments based on "systematics" to make accurate state assignments and transition-probability estimates on the basis of rather fragmentary data. (These ideas and their application to the level structure of the strongly-deformed odd-A nuclei in the rare-earth region have been treated in detail elsewhere, e.g., in [5].) In the strongly-deformed doubly-odd nuclei, the coupling of the two odd nucleons, each in a definite "single-particle" state, gives rise to two non-rotational states. In one of these the two intrinsic spins are parallel and in one they are antiparallel, the former lying lower in energy (the so-called Gallagher-Moszkowski rule [6]). The ordering of isomer pairs in doubly-odd deformed

nuclei appears to be quite well accounted for by this rule and it has been used to assign the relative positions of the two isomers observed in ^{236}Np and in ^{250}Es .

1.3.2. X-ray and discrete-electron spectra

The internal-conversion process is well understood theoretically, and the internal-conversion coefficients (ICC) can be calculated [7] with high accuracy. (For some multipolarities, small systematic differences between theory and experiment exist, but even here, these known differences can themselves be employed to provide reliable ICC values.) Consequently, the conversion-electron spectrum associated with a given γ ray can be accurately calculated from the γ -ray energy and multipolarity (the latter either measured or deduced as described in subsection 1.3.1 above).

The energies and relative intensities of the prominent components of the K x-ray spectrum produced in radioactive decay of a given nuclide can be predicted with sufficient accuracy to be useful for many applications, provided that the decay scheme is known. Recent relative K x-ray intensity data in the region $96 \leq Z \leq 99$ [8] and $81 \leq Z \leq 96$ [9] give generally good agreement with calculations for the stronger lines although they do indicate some disagreement ($\sim 7\%$ at $Z=96$) in the $K\beta/K\alpha$ intensity ratio. While the energies of the L x-ray series can be accurately obtained from the binding-energy data of Bearden and Burr [10], the relative intensities of the L lines cannot presently be accurately calculated. Nonetheless, estimates of the L x-ray intensity which are generally adequate for many applications (e.g., energy-release and dose-estimate calculations) can be made [11]. Similarly, realistic calculations of the Auger electron spectrum cannot be made but estimates adequate for many applications can be generated [11].

1.4 Topics to be discussed in this paper

In the remaining chapters of this review, we present the current status of selected categories of decay data for the transactinium nuclides. In Chapter 2, we discuss several important existing compilations (and some currently in preparation) of transactinium-nuclide decay data. Chapter 3, the main thrust of this paper, contains a discussion of the reasons for the selection of the data to be listed and a tabular summary of the decay data themselves. Chapter 4 contains a brief discussion of the yields and energy distributions of prompt and delayed neutrons from spontaneous fission. Chapter 5 presents some general observations con-

cerning the use of decay data in applied areas and the improving of conditions under which relevant data with the required accuracy can be identified and supplied in a timely manner.

In Appendix A, the data content and layout of the decay data for Version V of ENDF/B is discussed within the context of the ENDF/B Actinide File. Finally, a summary of delayed-neutron spectral measurements by Rudstam and co-workers at the OSIRIS Facility at Studsvik, Sweden is given in Appendix B.

2. REMARKS ON DECAY-DATA COMPILATIONS FOR THE TRANSACTINIUM NUCLIDES

While several compilations of decay data oriented specifically toward the fission-product nuclides exist (e.g., [12], [13], and the relevant portions of the ENDF/B-IV Fission-Product File), no equivalent such compilations presently exist solely oriented toward users of transactinium-nuclide decay data. Those compilations in which decay data for the transactinium nuclides do occur are generally oriented toward a much larger class of nuclides and/or a much broader (or restricted) category of data. Numerous compilations of a rather specialized data content (e.g., half-lives, γ -rays arranged according to energy, or nuclide, or nuclide half-life) exist in which transactinium nuclides are included. Some of these have been discussed in the review paper by Rudstam [14] in the context of their fission-product decay-data content; and the reader is referred to that review for further information concerning them.

We now briefly discuss several compilations containing transactinium-nuclide decay data which are quite useful to workers in both basic and applied areas. They have also been utilized in the preparation of much of the work contained in this paper.

2.1. Nuclear Data Sheets (Academic Press, New York, continuing)

These are standard reference material for non-neutron nuclear data. The most recent issues of this series which are relevant to the transactinium-nuclide decay data are the following:

A=230, 234, 238, 242 - Y. A. Ellis, Vol. 4, No. 6 (1970)

A=232, 236, 240 - M. R. Schmorak, Vol. 4, No. 6 (1970)

A=229, 233 - Y. A. Ellis, Vol. 6, No. 3 (1971)

A=231, 235 - A. Artna-Cohen, Vol. 6, No. 3 (1971)

A=237, 241 - Y. A. Ellis, Vol. 6, No. 6 (1971)

A=239 - A. Artna-Cohen, Vol. 6, No. 6 (1971)

243 \leq A \leq 261 - Y. A. Ellis and A. H. Wapstra, Vol. 3, No. 2 (1969)

The Data Sheets for the even-A nuclides with $A > 243$ are currently being revised [15], and some of their contents have been used in the preparation of the data summary given in Chapter 3 of this review.

These data sets are quite useful, particularly for the basic nuclear physicist and the specialized evaluator, but the quite broad coverage of different types of nuclear data renders its use difficult for many applications-oriented people. Somewhat disconcerting for many applied users is the practice of listing on the level schemes the transition (i.e., photon + conversion-electron) intensities for the γ -rays instead of simply the photon intensities. The relatively long cycle times between revisions of the A-chains also presents a problem for the applied users, although the issuing of the companion "Recent References" helps keep the nuclear physicist or evaluator aware of the fairly recent data. The files are presently being extensively computerized; and consideration is being given to various means of decreasing the cycle time.

2.2 C. M. Lederer, J. M. Hollander and I. Perlman, Table of Isotopes Sixth Edition (John Wiley and Sons, New York, 1967)

This has been a standard reference work for radioactive-nuclide decay data and has been widely used, especially by the applied user. Its major difficulty is long cycle time between editions. Somewhat disconcerting is the practice of listing the γ -ray intensities on the level schemes in such a fashion that the sum of these intensities out of each level is 100%, so that the actual γ -ray relative intensity data cannot easily be inferred by reference to the decay scheme. At present, this data file is extensively computerized, which should simplify editing and updating. A seventh edition is presently in preparation; and the data base for the nuclides with $A \geq 231$ for this edition, supplied by C. M. Lederer [16], was extensively used in the work described in Chapter 3 below.

2.3 A. H. Wapstra and N. B. Gove, The 1971 Atomic Mass Evaluation, Nuclear Data Tables A, Vol. 9, No. 4-5 (1971)

This compilation contains Q values for all relevant decay processes, derived from careful consideration and adjustment of all experimental information relating to atomic-mass differences. Also important is a listing of the uncertainties in these adopted values. The Q values used in this review paper were taken from an unpublished revision of this compilation [17].

2.4. R. Vaninbroux, Half-Lives of Some Long-Lived Actinides: a Compilation, Euratom Report EUR-5194e (1974)

This report contains an up-to-date collection of half-life data on a number of the longer-lived isotopes of U and Pu and of ^{241}Am and ^{252}Cf . Recommended half-life values are given; and generally these values are listed in the present paper.

2.5. F. Manero and V. A. Konshin, Status of the Energy-Dependent $\bar{\nu}$ -Values for the Heavy Elements ($Z > 90$) from Thermal to 15 MeV and of $\bar{\nu}$ -Values for Spontaneous Fission, Atomic Energy Review 10 (1972) 637

This excellent survey contains a complete compilation of the $\bar{\nu}$ data published up to August, 1972. Of relevance for the present review is the tabulation of the prompt $\bar{\nu}$ values for the spontaneous fission of 21 transactinium isotopes ranging from ^{232}Th to ^{257}Fm .

2.6. E. K. Hyde, I. Perlman and G. T. Seaborg, The Nuclear Properties of the Heavy Elements, Vol. I-III, (Prentice-Hall, Englewood Cliffs, 1964)

Very comprehensive, these three volumes treat essentially all aspects of transactinium nuclear data. As such, they are quite valuable reference material for those interested in gaining a knowledge of most facets of this subject. However, since they have not been updated, much of their data content is not up-to-date and hence not particularly useful to users whose data needs require a current and evaluated set of data.

2.7. Actinide Data File for ENDF/B, Version V

Mention should be made of the fact that a file of Actinide Nuclear Data is currently being prepared under the auspices of CSEWG for issue in Version V of ENDF/B. One component of this Actinide File will be evaluated decay data for the included isotopes. Because of its relevance to this meeting, the content and organization of the decay data on this file will be discussed in Appendix A below.

3. STATUS OF SELECTED DECAY DATA FOR TRANSACTINIUM ISOTOPEs

In Table I is summarized the current status of selected decay data on the transactinium isotopes in the mass region $228 \leq A \leq 257$. We first discuss the organization of the table and then briefly comment on some of the points to emerge from this assessment of the decay-data status.

TABLE I

Summary of selected decay data for the transactinium nuclides ($Z > 90$) with $228 < A < 257$. The quantities in parentheses represent the uncertainties in the last significant figure (or figures) of the associated value. For further discussion, see the text.

Nuclide	Decay Modes	Branching Ratios (%)	Half-life Data			Q (keV)	Intensity of ground-state transition ^[a] (%)	γ-ray transition data ^[b] E _γ (keV); I _γ (%)	Status of c.-e. data	Decay Scheme Status	References and Comments
			Value	Range	No. of Meas.						
²²⁸ Th	Decay chain terminating with ²⁰⁸ Pb		1.913(1)y	--	--	--	--	{2614.66(10); 35.93(6)} {583.14(3); 30.(2)}	--	--	[1]. I _γ values are equilibrium values for the decay chain.
²²⁹ Th	α	100.	7340.(160)y	--	--	5168.0(12)	0.01	193.63(6); 4.5	A(mag.)	B	[2]. I _γ value deduced from absolute c.e. intensities and theoretical ICC.
²²⁹ Pa	e.c. α	99.75 0.25	1.4(4)d --	-- --	-- --	306.(13) 5835.(5)	-- ≤0.5	-- --	-- --	C B	[2,3]
²²⁹ U	e.c. α	~80. ~20.	58.(3)m --	-- --	-- --	1318.(14) 6472.4(31)	-- 64.	-- --	-- --	C C	[2]
²³⁰ Th	α s.f.	100. ≤5×10 ⁻¹¹ [c]	7.7(2)×10 ⁴ y ≥1.5×10 ¹⁷ y	-- --	-- --	4767.2(15) --	76.3 --	67.73(3); 0.38 --	B(mag.) --	B --	[4,5]
²³⁰ Pa	e.c. β ⁻ α	89.6(5) 10.4(5) 0.0032	17.4(4)d -- --	-- -- --	-- -- --	1304.0(25) 560.(6) 5438.0(20)	0 0 23.(5)	951.99(5); 29.3 -- --	A(Si) -- --	A B C	[4,6-8]. I _γ value listed is average of 28.3(3)[6] and 30.3[8].
²³⁰ U	α	100.	20.8d	--	--	5991.4(20)	67.5(5)	72.13; 0.54	--	B	[4]
²³¹ Th	β ⁻	100.	25.52(1)h	--	--	387.(5)	0	84.17; 7(1)	A(mag.)	A	[2,9]
²³¹ Pa	α s.f.	~100. ~3×10 ⁻¹⁰ [c]	3.257(10)×10 ⁴ y 1.1×10 ¹⁶ y	{+0.014} {-0.023} --	3 --	5147.3(10) --	11. --	283.56(6); 1.3 --	A(mag.) --	A --	[2,9]. I _γ value estimated to be uncertain by ~ 20%.

Table I (continued)

^{231}U	e.c. α	~ 100 . 0.0055	4.2(1)d --	-- --	-- --	360.(50) 5550.(50)	-- --	84.18;-- --	B(mag.) --	B C	[2,9]. The value 7% is given for this absolute I_γ . It is unclear how this value was measured.
^{231}Np	e.c. α	<99. >1.	48.8(2)m --	-- --	-- --	1840.(80) 6400.(50)	-- --	370.9(3); -- --	-- --	B C	[9]
^{232}Th	α	100.	$1.407(7) \times 10^{10}\text{y}$	$\begin{Bmatrix} +0.043 \\ -0.017 \end{Bmatrix}$	5	4082.(4)	77.	59.(1);	B(emuls.)	B	[1,9]. γ not observed. Transition (i.e., γ +c.e.) intensity = 23.(2)%.
^{232}Pa	β^-	100.	1.31d	--	--	1337.(10)	0	150.(1);12.	A(mag., Si)	A	[4,9]. I_γ value from measured (β, γ) coincidences and conversion-electron intensities.
^{232}U	α s.f.	~ 100 . $\sim 10^{-10}[\text{c}]$	72.6(7)y $8.(6) \times 10^{13}\text{y}$	$\begin{Bmatrix} +1.0 \\ -0.9 \end{Bmatrix}$ --	2 --	5413.92(25) --	68.6(6) --	129.0(2);0.082 --	B(emuls.) --	B --	[4,9]. I_γ value from relative-intensity data [4,11] and $I_\gamma=0.21\%$ for the 57.6-keV γ . From α -intensity and c.e. data, however, I_γ is expected to be ~ 0.058 .
^{232}Np	e.c.	100.	14.7(3)m	--	--	2700(SYST.)	<1	327.3(3);52.	--	B	[4,9]
^{232}Pu	e.c. α	>80. <20.	34.1(7)m --	-- --	-- --	1060(SYST.) 6700.(50)	-- 62.	-- --	C C	C C	[9]
^{233}Th	β^-	100.	22.29(5)m	$\begin{Bmatrix} +1.31 \\ -0.17 \end{Bmatrix}$	4	1245.1(24)	85.	86.50(5);2.6(4)	A(mag.)	A	[2,9]. Sum of β^- intensities to ground and first excited state (6.7 keV).
^{233}Pa	β^-	100.	27.0(1)d	--	--	572.3(25)	3.	311.89(1);36.	A(mag.)	A	[2,9]
^{233}U	α s.f.	~ 100 . $1.3 \times 10^{-10}[\text{c}]$	$1.592(3) \times 10^5\text{y}$ $1.2(3) \times 10^{17}\text{y}$	$\begin{Bmatrix} +0.034 \\ -0.039 \end{Bmatrix}$ --	11 --	4908.5(12) --	84.4 --	317.15(2);0.008(1) --	A(mag.) --	A --	[2,9,12]. $T_{1/2}$ from [10]. This I_γ value is a factor of ~ 2 smaller than is obtained from the absolute γ -intensity normalization used in [2,9].
^{233}Np	e.c. α	~ 100 . ~ 0.001	36.2(1)m --	-- --	-- --	1100.(SYST) 5700.(SYST)	~ 96 . --	312.1(3); 0.75 ? --	-- --	B C	[9]. Sum of e.c. transition intensities to first three members of ground-state band.

Table I (Continued)

^{233}Pu	e.c. α	99.88 0.12(5)	20.9(4)m --	-- --	-- --	2030.(SYST) 6416.(20)	-- --	235.4(3); --	-- --	B C	[9]
^{234}Th	β^-	100.	24.101(25)d	--	--	262.5(25)	0	112.81(5);0.24(1)	A(mag.)	A	[4,9]
^{234}Pa	β^-	100.	6.68(1)h	{ ± 0.05 }	2	2208(5)	0	883.237(33);12.	A(mag.)	A	[4,9]
$^{234\text{m}}\text{Pa}$	β^- I.T.	99.87 0.13(3)	1.170(4)m --	{+0.08} {-0.03}	4	2292. --	98. --	1001.025(22);0.59 --	A(mag.) --	A --	[4,9]. Energy of isomeric state not precisely known. A value of ~ 84 keV is used in [9].
^{234}U	α s.f.	~ 100 $\sim 1 \times 10^{-9}[\text{C}]$	2.446(7) $\times 10^5\text{y}$ 2(1) $\times 10^{16}\text{y}$	{+0.074} {-0.007}	7	4856.4(19) --	72.5(30) --	{ 53.222(19);0.15 } {120.905(12);0.050}	-- --	B --	[4,9]. $T_{1/2}$ from [10]. Quoted $I_{\gamma}(120)$ values range from $\sim 0.04\%$ [4] to 0.23% [11].
^{234}Np	e.c.+ β^+	100.	4.40(5)d	--	--	1808.(9)	26.	1558.7(6);18.	A(mag.)	A	[4,9]
^{234}Pu	e.c.	94. 6.	8.8(1)h --	-- --	-- --	390.(12) 6310.(5)	-- 68.	{no γ 's observed}	C C	C C	[4,9]
^{235}Th	β^-	100.	6.9(2)m	--	--	--	0.	--	--	C	[2,9]
^{235}Pa	β^-	100.	24.0(2)m	{+0.2} {-0.3}	2	1400.(100)	--	--	--	C	[2,9]
^{235}U	α s.f.	~ 100 $2.6 \times 10^{-7}[\text{C}]$	7.038(20) $\times 10^8\text{y}$ 2.7(10) $\times 10^{17}\text{y}$	{+0.092} {-0.098}	8 2	4678.8(25) --	4.6 --	185.712(10);54. --	-- --	A --	[2,9]. $T_{1/2}$ from [10].
^{235}Np	e.c. α	~ 100 0.0014	396.(1)d --	-- --	-- --	123.(1) 5188.(4)	~ 100 1.5(2)	-- 84.2(1); 1.1×10^{-4}	-- --	C B	[2,9]. I_{γ} from measured γ/α intensity and α -decay branching ratio.
^{235}Pu	e.c. α	~ 100 0.0030(6)	25.0(1)m --	{ ± 0.7 }	2	1130.(60) 5958.(31)	~ 56 100.	49.3(3);1.84 --	-- --	B C	[2,9]
^{236}Th	β^-	100.	37.5(15)m	--	--	--	46.	110.7(5);5.	--	B	[9]. I_{β} and I_{γ} values inferred from γ -ray intensities from sources containing both parent and daughter activities.
^{236}Pa	β^-	100.	9.1(2)m	--	--	3100.(200)	--	642.0; --	--	C	[4,9]

Table I (Continued)

^{236}U	α	$\sim 100.$	$2.34(2)\times 10^7\text{y}$	$\left\{ \begin{smallmatrix} +0.12 \\ +0.0015 \end{smallmatrix} \right\}$	3	4569.2(24)	74.	112.750(16);0.019	B(emuls.)	B	[4,9]. $T_{1/2}$ from [10].
	s.f.	$1.2\times 10^{-7}[\text{c}]$	$2.\times 10^{16}\text{y}$	--	--	--	--	--	--	--	
^{236}Np	β^-	100.	$1.29(6)\times 10^6\text{y}$	--	--	986.(10)	--	--	--	C	[4,9]
$^{236\text{m}}\text{Np}$	β^-	48.(1)	22.5(4)h	--	--	537.(8)	38.(7) ^[d]	44.63(10);--	A(mag., Si)	A	[4,9]
	e.c.	52.(1)	--	--	--	986.(10)	40. ^[d]	642.42(10);1.0(2)	A(Si)	A	
^{236}Pu	α	$\sim 100.$	$2.851(8)\text{y}$	--	--	5866.7(20)	68.9(5)	109.0;0.012	--	B	[4,9]
	s.f.	$8\times 10^{-6}[\text{c}]$	$3.5(1)\times 10^9\text{y}$	--	--	--	--	--	--	--	
^{237}Pa	β^-	100.	8.7(2)m	--	--	2250.(10)	19.4	853.7(2);34.1(34)	--	B	[9,13,14]. Q_β from [13]. I_β is total β intensity to first 3 members of ground-state band. I_γ value from absolute β and γ measurements.
^{237}U	β^-	100.	6.75(1)d	--	--	519.3(11)	0.	208.005(23);23.3	A(mag.)	A	[9,14]. A 4π β - γ measurement (see [2]) gives $I_\gamma(208)=20.2\%$.
^{237}Np	α	100.	$2.14(1)\times 10^6\text{y}$	--	--	4957.2(14)	2.6	86.49(10);12.6(13)	A(mag., Si)	A	[9,14]
^{237}Pu	e.c.	$\sim 100.$	45.63(20)d	--	--	224.(5)	60.	59.54(1);--	--	B	[9,14]. Value given for α
	α	0.0033(3)	--	--	--	5754.(5)	21.(4)	--	--	C	branch is sum of intensities to ground and first excited states.
^{237}Am	e.c.	>99.	73.0(10)m	--	--	1540(SYST)	$\approx 5.$	280.230(20);47.3(20)	A(mag.,Si)	A	[9,15]
	α	0.025(3)	--	--	--	6200(SYST)	--	--	--	C	
^{238}Pa	β^-	100.	2.3(1)m	--	--	3960(300)	0.	--	--	B	[4,9]
^{238}U	α	$\sim 100.$	$4.468(10)\times 10^9\text{y}$	$\left\{ \begin{smallmatrix} +0.092 \\ +0.0003 \end{smallmatrix} \right\}$	4	4270.6(39)	77.	49.55(6);--	--	B	[4,9]. $T_{1/2}$ from [10].
	s.f.	$5.1\times 10^{-5}[\text{c}]$	$8.81(7)\times 10^{15}\text{y}$	$\left\{ \begin{smallmatrix} +1.29 \\ -0.81 \end{smallmatrix} \right\}$	7	--	--	--	--	--	
^{238}Np	β^-	100.	2.117(2)d	--	--	1292.5(32)	0.	984.45(2);24.	A(mag.)	A	[4,9]

^{238}Pu	α	$\sim 100.$	87.8(8)y	$\begin{Bmatrix} +0. \\ -1.4 \end{Bmatrix}$	4	5593.30(21)	71.1(12)	99.871(10); 0.0074(1)	B(mag., Si)	A	[4,9]. $T_{1/2}$ from [10]. I_Y measured [15]. A value of 0.080% is also reported [11] for $I_Y(99.8).$
	s.f.	$1.84(5) \times 10^{-7}$	$4.77(14) \times 10^{10} y^{[e]}$	--	--	--	--	--	--	--	
^{238}Am	e.c. α	$\sim 100.$ $1.0(4) \times 10^{-4}$	1.63(5)h --	-- --	-- --	2257.(32) 6042.(31)	$\sim 6.$ --	962.8(1); 29.(2) --	A(Si) --	A C	[4,9]
^{239}U	β^-	100.	23.54(5)m	--	--	1267.4(29)	20.	74.66(2); 59.3 ?	B(mag.)	B	[9,14]. I_β value represents sum of β intensity to ground and first excited states.
^{239}Np	β^-	100.	2.354(2)d	$\begin{Bmatrix} +0.012 \\ -0.008 \end{Bmatrix}$	4	721.5(19)	0.	$\{228.19(1); 11.3(2)\}$ $\{277.60(3); 14.3(2)\}$	A(mag.)	A	[9,14]. I_Y values from [17].
^{239}Pu	α s.f.	$\sim 100.$ $4.4 \times 10^{-10}[c]$	$2.430(25) \times 10^4 y$ $5.5 \times 10^{15} y$	$\begin{Bmatrix} +0.011 \\ -0.0235 \end{Bmatrix}$ --	10 1	5243.6(8) --	73. --	$\{129.28; 0.0062(1)\}$ $\{413.69; 0.00151(2)\}$	A(mag., Si)	A --	[9,14]. $T_{1/2}$ from [10]. Listed α -branch intensity is actually that feeding the 0.073-keV, 26.1-m isomeric state in ^{235}U . I_Y values are from [16]. Values of 0.0056% and 0.0015%, respectively, are reported for $I_Y(129)$ and $I_Y(413)$ in [11].
^{239}Am	e.c. α	>99.9 0.01(1)	11.9(1)h --	-- --	-- --	803.8(24) 5924.4(20)	$\sim 56.$ 0.33(2)	277.604(16); 15.(3) 48.3(15); 0.005(2)	A(mag., Si)	A B	[9]
^{240}U	β^-	100.	14.1(2)h	--	--	500.(60)	0.	44.10(7); 1.69(20)	B(mag.)	B	[4,9]. I_Y measured using equilibrium ^{244}Pu source.
^{240}Np	β^-	100.	65.(3)m	--	--	2090.(60)	0.	566.4(2); $\sim 29.$	--	B	[4,9]
^{240m}Np	β^- I.T.	99.9 ~ 0.1	7.50(6)m --	-- --	-- --	2090.(60) --	41.(5) --	597.40(7); 12.5(6) --	B(mag., emuls.)	A	[4,9]. This isomer probably lies above 65-m ^{240}Np , but the precise energy difference is unknown. The Q_β value listed is that of the ^{240}Np ground state. I_Y value measured using equilibrium ^{244}Pu source.

Table I (Continued)

^{240}Pu	α	$\sim 100.$	$6.55(7)\times 10^3\text{y}$	$\begin{Bmatrix} +0.21 \\ -0.31 \end{Bmatrix}$	7	5256.16(25)	76.	$\begin{Bmatrix} 45.235(20); 0.045(1) \\ 104.233(10); 0.0070(1) \\ 642.30; 1.45(5)\times 10^{-5} \end{Bmatrix}$	A(mag., Si)	A	[4,9]. $T_{1/2}$ from [10]. I_γ measured using assayed sources [16]. Values of 0.045%, 0.01% and $4.1\times 10^{-5}\%$, respectively, are given for these 3 γ rays in [11].
	s.f.	$5.0\times 10^{-6}[c]$	$1.313(10)\times 10^{11}\text{y}$	$\begin{Bmatrix} +0.137 \\ -0.143 \end{Bmatrix}$	5	--	--	--	--	--	
^{240}Am	e.c.	>99.7	$50.8(3)\text{h}$	--	--	1346.(20)	0.	$987.79(6); 73.3(25)$	B(Si)	B	[4,9]. $Q_{e.c.}$ value reported by [18], from K to total capture ratio.
	α	1.9×10^{-4}	--	--	--	5670.(SYST)	--	--	--	C	
^{240}Cm	α	$\sim 100.$	$28.\text{d}$	--	--	$6397.0(6)$	71.1	--	--	C	[4,9]
	s.f.	$4.0\times 10^{-6}[c]$	$1.9(4)\times 10^6\text{y}$	--	--	--	--	--	--	--	
^{241}Np	β^-	100.	$16.0(2)\text{m}$	--	--	$1360.(100)$	--	--	--	C	[9,14]
^{241}Pu	β^-	$\sim 100.$	$14.89(9)\text{y}$	$\begin{Bmatrix} +0.27 \\ -0.29 \end{Bmatrix}$	5	$20.81(20)$	100.	--	--	A	[9,14]. I_γ value from measured γ/α ratio and α branching ratio. An I_γ value of $2.2(2)\times 10^{-4}$ is deduced from the data of [19].
	α	$0.00245(8)$	--	--	--	$5139.4(11)$	0.35	$148.60(4); 1.90(2)\times 10^{-4}$	--	B	
^{241}Am	α	$\sim 100.$	$432.(4)\text{y}$	$\begin{Bmatrix} +26.1 \\ -5.7 \end{Bmatrix}$	6	$5637.93(14)$	0.35	$59.537(1); 35.9(3)$	A(mag.)	A	[9,14]. $T_{1/2}$ from [10].
	s.f.	$4.1\times 10^{-10}[c]$	$1.05(2)\times 10^{14}\text{y}$	$\begin{Bmatrix} +0.093 \\ -0.247 \end{Bmatrix}$	2	--	--	--	--	--	
^{241}Cm	e.c.	99.0	$32.8(2)\text{d}$	--	--	$771.(5)$	$<4.$	$471.805(20); 72.(3)$	A(mag.)	A	[9,15]
	α	$1.0(1)$	--	--	--	$6184.8(15)$	0.15	$145.536(9); --$	--	C	
^{242}Pu	α	$\sim 100.$	$3.87(5)\times 10^6\text{y}$	$\begin{Bmatrix} +0.01 \\ -0.22 \end{Bmatrix}$	5	$4981.7(12)$	78.9	$44.915(13); 0.042$	--	B	[4,9]. $T_{1/2}$ from [10]. Four of the $T_{1/2}$ values are measured relative to half-lives of other Pu isotopes.
	s.f.	$5.55\times 10^{-4}[c]$	$6.97(8)\times 10^{10}\text{y}$	$\begin{Bmatrix} +0.48 \\ -0.51 \end{Bmatrix}$	3	--	--	--	--	--	
^{242}Am	β^-	82.7	$16.01(2)\text{h}$	--	--	$665.(5)$	$37.[d]$	$42.12; --$	B(mag.)	B	[4,9]
	e.c.	$17.3(3)$	--	--	--	$752.(5)$	$6.[d]$	$44.54; --$	B(mag.)	B	
$^{242\text{m}}\text{Am}$	I.T.	$99.5^{+0}_{-0.2}$	$152.(7)\text{y}$	--	--	48.63	--	$48.63; --$	A(mag.)	A	[4,9]. Q_{IT} value is the energy of the isomeric state. Q_α value is that of ground state + E(I.T.). $I_\gamma(49.3)$ is obtained from α -branching intensity and measured γ/α value.
	α	$0.476(14)$	--	--	--	$5637.5(38)$	0.	$49.3; 0.20$	--	B	
	s.f.	$1.6\times 10^{-8}[c]$	$9.5(35)\times 10^{11}\text{y}$	--	1	--	--	--	--	--	

Table I (Continued)

^{242}Cm	α	$\sim 100.$	162.9(1)d	$\begin{Bmatrix} +1.5 \\ -0.44 \\ +0.6 \\ -0.5 \end{Bmatrix}$	4	6215.96(14)	74.0(5)	$\begin{Bmatrix} 44.08(5); 0.030(5) \\ 157.6(3); 0.20(5) \end{Bmatrix}$	B(mag.)	A	[4,9]
	s.f.	$6.8 \times 10^{-6} [^c]$	$6.6(1) \times 10^6 \text{y}$	$\begin{Bmatrix} +0.6 \\ -0.5 \end{Bmatrix}$	2	--	--	--	--	--	
^{243}Pu	β^-	100.	4.957(2)h	--	--	583.2(39)	58.	84.0(2); 23.(2)	A(Si)	A	[9]. I_γ value from measurements of ^{243}Pu γ 's in equilibrium with ^{247}Cm . An $I_\gamma(84)$ value of 27.6% is also reported:
^{243}Am	α	$\sim 100.$	7370(40)y	--	--	5438.1(10)	0.16	74.67; 66.(3)	A(Si)	A	[9]. I_γ value from determination of absolute γ -ray emission rates from calibrated source [20].
	s.f.	$1.8 \times 10^{-8} [^c]$	$4.2(4) \times 10^{13} \text{y}$	$\begin{Bmatrix} +15.8 \\ -0.9 \end{Bmatrix}$	2	--	--	--	--	--	
^{243}Cm	α	99.7	30y	$\begin{Bmatrix} +2. \\ -1.5 \end{Bmatrix}$	2	6168.3(10)	1.5	228.2; 10.6(3)	B(mag.)	A	[9]. I_γ value from absolute γ -ray emission rates from calibrated source [20].
	e.c.	0.26	--	--	--	8.7(24)	100.	277.6; 14.0(4)	--	A	
^{243}Bk	e.c.	>99.	4.6(2)h	--	--	1507.(6)	--	87.4(1); --	C(Si)	C	[9,21]. I_γ value from measured γ/α ratio and α -decay branching.
	α	0.15	--	--	--	6871.(5)	15.4(10)	187.1(5); 0.06	--	B	
^{244}Pu	α	$\sim 100.$	$8.2(1) \times 10^7 \text{y}$	$\begin{Bmatrix} +0.08 \\ -0.7 \end{Bmatrix}$	4	4663.7(10)	80.6(8)	--	--	C	[9,21,22]. $T_{1/2}$ from [10].
	s.f.	$0.12 [^c]$	$6.55(32) \times 10^{10} \text{y}$	--	--	--	--	--	--	--	
^{244}Am	β^-	100.	10.1(1)h	--	--	1429.0(20)	0.	744.1; 61.	B(mag.)	B	[9,21,22]
^{244}mAm	β^-	$\sim 100.$	26.m	--	--	1498.(10)	$\sim 80.$	42.9; --	C(mag.)	B	[9,21,22]. Q_β value taken from measured energy of ground-state β^- transition.
	e.c.	0.039(3)	--	--	--	72.(7)	--	--	--	C	
^{244}Cm	α	$\sim 100.$	18.11(1)y	$\begin{Bmatrix} +0.01 \\ -0.011 \end{Bmatrix}$	2	5901.70(11)	76.4(2)	42.824(8); 0.026	B(mag.)	B	[9,21,22]
	s.f.	$1.346(2) \times 10^{-4}$	$1.345(3) \times 10^7 \text{y} [^e]$	$\begin{Bmatrix} +0.115 \\ -0.093 \end{Bmatrix}$	5	--	--	--	--	--	
^{244}Bk	e.c.	>99.	4.35(15)h	--	--	2280(SYST)	--	217.6(3);	--	C	[9,21]
	α	0.006	--	--	--	6777.(10)	$\sim 50.$	--	--	C	

Table I (Continued)

^{245}Pu	β^-	100.	10.56(2)h	$\begin{Bmatrix} +0.03 \\ -0.08 \end{Bmatrix}$	2	1260.(30)	$\sim 10.$	327.2(5);23.3	B(Si)	B	[9,21]. I_{β^-} value is sum of β^- branch intensities to the lowest 7 states.
^{245}Am	β^-	100.	2.05(1)h	--	--	898.3(25)	78.	252.3(7);6.1(6)	B(Si, mag.)	B	[9,21]. I_{γ} value is from measured γ/β ratio.
^{245}Cm	α	100.	8475.(58)y	$\begin{Bmatrix} +62. \\ -210. \end{Bmatrix}$	2	5623.5(19)	0.5	173.;14.	--	C	[9,21]. I_{γ} value from γ/α ratio. $T_{1/2}$ values measured relative to $T_{1/2}(^{244}\text{Cm})$.
^{245}Bk	e.c.	99.9	4.98(2)d	--	--	819.(5)	0.	252.7(3);30.	B(mag.,Si)	C	[9,21]. Value of $I_{\gamma}(474)$ from γ/α ratio.
	α	0.105	--	--	--	6464.(5)	15.5(5)	474.5(15);0.022	--	C	
^{245}Cf	e.c.	~ 70	43.6(8)m	--	--	1563.(7)	--	--	--	C	[9,21]
	α	~ 30	--	--	--	7255.8(20)	--	--	--	C	
^{246}Pu	β^-	100.	10.85(2)d	--	--	374.(10)	0.	223.75(2);28(2)	C(mag.)	B	[9,21,22]
^{246}Am	β^-	100.	39.(3)m	--	--	2300.(50)	0.	679.(1);53.	--	B	[9,21,22]
^{246}mAm	β^-	100.	25.0(2)m	--	--	2300.(50)	$\sim 0.$	798.80(4);26.	B(Si)	A	[9,21-23]. Q_{β} assumed same as for ground state.
^{246}Cm	α	$\sim 100.$	4748.(14)y	$\begin{Bmatrix} +77. \\ -94. \end{Bmatrix}$	3	5476.1(26)	79.(1)	44.545(9);	--	C	[9,21,22]. $T_{1/2}$ values generally given relative to $T_{1/2}(^{244}\text{Cm})$.
	s.f.	0.0261(1)	$1.82(1)\times 10^7\text{y}^{[e]}$	$\begin{Bmatrix} +0.03 \\ -0.02 \end{Bmatrix}$	2	--	--	--	--	--	
^{246}Bk	e.c.	100.	1.83(15)d	--	--	1600.(SYST)	see comment	800.0(5);70.	B(Si)	B	[9,21,22]. Feeding of ground-state band <20%. Intensity of ground-state branch assumed to be zero. I_{γ} value from [22]. [9] gives 56% for this value.
^{246}Cf	α	$\sim 100.$	35.7(5)h	--	--	5476.1(26)	77.9(2)	147(4);0.0035(2)	--	C	[9,21,22]. I_{γ} from $\alpha\gamma$ coincidence measurements.
	s.f.	$2.3\times 10^{-4}[c]$	$1.74(12)\times 10^3\text{y}$	$\begin{Bmatrix} +0.36 \\ -0.4 \end{Bmatrix}$	3	--	----	--	--	--	
^{246}Es	e.c.	90.	7.7(5)m	--	--	3830(SYST)	--	--	--	C	[9,21,22]
	α	10(2)	--	--	--	7700(SYST)	--	--	--	C	

Table I (Continued)

^{247}Am	β^-	100.	22(2)m	--	--	--	--	285.(2);--	C(S1)	C	[9,21]
^{247}Cm	α	100.	$1.56(5)\times 10^7\text{y}$	--	--	5352.1(35)	13.8(7)	402.4(5);72.(6)	--	B	[9,21]. I_γ value determined from relative α - and γ -emission rates.
^{247}Bk	α	100.	$1.38(25)\times 10^3\text{y}$	--	--	5889.(5)	5.5(5)	265.(10);~30.	--	C	[9,21]
^{247}Cf	e.c.	100.	2.45(15)h	--	--	6600.(SYST)	0. ?	295.(5); --	--	C	[9,21]
^{247}Es	e.c.	93.	4.8(2)m	---	--	2350.(SYST)	--	--	--	C	[9,21]
	α	7.	--	--	--	7441.(30)	--	--	--	C	
^{248}Cm	α	91.67	$3.50(4)\times 10^5\text{y}$	$\left\{ \begin{smallmatrix} +0.11 \\ -0.103 \end{smallmatrix} \right\}$	3	5161.(5)	81.9(13)	--	--	C	[9,21,22]. $T_{1/2}$ and $T_{1/2}(\text{s.f.})$ values from averaged $T_{1/2}(\alpha)$ and $\alpha/\text{s.f.}$ values. $T_{1/2}(\alpha)$ generally obtained relative to $T_{1/2}(^{244}\text{Cm})$.
	s.f.	8.33(7)	$4.20(4)\times 10^6\text{y}$	$\left\{ \begin{smallmatrix} +0. \\ -0.085 \end{smallmatrix} \right\}$	2	--	--	--	--	--	
^{248}Bk	β^-	--	>9y	--	--	750.(SYST)	--	--	--	C	[9,21,22]
	e.c.	--	--	--	--	600.(SYST)	--	--	--	C	
$^{248\text{m}}\text{Bk}$	β^-	70.	19(3)h	$\left\{ \begin{smallmatrix} +4. \\ -3. \end{smallmatrix} \right\}$	2	750.(SYST)	--	--	--	C	[9,21,22]. Q values assumed the same as those for the ground state.
	e.c.	30.	--	--	--	600.(SYST)	--	--	--	C	
^{248}Cf	α	~100.	335.3(33)d	$\left\{ \begin{smallmatrix} +9.7 \\ -1.8 \end{smallmatrix} \right\}$	2	6369.(30)	83.0(5)	--	--	C	[9,21,22]
	s.f.	$0.0026^{[c]}$	$3.5(2)\times 10^4\text{y}$	$\left\{ \begin{smallmatrix} +0.5 \\ -0.3 \end{smallmatrix} \right\}$	2	--	--	--	--	--	
^{248}Es	e.c.	>99.	26.(4)m	$\left\{ \begin{smallmatrix} +2. \\ -1. \end{smallmatrix} \right\}$	2	3060.(SYST)	--	--	--	C	[9,21,22]
	α	~0.25	--	--	--	7150.(SYST)	--	--	--	C	
^{248}Fm	α	99.9	37.(4)s	--	--	8001.(20)	80.	--	--	C	[9,21,22]
	s.f.	0.1	10.(5)h	--	--	--	--	--	--	--	
^{248}Md	e.c.	80.(10)	7.(3)s	--	--	5110.(SYST)	--	--	--	C	[9,22]
	α	20.	--	--	--	6800.(SYST)	25.	--	--	C	
^{249}Cm	β^-	100.	64.(3)m	--	--	903.(9)	--	--	---	C	[9,21]

Table I (Continued)

^{249}Bk	β^- α s.f.	$\sim 100.$ 0.00145(8) $4.6 \times 10^{-8} [\text{c}]$	314.(8)d -- $1.87(9) \times 10^9 \text{y}$	-- -- --	-- -- --	126.1(19) 5523.3(19) --	100. 6.7 --	-- 327.2(5); -- --	-- -- --	A B --	[9,21]
^{249}Cf	α s.f.	$\sim 100.$ $5.0(1) \times 10^{-7}$	350.4(24)y $6.98(15) \times 10^{10} \text{y}^{[e]}$	$\begin{Bmatrix} +1.6 \\ -5.4 \end{Bmatrix}$ $\begin{Bmatrix} -0.11 \\ -0.84 \end{Bmatrix}$	3 2	6295.6(7) --	2.4(1) --	388.1(1); 66.(2) --	B(Si) --	A --	[9,21]. I_γ value from measured γ -ray emission rate.
^{249}Es	e.c. α	99.5 0.5(1)	1.7(1)h --	-- --	-- --	1405.(7) 6881.(5)	$\sim 46.$ --	379.4(5); $\sim 46.$ --	C(Si) --	B C	[9]. $I_{\text{e.c.}}$ value is sum of feeding to lowest 2 states.
^{249}Fm	α	100.	2.6(7)m	--	--	7700.(SYST)	--	--	--	C	[9,21]
^{249}Md	e.c. α	$\sim 80.$ $\sim 20.$	24.(4)s --	-- --	-- --	3760.(SYST) 8460.(SYST)	-- --	-- --	-- --	C C	[9]
^{250}Cm	s.f.	100.	$1.13(5) \times 10^4 \text{y}$	--	--	--	--	--	--	--	[9,21]
^{250}Bk	β^-	100.	3.222(5)h	--	--	1775.(8)	5.	988.96(15); 45.	B(mag.)	B	[9,21,22]
^{250}Cf	α s.f.	$\sim 100.$ 0.077(2)	13.08(9)y $1.69(4) \times 10^4 \text{y}^{[e]}$	-- $\begin{Bmatrix} +0.04 \\ -0.03 \end{Bmatrix}$	-- 2	6129.2(6) --	83.5(12) --	42.852(5); -- --	B(mag.) --	B --	[9,21,22]
$^{250}\text{Es}^{[f]}$	e.c.	100.	8.3(2)h	--	--	2000.(SYST)	--	--	B(Si)	C	[9,22]
$^{250\text{m}}\text{Es}^{[f]}$	e.c.	100	2.1(2)h	--	--	2000.(SYST)	--	--	--	C	[9,22]. Q value listed is the same as that for the ground state.
^{250}Fm	α s.f.	$> 90.$ $\sim 10.\text{y}$	30.(3)m $\sim 10.\text{y}$	-- --	-- --	7548.(30) --	-- --	-- --	-- --	C --	[9]
$^{250\text{m}}\text{Fm}$	I.T.	--	1.8(1)s	--	--	--	--	--	--	C	[9]
^{250}Md	e.c. α	94.(3) 6.	52.(6)s --	-- --	-- --	4530.(SYST) 8250.(SYST)	-- --	-- --	-- --	C C	[9]
^{251}Bk	β^-	100.	57.0(17)m	--	--	1130.(SYST)	0.	--	--	C	[9,21]. Intensity of ground-state β^- branch deduced from probable difference in ground-state spins and parities ($\Delta I=3, \Delta \pi=\text{no.}$).

Table I (Continued)

^{251}Cf	α	100.	897.(45)y	$\begin{Bmatrix} +3. \\ -5. \end{Bmatrix}$	2	6171.8(14)	2.7(3)	176.6(1);17.(1)	B(Si)	B	[24]. $T_{1/2}$ from data in [21]. I_{γ} value from $\alpha\gamma$ -coincidence measurements
^{251}Es	e.c. α	>99. 0.52	33.(1)h --	-- --	-- --	375.(9) 6593.(5)	$\sim 65.$ $\sim 80.$	177.6(3); 5. --	-- --	C C	[9,21]. Value given for ground-state e.c. branch is total feeding of first 3 members of ground-state band.
^{251}Fm	e.c. α	98.1 1.9(2)	5.30(8)h --	-- --	-- --	1490.(SYST) 7366.(15)	-- 1.5(1)	425.4(1);0.97(13)	B(Si)	C A	[9]. I_{γ} (425) determined from measured γ and α intensities together with α /e.c. branching.
^{251}Md	e.c. α	$\sim 90.$ --	4.0(5)m --	-- --	-- --	3030.(SYST) 8050.(SYST)	-- --	-- --	-- --	C C	[9]
^{252}Cf	α s.f.	96.90 3.10(2)	2.640(3)y 85.3(5)y ^[e]	± 0.019	4	6217.0(5)	84.2(3)	$\{43.399(25);0.0148(9)\}$ $\{160.(15);0.0020(6)\}$	--	B --	[9,22]. I_{γ} values from $\alpha\gamma$ -coincidence measurements.
^{252}Es	α e.c.	78.(6) 22.(2)	350.(50)d --	-- --	-- --	6746.(5) 1130.(SYST)	80.2(9) 0.	$\{399.7(3);0.23(3)\}$ $\{418.5(3);0.23(3)\}$ 785.1(1);15.(2)	-- B(Si)	A A	[9,22]. I_{γ} (399,418) values determined from $\alpha\gamma$ -coincidence measurement and listed α -branching ratio. I_{γ} (785) deduced from intensity-balance considerations and e.c.-branching ratio.
^{252}Fm	α s.f.	$\sim 100.$ 0.002 ^[e]	22.8(6)h 115.(60)y	$\begin{Bmatrix} +0.2 \\ -0.1 \end{Bmatrix}$ --	2 1	7154.(20) --	$\sim 85.$ --	-- --	-- --	C --	[9,21,22]
^{252}Md	e.c.	--	2.3(8)m	--	--	3750.(SYST)	--	--	--	C	[9]
^{252}No	α s.f.	$\sim 70.$ $\sim 30.$	2.4(2)s $\sim 7.s$	-- --	-- --	8546.(15) --	-- --	-- --	-- --	C --	[9]
^{253}Cf	β^- α	99.69 0.31(4)	17.82(9)d --	-- --	-- --	299.(10) 6136.(5)	$\sim 100.$ 0.	{no γ 's reported}	-- --	C C	[9,21]
^{253}Es	α s.f.	$\sim 100.$ $8.7(2)\times 10^{-6}$	20.47(2)d $6.4(2)\times 10^5 y^{[e]}$	-- --	-- --	6739.58(23) --	89.8(2) --	389.18(4);0.026 --	A(mag.) --	A --	[9,21,25]

Table I (Continued)

^{253}Fm	e.c. α	88. 12.(1)	3.00(13)d --	-- --	-- --	341.(4) 7206.(4)	-- 1.3(2)	-- 271.8(4);2.6(4)	-- B(Si)	C B	[9,21]. I_γ value from $\alpha\gamma$ -coincidence measurements and α -branching ratio.
^{254}Cf	α s.f.	0.310(16) 99.690	60.5(2)d 60.7(2)d	-- --	-- --	5931.4 --	83.(2) --	-- --	-- --	C --	[9,21,22]. $T_{1/2}$ (s.f.) calculated from $\alpha/(\alpha+s.f.)$ ratio and listed $T_{1/2}$ value.
^{254}Es	α	100.	276.d	--	--	6626.(5)	~ 0.005	{ 63.(2);2.0(3) } { 150.(2);0.020(3) }	B(emuls.)	B	[9,21,22]. I_γ (63) value from $\alpha\gamma$ -coincidence and γ -emission rate measurements.
^{254m}Es	β^- α e.c.	99.6 0.33(1) 0.078(6)	39.3(2)h -- --	-- -- --	-- -- --	1164.(11) 6704.(5) 668.(SYST)	$\sim 16.$ 4.0(5) 100.	693.67(7);24.7(17) 211.8(1);0.10(1)	B(mag.) B(Si)	A A C	[9,21,22]. I_γ values from measured γ -emission rate relative to α -rate from ^{254}Fm in equilibrium. Q values calculated from those for the ground state assuming an isomeric-state energy of 78(1) keV.
^{254}Fm	α s.f.	99.941 0.0590(3)	3.24(1)h 229.(1)d[e]	-- --	-- --	7315.(5) --	85.(1) --	151.(5);0.0010(3) --	-- --	C --	[9,21,22]
^{254}Md (1)[g]	e.c.	--	10.(3)m	--	--	2490.(SYST)	--	--	--	C	[9]. $Q_{e.c.}$ value is that for the ground-state decay.
^{254}Md (2)[g]	e.c.	--	28.(8)m	--	--	2490.(SYST)	--	--	--	C	[9]. $Q_{e.c.}$ value is that for the ground-state decay.
^{254}No	α	100.	55(5)s	--	--	8235.(15)	$\sim 85.$	--	--	C	[9,21,22]
^{254m}No	I.T.	--	0.28(4)s	--	--	--	--	--	--	C	[9]
^{255}Es	β^- α s.f.	92.0 8.0(4) 0.0041(2)	39.8(12)d -- 2.63(15) $\times 10^3$ y	-- -- --	-- -- --	290.(SYST) 6400.2(15) --	-- 87.7 --	-- -- --	-- -- --	C C --	[9,21]. $T_{1/2}$ (s.f.) derived from $\beta^-/s.f.$ ratio and $T_{1/2}$.
^{255}Fm	α s.f.	$\sim 100.$ 2.4(10) $\times 10^{-5}$	20.04(8)h (9.6 $^{+5.7}_{-3.0}$) $\times 10^3$ y[e]	{+0.03} {-0.14}	2	7242.(4) --	0.070(7) --	204.1(2);0.024(2) --	A(mag., Si) --	A --	[9,21,25]. I_γ value from γ - and α -emission-rate measurements.

Table I (Continued)

^{255}Md	e.c. α	90. 10.(1)	27.(2)m --	-- --	-- --	1080.(SYST) 7950.(SYST)	-- --	-- 430.(40); --	-- --	C C	[9]. A value for e.c./ α of 93/7(1) is also reported.
^{255}No	α	100.	3.16(12)m	$\begin{Bmatrix} +0.17 \\ -0.16 \end{Bmatrix}$	3	8445.(9)	3.(1)	--	--	C	[9,21]
^{256}Fm	α s.f.	8.1(3) 91.9	157.(2)m 2.85(4)h	-- --	-- --	7034.(5) --	-- --	-- --	-- --	C	[9,22]. $T_{1/2}$ (s.f.) calculated from measured $\alpha/(\alpha+s.f.)$ ratio and listed $T_{1/2}$ value.
^{256}Md	e.c. α	90.6 9.4(4)	76.(3)m --	$\{\pm 1.\}$ --	2 --	1940.(SYST) 7843.(20)	-- 4.(1)	-- 400.(20); --	-- --	C C	[9,22]. E.c. and α branch intensities are an average of 2 reported values, 90.1/9.9(5) and 91.5/8.5(8), for $\alpha/(e.c.+ \alpha)$.
^{257}Fm	α s.f.	99.79 0.210(5)	100.5(2) d 131.(3) y [e]	-- --	-- --	6866.2(31)	0.4(2)	241.2(7); 10.(1)	B(Si)	B	[9,21]. I_γ values from $\alpha\gamma$ -coincidence measurements.
^{257}Md	e.c. α	90. 10.(3)	5.2(3)h --	$\{\pm 0.2\}$ --	2 --	430.(SYST) 7600.(SYST)	-- --	-- --	-- --	C C	[9,21]
^{257}No	α	100.	24.5(14)s	$\{\pm 1.5\}$	2	8452.(30)	--	--	--	C	[9,21]

- [a]. Unless otherwise indicated, these intensity values give the percent of a given decay mode which directly populates the ground state of the respective daughter nucleus. Consequently, in those cases where more than one decay mode of a nucleus has an appreciable intensity, they must not be interpreted as being expressed as % of decays of the parent nucleus.
- [b]. Unless otherwise noted, the listed absolute I_γ values are derived from intensity-balance considerations within the decay scheme. They are always given in %/decay (i.e., photons/100 decays) of the parent nuclides.
- [c]. Spontaneous-fission branching ratio calculated from the listed values of $T_{1/2}$ (s.f.) and $T_{1/2}$.
- [d]. (^{236}mNp , ^{242}Am). These values represent intensities in % of decays of the parent nuclide rather than in % of decays via the respective decay mode.
- [e]. $T_{1/2}$ (s.f.) value derived from the $\alpha/s.f.$ ratio and the listed value of $T_{1/2}$.
- [f]. (^{250}Es , $^{250\text{m}}\text{Es}$). The relative ordering of the ground and isomeric states is not experimentally established. The ordering given here is based on the expectation that the coupling of the odd neutron and the odd proton will produce a high-spin ground state and a low-spin isomeric state. The short-lived activity is observed to feed low-spin states in the daughter nucleus, while the longer-lived activity does not. This indicates that the short-lived activity has a low spin and thus strongly suggests that it is the isomeric state.

Table I (Continued)

[g]. ($^{254}\text{Md}(1)$, $^{254}\text{Md}(2)$). The relative position in ^{254}Md of these two activities is not yet established.

REFERENCES FOR TABLE I

- [1]. M. J. Martin and P. H. Blichert-Toft, Nuclear Data Tables A 8, Nos. 1-2, (1970) 1.
- [2]. Nuclear Data Sheets 6, No. 3, (1971).
- [3]. P. Aguer, A. Peghaire and C. F. Liang, Nucl. Phys. A202 (1973) 37.
- [4]. Nuclear Data Sheets B 4, No. 6, (1970).
- [5]. E. F. Tret'yakov, N. I. Tret'yakova and V. F. Konyaev, Izv. Akad. Nauk SSSR, Ser. fiz. 35 (1971) 2306; Bull. Acad. Sci. USSR, Phys. Ser. 35 (1972) 2094.
- [6]. W. Lourens, B. O. Ten Brink and A. H. Wapstra, Nucl. Phys. A152 (1970) 463.
- [7]. W. Kurcewicz, K. Stryczniewicz, J. Zylicz, S. Chojnacki, T. Morek and I. Yutlandov, Acta Phys. Polonica B2 (1971) 451.
- [8]. T. Valkeapää, J. Heinonen and G. Graeffe, Phys. Scripta 5 (1972) 119.
- [9]. C. M. Lederer, private communication (July, 1975) (to appear in Table of Isotopes, Seventh Edition).
- [10]. R. Vaninbroux, Euratom Report EUR-5194e (1974).
- [11]. J. E. Cline, USAEC Report IN-1448 (rev.), (Jan., 1971); see also J. E. Cline, R. J. Gehrke and L. D. McIsaac, USAEC Report ANCR-1069 (Supplement to IN-1448), (July, 1972).
- [12]. L. A. Kroger, C. W. Reich and J. E. Cline, USAEC Report ANCR-1016 (1971) 68; L. A. Kroger and C. W. Reich (to be submitted for publication).
- [13]. N. Kaffrell, N. Trautmann and R. Denig, Z. Physik 266 (1974) 21.
- [14]. Nuclear Data Sheets 6, No. 6, (1971).
- [15]. I. Ahmad, F. T. Porter, M. S. Freedman, R. K. Sjoblom, J. Lerner, R. F. Barnes, J. Milsted and P. R. Fields, Phys. Rev. C. (to be published).
- [16]. R. Gunnink and R. J. Morrow, USAEC Report UCRL-51087 (July, 1971).
- [17]. R. G. Helmer and R. C. Greenwood, Nucl. Technology 25 (1975) 258.

Table I (Continued)

- [18]. I. Ahmad, R. F. Barnes, R. K. Sjoblom and P. R. Fields, J. Inorg. Nucl. Chem. 34 (1972) 3335.
- [19]. I. Ahmad, A. M. Friedman and J. P. Unik, Nucl. Phys. A119 (1968) 27.
- [20]. I. Ahmad and M. Wahlgren, Nucl. Instr. and Methods 99 (1972) 333.
- [21]. Nuclear data Sheets B 3, No. 2 (1969).
- [22]. M. R. Schmorak, private communication (July, 1975) (to appear in Nuclear Data Sheets).
- [23]. L. G. Multhauf, K. G. Tirsell and R. A. Meyer, Phys. Rev. C (to be published).
- [24]. E. Browne and F. Asaro, USAEC Report UCRL-19530 (1969) 8.
- [25]. I. Ahmad and J. Milsted, Nucl. Phys. A239 (1975) 1.

3.1. Comments on the Content and Organization of the Table

Entries for 142 nuclides and isomeric states are contained in Table I. These constitute essentially all the nuclides in this mass region for which some decay data, other than simply a half-life, are available. In the table, we have listed numerical values and their uncertainties for the various quantities. To the extent that these uncertainties are correct, they indicate the "status" of a given quantity. It should be emphasized that these values are in no way intended to serve as a set of "recommended data."

In the table, some of the listed data refer to α transitions and α -decay-related half-lives. These are included to illustrate the various data categories and are not to be regarded as being in contradiction to the more extensive treatment of α -particle data in the review paper B6 [18] presented at this meeting.

For each nuclide, the observed decay modes and their branching ratios (in percent) are given. This is followed by the half-life data, which include the total nuclide half-life in all cases and the spontaneous-fission (s.-f.) half-life where it exists. In some cases, the s.-f. half-life is measured directly (and the s.-f. branching ratio is inferred) and in some cases the s.-f. branching ratio is measured directly (and the s.-f. half-life is inferred). The manner in which these two quantities were derived for the various nuclides is indicated in footnotes to the table.

In a number of cases, several measurements of the nuclide half-life have been made; and it is frequently found that the measured values differ from each other by amounts that are much larger than the quoted uncertainties. In these cases, we have listed (1) an "averaged" value for the half-life and its uncertainty, together with (2) the range (above and below the average) spanned by the measured values and (3) the number of measurements included. In arriving at those measurements to be included, we have occasionally discarded some older measurements (where more recent ones seemed more reliable) and some whose quoted uncertainties were significantly larger than those of the ones used. Where indicated in the References Column, these "averaged" values were taken from the recent compilation of Vaninbroukx [19]. In the remainder of the cases, the listed value is a weighted average of the measurements, with a $1/\sigma$ weighting factor used. The uncertainty given is the "internal" error, namely,

$$\sigma (T_{1/2}) = \sqrt{n / \sum_i w_i}$$

where n is the number of measurements and w_i is the weighting factor (i.e., $1/\sigma_i$) of the i^{th} measurement. Comparison of this internal-error estimate with the range of values gives some indication of how the differences among the measured values compare with their quoted uncertainties. As stated above, it is not the purpose of this procedure to produce "recommended" half-life values in these cases; it is merely intended to illustrate in a fairly concise way the status of the experimental situation.

In the table are listed the Q -values for each decay mode (except spontaneous fission). This gives the total energy available to the decay. The notation "SYST" accompanying a value indicates that is estimated from systematics. Listed next is the intensity of the transition directly from the parent state to the ground state of the daughter nucleus (excluding isomeric-transition decay). This has been included since, in many cases, it indicates the precision with which γ -ray intensities can be inferred from intensity-balance considerations within the decay scheme. These absolute intensities, where not directly measured (i.e., by $\alpha\gamma$ - or $4\pi\beta\gamma$ - coincidence measurements) are generally deduced by requiring that the sum of the transition (i.e., photon + conversion-electron) intensities of all the γ -rays feeding the ground state and the direct feeding from the parent nucleus equal 100%. Weak ground-state feeding indicates that, in principle, fairly precise absolute γ -ray intensities can be deduced, while strong direct feeding of the ground state generally indicates that the derived absolute-intensity values will be less precise.

Also given in the table are energy and absolute-intensity values for a prominent γ -ray (or γ -rays) associated with the various decay modes (except spontaneous fission) of each nuclide. Because of the widespread use of γ -ray spectroscopy for quantitative assay of radioactivity and of the many applications involving such assay, these data are of considerable importance.

We have given only qualitative indicators for the status of the conversion-electron data and of the deduced decay scheme. In this notation, A indicates a quite well studied and reasonably complete situation; B denotes some data, but an incomplete situation; while C indicates only fragmentary data or decay scheme. If no c.-e. data exist, this column is left blank, while if the decay scheme is completely unknown, a C is still indicated in that column. Clearly, the borders between these various symbols are not sharply drawn. The notations "mag.", "emuls." and "Si"

in the c.-e. status column indicate that magnetic spectrometers, magnetic spectrographs, and silicon detectors, respectively, were utilized in the conversion-electron measurements.

Where the various quantities are not known, generally no entry appears in the table.

At the right in the table are given the references from which the data have been taken and appropriate comments. The numbering of the references refers to those at the bottom of the table and is separate from that employed in the text. While it would have been generally desirable to refer in all cases to the original papers for the data included in Table I, this was not done because of the quite extensive referencing which this would have required.

A large body of data on the spontaneous-fission isomers, whose existence and properties provide a striking illustration of the influence of shell-structure effects on the formation of a second minimum in the nuclear potential well, is not included here. It was felt that a treatment of these interesting nuclear states lay outside the scope of this meeting.

3.2. Discussion of specific points

Because of the widespread use of γ -ray spectroscopy as a means of both qualitative and quantitative assay of radioactivity, the γ -ray-energy and especially the absolute-intensity data are of great importance. For this reason, comments pointing up discrepancies and differences in reported intensity values are occasionally included in Table I (see, e.g., ^{232}U). The intensity of the prominent 185.71-keV γ -ray from the ^{235}U decay represents an interesting situation. Only one measurement of this quantity is reported [20]--in an APS Bulletin Abstract in 1957--and no uncertainty was quoted. Hence, quantitative assay of ^{235}U samples using only γ -ray spectrometry involves data of unknown accuracy.

The absolute intensities of the γ -rays from the more common Pu isotopes present unresolved problems at this time, in that the two most extensive reported measurements [21,22] exhibit considerable disagreements. This situation has been studied in detail in the context of safeguards research by Ottmar and Weitkamp [23], who compare isotopic ratios of Pu isotopes determined from mass-spectrometric analyses with those determined

from γ -ray spectrometry. These results are shown in Table II. Ottmar and Weitkamp report:

For computation of the γ -spectrometric isotopic ratio values as listed in the Table, absolute γ intensities have been used. The results in columns 3 and 4 are calculated from the only two comprehensive sets of absolute γ intensities of plutonium and americium isotopes published until now [21,22]. The agreement of the two sets of results with each other and with the mass-spectrometric data is poor. This indicates that the reported error values for the absolute intensities are too optimistic.

Among other things, they conclude:

One prerequisite for the accurate γ spectrometric determination of plutonium isotopic ratios is the availability of better nuclear data. Since absolute γ intensities can hardly be measured to the degree of accuracy necessary, intensity ratios should be determined as outlined in Chapter 4. This requires samples with very accurately known isotopic composition.

As a daughter nucleus from ^{239}U decay, ^{239}Np is important in a number of applications such as, e.g., measurements of the neutron capture cross section of ^{238}U . As indicated in Table I, the absolute intensities of the two prominent γ -rays near ~ 0.2 MeV are known with precisions somewhat better than 2%. A γ -ray doublet at ~ 106 keV, more intense than either of these two, also occurs in the ^{239}Np decay. Its use in quantitative spectral analysis is not generally advisable, partly because at that energy absorption within the samples can be important and partly because it lies in the energy region of the K x-rays from the near-lying elements.

The intensity of the prominent 59.5-keV γ -ray from ^{241}Am decay is now quoted with an uncertainty of $\sim 1\%$. We have derived the value given in Table I from a $1/\sigma$ -weighted average of the two most recent measurements, $35.3 \pm 0.6\%$ [24] and $36.3 \pm 0.4\%$ [25]. It is interesting and perhaps fortuitous that this value is now back to what it was in 1957 [26] and used by IAEA, namely 35.9%, although the uncertainty is now roughly a factor of 2 smaller.

The low-energy (≤ 30 keV) photons from ^{241}Am are frequently used as intensity-calibration standards for low-energy photon detectors. Five peaks are commonly utilized, namely the $L\beta$, $L\alpha$, $L\gamma\beta$, and $L\gamma$ lines at 11.9, 13.9, 17.8 and 20.8 keV, respectively, and the 26.35-keV γ -ray. A detailed treatment of the absolute-intensity values of these lines has been reported by Campbell and McNelles [27]. They conclude that the uncertainties in these absolute intensities range from $\sim 2.5\%$ for the $L\alpha$ line to $\sim 4\%$ for weaker $L\beta$ and 26.35-keV lines.

TABLE II. RESULTS OF A GAMMA SPECTROMETRIC DETERMINATION OF ISOTOPIC RATIOS IN PLUTONIUM. (This table is taken from Ottmar and Weitkamp[23].)

Isotopic ratio	Mass spectro-metric value	γ-spectrom. values calculated with absolute intensities from refs.		γ lines used for analysis (keV)		Error components(*) [†]		
						F _I	F _H	F _P
		[21]	[22]	²³⁹ Pu γ	Other γ	[21]		
²³⁹ Pu/ ²³⁸ Pu	3118 (10)*	3260 (6)	4809 (22)	203.55	152.77	4	0.2	2
		3333 (14)	4513 (32)	769.38	742.77 ⁺	2	0.2	12
		2753 (4)	3680 (21)	769.38	766.41 ⁺	2	0.2	2
		2855 (10)	6673 (18)	769.38	786.30	2	0.2	8
²³⁹ Pu/ ²⁴⁰ Pu	10.512(0.4)	12.57(10)	40.41(25)	161.45	160.35	4	0.3	5
		12.74 (8)	40.21(22)	646.02	642.30	5	0.3	2.5
²³⁹ Pu/ ²⁴¹ Pu	121.39(1.1)	113.7(10)	139.6(22)	203.55	208.00	8	1.1	0.3
²³⁹ Pu/ ²⁴¹ Am	901.6(2.3)	635.2(11)	671.0(26)	422.57	419.19	5	0.3	6
		846.9(20)	1214 (33)	451.45	454.58	7	0.3	13
		588.1(18)	1232 (31)	640.15	641.37	7	0.3	11
		604.6 (4)	819.9(11)	646.02	662.37 ⁺	3	0.3	0.6
		498.3 (9)	639.0(24)	652.19	652.38	5	0.3	4
		607.6 (5)	618.7(11)	658.99	662.37	4	0.3	0.7
		601.0 (9)	-	686.16	688.70	6	0.3	2.7
		599.4 (7)	913.2(23)	717.76	721.92	4	0.3	2.6

[†]F_I, F_H, F_P denote errors for the ratios of absolute intensities, half-lives and measured peak areas, respectively.

*Values in parentheses are errors in percent (emphasis ours).

[†]Possible interference from fission-product γ rays.

4. SELECTED SPONTANEOUS-FISSION DATA

The spontaneous-fission half-life data are summarized in Table I above. The subjects of prompt and delayed neutron yields and energy spectra from spontaneous fission are characterized by an extensive literature; and we consequently confine our remarks here to brief comments concerning a few recent developments.

4.1. $\bar{\nu}$ values from spontaneous fission

The subject of $\bar{\nu}$, the average number of neutrons emitted per fission, has been treated exhaustively in the excellent recent review by Manero and Konshin [28]. Since that time a few additional measurements of $\bar{\nu}$ from the spontaneous fission of several nuclides have been reported. However, these values are in essential agreement with those given in [28], so that this review still presents a good overall picture of the status of spontaneous-fission $\bar{\nu}$ values.

The value of $\bar{\nu}$ for the spontaneous fission of ^{252}Cf occupies a central position in the area of $\bar{\nu}$ measurements since it is the "standard" relative to which other $\bar{\nu}$ values are measured. This is the case not only for the other spontaneously fissioning isotopes, but also --and more important--for the fissionable isotopes as well. However, at the present time there are still discrepancies in the value of this quantity as determined using different measurement techniques (see the discussion in [29] and [28]). In this context, it is appropriate to point out that a remeasurement of $\bar{\nu}$ for ^{252}Cf is currently in progress [30]. This experiment utilizes the manganese-bath technique; and particular attention has been given to identifying the various sources of error and to the quantitative determination of their effects. At the time of the writing of this review the results from this experiment are not available.

4.2. Neutron energy spectra from spontaneous fission

The prompt-neutron energy spectrum following spontaneous fission is customarily assumed to be well described by a Maxwellian distribution function, viz.

$$N(E) \propto E^{1/2} \exp(-1.5E/E_{av.}),$$

with the quantity $E_{av.}$ being determined from the data. The two most widely studied fission-neutron spectra are those from spontaneous fission of ^{252}Cf and thermal-neutron-induced fission of ^{235}U . The extensive data on these two energy spectra have quite recently been carefully evaluated by Grundl and Eisenhauer [31] to determine to what extent they can be described by a Maxwellian function. These authors conclude that, over the energy range 0.25 to 8 MeV, the reference Maxwellian shapes differ from the final evaluated shapes by $\sim 2\%$, with the average-energy parameters ($E_{av.}$) determined to be 2.13 ± 0.027 MeV and 1.97 ± 0.014 MeV, respectively, for ^{252}Cf spontaneous fission and ^{235}U thermal-neutron-induced fission.

In the area of the energy distribution of delayed neutrons following spontaneous fission, we wish to call attention to a series of quite interesting experiments being carried out at the OSIRIS Facility at Studsvik, Sweden. In these experiments the individual delayed-neutron precursors, produced in thermal-neutron fission of ^{235}U , are isolated for detailed study using on-line isotope separation. While these studies do not provide "integral" energy-spectral information, they can (in principle) yield such information when combined with the appropriate fission-product yields. A number of interesting features of the delayed-neutron energy distributions of individual precursors are observed, such as the occurrence of both discrete and continuous components. A summary of the present status of these results has been prepared by Professor Rudstam. This is included as Appendix B of this review.

5. COMMENTS AND OBSERVATIONS

To make the most effective use of available resources in the area of Nuclear Data, good communication among the measurers, the users, and the compilers and evaluators of nuclear data should exist. The field of neutron cross sections provides an excellent example of one category of nuclear data in which a fruitful interaction has existed among these three components of nuclear-data activity. At the present time, however, no relationship of comparable scope exists within the area of radioactive-nuclide decay data. This situation has been commented on before (see, e.g., [1,32]).

Because of the use of radioactivity in a number of widely varied applied areas and scientific disciplines, the "user community" of decay data is quite diverse. Consequently, the identification of a satisfactorily representative sample of such users represents a formidable problem.

The existence of different categories of measurers of decay data needs to be recognized. The vast majority of information constituting the present base of decay data has been provided by those interested in nuclear-structure physics. Generally speaking, these workers are not aware of the specific data needs of applied users, particularly specific accuracy requirements. This is especially true with respect to absolute γ -ray intensities and half-life values, which are necessary for any applications where quantitative assay of γ -radioactivity is required. High-precision measurements of these quantities are not generally required in order to extract the interesting basic nuclear-physics information

from a decay study. In addition, the measurement of these quantities with the desired precisions (say, <5% for absolute γ -ray intensities) requires specialized calibration techniques and instrumentation. For these reasons many of the data needs of users are inadequately satisfied at the present time.

Important in the development of a program to meet the requirements for decay data is recognition of the importance of radioactive-nuclide metrology. This metrology function would be mainly to develop and improve selected measurement techniques to provide a recognized capability for performing measurements requiring high precision. While in fact these measurements are of basic nuclear-physics quantities, the orientation of the effort would be to provide specific information for application to specific problems. Such a metrology program would most effectively be organized around existing capability in major laboratories engaged in nuclear research in order to provide continuity and the required technical support in associated disciplines. Examples of high-precision measurements of selected decay-scheme parameters for applications-oriented purposes are provided by work carried on in several Western-European laboratories (see, e.g., [33,34]).

Attention should also be given to the desirability of utilizing a common data content and format for the organization of decay data to meet applied needs. A common base of data presents a number of advantages to the applied user, among which we indicate two. First, it possesses "traceability," that is, it provides a standard origin for the data used by different groups. Second, it permits uniformity in the application of decay data to the quantitative measurement of radioactivity. Examples of applied needs include environmental monitoring and radiological health-hazard evaluations. In the preparation of regulations and guidelines by regulatory agencies to insure uniformity in the reported results of measurements, the standardization of reference material afforded by a common data base is a necessity and has legal implications. A structure for such data modeled along that for the ENDF/B decay-data file might be useful.

Interest has been expressed concerning what type of presentation (computer media or published form) of decay data is the most convenient from the point of view of the user. It is our opinion that such data should certainly be available in a simple and easily readable form, i.e., in print. Compared with categories of nuclear data such as, e.g.,

neutron cross sections, the amount of information involved is relatively small and having it available in handbooks, reports or tables makes its use quite straightforward and simple. If required for some applications, e.g., for use in data-analysis codes, the relevant data can readily be prepared in a suitable computer-based medium. (In fact, the decay data on ENDF/B-IV are stored on computer tape, although they are also available in the form of computer listings in a "people-readable" format [2] if desired.)

ACKNOWLEDGEMENTS

Contributions and communications from a number of interested people are gratefully acknowledged. A major source of decay data for this review was provided by the extensive data sets for individual transactinium nuclides with $A > 230$ supplied by C. M. Lederer of the Table of Isotopes Project at LBL. M. R. Schmorak of the Nuclear Data Project at ORNL supplied listings of selected decay data from his recent revision of the Nuclear Data Sheets for the even- A mass chains with $A > 243$. R. M. Harbour of SRL produced and supplied a listing of references to spontaneous-fission-related data from the Nuclear Science Abstracts. G. Rudstam has prepared the summary of delayed-neutron energy spectra given in Appendix B. Data requirements and helpful comments were sent by R. Dierckx of Euratom, Ispra and by A. H. W. Aten, Jr., of the IKO, Amsterdam. Communications of data on various aspects of transactinium-isotope nuclear data were received from: E. Takekoshi and H. Umezawa of JAERI; A. Hashizume and H. Kawakami of the Institute of Physical and Chemical Research, Wako-Shi, Saitama, Japan and the Institute for Nuclear Study, University of Tokyo, Japan, respectively; and A. B. Smith and J. W. Meadows of ANL. Helpful discussions were held with J. R. Smith, R. L. Heath and R. G. Helmer of the INEL. Finally, the constructive comments of R. G. Helmer and his careful reading of the manuscript were most helpful.

REFERENCES

- [1] Fission Product Nuclear Data (Proc. Conf. Bologna, 1973), IAEA - 169, IAEA, Vienna (1974).
- [2] REICH, C. W., HELMER, R. G., PUTNAM, M. H., Radioactive-Nuclide Decay Data for ENDF/B, U.S. AEC Report ANCR-1157 (August, 1974).

- [3] NATHAN, O., NILSSON, S. G., "Collective Nuclear Motion and the Unified Model," Ch. 10, Alpha-, Beta-, and Gamma-Ray Spectroscopy (SIEGBAHN, K., Ed.), North-Holland, Amsterdam, (1966).
- [4] NILSSON, S. G., Mat. Fys. Medd. Dan. Vid. Selsk. 29 (1955) No. 16; GUSTAFSON, C., LAMM, I.-L., NILSSON, B., NILSSON, S. G., Ark. Fys. 36 (1967) 613; NILSSON, S.G., TSANG, C.F., SOBICZEWSKI, A., SZYMANSKI, Z., WYCECH, S., GUSTAFSON, C., LAMM, I.-L., MÖLLER, P., NILSSON, B., Nuclear Physics A131 (1969) 1.
- [5] BUNKER, M.E., REICH, C. W., Revs. Mod. Phys. 43 (1971) 348.
- [6] GALLAGHER, C. J., MOSZKOWSKI, S. A., Phys. Rev. 111 (1958) 1282.
- [7] HAGER, R. S., SELTZER, E. C., Nuclear Data A 4 (1968) 1.
- [8] DITTNER, P. F., BEMIS, C. E., Jr., Phys. Rev. A 5 (1972) 481.
- [9] SCHMIDT-OTT, W.-D., HANSEN, J. S., FINK, R. W., Z. Physik 250 (1972) 191.
- [10] BEARDEN, J. A., BURR, A. F., Revs. Mod. Phys. 39 (1967) 125.
- [11] MARTIN, M. J., BLICHERT-TOFT, P. H., Nuclear Data Tables A8 (1970) 1.
- [12] BLACHOT, J., deTOURREIL, R., CEA Report CEA-N-1526 (1972); DEVILLERS, C., BLACHOT, J., LOTT, M., NIMAL, B., N'GUYEN VAN DAT, NOEL, J.P., deTOURREIL, R., Nuclear Data in Science and Technology (Proc. Conf. Paris, 1973), Vol. I, 477, IAEA SM-170/63, IAEA, Vienna (1973).
- [13] TOBIAS, A., Data for the Calculation of Gamma Radiation Spectra and Beta Heating from Fission Products (Revision 3), Central Electricity Generating Board Report RD/B/M2669 CNDG (73) P4 (June, 1973).
- [14] RUDSTAM, G., Fission Product Nuclear Data (Proc. Conf. Bologna, 1973), Review Paper 12, Vol. II, 1. IAEA-169, IAEA Vienna (1974).
- [15] SCHMORAK, M. R., Private Communication (July, 1975).
- [16] LEDERER, C. M., Private Communication (July, 1975).
- [17] GOVE, N. B., Private Communication (May, 1973).
- [18] ZELENKOV, A., Review Paper B6 submitted to this conference.
- [19] VANINBROUKX, R., Half-Lives of Some Long-Lived Actinides: A Compilation, Euratom Report EUR-5194e (1974).
- [20] PILGER, R. C., STEPHENS, F. S., ASARO, F., PERLMAN, I., Bull. Am. Phys. Soc., Ser. II 2 (1957) 394.
- [21] GUNNINK, R., MORROW, R. J., U.S. AEC Report UCRL-51087 (July, 1971).

- [22] CLINE, J. E., U.S. AEC Report IN-1448 (rev.) (January, 1971); CLINE, J. E., GEHRKE, R. J., McISAAC, L. D., U.S. AEC Report ANCR-1069 (Supplement to IN-1448) (July, 1972).
- [23] OTTMAR, H., WEITKAMP, C., Symposium on Practical Applications of Research and Development in the Field of Safeguards (Proc. Conf. Rome, 1974), IAEA, Vienna, (1974).
- [24] PEGHAIRE, A., Nuclear Instr. and Methods 75 (1969) 66.
- [25] LEGRAND, J., PEROLAT, J. P., BAC, C., GORRY, J., Int'l. J. Appl. Rad. and Isotopes 26 (1975) 179.
- [26] MAGNUSSON, L. B., Phys. Rev. 107 (1957) 161.
- [27] CAMPBELL, J. L., McNELLES, L. A., Nuclear Instr. and Methods 117 (1974) 519.
- [28] MANERO, F., KONSHIN, V. A., At. Energy Rev. 10 (1972) 637.
- [29] AXTON, E. J., Neutron Standard Reference Data (Proc. Conf. Vienna, 1972), 261, IAEA-PI-246-2/31, IAEA, Vienna (1974).
- [30] SMITH, J. R., Private Communication (August, 1975).
- [31] GRUNDL, J. A., EISENHAUER, C. M., Bulletin Am. Phys. Soc. Ser. II 20 (1975) 145; and Proc. Conf. on Nuclear Cross Sections and Technology, Washington, D.C. (1975) (to be published).
- [32] REICH, C. W., HELMER, R. G., Bull. Am. Phys. Soc., Ser. II 20 (1975) 134; and Proc. Conf. on Nuclear Cross Sections and Technology, Washington, D.C. (1975) (to be published).
- [33] HANSEN, H. H., deROOST, E., van der EIJK, W., VANINBROUKX, R., Z. Physik 269 (1974) 155, and references contained therein.
- [34] DEBERTIN, K., SCHÖTZIG, U., WALZ, K. F., WEISS, H. M., Private Communication (March, 1974).

APPENDIX A

THE ENDF/B DECAY-DATA FILE

As mentioned in Chapter 1 above, a file of actinide-nuclide decay data is currently being prepared for inclusion in Version V of ENDF/B. It will contain data on 46 nuclides and isomeric states. It thus seems appropriate within the context of this meeting to present a discussion of the philosophy underlying the ENDF/B decay-data file and to describe its organization and the types of information it contains.

As originally set up for Version IV of ENDF/B, the decay-data file was oriented toward the specific objective of providing a data base adequate for use in summation-type calculations of the fission-product decay-heat source term in reactor cores. However, in the planning of the file organization and content it was recognized that such a file--within the ENDF/B structure--should address itself to as broad a range of reactor-related applications (and, by implication, to use in other areas as well) as possible, within the limits of a realistic content and size. As such, the file was not intended to replace such broadly based data compilations as the Nuclear Data Sheets or the Table of Isotopes (see Chapter 2 above) but rather to represent a carefully evaluated subset of those data, oriented toward the needs of a certain identified group of users and presented in a format readily usable by them. The Version-IV data file which was set up to satisfy these requirements has been discussed in detail elsewhere [2,32][†]. For ENDF/B-V, the content has been expanded somewhat to permit detailed information on more radiation forms.

The file is most simply discussed by reference to actual examples of specific data sets. We have chosen two examples, ^{85m}Kr and ^{128}I , to serve as vehicles for the discussion. Although not actinides, these relatively simple cases provide a good orientation to the file structure.

Decay-data sets, in card-image format, as prepared for our laboratory, or "working," file for ^{85m}Kr and ^{128}I are shown in Tables A-I and A-II, respectively. (The process by which they are transcribed into final ENDF/B format will be mentioned below.) The first card contains the following information: Z and A values (in the form 1000 Z + A) followed immediately by an isomer flag. A blank or zero in the latter column indicates the ground state of the nucleus, a 1,2... indicates a first, second ... isomeric state. (Isomers are arbitrarily restricted to nuclear states with half-lives >0.1 sec. and are listed as separate "nuclides" in the file.) Following this on the first card are the chemical symbol, the spin and parity of the state and a number indicating the numbers of "comment cards" to follow.

Next comes a group of cards which provide the documentation for and pertinent comments about the data set. These are followed by a card giving the half-life, its uncertainty, the units, the number of decay modes of the nuclide and the number of energy spectra to be listed.

[†] The numbering of the references is that used in the text.

This is followed by cards (equal in number to the indicated number of decay modes) giving the following information about each decay mode: the type of decay; whether or not an isomeric state in the daughter is fed; the Q-value in keV for the decay mode; its uncertainty; the branching ratio (in percent) of the decay mode; and its uncertainty. The decay modes thus far treated are denoted as follows: β^- , 1; electron-capture and/or β^+ , 2; isomeric-transition, 3; α -particle, 4; neutron, 5; spontaneous fission, 6; and proton, 7. If one type of decay (e.g., β^-) feeds both the ground state and an isomeric state in the daughter nucleus, this is treated as two distinct decay modes. Any radiations (e.g., an isomeric transition) associated with the decay of the daughter-nucleus isomeric state are listed with the daughter-nucleus decay data.

The next card contains the average-energy information in keV/disintegration) in the order: $\langle E \text{ electron} \rangle$; its uncertainty; $\langle E \text{ photon} \rangle$; its uncertainty; $\langle E \text{ heavy particle} \rangle$; and its uncertainty. These average energies contain the following contributions. $\langle E \text{ electron} \rangle$ includes the average energy from all processes involving electrons, such as β^- , β^+ , conversion electrons and Auger electrons. The photon term includes not only γ -rays, but also all other electromagnetic radiation (e.g., x-rays and annihilation radiation) emitted in the decay process. The third energy includes contributions from α -particle emission, protons and neutrons. (It could also include spontaneous-fission fragment contributions as well, if desired.)

Next comes the listing of the various radiation spectra. Each listing consists of two types of cards. The first of these contains the following information: a normalization factor (to convert relative intensities to absolute intensities); its uncertainty; the number of individual transitions listed; the radiation type; the average energy (in keV per decay) associated with the radiation type; and its uncertainty. The numbering of the radiation types is similar to that given above for the decay modes, with the additional conventions: 8 denotes discrete electrons (e.g., conversion electrons); 9 denotes photons not arising as transitions between nuclear states; and 0 denotes γ radiation. The second of these card types contains the specific spectral information, with one card for each individual transition. Except for the cases discussed below, the data given here are listed in the order: energy, its uncertainty; intensity and its uncertainty. For e.-c. and β^+ decay (radiation type 2, see Table A-II) two sets of intensity information are given: namely that of the electron-capture component of the transition and that of the β^+ component.

In this case the average energy listed is that of the β^+ component only. For β^+ and β^- transitions, provision is also made for including a "multipolarity flag," giving the spectrum shape of the particular transition. The symbol "1U" indicates a first-forbidden unique shape; and the computer program takes this into account in its calculation of $\langle E_\beta \rangle$ for that transition. In the absence of such a notation (which is the case for allowed or first-forbidden non-unique transitions) an allowed shape is assumed.

The data for radiation type 9, x-rays and annihilation radiation, are entered somewhat differently. The first ("normalization") card has the same arrangement as for the other radiation types, but only the intensity data are given (since the energies in this case are in principle known). These are entered in the order: K-x-ray intensity, its uncertainty; L-x-ray intensity, its uncertainty; annihilation radiation intensity, its uncertainty; and a "source flag." This latter quantity indicates the decay process with which the radiation is associated, and hence indicates the Z-values of which the x-rays are characteristic. In Table A-I, for example, there are two sets of x-rays, one of which follows β^- decay (and hence is characteristic of $Z=37$) and one which is associated with isomeric-transition decay (and hence is characteristic of $Z=36$). Where measured x-ray intensities exist, they are listed here. In most cases, however, such measurements do not exist, and these intensity data will have to be calculated from the other decay-scheme data, as mentioned in Section 1.1. above. The values listed in Table A-I are in fact theoretical values, calculated from the decay-scheme data by the procedures outlined in [11].

Radiation type 0 (γ radiation), when available, is always the last data set listed. Provision is made for the existence of two cards for each γ -ray transition. The first of these contains the following information: energy, its uncertainty; intensity, its uncertainty; multipolarity and a source flag, indicating with which decay process the γ -ray is associated. (Although only pure multipoles are indicated, the alphanumeric information here can describe mixed multipoles and uncertainties in the contributions of these different multipoles.) If internal-conversion-coefficient data are known (or, in some cases, can be inferred), a second card is included. This contains the K-shell ICC (α_K), its uncertainty), α_L , its uncertainty, α_M and its uncertainty. To avoid confusion with the energy cards, the first 10 columns of these ICC cards (corresponding to the location of the energy value) are left blank, as shown in Table A-I.

More complicated decay processes can be treated within the structure of this data file. Delayed-neutron emission (β^- decay followed by neutron emission), for example, would be listed as decay mode "15" - 1 for β^- and 5 for neutron. And, a γ -ray emitted from an excited state of the nucleus remaining after the neutron emission would carry a source flag "15." Spectra characterized by both a discrete and a continuous component, such as delayed neutron spectra, are listed in the following manner. The discrete components are listed as usual: energy, uncertainty; intensity, and uncertainty. For the continuous component, the energy values are chosen (and listed) at equally spaced intervals across the distribution, with a sufficient number of points chosen to permit a suitably accurate representation of the distribution. The intensity (and where appropriate, the uncertainty) values corresponding to these energy points are listed, not in the columns where the discrete data are given, but in the next two groups of columns (corresponding to positions of a fifth and a sixth entry). In this fashion, the discrete and the continuous components can be readily recognized.

Before the data described above are entered into ENDF/B, two separate processings are carried out. The first of these, carried out at our laboratory, consists primarily of listing all the data in an "energy-intensity" format and affects only the listings for radiation types 8, 9, and 0. Conversion-electron and Auger-electron spectra, which are not listed as such on our laboratory file, could be calculated theoretically from the data given in this file and entered as a listing of energy and intensity values for the various lines. Where desired, lines from a given subshell can be grouped as a single line, with an appropriate averaged energy for that shell. The x-ray and annihilation data are converted into a listing of energy and intensity values for the individual transitions. The partial ICC data for the various γ -ray transitions are deleted and the data cards for the individual transitions are prepared in the format: energy, uncertainty; intensity, uncertainty; total conversion coefficient, uncertainty; and the source flag.

Following this, these data are transmitted to the NNCSC at BNL for conversion to the standard ENDF/B format (e.g., half-lives in sec., energies in eV, etc.).

TABLE A-I. Sample listing of decay data for ^{85m}Kr decay prepared in the INEL format.

Z	A	IS	I_{π}	No. of Comment Cards
36	85	1 KR	1/2-	4

COMMENTS AND DOCUMENTATION

PREPARED FOR FILE : 1/75 CWR
 REFERENCES: Q- 1973 REVISION OF WAPSTRA-GOVE MASS TABLES.
 OTHER- F.K. WOHN, W.L. TALBERT, JR. AND J.K. HALBIG,
 NUCL. PHYS. A152, 561 (1970).

$T_{1/2}$	σ	Units	No. of Decay Modes	No. of Spectra		
4.480	0.008	H	2	3		
Decay Mode	Final-state isomer	Q	σ	Branching	σ	
1	0	991.7	2.0	78.8	1.3	
3	0	304.47	0.05	21.2	1.3	
$\langle E_{\text{elect.}} \rangle$	σ	$\langle E_{\text{phot.}} \rangle$	σ	$\langle E_{\text{h.p.}} \rangle$	σ	
251.62		157.14				
Normalization	σ	No. of Transitions	Radiation Type	$\langle E_{\beta^-} \rangle$	σ	
0.788	0.013	1	1	226.1	2.0	
E_{β^-}	σ	I_{β^-}	σ			
840.7	2.0	100.0				
Normalization	σ	No. of Entries	Radiation Type	$\langle E \rangle$	σ	
1.0		2	9	0.792		
K x-ray Int.	σ	L x-ray Int.	σ	ann. rad. Int.	σ	source flag
2.05		0.13				1
3.96		0.23				3
Normalization	σ	No. of Transitions	Radiation Type	$\langle E_{\gamma} \rangle$	σ	
1.40		2	0	156.35		
E_{γ}	σ	I_{γ}	σ	Multipolarity	Source flag	
150.99	0.05	53.8	1.8	M1	1	
	0.0400	0.0008	0.0045	0.0002	0.0010	0.0001
304.47	0.05	10.0	0.4	M4	3	
	0.432	0.020	0.064	0.003	0.013	0.001

TABLE A-II. Sample listing of decay data for ^{128}I decay, prepared in the INEL format.

Z	A	IS	I π		No. of Comment Cards	
53	128	I	1+		3	
COMMENTS AND DOCUMENTATION						
PREPARED FOR FILE: 1/75 CWR						
REFERENCES: Q- 1973 REVISION OF WAPSTRA-GOVE MASS TABLES.						
OTHER- SEE R.L. AUBLE, NUCL. DATA SHEETS 9, 157(1973)						
T _{1/2}	σ	Units	No. of Decay Modes	No. of Spectra		
24.99	0.02	M	2	4		
Decay Mode	final-state isomer	Q	σ	Branching	σ	
1	0	2127.	5.	93.9		
2	0	1258.	5.	6.1		
$\langle E_{\text{elect.}} \rangle$	σ	$\langle E_{\text{phot.}} \rangle$	σ	$\langle E_{\text{h.p.}} \rangle$	σ	
751.1		85.2				
Normalization	σ	No. of transitions	Radiation type	$\langle E_{\beta^-} \rangle$	σ	
1.0		4	1	751.1		
E $_{\beta^-}$	σ	I $_{\beta^-}$	σ			
544.	5.	0.012				
1158.	5.	1.9				
1684.	5.	15.				
2127.	5.	77.				
Normalization	σ	No. of transitions	Radiation type	$\langle E_{\beta^+} \rangle$	σ	
1.0		2	2	0.0013		
E	σ	I $_{e.c.}$	σ	I $_{\beta^+}$	σ	
510.	5.	0.14		0.0		
1258.	5.	6.		0.002		
Normalization	σ	No. of Entries	Radiation type	$\langle E \rangle$	σ	
1.0		1	9	1.28		
K x-ray Int.	σ	L x-ray Int.	σ	ann. rad. Int.	σ	Source flag
4.48		0.72		0.004		2
Normalization	σ	No. of transitions	Radiation type	$\langle E_{\gamma} \rangle$	σ	
0.16		7	0	83.88		
E $_{\gamma}$	σ	I $_{\gamma}$	σ	Multipolarity		Source flag
442.91	0.07	100.				1
526.62	0.10	9.6				1
613.1	0.5	0.015	0.004			1
743.5	0.2	0.9	0.1			2
969.4	0.4	2.4	0.3			1
1139.7	0.2	0.060	0.008			1
1434.5	0.5	0.0033	0.0007			1

APPENDIX B

For the IAEA meeting on "Transactinium Isotope Nuclear Data"

Summary of delayed-neutron work at the Research Councils' Laboratory, Studsvik

G Rudstam

The Swedish Research Councils' Laboratory, Studsvik, Nyköping, Sweden

The isotope-separator-on-line facility "OSIRIS" has been used for a survey of delayed-neutron activities including accurate half-life determinations (17 new delayed-neutron precursors were detected in the course of the work). In addition to this, the energy spectra of the neutrons have been measured for 24 precursors. The results are summarized below, and references to the original publications or manuscripts are given.

Precursor	Half-life measured sec	Energy spectrum of the delayed neutrons
$^{79}_{\text{(Zn,Ga)}}$	$2.63 \pm 0.09^{\text{a)}}$	The energy spectrum has been measured ^{b)}
$^{80}_{\text{Ga}}$	$1.66 \pm 0.02^{\text{a)}}$	The energy spectrum has been measured ^{b)}
$^{81}_{\text{Ga}}$	$1.23 \pm 0.01^{\text{a)}}$	The energy spectrum has been measured ^{b)}
$^{82}_{\text{Ga}}$	$0.60 \pm 0.01^{\text{a)}}$	
$^{83}_{\text{Ga}}$	$0.31 \pm 0.01^{\text{a)}}$	
$^{85}_{\text{As}}$	$2.08 \pm 0.05^{\text{a)}}$	
$^{87}_{\text{Br}}$	$55.5 \pm 0.03^{\text{a)}}$	The energy spectrum contains several prominent peaks, notably at energies 130, 183, 253, and 440 keV. Smaller peaks are found at 315, 400, 534 and 614 keV ^{c)}
$^{88}_{\text{Br}}$	$16.7 \pm 0.02^{\text{a)}}$	Structure in the spectrum with peaks at 127, 160, 205, 235, 390, 540 and 670 keV ^{d,e)}
$^{89}_{\text{Br}}$	$4.37 \pm 0.03^{\text{a)}}$	Peaks (although not very pronounced) found at energies 270, 400, 610, 680, 740, 800 and 900 keV ^{f)}
$^{90}_{\text{Br}}$	$1.96 \pm 0.05^{\text{a)}}$	Energy spectrum without discrete structure ^{d)}

Precursor	Half-life measured, sec	Energy spectrum of the delayed neutrons
^{91}Br	0.541 ± 0.005	The energy spectrum has been measured ^{f)}
^{92}Br	$0.365 \pm 0.007^a)$	
^{92}Rb	$4.34 \pm 0.06^a)$	
^{93}Kr	$1.33 \pm 0.05^a)$	
^{93}Rb	$5.85 \pm 0.03^a)$	The energy spectrum shows some structure with peaks at 155, 200, 235, 275, 330, 365 and 460 keV ^{f)}
^{94}Rb	$2.69 \pm 0.02^a)$	The energy spectrum has been measured ^{g)}
^{95}Rb	$0.400 \pm 0.004^a)$	The energy spectrum has been measured ^{g)}
^{96}Rb	$0.203 \pm 0.003^a)$	
^{97}Rb	$0.172 \pm 0.003^a)$	
^{98}Rb	$0.141 \pm 0.010^a)$	
^{123}Ag	$0.39 \pm 0.03^h)$	
^{127}In	$3.76 \pm 0.03^h)$	
$^{128}(\text{Cd}, \text{In})$	$0.94 \pm 0.05^h)$	
^{128}In	$11 \pm 1^h)$	
^{129}In	$0.99 \pm 0.02^h)$	The combined spectrum for the two isomers at mass 129 has been measured ^{b)}
^{129}In	$2.5 \pm 0.2^h)$	
^{130}In	$0.58 \pm 0.01^h)$	The energy spectrum has been measured ^{b)}
^{131}In	$0.29 \pm 0.01^h)$	
^{132}In	$0.3 \pm 0.1^h)$	

Precursor	Half-life measured sec	Energy spectrum of the delayed neutrons
^{133}Sn	$1.47 \pm 0.07^{\text{h}}$	
^{134}Sn	$1.04 \pm 0.02^{\text{h}}$	The energy spectrum contains one very prominent peak at 500 keV and, in addition, some smaller peaks at 320, 435, 760, 860 and 1020 keV ^{c)}
^{134}Sb	$10.3 \pm 0.4^{\text{h}}$	
^{135}Sb	$1.82 \pm 0.04^{\text{h}}$	The energy spectrum contains three large peaks at 1040, 1205 and 1450 keV ^{c)}
^{136}Sb	$0.82 \pm 0.02^{\text{h}}$	
^{136}Te	$17.5 \pm 0.4^{\text{h}}$	The spectrum contains a single dominant peak at 429 keV and, in addition, a series of smaller peaks at 251, 313, 466, 525, 593, 692 and 766 keV ^{c)}
^{137}I	$24.25 \pm 0.12^{\text{h}}$	A spectrum with very pronounced structure. Large peaks are found at 272, 380, 487, 583, 756, 863, 965 and 1140 keV and smaller ones at 166, 325, 425, 515, 695 and 1063 keV ^{c)}
^{138}I	$6.46 \pm 0.15^{\text{h}}$	Some structure, in particular at 370 keV, found in the spectrum ^{d,e)}
^{139}I	$2.30 \pm 0.05^{\text{h}}$	The spectrum contains some evidence for structure with peaks at 130, 190, 290, 485 and 565 keV ^{f)}
^{140}I	$0.59 \pm 0.01^{\text{h}}$	Indication of peaks at 450, 550 and 800 keV ^{d)}
^{141}I	$0.48 \pm 0.03^{\text{h}}$	In the combined energy spectrum from ^{141}I and ^{141}Cs peaks are found at 160, 300, 395, 450 and 550 keV with indications of further peaks at 225, 340, 610 and 685 keV ^{f)}
^{141}Cs	$22.2 \pm 0.4^{\text{h}}$	
^{142}Cs	$1.69 \pm 0.09^{\text{h}}$	Peaks are found at 370 and 750 keV ^{d)}

Precursor	Half-life measured sec	Energy spectrum of the delayed neutrons
^{143}Cs	$1.78 \pm 0.01^{\text{h)}}$	Peaks are seen at 125, 180, 225, 310 and 350 keV ^{f)}
^{144}Cs	$1.00 \pm 0.02^{\text{h)}}$	Little structure but some suggestion of peaks at 130 and 180 keV ^{d)}
^{145}Cs	$0.58 \pm 0.01^{\text{h)}}$	
^{146}Cs	$0.343 \pm 0.007^{\text{h)}}$	

The techniques used in the half-life measurements are described in ref.^{a)}. The energy measurements were carried out using a ^3He -spectrometer, as described in ref.ⁱ⁾.

As a continuation of the studies on delayed neutrons a series of measurements of neutron branching ratios is being planned. The equipment is completed, and the experiments are ready to start.

References

- a) G. Rudstam and E. Lund, Delayed-Neutron Activities Produced in Fission. Mass Range 79-98, to be published in Phys. Rev.
- b) G. Rudstam and S. Shalev, work in progress.
- c) S. Shalev and G. Rudstam, Nucl. Phys. A230 (1974) 153.
- d) S. Shalev and G. Rudstam, manuscript under preparation for publication.
- e) S. Shalev and G. Rudstam, Proceedings of a Panel on Fission Product Nuclear Data, Bologna, 26-30 November 1973, Vol. III p. 367.
- f) G. Rudstam and S. Shalev, Nucl. Phys. A235 (1974) 397.
- g) E. Lund and G. Rudstam, work in progress.
- h) E. Lund and G. Rudstam, Half-Lives of Delayed-Neutron Activities Produced in Fission. Mass Range 122-146, submitted to Nucl. Phys.
- i) G. Rudstam, S. Shalev and O.C. Jonsson, Nucl. Instr. and Methods 120 (1974) 333.